Molecular and Cellular Defects Driving the Leukemic Progression of Severe Congenital Neutropenia

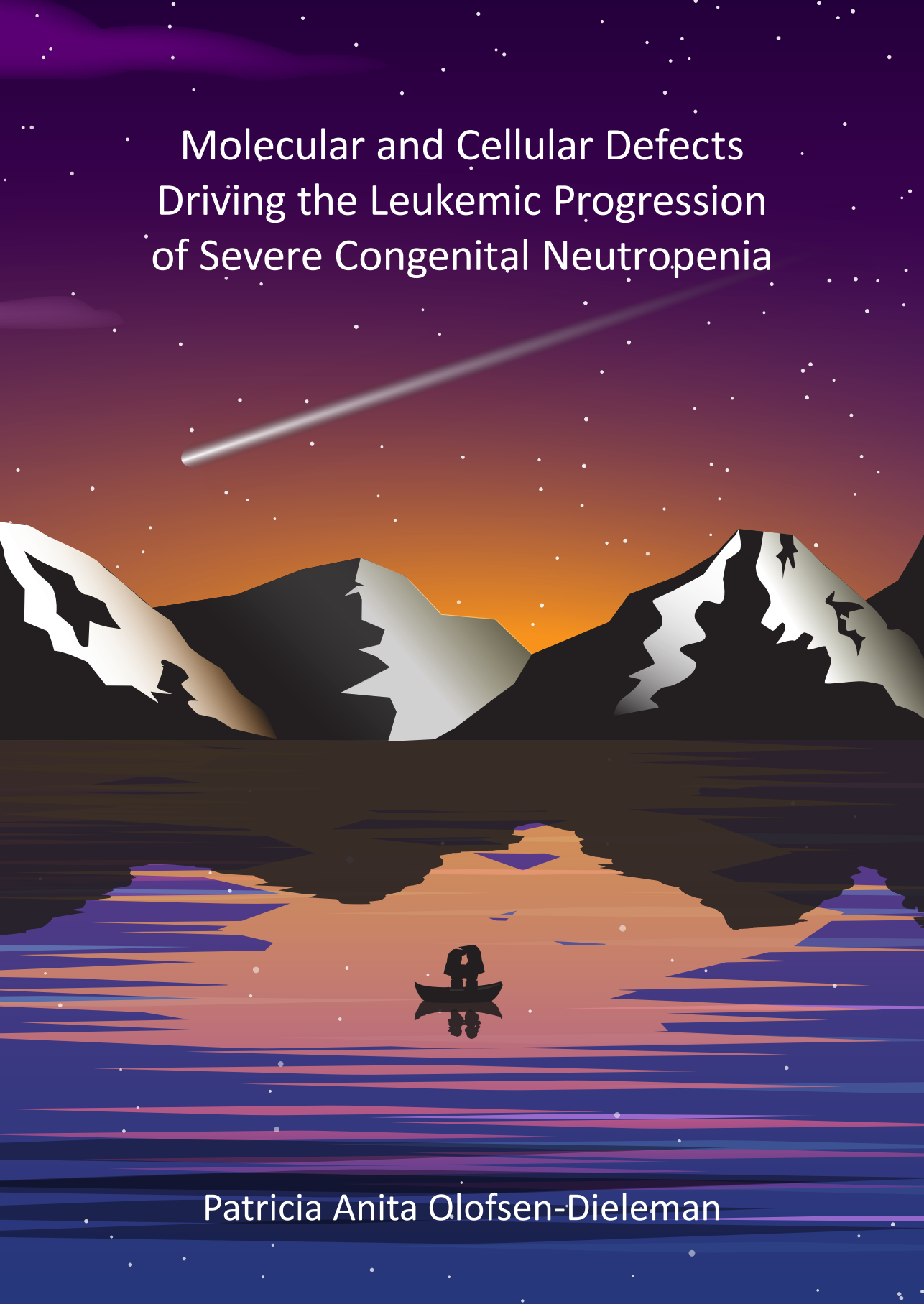

Patricia Anita Olofsen-Dieleman

Molecular and Cellular Defects Driving the Leukemic Progression of Severe Congenital Neutropenia

Patricia Anita Olofsen-Dieleman

Erasmus MC
Universitair Medisch Centrum Rotterdam

About the book cover:

Artistic impression of a PhD project.

The mountains represent the ups and downs of a PhD. The people in the boat stand for the fact that science is a team effort, you cannot do it alone. To see a comet you have to be lucky, and the same holds true if you want to catch a scientific breaktrough.

ISBN: 978-94-6361-540-2
Layout: Patricia A. Olofsen-Dieleman
Cover: Patricia A. Olofsen-Dieleman
Printing: Optima Grafische Communicatie (https://www.ogc.nl)

The work described in this thesis was performed at the Department of Hematology, Erasmus University Medical Center, Rotterdam, the Netherlands.

Printing of this thesis was financially supported by the Erasmus University Rotterdam.

Molecular and Cellular Defects Driving the Leukemic Progression of Severe Congenital Neutropenia

Moleculaire en cellulaire afwijkingen betrokken bij de leukemische ontaarding van ernstige aangeboren neutropenie

Proefschrift

ter verkrijging van de graad van doctor aan de
Erasmus Universiteit Rotterdam
op gezag van de rector magnificus

Prof.dr. F.A. van der Duijn Schouten

en volgens besluit van het College voor Promoties.
De openbare verdediging zal plaatsvinden op
woensdag 26 mei 2021 om 15:30 uur

door

Patricia Anita Olofsen-Dieleman

geboren te Amsterdam

Erasmus University Rotterdam

Erasmus

Promotiecommissie

Promotor:	Prof. dr. I.P. Touw
Overige leden:	Prof. dr. H.G.P. Raaijmakers
	Dr. M.M. von Lindern
	Dr. B.A. van der Reijden
Copromotor:	Dr. E.M. de Pater

Table of contents

Chapter 1

General Introduction

1.1. Hematopoiesis

Blood cells are generated in the bone marrow in a process known as hematopoiesis, and subsequently released in the circulation. Blood is comprised of various mature blood cells; red blood cells/erythrocytes which are important for oxygen transport, platelets which are best known for their role in blood clotting, and white blood cells/leukocytes which are the bodies defense mechanism against pathogens. There are several types of leukocytes; T-cells and B-cells which play an important role in adaptive immunity by creating an immunological memory after an initial response to a pathogen, and neutrophils, eosinophils, basophils, monocytes/macrophages, dendritic cells, and natural-killer cells which are the bodies first line of defense known as innate immunity. Neutrophils, eosinophils, and basophils are subclassified as granulocytes since these blood cells comprise various granules, which contain proteins important for the killing of pathogens, like bacteria and parasites. Mature blood cells have a limited lifespan making a constant production of new cells necessary to maintain adequate cell numbers.

All blood cells are generated from a rare, self-renewing, population of pluripotent hematopoietic stem cells (HSCs) which are located in the bone marrow and of which the self-renewal (symmetric cell division), and proliferation/differentiation (asymmetric cell division) is tightly regulated by, e.g., the bone marrow microenvironment/niche comprised of various non-hematopoietic cells.[1,2] Downstream of the so-called long-term hematopoietic stem cell (LT-HSC) are various hematopoietic stem- and progenitor cells (HSPCs), e.g., multipotent progenitor (MPP) cells.[3] The MPPs give rise to either lymphoid progenitors, which eventually produce T-, B-, dendritic-, and NK-cells, or myeloid progenitors which can give rise to the other mature blood cells, e.g., neutrophils and red blood cells. Growth factors play an important role in stimulating differentiation into a specific lineage. A schematic overview of the classical, linear, hematopoietic hierarchy, including the most important growth factors to stimulate differentiation, is shown in Figure 1.[4,5] The production of (mature) blood cells is a tightly regulated process, as well as preventing the uncontrolled growth of progenitors. However, discrepancies in these processes can occur resulting in (severely) increased or decreased levels of certain blood cells. For example, uncontrolled growth resulting in an increased number of myeloid progenitors, which have lost their ability to differentiate, can result in acute myeloid leukemia (AML), whereas a decreased number of neutrophils results in neutropenia.

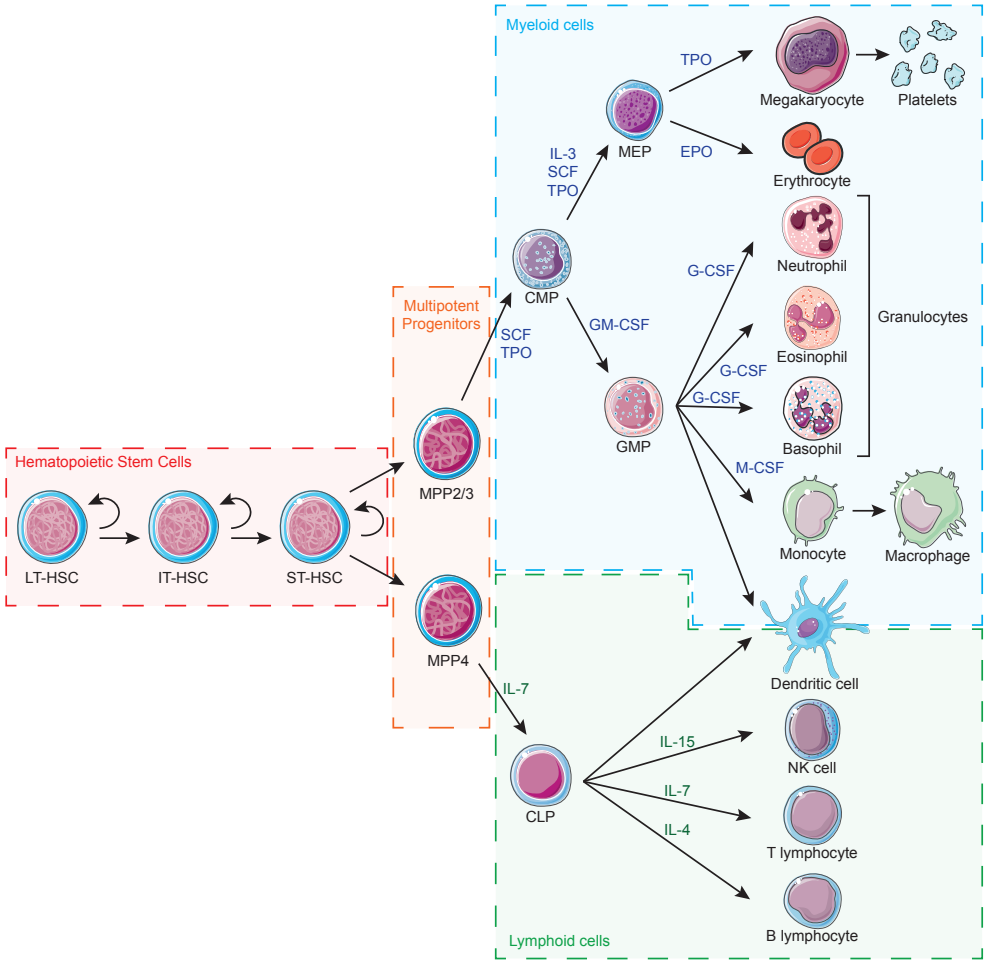

Figure 1: Schematic overview of the classical, linear, hematopoietic hierarchy.
Pluripotent hematopoietic stem cells can self-renew and differentiate into more mature multipotent progenitors, which can either become myeloid- or lymphoid progenitors, and further differentiate into mature progeny. Growth factors play an important role in stimulating differentiation and the most important ones are depicted here. For visualization purposes, not all differentiation stages and growth factors are depicted.

1.2. Severe congenital neutropenia

Severe congenital neutropenia (SCN) patients have a hereditary bone marrow failure syndrome characterized by a block in neutrophil differentiation at the promyelocyte stage (Figure 2), resulting in severely reduced absolute neutrophil counts (<0.5x10^9/L). Because neutrophils are essential effector cells of the innate immune system for killing bacteria, SCN patients show severe, recurrent, and sometimes life-threatening, bacterial infections such as gingivitis (infection of the gums), otitis (ear infection), pneumonia and skin infections starting within the first 4 weeks after birth.[6,7] SCN is a rare condition with a prevalence estimated between 3-8.5 cases per million individuals.[8] Before treatment with recombinant granulocyte colony-stimulation factor (G-CSF) became available for clinical use, the majority of SCN patients (>80%) used to die from severe bacterial infections.[9] Intriguingly, most patients respond to G-CSF therapy despite the fact that endogenous G-CSF serum levels are normal or even slightly elevated, raising the question why administration of exogenous G-CSF is effective. A plausible explanation for this apparent paradox is that SCN patients are hampered in their basal state of granulopoiesis, driven by the transcriptional regulator C/EBPα.[10] However, at high dosages of G-CSF a state termed “emergency” granulopoiesis is induced, which is controlled by C/EBPβ. In healthy individuals, emergency granulopoiesis is activated during phases of bacterial infections. In SCN patients, sustained G-CSF treatment activates C/EBPβ-dependent emergency granulopoiesis, alleviating the severe neutropenia in the absence of infections.[10] Nowadays, the majority of SCN patients (>90%) are effectively treated with G-CSF (officially called colony stimulating factor 3 or CSF3), alleviating the differentiation block and resulting in increased numbers of mature neutrophils, reduced numbers and severity of bacterial infections, and a dramatic improvement in quality of life.[11] However, follow-up studies revealed that SCN patients have an increased risk of developing leukemia.

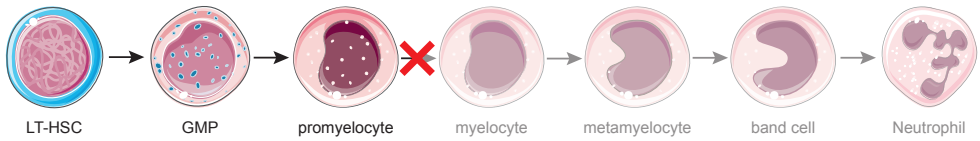

Figure 2: SCN patients show a neutrophil differentiation arrest at the promyelocyte stage.
Schematic overview of the myeloid differentiation pathway resulting in mature neutrophils, which is blocked at the promyelocyte stage in SCN patients. For visualization purposes, several HSC and progenitor stages have not been depicted.

1.2.1 Genetic alterations underlying SCN

An intriguing, yet puzzling characteristic of SCN is its wide genetic diversity. Currently, mutations in more than 20 genes have been implicated as the cause of SCN.[12] The majority of SCN patients (~50%) present with autosomal dominant or sporadic mutations in the gene *ELANE*, encoding for the primary granule protein neutrophil elastase (NE), which is highly expressed in promyelocytes.[13,14] A prevailing hypothesis is that *ELANE* mutations cause misfolding of the mutant NE protein, evoking an unfolded protein response (UPR) and cellular stress, eventually resulting in accelerated cell death beyond the promyelocyte stage.[15] To date more than 200 different *ELANE* mutations are identified, distributed throughout the whole exome. Because not all *ELANE* mutations predictably result in protein misfolding, alternative hypotheses as to how they may cause neutropenia have been proposed, e.g., involving altered substrate specificities and/or mis-trafficking of mutant NE from their normal residence in granules.[16]

Although the majority of SCN patients present with a mutation in *ELANE*, the first case of SCN, described in 1956 by Rolf Kostmann, was the result of an autosomal recessive mutation in the mitochondrial protein *HAX1.*[6,17] The prevalence of *HAX1* mutations varies a lot. Whereas ~11% of European SCN patients show homozygous mutations in *HAX1*, *HAX1*-mutant SCN patients are not yet detected in the United States.[12] This could be explained by the large number of consanguineous families in Europe (mainly from Arabic and Turkish origin), significantly increasing the possibility to obtain a mutation in both alleles of the *HAX1* gene. Mutations in *HAX1* are described to activate the nonsense-mediated mRNA decay pathway, resulting in loss of the HAX1 protein and mitochondrial leakage.[17]

In addition to mutations in genes encoding a granule protein (*ELANE*) or a mitochondrial protein (*HAX1*), mutations in genes encoding, e.g., a cytoskeletal protein (*WAS*)[18], a metabolic enzyme (*G6PC3*)[19], an endosomal membrane trafficking protein (*VPS45*)[20], a myeloid transcription factor (*GFI1*)[21], a transmembrane protein (*JAGN1*)[22], and a cytokine receptor (*CSF3R*)[23] can cause SCN. All these genes affect different proteins with completely different functions, and how these mutations result in a promyelocyte differentiation arrest and give rise to severe neutropenia is still largely unknown.[12] It has been suggested that a common mechanism of disease pathogenesis could be increased oxidative stress caused by the mutation. For example, mutations in *HAX1* result in mitochondrial leakage, while mutations in *ELANE* can cause NE protein misfolding, both possibly resulting in increased oxidative stress levels.

1.3. Oxidative stress

The term oxidative stress describes an imbalance between the production of the natural occurring reactive oxygen species (ROS) and the cell's ability to detoxify the reactive intermediates. ROS are natural by-products of cell metabolism but can also be generated by (dis)regulation of other processes in, for example, the mitochondria or endoplasmic reticulum (ER) or via extracellular stimuli. DNA oxidation is a major contributor to genomic instability and decay by, e.g., acquisition of mutations.[24] However, it has become clear that ROS are also important for several physiological responses, like cell proliferation and differentiation, by oxidation of various phosphatases and protein kinases.[25-27] The degree of stress ranges from physiological oxidative stress (eustress) to excessive and toxic oxidative stress burden (distress, resulting in DNA, protein and lipid damage). Of note, cells produce antioxidants to neutralize the excessive ROS to maintain the reduction-oxidation (redox) homeostasis.[24]

1.3.1 NRF2

The master regulator of this redox balance is NRF2. NRF2 is under homeostatic conditions located in the cytoplasm in a complex with KEAP1, where KEAP1 ubiquitinates NRF2 resulting in its rapid degradation.[28] Under oxidative stress conditions cysteinyl residues of KEAP1 are modified and KEAP1 loses its ability to ubiquitinate NRF2. NRF2 can then translocate to the nucleus, inducing the transcription of various antioxidant proteins which can neutralize the excessive ROS.[28]

1.3.2 PML

In addition to NRF2, the promyelocytic leukemia (PML) protein has also been described to act as ROS sensor. PML is a cysteine-rich protein and, similar to KEAP1, these cystine residues are oxidized upon oxidative stress. Oxidized PML forms multimers that self-organize into PML nuclear bodies (PML-NBs) which serve as SUMOylation factories (Small Ubiquitin-like Modifier).[29] Dozens of unrelated proteins are described to be able to be present in these PML-NBs, varying with cell type or stress conditions.[30] By SUMOylating these proteins PML is able to regulate their function and degradation. In line with this, PML-NBs have been linked to a plethora of cellular processes, e.g., clearing of misfolded proteins[31], cell cycle arrest[32], the DNA damage response[33], and metabolism.[34] PML downregulates ROS by inducing the expression of a subset of p53 targets, which induce antioxidants in response to basal oxidative stress.[35] Importantly, with active PML mediated antioxidant signaling, NRF2 responses are blunted, while loss of PML results in increased NRF2 levels.[35] In acute stress situations, PML NBs activate p53 targets resulting in cell death or senescence.[35]

1.4. Leukemic progression of SCN

As mentioned previously, G-CSF/CSF3 treatment significantly reduced occurances and severity of bacterial infections while increasing the quality of life in patients with SCN. In line with this, a large SCN patient cohort, comprised of 374 SCN patients on long-term CSF3 treatment enrolled in the SCN International Registry, showed that the mortality rate due to infections was severely reduced upon CSF3 treatment.[36] However, after 12 years on CSF3 treatment the cumulative incidence of progression to myelodysplastic syndrome (MDS) or AML was 21%, indicating that SCN patients on CSF3 treatment have a highly increased risk of leukemic progression.[36]

1.4.1 Mutations in the CSF3 receptor

Progression to MDS/AML is associated with the appearance of hematopoietic clones with somatic mutations in the gene encoding the G-CSF/CSF3 receptor (*CSF3R*). C-to-T transitions converting glutamine codons into stop codons in the cytoplasmic domain of the CSF3R, resulting in a truncated CSF3R, were detected in SCN patients in the early 1990s.[37,38] It was shown that these mutations were acquired, and not inherited, and present in ~80% of SCN patients that progressed to AML.[39,40] CSF3R-truncating mutations result in loss of a large portion of the cytoplasmic domain of the receptor. This domain contains, among others, a lysine residue critical for degradation of the CSF3R, resulting in increased numbers of receptors on the plasma membrane and sustained CSF3-induced signaling.[41,42] CSF3 treatment induced proliferation, phosphorylation of Stat5, and transcription of Stat5 target genes in *Csf3r*-truncation mutant mice, indicating that inappropriate Stat5 activation plays a key role in establishing clonal dominance by *Csf3r*-mutant HSCs.[43] In addition, increased levels of ROS were observed in *Csf3r*-mutant mice upon CSF3 treatment, possibly resulting in a more “mutation-prone” environment involved in leukemic progression.[44]

Several clones with different mutations leading to the expression of truncated CSF3R proteins could be detected in patients that did not (yet) show signs of leukemic progression, suggesting that *CSF3R* mutations are acquired early during leukemic transformation.[39,40] In addition, the existence of multiple *CSF3R* mutant clones suggest a strong selective pressure for acquisition of this type of mutations.[40] However, *CSF3R* mutant clones can persist for years as a minor clone before leukemia becomes clinically overt, indicating that additional mutations are needed for full malignant transformation.[45]

1.4.2 Mutations in RUNX1

Mutations in *RUNX1*, in addition to *CSF3R* mutations, were shown to be the most often acquired in 31 SCN patients who progressed to MDS or AML (20/31=64.5%).[46] RUNX1 is a member of the runt transcription factor family and is essential for foetal and adult haematopoiesis.[47,48] The majority of the *RUNX1*-mutant SCN-MDS/AML patients already

harbored mutations in the *CSF3R* (17/20=85%), suggesting an important (cooperative) role of these mutations in leukemic progression.[46] Where *CSF3R* mutations are all located in the C-terminal part of the gene, resulting in a truncated protein, mutations in *RUNX1* are found throughout the gene. However, the majority of the mutations were located in the runt homology domain (RHD) of the protein, important for DNA binding and interaction with the regulatory protein core-binding factor β (CBF-β).[45,46,49] *RUNX1* mutations were only observed shortly before leukemia became clinically overt, indicating that this is a late event during transformation.[45,46]

1.4.3 Mutations in epigenetic modifiers

Mutations in epigenetic modifiers, e.g., SUZ12/EZH2/ASXL1/EP300, are also observed, albeit less frequently than *CSF3R* and *RUNX1* mutations.[45,46] Epigenetics involves changes that affect gene expression, but do not involve alterations in the DNA sequence, and are therefore reversible. Simplified; gene expression is regulated by the packaging of DNA by histones, forming a DNA-protein complex called chromatin. Open chromatin allows for the transcription of genes in this region, while closed chromatin prevents this.[50] Epigenetic modifiers are important for this regulation and mutations in these genes could, for example, result in transcriptional silencing of tumor suppressor genes or activation of oncogenes without affecting the DNA sequence of these specific genes.[50] In addition to histone modification, also epigenetic changes on DNA level are important for cellular processes, e.g., DNA methylation. Various proteins involved in this process, TET2/IDH2/DNMT3A, are found frequently mutated in AML. In this thesis we describe a newly acquired driver mutation in *Cxxc4* found in a mouse model of leukemic progression of SCN **(Chapter 7)**. CXXC4 has been described to be able to bind TET2 and induce its protein degradation, thereby modulating TET2 protein abundance.[51]

1.4.4 Chromosomal aberrations

In addition to epigenetic deregulation, also chromosomal aberrations resulting in monosomy 7 or trisomy 21 are observed in SCN-MDS/AML patients.[45,46] These aberrations are only observed in leukemic samples and are therefore considered late alterations.[45,46] Why these 2 chromosomal aberrations are frequently observed and how they contribute to leukemic transformation is not yet known. However, several tumor suppressor genes, e.g., *EZH2*, are present on chromosome 7, while chromosome 21 contains various oncogenes, e.g., *RUNX1,* and one could imagine that loss or gain of these genes might affect the cells characteristics, especially when an additional mutation in one of these genes is acquired.

1.5. Overlap with chronic neutrophilic leukemia (CNL)

Alterations in *RUNX1, SUZ12, EZH2, ASXL1, EP300* and chromosomal aberrations can

also be present in other leukemias like *de novo* AML (AML without prior hematological disease) or MDS. However, *CSF3R* mutations are exclusively found in SCN-MDS/AML, chronic neutrophilic leukemia (CNL)[42,52], and rare cases of *de novo* AML with mutations in *CEBPA*.[53-55] The majority of CNL patients acquire a *CSF3R*-T618I mutation, but also truncating mutations are observed.[52] In addition, the *CSF3R*-T618I mutation can be detected in SCN-MDS/AML patients.[45] The *CSF3R*-T618I mutation provides autonomous signaling, supporting hyperproliferation of mature neutrophil progenitors.[52] The truncating and auto-activating mutation can be found in the same patient and even on the same allele in both SCN and CNL, indicating a strong selective pressure for acquisition of *CSF3R* mutations in both SCN and CNL.[45,52] These findings suggest that SCN and CNL might share a similar CSF3 hyporesponsive pre-leukemic state, from which cells can escape by acquiring *CSF3R*-mutations.

1.6. Outline and scope of this thesis

SCN is a complex disease caused by mutations in several different genes, associated with different cellular localization and function. How these genes cause a promyelocytic differentiation arrest is largely unknown, but it has been suggested that increased oxidative stress levels might play an important role. Additionally, why SCN patients have an increased risk of leukemic transformation remains an important point of study. The presence of multiple *CSF3R*-truncating mutations/clones suggests a strong selective pressure for acquisition of these mutations, possibly induced by the sustained life-long CSF3 treatment that the majority of patients with SCN receive. How truncated-CSF3Rs function in a SCN-mutant background is unknown, since mouse models do not mimic the neutropenic phenotype observed in patients with SCN. In addition, the observation that patients with SCN-MDS/AML often acquire *RUNX1* merits for interesting further studies, e.g., the effect of these mutations on hematopoietic cells, and why they frequently co-occur with *CSF3R*-mutations. Whether the combination of *CSF3R*- and *RUNX1*-mutations is sufficient for leukemic transformation, possibly in combination with CSF3-therapy, remains to be determined. The work presented in these thesis focuses on unraveling these questions, using *in vitro* SCN patient- and control-derived induced pluripotent stem cells (iPSCs), and *in vivo* mouse models to mimic several steps of leukemic transformation.

In **Chapter 2** we describe the pros and cons of different models to study SCN and its leukemic progression, mainly focusing on the newest disease model; induced pluripotent stem cells (iPSCs). iPSCs can be generated from SCN-patient material making it possible to study the effect of, e.g., *ELANE/HAX1*-mutations, as well as the acquisition of *CSF3R*-mutations, in a disease-relevant background.

In **Chapter 3** the generation of 3 SCN-patient-derived iPSCs are described, in addition to iPSCs derived from a healthy control. We employed these SCN- and control-derived iPSC to investigate if different SCN mutations show overlapping cellular responses, possibly explaining why mutations in different genes have the same disease phenotype. Albeit having different SCN-causing mutations, the HPCs generated from these iPSCs showed increased oxidative stress levels in all 3 SCN-patients compared to the healthy control. Additionally, the *ELANE*-mutant patient of which the mutation predicted NE protein misfolding showed increased numbers of PML-NBs, a marker of more excessive oxidative stress. We showed that PML not only played a role in lowering oxidative stress levels but is also involved in several biological processes important for SCN pathogenesis, like CSF3-therapy responsiveness.

In **Chapter 4** we mimic the first acquired step of leukemic progression of SCN in iPSC by introducing a patient-specific *CSF3R*-truncating mutation using CRISPR-Cas9-mediated genome editing. This data provides evidence for the involvement of the SCN mutation in disease progression by tipping the balance between proliferative signaling and inflammatory signaling towards the latter, making it possible for *CSF3R*-mutations to be present as minor clones for years while creating a mutation-prone environment ideal for the acquisition of mutations that are more resistant to inflammatory stimuli like *TET2* and *RUNX1*.

In **Chapter 5** a perspective (p)review discusses the role of *RUNX1* mutations in the leukemic progression of SCN.

In **Chapter 6** we addressed the question how truncated *CSF3R* and *RUNX1* mutations, in conjunction with CSF3 treatment, contribute to AML development. To study this, we used a combination of mouse- and iPSC-models and showed that the combination of mutant *Csf3r,* mutant *RUNX1* and CSF3 treatment resulted in a pre-leukemic state in mice. An additional acquired mutation in *Cxxc4* resulted in full-blown AML by inhibiting TET2 protein levels. Mutations in *CXXC4* can also be found in human AML and MDS patients, of whom the clinical, molecular, and cytogenetic characteristics are described in **Chapter 7**.

In **Chapter 8** we describe a patient with severe aplastic anemia (SAA) who progressed to CNL and AML with mutations that are frequently found in the leukemic progression of SCN. Non-leukemic HPCs from the SAA and SCN patient showed activation of interferon signaling pathways, indicating an important role for inflammation in leukemic progression from bone marrow failure syndromes.

Finally, in **Chapter 9** we summarize the findings described in this thesis and discuss how to further investigate the leukemic progression of SCN.

References

1. Scadden DT. The stem cell niche in health and leukemic disease. *Best Pract Res Clin Haematol*. 2007;20(1):19-27.
2. Mendez-Ferrer S, Michurina TV, Ferraro F, et al. Mesenchymal and haematopoietic stem cells form a unique bone marrow niche. *Nature*. 2010;466(7308):829-834.
3. Doulatov S, Notta F, Laurenti E, Dick JE. Hematopoiesis: a human perspective. *Cell Stem Cell*. 2012;10(2):120-136.
4. Zhang Y, Gao S, Xia J, Liu F. Hematopoietic Hierarchy - An Updated Roadmap. *Trends Cell Biol*. 2018;28(12):976-986.
5. Kaushansky K. Lineage-specific hematopoietic growth factors. *N Engl J Med*. 2006;354(19):2034-2045.
6. Kostmann R. Infantile genetic agranulocytosis; agranulocytosis infantilis hereditaria. *Acta Paediatr Suppl*. 1956;45(Suppl 105):1-78.
7. Welte K, Zeidler C, Dale DC. Severe congenital neutropenia. *Semin Hematol*. 2006;43(3):189-195.
8. Donadieu J, Beaupain B, Mahlaoui N, Bellanne-Chantelot C. Epidemiology of congenital neutropenia. *Hematol Oncol Clin North Am*. 2013;27(1):1-17, vii.
9. Souza LM, Boone TC, Gabrilove J, et al. Recombinant human granulocyte colony-stimulating factor: effects on normal and leukemic myeloid cells. *Science*. 1986;232(4746):61-65.
10. Skokowa J, Cario G, Uenalan M, et al. LEF-1 is crucial for neutrophil granulocytopoiesis and its expression is severely reduced in congenital neutropenia. *Nat Med*. 2006;12(10):1191-1197.
11. Dale DC, Bonilla MA, Davis MW, et al. A randomized controlled phase III trial of recombinant human granulocyte colony-stimulating factor (filgrastim) for treatment of severe chronic neutropenia. *Blood*. 1993;81(10):2496-2502.
12. Skokowa J, Dale DC, Touw IP, Zeidler C, Welte K. Severe congenital neutropenias. *Nat Rev Dis Primers*. 2017;3:17032.
13. Horwitz M, Benson KF, Person RE, Aprikyan AG, Dale DC. Mutations in ELA2, encoding neutrophil elastase, define a 21-day biological clock in cyclic haematopoiesis. *Nat Genet*. 1999;23(4):433-436.
14. Dale DC, Person RE, Bolyard AA, et al. Mutations in the gene encoding neutrophil elastase in congenital and cyclic neutropenia. *Blood*. 2000;96(7):2317-2322.
15. Grenda DS, Murakami M, Ghatak J, et al. Mutations of the ELA2 gene found in patients with severe congenital neutropenia induce the unfolded protein response and cellular apoptosis. *Blood*. 2007;110(13):4179-4187.

16. Horwitz MS, Duan Z, Korkmaz B, Lee HH, Mealiffe ME, Salipante SJ. Neutrophil elastase in cyclic and severe congenital neutropenia. *Blood*. 2007;109(5):1817-1824.
17. Klein C, Grudzien M, Appaswamy G, et al. HAX1 deficiency causes autosomal recessive severe congenital neutropenia (Kostmann disease). *Nat Genet*. 2007;39(1):86-92.
18. Devriendt K, Kim AS, Mathijs G, et al. Constitutively activating mutation in WASP causes X-linked severe congenital neutropenia. *Nat Genet*. 2001;27(3):313-317.
19. Boztug K, Appaswamy G, Ashikov A, et al. A syndrome with congenital neutropenia and mutations in G6PC3. *N Engl J Med*. 2009;360(1):32-43.
20. Vilboux T, Lev A, Malicdan MC, et al. A congenital neutrophil defect syndrome associated with mutations in VPS45. *N Engl J Med*. 2013;369(1):54-65.
21. Person RE, Li FQ, Duan Z, et al. Mutations in proto-oncogene GFI1 cause human neutropenia and target ELA2. *Nat Genet*. 2003;34(3):308-312.
22. Boztug K, Jarvinen PM, Salzer E, et al. JAGN1 deficiency causes aberrant myeloid cell homeostasis and congenital neutropenia. *Nat Genet*. 2014;46(9):1021-1027.
23. Triot A, Jarvinen PM, Arostegui JI, et al. Inherited biallelic CSF3R mutations in severe congenital neutropenia. *Blood*. 2014;123(24):3811-3817.
24. Sies H, Berndt C, Jones DP. Oxidative Stress. *Annu Rev Biochem*. 2017;86:715-748.
25. Rhee SG. Cell signaling. H2O2, a necessary evil for cell signaling. *Science*. 2006;312(5782):1882-1883.
26. Rhee SG, Bae YS, Lee SR, Kwon J. Hydrogen peroxide: a key messenger that modulates protein phosphorylation through cysteine oxidation. *Sci STKE*. 2000;2000(53):pe1.
27. Sundaresan M, Yu ZX, Ferrans VJ, Irani K, Finkel T. Requirement for generation of H2O2 for platelet-derived growth factor signal transduction. *Science*. 1995;270(5234):296-299.
28. Suzuki T, Yamamoto M. Molecular basis of the Keap1-Nrf2 system. *Free Radic Biol Med*. 2015;88(Pt B):93-100.
29. Sahin U, de The H, Lallemand-Breitenbach V. PML nuclear bodies: assembly and oxidative stress-sensitive sumoylation. *Nucleus*. 2014;5(6):499-507.
30. Tessier S, Martin-Martin N, de The H, Carracedo A, Lallemand-Breitenbach V. Promyelocytic Leukemia Protein, a Protein at the Crossroad of Oxidative Stress and Metabolism. *Antioxid Redox Signal*. 2017;26(9):432-444.
31. Guo L, Giasson BI, Glavis-Bloom A, et al. A cellular system that degrades misfolded proteins and protects against neurodegeneration. *Mol Cell*. 2014;55(1):15-30.
32. Dellaire G, Bazett-Jones DP. PML nuclear bodies: dynamic sensors of DNA damage and cellular stress. *Bioessays*. 2004;26(9):963-977.

33. Chang HR, Munkhjargal A, Kim MJ, et al. The functional roles of PML nuclear bodies in genome maintenance. *Mutat Res*. 2018;809:99-107.
34. Niwa-Kawakita M, Wu HC, The H, Lallemand-Breitenbach V. PML nuclear bodies, membrane-less domains acting as ROS sensors? *Semin Cell Dev Biol*. 2018;80:29-34.
35. Niwa-Kawakita M, Ferhi O, Soilihi H, Le Bras M, Lallemand-Breitenbach V, de The H. PML is a ROS sensor activating p53 upon oxidative stress. *J Exp Med*. 2017;214(11):3197-3206.
36. Rosenberg PS, Alter BP, Bolyard AA, et al. The incidence of leukemia and mortality from sepsis in patients with severe congenital neutropenia receiving long-term G-CSF therapy. *Blood*. 2006;107(12):4628-4635.
37. Dong F, Hoefsloot LH, Schelen AM, et al. Identification of a nonsense mutation in the granulocyte-colony-stimulating factor receptor in severe congenital neutropenia. *Proc Natl Acad Sci U S A*. 1994;91(10):4480-4484.
38. Dong F, Brynes RK, Tidow N, Welte K, Lowenberg B, Touw IP. Mutations in the gene for the granulocyte colony-stimulating-factor receptor in patients with acute myeloid leukemia preceded by severe congenital neutropenia. *N Engl J Med*. 1995;333(8):487-493.
39. Tidow N, Pilz C, Teichmann B, et al. Clinical relevance of point mutations in the cytoplasmic domain of the granulocyte colony-stimulating factor receptor gene in patients with severe congenital neutropenia. *Blood*. 1997;89(7):2369-2375.
40. Germeshausen M, Ballmaier M, Welte K. Incidence of CSF3R mutations in severe congenital neutropenia and relevance for leukemogenesis: Results of a long-term survey. *Blood*. 2007;109(1):93-99.
41. Palande K, Meenhuis A, Jevdjovic T, Touw IP. Scratching the surface: signaling and routing dynamics of the CSF3 receptor. *Front Biosci (Landmark Ed)*. 2013;18:91-105.
42. Touw IP. Game of clones: the genomic evolution of severe congenital neutropenia. *Hematology Am Soc Hematol Educ Program*. 2015;2015:1-7.
43. Liu F, Kunter G, Krem MM, et al. Csf3r mutations in mice confer a strong clonal HSC advantage via activation of Stat5. *J Clin Invest*. 2008;118(3):946-955.
44. Zhu QS, Xia L, Mills GB, Lowell CA, Touw IP, Corey SJ. G-CSF induced reactive oxygen species involves Lyn-PI3-kinase-Akt and contributes to myeloid cell growth. *Blood*. 2006;107(5):1847-1856.
45. Beekman R, Valkhof MG, Sanders MA, et al. Sequential gain of mutations in severe congenital neutropenia progressing to acute myeloid leukemia. *Blood*. 2012;119(22):5071-5077.

46. Skokowa J, Steinemann D, Katsman-Kuipers JE, et al. Cooperativity of RUNX1 and CSF3R mutations in severe congenital neutropenia: a unique pathway in myeloid leukemogenesis. *Blood*. 2014;123(14):2229-2237.
47. Sroczynska P, Lancrin C, Kouskoff V, Lacaud G. The differential activities of Runx1 promoters define milestones during embryonic hematopoiesis. *Blood*. 2009;114(26):5279-5289.
48. Bee T, Liddiard K, Swiers G, et al. Alternative Runx1 promoter usage in mouse developmental hematopoiesis. *Blood Cells Mol Dis*. 2009;43(1):35-42.
49. Miyoshi H, Ohira M, Shimizu K, et al. Alternative splicing and genomic structure of the AML1 gene involved in acute myeloid leukemia. *Nucleic Acids Res*. 1995;23(14):2762-2769.
50. Zentner GE, Henikoff S. Regulation of nucleosome dynamics by histone modifications. *Nat Struct Mol Biol*. 2013;20(3):259-266.
51. Ko M, An J, Bandukwala HS, et al. Modulation of TET2 expression and 5-methylcytosine oxidation by the CXXC domain protein IDAX. *Nature*. 2013;497(7447):122-126.
52. Maxson JE, Gotlib J, Pollyea DA, et al. Oncogenic CSF3R mutations in chronic neutrophilic leukemia and atypical CML. *N Engl J Med*. 2013;368(19):1781-1790.
53. Maxson JE, Ries RE, Wang YC, et al. CSF3R mutations have a high degree of overlap with CEBPA mutations in pediatric AML. *Blood*. 2016;127(24):3094-3098.
54. Lavallee VP, Krosl J, Lemieux S, et al. Chemo-genomic interrogation of CEBPA mutated AML reveals recurrent CSF3R mutations and subgroup sensitivity to JAK inhibitors. *Blood*. 2016;127(24):3054-3061.
55. Zhang Y, Wang F, Chen X, et al. CSF3R Mutations are frequently associated with abnormalities of RUNX1, CBFB, CEBPA, and NPM1 genes in acute myeloid leukemia. *Cancer*. 2018;124(16):3329-3338.

Chapter 2

Modeling severe congenital neutropenia in induced pluripotent stem cells

Patricia A. Olofsen[1] and Ivo P. Touw[1]

[1] Department of Hematology, Erasmus University Medical Center, 3015 CN,Rotterdam, The Netherlands

Birbrair A, ed. Recent Advances in iPSC Disease Modeling, Volume 1: Academic Press; 2020:85-101

Abstract

Patients with severe congenital neutropenia (SCN) suffer from a severe shortage of neutrophilic granulocytes, leading to life-threatening bacterial infections. The severe neutropenia and infectious episodes can be alleviated by life-long treatment with granulocyte colony-stimulating factor (G-CSF or CSF3). G-CSF therapy has unveiled an increased risk of developing myelodysplastic syndromes or acute myeloid leukemia, which is often preceded by the expansion of myeloid cell clones with somatic mutations in the CSF3 receptor gene (*CSF3R*). Genetically, SCN is a heterogeneous condition, with over 15 genes identified as causative to the disease. Most commonly, mutations are found in *ELANE*, the gene encoding neutrophil elastase, leading to autosomal dominant or sporadic forms of SCN. SCN caused by mutations in *HAX1* is best known, as this represents the recessive condition originally described as Kostmann disease. Despite our knowledge of the genetic causes of SCN, it remains ill-understood how the mutations cause neutropenia and why they predispose to myeloid malignancies. In this chapter, we will discuss the clinical characteristics of SCN and summarize the properties and limitations of the current *in vitro* and *in vivo* models used to study the pathobiology of the disease. Subsequently, we will review the current status of induced pluripotent stem cell models of SCN and discuss their potential and current limitations for elucidating disease mechanisms of neutropenia and leukemic progression, as well as for developing curative therapies.

Severe congenital neutropenia

Severe congenital neutropenia (SCN) is a bone marrow failure syndrome characterized by low absolute neutrophil counts (<0.5x10^9/L) caused by a granulocytic differentiation block at the promyelocyte stage, resulting in increased bacterial infections in patients (Figure 1). SCN is a rare condition with a prevalence estimated between 3-8.5 cases per million individuals [1].

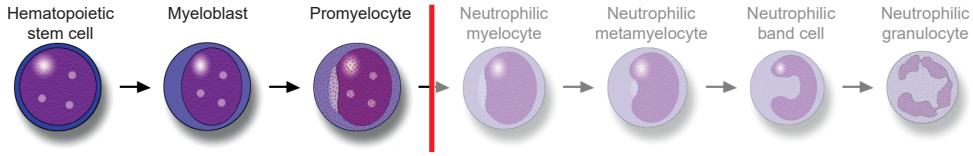

Figure 1: Sequential steps in normal neutrophil differentiation; the maturation arrest in SCN patients is marked by the red bar

Congenital forms of neutropenia were first reported by Rolf Kostmann in 1956, who described a family with inherited severe neutropenia, which he termed infantile genetic agranulocytosis[2]. More than 50 years later, mutations in the gene encoding HCLS1-associated protein X-1 (*HAX1*) were found to be the cause of this autosomal recessive form of SCN[3]. *HAX1*-mutant SCN is confined to consanguineous populations covering less than 5% of patients worldwide. Mutations in *HAX1* introduce a premature stop codon resulting in nonsense-mediated messenger RNA decay leading to the loss of HAX1 protein. Although multiple functions have been assigned to HAX1, its loss resulting in destabilization of the mitochondrial membrane potential and mitochondrial leakage are currently thought to explain the SCN phenotype[3].

Mutations in *ELANE*, encoding the primary granule protein neutrophil elastase (NE), are the most frequent cause of SCN, responsible for approximately 30%-40% of cases[4,5]. *ELANE* mutations result in an autosomal dominant form of SCN and, in contrast to HAX1 mutations, the mutational spectrum observed in patients encompasses the entire *ELANE* gene[6]. How mutations in *ELANE* cause neutropenia is still unclear. Mislocalization of the mutant NE protein[7], altered enzymatic activity[8] and protein misfolding resulting in activation of the unfolded protein response (UPR)[7,9] have all been suggested as potential initiators causing neutropenia, through the activation of cell death mechanisms at the promyelocyte stage. However, definitive proof for the involvement of these mechanisms is still lacking.

In addition to mutations in *ELANE* and *HAX1*, mutations in, e.g., *GFI1*[10], *WAS*[11] *JAGN1*[12] and *G6PC3*[13] have been shown to cause SCN. A recent review provides a comprehensive overview of the genetic causes of SCN, their hereditary patterns, proposed mechanisms of action, and clinical features[14].

A unique aspect of SCN is that the majority of patients are treated with the hematopoietic growth factor granulocyte colony-stimulating factor (G-CSF), now renamed colony-stimulating factor 3 (CSF3), to alleviate the life-threatening neutropenia[15]. As will

be discussed later in this chapter, patients with SCN may develop myeloid malignancies, preceded by a preleukemic phase characterized by hematopoietic clones with somatic mutations in the CSF3 receptor (CSF3R)[16].

Severe congenital neutropenia mouse models

Mouse models with representative SCN-derived *HAX1* and *ELANE* mutations have been generated to gain insight into how these mutations cause neutropenia[17]. Quite surprisingly, neither HAX1-deficient mice nor mice with human-equivalent *Elane* mutations (V72M, G193X) showed signs of neutropenia or a granulocytic differentiation block, neither under basal conditions nor after induction of emergency granulopoiesis[18-20]. Theoretically, this could be due to differences between mice and humans in the NE and HAX1 protein composition, because only 72% and 80%, respectively, of the amino acids are identical (Figures 2 and 3). However, over-expression of human NE mutants in murine HoxB8-driven cell lines derived from $NE^{-/-}$ mice also did not result in a granulocytic differentiation defect, neither *in vitro* nor *in vivo*[21], indicating that there are more differences between mice and human granulopoiesis besides the structure of NE and possibly HAX1.

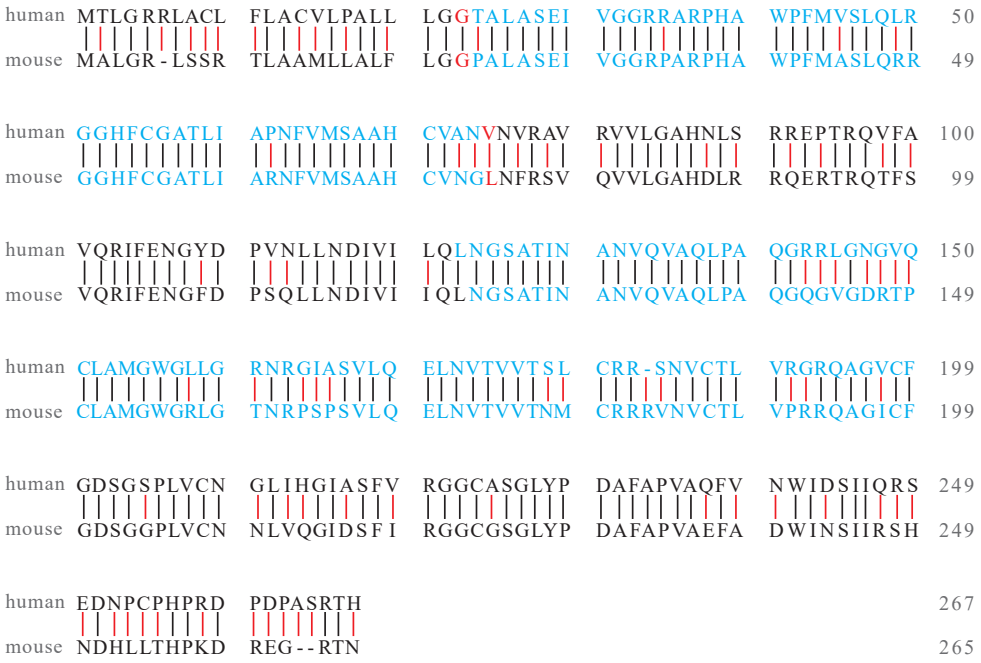

Figure 2: Human and mouse NE protein sequences show 72% overlapping amino acids (191/267)
Black bars indicate overlapping amino acids, where red bars show mismatched amino acids. Exons are shown alternating in black and blue, indicating the 5 different coding exons of the ELANE gene. The red characters indicate amino acids generated through splicing.

Figure 3: Human and mouse HAX1 protein sequences show 80% overlapping amino acids (224/280)
Black bars indicate overlapping amino acids, where red bars show mismatched amino acids. Exons are shown alternating in black and blue, indicating the 7 different coding exons of the HAX1 gene. The red characters indicate amino acids generated through splicing.

Human cell line models

Before the introduction of induced pluripotent stem cell (iPSC) technology, attempts to model SCN in human cells have been mainly restricted to retroviral introduction of *ELANE* mutations in the promyelocytic leukemia cell line HL-60. Although HL-60 cells have retained some ability to differentiate to neutrophils when stimulated with all-trans retinoic acid (ATRA), an obvious caveat of this model is its leukemic nature. Furthermore, retroviral introduction of *ELANE* mutants has the drawback that it will cause expression at nonphysiological levels and can create potential off-target effects due to the site of integration. The outcome of these experiments was mixed. In one study, overexpression of the *ELANE*-V174_C181del mutant under the control of the tet-regulated promoter resulted in less mature neutrophils induced by ATRA relative to controls[22], whereas in a comparable study, introduction of *ELANE*-G185R failed to show reduced neutrophil differentiation[23]. Taken together, the myeloid leukemia cell line-based models of SCN are now generally considered as less suitable for studying the biology of SCN.

Induced pluripotent stem cell models for severe congenital neutropenia

SCN-iPSCs have been generated using different protocols for reprogramming. The first published studies made use of retroviral vectors to reprogram skin or bone marrow fibroblast derived from patients with *ELANE*-C194X or *HAX1*-R86X mutations[24,25]. Later, lentiviral vectors or integration-free episomal vectors were used to avoid off-target effects of integration[26]. A now-well-recognized problem is that iPSC lines may display a significant level of variation, owing to phenotypic changes caused by the reprogramming process[27]. To avoid misinterpretations based on such non-disease-relevant shifts in phenotypes, it is important to generate multiple clones derived from the same starting material. Also, the introduction of CRISPR-Cas9 mediated genome editing made it feasible to precisely target modifications in iPSCs, e.g., to repair the disease-causing gene defects in patient-derived lines or to introduce patient-derived mutations in normal controls[28]. In this way the phenotypic consequences of mutations can be definitively assessed. Because the majority of studies on SCN-iPSCs published to date did not yet make use of multiple clones or isogenic lines, the results discussed in the following sections should be interpreted with some caution.

Hematopoietic induction of induced pluripotent stem cells

To study how the underlying genetic defects affect neutrophil development, hematopoietic progenitor cells (HPCs) first need to be generated from SCN-iPSCs. Different methods have been developed to generate HPCs and their more mature myeloid progeny from iPSCs. These protocols are somewhat variable but have in common that in the first 3-4 days mesodermal differentiation is induced by the addition of BMP4, after which hematopoietic cytokines (e.g., vascular endothelial growth factor (VEGF), interleukin 3 (IL-3), stem cell factor (SCF), and CSF3) are added to the cultures to generate the HPCs, as visualized in Figure 4 [22,24,25,29-32]. Nowadays, complete hematopoietic induction kits, e.g., STEMdiff Hematopoietic Kit (STEMCELL Technologies) can be purchased, minimizing batch effects due to extensive testing.

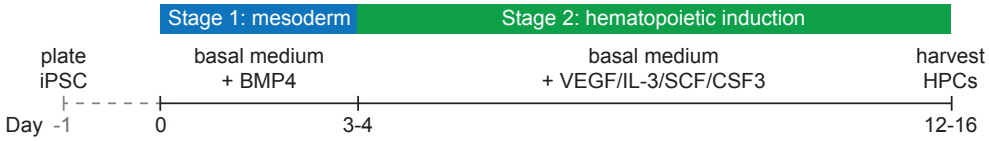

Figure 4: Standard protocol for the induction of HPCs

Mesoderm differentiation is induced by addition of BMP4, after which the medium is replaced with hematopoietic cytokines e.g. VEGF/IL-3/SCF/CSF3 to induce hematopoietic differentiation. Cells are generally harvested between days 12 and 16 to yield the highest number of HPCs.

The potential of HPCs to produce differentiated progeny can be further tested in colony-forming unit (CFU) assays, in which cells are plated into semisolid medium with the addition of lineage-specific cytokines. Typically, a CFU-G assay can be done to test SCN-iPSC-derived HPCs for their ability to respond to G-CSF/CSF3. In addition to the generation of HPCs, cells need to be differentiated further into the granulocytic lineage if one wishes to study the mechanisms underlying the differentiation block observed in patients with SCN. CSF3 is a key hematopoietic cytokine driving the maturation of granulocytes in culture. Importantly, it must be kept in mind that CSF3 dosage has a major impact on the outcome of such experiments, as the differentiation block can be alleviated in the majority of patients with SCN by pharmacological dosages of this cytokine (discussed later in more detail). Different stages of neutrophil development based on surface antigen expression can be conveniently assayed by flow cytometry[33]. The EuroFlow consortium defined the combination of antibodies to discriminate the different stages of human neutrophil differentiation based on expression of HLA-DR, CD45, CD16, CD13, CD34, CD117, and CD11b, as shown in Figure 5, which can also be applied in SCN-iPSC models[34].

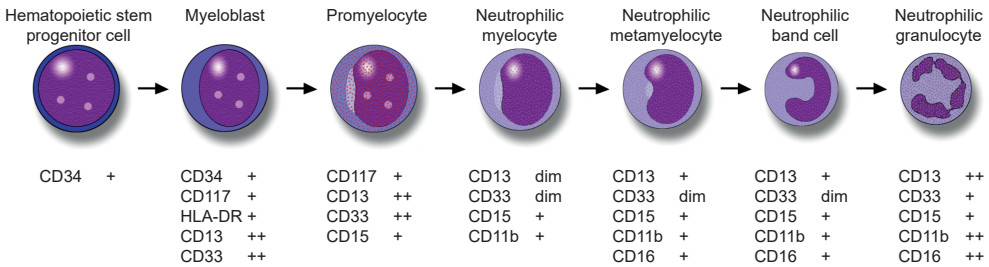

Figure 5: EuroFlow defined flow cytometry markers to differentiate the various neutrophil differentiation stages

HAX1-mutant induced pluripotent stem cells

To date, two studies on *HAX1*-mutant iPSC derived from patients with SCN have been published. Morishima et al. focused on trying to correct the *HAX1* mutation by lentiviral overexpression of wild-type HAX1[25]. They showed that the *HAX1*-R86X mutant cells generate a smaller proportion of mature neutrophils upon differentiation and produce less myeloid colonies in semisolid medium compared with normal controls. Introduction of HAX1 restored the production of mature neutrophils and myeloid colony-forming cells (CFU-G) [25]. Similarly, CRISPR-Cas9-mediated correction of an *HAX1*-W44X mutation in iPSCs resulted in an increased proportion of mature neutrophils[31]. Both studies confirmed that mutations in *HAX1* resulted in disruption of the mitochondrial membrane potential, as shown before in primary bone marrow cells from patients with *HAX1*-SCN[3]. These findings validate the use of patient-derived iPSC for studying the cellular consequences of *HAX1* mutations for

neutrophil development, but at this point, they provide only limited additional mechanistic insights.

ELANE-mutant induced pluripotent stem cells

Because mutations in *ELANE* occur throughout the gene, it is likely that different mutations may affect the NE protein differently, which might explain observed variations in clinical symptoms of SCN. To date, 11 distinct *ELANE*-mutant iPSC lines have been published (Figure 6)[22,24,29,30,32,35,36]. The majority of these studies showed reduced neutrophilic differentiation potential of *ELANE*-mutant lines, but discrepancies between distinct mutants have also been observed. While possibly relevant to the type of mutation, it cannot be excluded that differences in culture conditions, especially concentrations of G-CSF/CSF3 used in myeloid differentiation cultures, contributed to these variations. This asks for some caution in the interpretation of these findings, also because most of these studies did not include validations in multiple independent clones and/or use of gene-corrected isogenic lines to confirm phenotypic reversion.

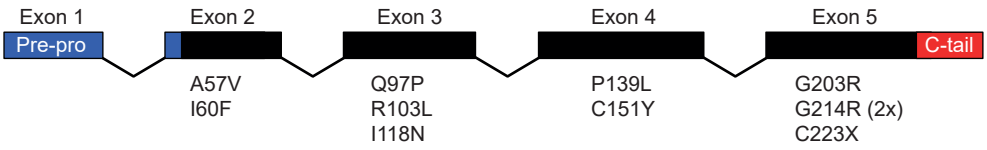

Figure 6: Overview of the ELANE gene indicating the different positions of the iPSC generated from ELANE-mutant patients

Unfolded protein response activation in _ELANE_-mutant cells

Studies published thus far mainly aimed at activation of the UPR and increased apoptosis in *ELANE*-mutant myeloid progenitor cells as the cause of neutropenia in SCN. However, as explained earlier, not all *ELANE* mutations predictably result in protein misfolding, leaving room for alternative explanations as to how *ELANE* mutations affect neutrophil development. Most *ELANE* mutations in currently published SCN-iPSCs are predicted to result in protein misfolding (Figure 7, C223X cannot be assessed because of the premature stop codon)[37]. However, these lines did not uniformly show induction of the classical UPR because often only a few UPR-related transcripts were found to be upregulated, whereas others were unchanged or even downregulated[24,29,35]. Besides the classical UPR pathway, the promyelocytic leukemia protein has been reported to recognize and degrade misfolded proteins[38]. We have shown that this alternative “noncanonical” UPR pathway is activated in some *ELANE*-mutant patients associated with NE protein misfolding[36] (and Olofsen PA et al., manuscript submitted).

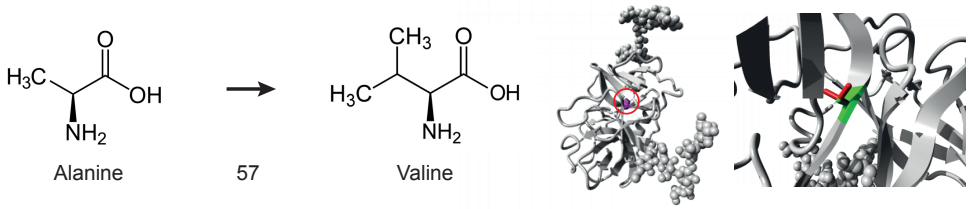

The residue is buried in the core of the protein. The mutant residue is bigger and probably will not fit.

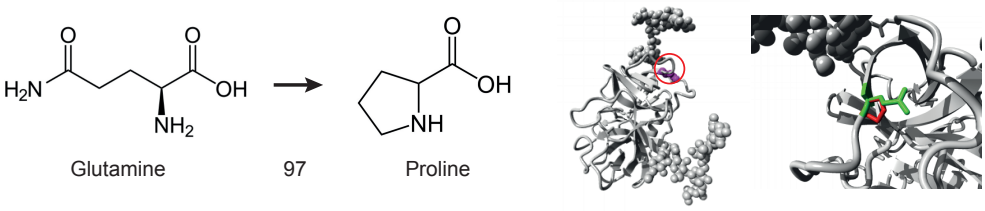

The mutation will cause loss of hydrogen bonds in the core of the protein and disturb correct folding.

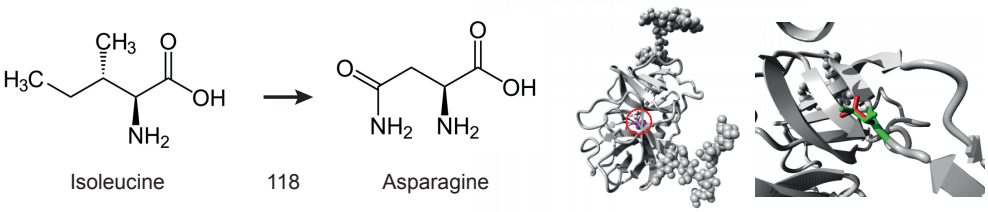

The residue is buried in the core of the protein. The mutant residue is bigger and probably will not fit.
The mutation will cause loss of hydrophobic interactions in the core of the protein.

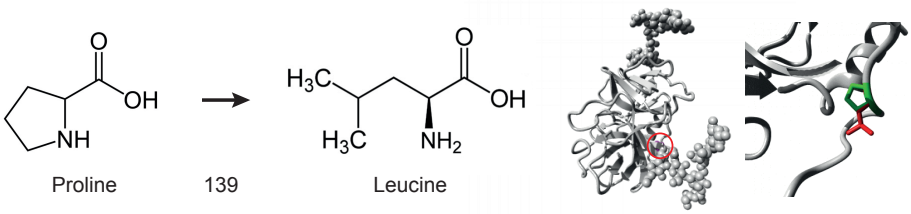

The residue is buried in the core of the protein. The mutant residue is bigger and probably will not fit.

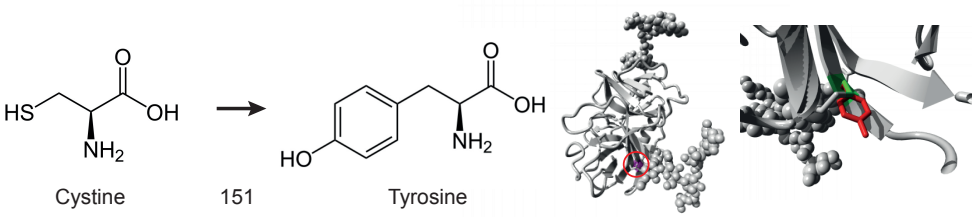

The residue is buried in the core of the protein. The mutant residue is bigger and probably will not fit.
The mutation will cause loss of hydrophobic interactions in the core of the protein.

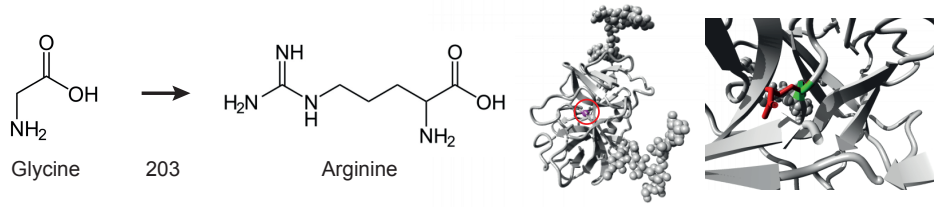

Figure 7: Predicted effect of the amino acid alterations induced by mutations in ELANE
The location of the altered amino acid is shown in purple. The wild type residue is shown in green, whereas the mutant residue is shown in red [37].

Use of SCN-iPSCs to develop new therapeutic strategies

Although patients with SCN are effectively treated by administration of recombinant CSF3, better known as G-CSF, neupogen or filgrastim[39], they face an increased risk of progression toward myelodysplastic syndromes (MDS) or acute myeloid leukemia (AML) while on this treatment[40,41]. There are concerns that CSF3 therapy might contribute to the leukemic progression, especially because the majority of patients with SCN acquire truncating mutations in the G-CSF receptor *(CSF3R)* early during disease progression[16,42].

SCN-iPSC models have been used to find new treatment strategies as alternatives for CSF3 therapy, as options for patients who fail to respond to CSF3 or to avoid development of malignancies in patients who need excessive CSF3 dosages to alleviate neutropenia [40,41]. For example, Hiramoto et al. showed that Wnt3a combined with CSF3, but not alone, stimulated the maturation of neutrophils in *ELANE*-C223X iPSC-derived hematopoietic cells. They propose that, by using the combination therapy including compounds activating the Wnt3a/β-catenin axis, CSF3 doses can be lowered in patients, potentially reducing the risk of leukemic transformation[24].

Another new treatment option that has been proposed is the use of the NE-specific cell-permeant serine protease inhibitor sivelestat. Sivelestat, in combination with 50 ng/

ml CSF3, mimicked high dose CSF3 treatment and ameliorated endoplasmic reticulum (ER) stress and enhanced cellular survival in *ELANE*-Q97P and *ELANE*-I118N mutant cells[35]. These data differ from those reported by Makaryan et al. who showed that the β-lactam-based inhibitor MK0339, but not sivelestat, significantly increased the proportion of mature neutrophils ($CD11b^+$ cells) in both *ELANE*-P139L, *ELANE*-G214R and control iPSCs[22].

Finally, genetic therapeutic options that are currently being explored involve the deletion of *ELANE* by CRISPR-Cas9-mediated genome editing, disrupting both the mutant and wild-type alleles[30,43]. The underlying rationale for this strategy is that the lack of NE may not have a major impact on neutrophil function, based on studies in mice and on the premise that individuals suffering from Papillon-Lefèvre syndrome, a condition characterized by a combined serine protease deficiency, show relatively mild symptoms[43,44]. Introducing indels at exon 2 of *ELANE* efficiently triggered nonsense-mediated decay and loss of NE in hematopoietic stem and progenitor cells (HSPCs) derived from healthy controls or *ELANE*-mutant patients with SCN[43]. The same strategy was explored by Nasri et al., who introduced indels in exon 2 of *ELANE*-mutant iPSCs (A57V and C151Y)[30]. Both studies show that loss of NE resulted in alleviation of the differentiation block, both in HSPCs and iPSC-derived cells. Although the first results look promising, the long-term clinical impact of NE loss remains uncertain. Therefore efforts to correct rather than delete mutant (and wild type) *ELANE* should continue, even though the repair protocols are currently far from fit to successfully implement this clinically. Given the large diversity of *ELANE* mutations found in patients with SCN, a major hurdle to be taken will be to avoid off-target effects of the individual gene correction strategies, an essential step before they can be advanced towards clinical grade. Clearly, the iPSC lines from patients harboring different *ELANE* mutations serve as valuable tools for fine-tuning these approaches.

Induced pluripotent stem cells to study leukemic progression

Hematopoietic cell clones with somatic mutations in *CSF3R* truncating the membrane-distal cytoplasmic region of CSF3R are frequently observed in patients who progress to MDS or AML. These *CSF3R*-mutant cells can be present as minor clones years before the leukemia becomes clinically overt[16]. At the final stage of transformation, a majority of patients with SCN-MDS/AML acquire mutations in the myeloid transcription factor *RUNX1* (64.5%), of which the majority were found in clones already harboring *CSF3R* mutations (85%)[45]. Mouse models have been used to study the combination of *CSF3R* and *RUNX1* mutations, in conjunction with CSF3 treatment, in the leukemic progression of SCN[46,47]. Although these mice lack a SCN disease-causing mutation, these studies do give insights in the mechanisms of leukemic transformation. We showed that the combination of *CSF3R* and *RUNX1* mutations, in conjunction with CSF3 treatment, resulted in a preleukemic stage indicated by increased blasts in the peripheral blood but not over AML. An additional novel mutation

in a gene affecting TET2 levels was acquired, resulting in the possibility to perform serial transplantation while mice developed full-blown AML[47].

To study the combinatorial effects of *CSF3R, RUNX1* in an SCN background, the *ELANE/HAX1*-mutant iPSCs serve as valuable models. We used CRISPR-Cas9-mediated genome editing and lentiviral transduction to introduce *CSF3R* and *RUNX1* mutations, respectively. iPSCs derived from healthy donors with *CSF3R* and *RUNX1* mutations mimicked the findings in the mouse model, where an increase in immature myeloid progenitors was observed due to increased proliferative signaling in response to CSF3[48]. Importantly, similar studies in ELANE-iPSC-derived myeloid progenitors showed that this proliferative signature was absent. Instead, transcriptome analysis revealed that *CSF3R* and *RUNX1* mutant HPCs showed induced expression of inflammatory-related signatures (Olofsen PA et al., manuscript submitted).

Outlook

iPSCs have qualified as potentially useful models for studying the underlying biology of SCN and its leukemic progression, but major challenges remain. First of all, it is still uncertain to what extent the promyelocyte maturation arrest seen in patients with SCN can be faithfully reproduced in iPSC models. Thus far, the reported results are mixed and one may even wonder whether this endpoint has a major significance for understanding disease mechanisms, given that most patients with SCN can produce mature neutrophils if CSF3 is administered. Because little is known about how dosages applied *in vivo* translate to the *in vitro* context of iPSC cultures, the observed differences in the ability to produce neutrophils may depend at least partly on variations in culture conditions, rather than cell-intrinsic defects of the myeloid progenitors produced by SCN-iPSCs. Hence, it remains largely unexplained how the variety of mutations found to cause SCN, affecting such functionally distinct proteins, all lead to a severe shortage of neutrophils. Similarly, it remains unclear why neutropenia can be alleviated by CSF3 treatment in the majority of patients with SCN, despite their underlying genetic heterogeneity. Although still only limited in number, studies from several laboratories including ours begin to reveal that elevated oxidative stress caused by, e.g., mitochondrial damage (*HAX1* mutations) or increased ER stress (*ELANE* mutations), rewiring of cytokine signal transduction and transcriptional programs in myeloid progenitors are common denominators in different genetic SCN subtypes, features that can faithfully be reproduced in iPSC models [29,31,35,36]. Future studies should focus on how these alterations affect myeloid progenitors and prevent them from producing adequate numbers of neutrophils under both homeostatic and infectious conditions, keeping in mind that these defects are reversible by CSF3 treatment, hence subtle rather than absolute.

Also, one needs to take into consideration that factors that may aggravate neutropenia in patients, such as febrile and infectious episodes, are not easily captured *in vitro* and this limitation obviously also applies to the iPSC-SCN models. To cope with this, it will remain essential to cross-validate observations in the iPSC models with primary patient samples, which has become feasible now that epigenetic/transcriptome profiling by next-generation sequencing can be performed on small cell numbers. If these criteria are met, valid endpoints for, e.g., compound testing and functional CRISPR-based screens can be defined. A comparable approach can be followed to unravel the functional consequences of *ELANE/HAX1* mutations, in combination with *CSF3R* and *RUNX1* mutations and the role of CSF3 treatment herein, for leukemic progression [36] (Olofsen PA et al., manuscript submitted).

Acknowledgements

This work was supported by grants from KWF Kankerbestrijding (EMCR 2013-5755 and EMCR 2014-6780) and the KiKa foundation (project 152).

References

1. Donadieu J, Beaupain B, Mahlaoui N, Bellanne-Chantelot C. Epidemiology of congenital neutropenia. *Hematol Oncol Clin North Am.* 2013;27(1):1-17, vii.
2. Kostmann R. Infantile genetic agranulocytosis; agranulocytosis infantilis hereditaria. *Acta Paediatr Suppl.* 1956;45(Suppl 105):1-78.
3. Klein C, Grudzien M, Appaswamy G, et al. HAX1 deficiency causes autosomal recessive severe congenital neutropenia (Kostmann disease). *Nat Genet.* 2007;39(1):86-92.
4. Horwitz M, Benson KF, Person RE, Aprikyan AG, Dale DC. Mutations in ELA2, encoding neutrophil elastase, define a 21-day biological clock in cyclic haematopoiesis. *Nat Genet.* 1999;23(4):433-436.
5. Dale DC, Person RE, Bolyard AA, et al. Mutations in the gene encoding neutrophil elastase in congenital and cyclic neutropenia. *Blood.* 2000;96(7):2317-2322.
6. Horwitz MS, Corey SJ, Grimes HL, Tidwell T. ELANE mutations in cyclic and severe congenital neutropenia: genetics and pathophysiology. *Hematol Oncol Clin North Am.* 2013;27(1):19-41, vii.
7. Kollner I, Sodeik B, Schreek S, et al. Mutations in neutrophil elastase causing congenital neutropenia lead to cytoplasmic protein accumulation and induction of the unfolded protein response. *Blood.* 2006;108(2):493-500.
8. Germeshausen M, Deerberg S, Peter Y, Reimer C, Kratz CP, Ballmaier M. The spectrum of ELANE mutations and their implications in severe congenital and cyclic neutropenia. *Hum Mutat.* 2013;34(6):905-914.
9. Grenda DS, Murakami M, Ghatak J, et al. Mutations of the ELA2 gene found in patients with severe congenital neutropenia induce the unfolded protein response and cellular apoptosis. *Blood.* 2007;110(13):4179-4187.
10. Person RE, Li FQ, Duan Z, et al. Mutations in proto-oncogene GFI1 cause human neutropenia and target ELA2. *Nat Genet.* 2003;34(3):308-312.
11. Devriendt K, Kim AS, Mathijs G, et al. Constitutively activating mutation in WASP causes X-linked severe congenital neutropenia. *Nat Genet.* 2001;27(3):313-317.
12. Boztug K, Jarvinen PM, Salzer E, et al. JAGN1 deficiency causes aberrant myeloid cell homeostasis and congenital neutropenia. *Nat Genet.* 2014;46(9):1021-1027.
13. Boztug K, Appaswamy G, Ashikov A, et al. A syndrome with congenital neutropenia and mutations in G6PC3. *N Engl J Med.* 2009;360(1):32-43.
14. Skokowa J, Dale DC, Touw IP, Zeidler C, Welte K. Severe congenital neutropenias. *Nat Rev Dis Primers.* 2017;3:17032.
15. Dale DC, Bonilla MA, Davis MW, et al. A randomized controlled phase III trial of recombinant human granulocyte colony-stimulating factor (filgrastim) for treatment of severe chronic neutropenia. *Blood.* 1993;81(10):2496-2502.

16. Touw IP. Game of clones: the genomic evolution of severe congenital neutropenia. *Hematology Am Soc Hematol Educ Program.* 2015;2015:1-7.
17. Schaffer AA, Klein C. Animal models of human granulocyte diseases. *Hematol Oncol Clin North Am.* 2013;27(1):129-148, ix.
18. Chao JR, Parganas E, Boyd K, Hong CY, Opferman JT, Ihle JN. Hax1-mediated processing of HtrA2 by Parl allows survival of lymphocytes and neurons. *Nature.* 2008;452(7183):98-102.
19. Grenda DS, Johnson SE, Mayer JR, et al. Mice expressing a neutrophil elastase mutation derived from patients with severe congenital neutropenia have normal granulopoiesis. *Blood.* 2002;100(9):3221-3228.
20. Nanua S, Murakami M, Xia J, et al. Activation of the unfolded protein response is associated with impaired granulopoiesis in transgenic mice expressing mutant Elane. *Blood.* 2011;117(13):3539-3547.
21. Wiesmeier M, Gautam S, Kirschnek S, Hacker G. Characterisation of Neutropenia-Associated Neutrophil Elastase Mutations in a Murine Differentiation Model In Vitro and In Vivo. *PLoS One.* 2016;11(12):e0168055.
22. Makaryan V, Kelley ML, Fletcher B, Bolyard AA, Aprikyan AA, Dale DC. Elastase inhibitors as potential therapies for ELANE-associated neutropenia. *J Leukoc Biol.* 2017;102(4):1143-1151.
23. Massullo P, Druhan LJ, Bunnell BA, et al. Aberrant subcellular targeting of the G185R neutrophil elastase mutant associated with severe congenital neutropenia induces premature apoptosis of differentiating promyelocytes. *Blood.* 2005;105(9):3397-3404.
24. Hiramoto T, Ebihara Y, Mizoguchi Y, et al. Wnt3a stimulates maturation of impaired neutrophils developed from severe congenital neutropenia patient-derived pluripotent stem cells. *Proc Natl Acad Sci U S A.* 2013;110(8):3023-3028.
25. Morishima T, Watanabe K, Niwa A, et al. Genetic correction of HAX1 in induced pluripotent stem cells from a patient with severe congenital neutropenia improves defective granulopoiesis. *Haematologica.* 2014;99(1):19-27.
26. Yu J, Hu K, Smuga-Otto K, et al. Human induced pluripotent stem cells free of vector and transgene sequences. *Science.* 2009;324(5928):797-801.
27. Soldner F, Jaenisch R. Medicine. iPSC disease modeling. *Science.* 2012;338(6111):1155-1156.
28. Cong L, Ran FA, Cox D, et al. Multiplex genome engineering using CRISPR/Cas systems. *Science.* 2013;339(6121):819-823.
29. Dannenmann B, Zahabi A, Mir P, et al. Human iPSC-based model of severe congenital neutropenia reveals elevated UPR and DNA damage in CD34(+) cells preceding leukemic transformation. *Exp Hematol.* 2019;71:51-60.

30. Nasri M, Ritter M, Mir P, et al. CRISPR/Cas9 mediated ELANE knockout enables neutrophilic maturation of primary hematopoietic stem and progenitor cells and induced pluripotent stem cells of severe congenital neutropenia patients. *Haematologica.* 2019.
31. Pittermann E, Lachmann N, MacLean G, et al. Gene correction of HAX1 reversed Kostmann disease phenotype in patient-specific induced pluripotent stem cells. *Blood Adv.* 2017;1(14):903-914.
32. Shigemura T, Kobayashi N, Agematsu K, Ohara O, Nakazawa Y. Mosaicism of an ELANE Mutation in an Asymptomatic Mother. *J Clin Immunol.* 2019;39(1):106-111.
33. van Lochem EG, van der Velden VH, Wind HK, te Marvelde JG, Westerdaal NA, van Dongen JJ. Immunophenotypic differentiation patterns of normal hematopoiesis in human bone marrow: reference patterns for age-related changes and disease-induced shifts. *Cytometry B Clin Cytom.* 2004;60(1):1-13.
34. van Dongen JJ, Lhermitte L, Bottcher S, et al. EuroFlow antibody panels for standardized n-dimensional flow cytometric immunophenotyping of normal, reactive and malignant leukocytes. *Leukemia.* 2012;26(9):1908-1975.
35. Nayak RC, Trump LR, Aronow BJ, et al. Pathogenesis of ELANE-mutant severe neutropenia revealed by induced pluripotent stem cells. *J Clin Invest.* 2015;125(8):3103-3116.
36. Olofsen PA, van Strien PMH, Roovers O, et al. PML Plays a Key Role in Severe Congenital Neutropenia with Mutant ELANE Causing Neutrophil Elastase Protein Misfolding. *Blood.* 2019;134:213.
37. Venselaar H, Te Beek TA, Kuipers RK, Hekkelman ML, Vriend G. Protein structure analysis of mutations causing inheritable diseases. An e-Science approach with life scientist friendly interfaces. *BMC Bioinformatics.* 2010;11:548.
38. Guo L, Giasson BI, Glavis-Bloom A, et al. A cellular system that degrades misfolded proteins and protects against neurodegeneration. *Mol Cell.* 2014;55(1):15-30.
39. Bonilla MA, Gillio AP, Ruggeiro M, et al. Effects of recombinant human granulocyte colony-stimulating factor on neutropenia in patients with congenital agranulocytosis. *N Engl J Med.* 1989;320(24):1574-1580.
40. Rosenberg PS, Alter BP, Bolyard AA, et al. The incidence of leukemia and mortality from sepsis in patients with severe congenital neutropenia receiving long-term G-CSF therapy. *Blood.* 2006;107(12):4628-4635.
41. Rosenberg PS, Zeidler C, Bolyard AA, et al. Stable long-term risk of leukaemia in patients with severe congenital neutropenia maintained on G-CSF therapy. *Br J Haematol.* 2010;150(2):196-199.

42. Donadieu J, Leblanc T, Bader Meunier B, et al. Analysis of risk factors for myelodysplasias, leukemias and death from infection among patients with congenital neutropenia. Experience of the French Severe Chronic Neutropenia Study Group. *Haematologica.* 2005;90(1):45-53.
43. Rao S, Brito-Frazao J, Serbin AV, et al. Gene Editing ELANE in Human Hematopoietic Stem and Progenitor Cells Reveals Disease Mechanisms and Therapeutic Strategies for Severe Congenital Neutropenia. *Blood.* 2019;134(Supplement_1):3.
44. Sreeramulu B, Shyam ND, Ajay P, Suman P. Papillon-Lefevre syndrome: clinical presentation and management options. *Clin Cosmet Investig Dent.* 2015;7:75-81.
45. Skokowa J, Steinemann D, Katsman-Kuipers JE, et al. Cooperativity of RUNX1 and CSF3R mutations in severe congenital neutropenia: a unique pathway in myeloid leukemogenesis. *Blood.* 2014;123(14):2229-2237.
46. Ritter MU, Klimiankou M, Schmidt AE, et al. Understanding the Role of CSF3R and Runx1 Runt Homology Domain Missense Mutations in Leukemic Transformation of Hematopoietic Stem Cells. *Blood.* 2018;132:1101.
47. Olofsen PA, Fatrai S, van Strien PMH, et al. Malignant Transformation Involving CXXC4 Mutations Identified in a Leukemic Progression Model of Severe Congenital Neutropenia. *Cell Reports Medicine.* 2020;1(5):100074.
48. Olofsen PA, Touw IP. RUNX1 Mutations in the Leukemic Progression of Severe Congenital Neutropenia. *Mol Cells.* 2020;43(2):139-144.

Chapter 3

PML-controlled responses in severe congenital neutropenia with *ELANE*-misfolding mutations

Patricia A. Olofsen[1], Dennis A. Bosch[1*], Onno Roovers[1*], Paulina M.H. van Strien[1*], Hans W.J. de Looper[1], Remco M. Hoogenboezem[1], Sander Barnhoorn[2], Pier G. Mastroberardino[2], Mehrnaz Ghazvini[3], Vincent H.J. van der Velden[4], Eric M.J. Bindels[1], Emma M. de Pater[1], Ivo P. Touw[1]

[1] Department of Hematology, Erasmus University Medical Center, Rotterdam 3015 CN, the Netherlands
[2] Department of Molecular Genetics, Erasmus University Medical Center, Rotterdam 3015 CN, the Netherlands
[3] Department of Developmental Biology, iPS Core Facility, Erasmus University Medical Center, Rotterdam 3015 CN, the Netherlands
[4] Department of Immunology, Erasmus University Medical Center, Rotterdam 3015 CN, the Netherlands
* These authors contributed equally to this work

Short title: PML in severe congenital neutropenia

Blood Advances, 2021 Feb 9; 5(3):775-786.

Abstract

Mutations in *ELANE* cause severe congenital neutropenia (SCN), but how they affect neutrophil production and contribute to leukemia predisposition is unknown. Neutropenia is alleviated by CSF3 (G-CSF) therapy in most cases, but dose requirements vary between patients. Here, we show that $CD34^{+}CD45^{+}$ hematopoietic progenitor cells (HPCs) derived from induced pluripotent stem cell lines (iPSCs) from patients with SCN that have mutations in *ELANE* (n=2) or *HAX1* (n=1) display elevated levels of reactive oxygen species (ROS) relative to normal iPSC-derived HPCs. In patients with *ELANE* mutations causing misfolding of the neutrophil elastase (NE) protein, HPCs contained elevated numbers of promyelocyte leukemia protein nuclear bodies (PML-NBs), a hallmark of acute oxidative stress. This was confirmed in primary bone marrow cells from 3 additional ELANE-mutant SCN patients. Apart from responding to elevated ROS levels, PML controlled the metabolic state of these *ELANE*-mutant HPCs as well as the expression of *ELANE*, suggestive of a feed-forward mechanism of disease development. Both *PML* deletion and correction of the *ELANE* mutation restored CSF3 responses of these *ELANE*-mutant HPCs. These findings suggest that PML plays a crucial role in the disease course of *ELANE*-SCN characterized by NE-misfolding, with potential implications for CSF3 therapy.

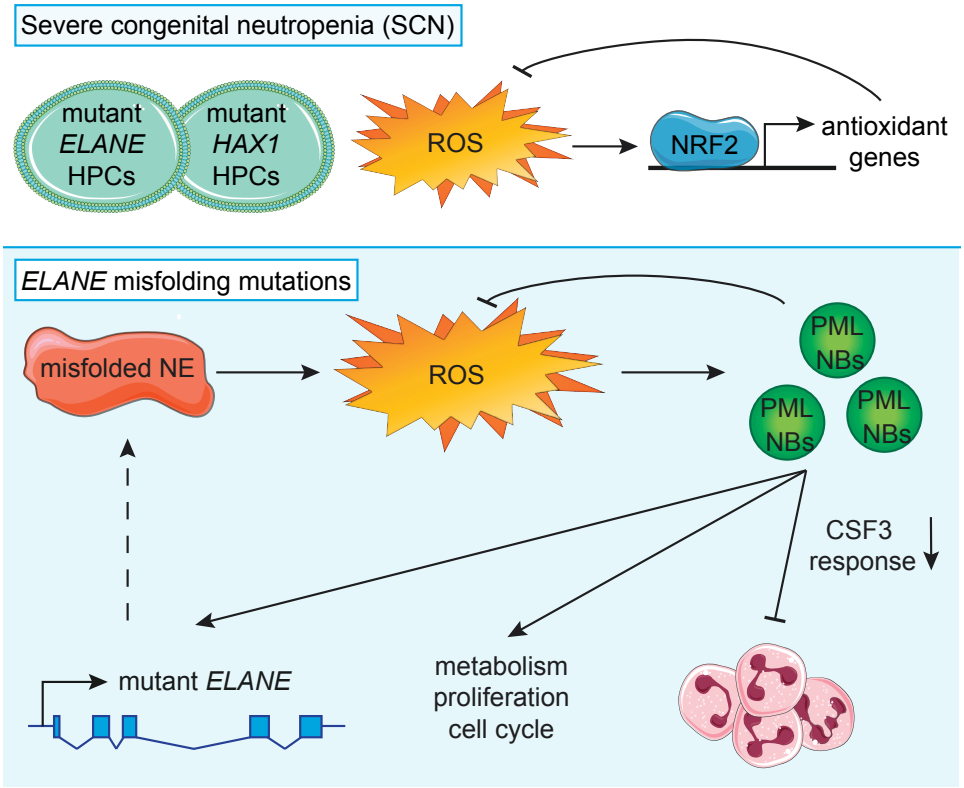

Introduction

Severe congenital neutropenia (SCN) is a genetically heterogeneous disease that, when left untreated, leads to life-threatening bacterial infections from the lack of neutrophils.[1] Autosomal dominant or sporadic mutations in *ELANE*, the gene encoding neutrophil elastase (NE), are the most frequent cause of SCN, whereas mutations in *HAX1*, encoding a multifunctional protein associated with mitochondrial integrity and cytoskeleton organization, are responsible for the autosomal recessive form of SCN originally described as Kostmann syndrome.[2,3] Most patients with SCN receive life-long therapy with colony stimulating factor 3 (CSF3/ granulocyte colony-stimulating factor [G-CSF]) to alleviate the neutrophilic differentiation block. While the majority of patients repond favorably to relatively modest dosages of CSF3 (5-10 μg/kg/day), others need more excessive dosages (>50-100 μg/kg/day) to reach clinically beneficial neutrophil levels, whereas some patients fail to respond to CSF3 therapy altogether.[4] Patients with SCN have an increased risk of developing myelodysplastic syndrome (MDS) or acute myeloid leukemia (AML) while under CSF3 treatment. This particularly applies to patients needing high CSF3 dosages to alleviate neutropenia.[5,6]

How *ELANE*, *HAX1*, and other mutations causing SCN affect neutrophil production is still largely unknown. A prevailing hypothesis is that cellular stresses, in *ELANE*-SCN caused by NE protein misfolding and in *HAX1*-SCN by mitochondrial leakage, are drivers of the neutropenia.[3,7,8] However, the wide spectrum of *ELANE* mutations found in SCN are not all predicted to cause NE misfolding; therefore, alternative mechanisms of how *ELANE* mutations cause neutropenia have been proposed.[9-11] This heterogeneity of mutations may explain the variability in CSF3 responses seen in patients and possibly also determine leukemia risk.[4,5,9]

The promyelocytic leukemia protein (PML), originally identified as a fusion partner in a chromosomal translocation causing acute promyelocytic leukemia, has been studied extensively for its role in controlling cell cycle, DNA damage, and inflammation.[12-17] Particularly, these studies dealt with the role of PML nuclear bodies (PML-NBs), hollow spherical structures that contain a plethora of regulatory molecules controlling the previously mentioned processes. Moreover, PML-NBs have been implicated in degrading misfolded proteins by a mechanism not involving the canonical unfolded protein response (UPR) signaling pathways.[18] Finally, PML plays an important role in how cells deal with oxidative stress caused by reactive oxygen species (ROS).[19] Whereas nuclear factor erythroid 2-related factor 2 (NRF2) transcriptionally activates antioxidant pathways at relatively low levels of ROS, this role can be taken over by PML upon the acute generation of excess ROS,

e.g., induced by exposure of cells to arsenic trioxide (As_2O_3) or irradiation.[19]

To investigate the involvement of PML in SCN, we created patient- and control-derived induced pluripotent stem cells (iPSCs) and generated $CD34^+CD45^+$ hematopoietic progenitor cells (HPCs) from these lines. We show that PML-NBs are elevated in SCN-HPCs with predicted NE misfolding mutations and that PML deletion reduces the metabolic activity and partly restores CSF3 responses of these cells. In addition, we show that loss of PML reduces the levels of mutant *ELANE* transcript and NE protein, indicating that PML may aggravate the SCN phenotype through a feed-forward mechanism.

Materials and Methods

Patient samples

Ficoll-gradient separated bone marrow (BM) and blood cells were obtained and frozen according to established procedures for viable cell cryopreservation. The study was performed under the permission of the institutional review boards of the Erasmus Medical Center.

Generation of iPSC

BM fibroblasts cultured from patients with SCN harboring *ELANE* mutation p.I60F (NC_000019.10:g.852986A>T), *ELANE* mutation p.R103L (NC_000019.10:g.853345G>T), or *HAX1* mutation p.W44X (NC_000001.11:g.154273412_154273413insA), and from a healthy control BM were reprogrammed, as described previously.[20] Cells were cultured in mTeSR1 (STEMCELL Technologies) on Geltrex LDEV-Free Reduced Growth Factor Basement Membrane Matrix (Thermo Fisher Scientific) and were regularly checked for pluripotency, correct karyotype and their ability to generate hematopoietic progenitor cells and mature neutrophils.

CRISPR/Cas9-mediated genome editing

CRISPR/Cas9-mediated genome editing was used to create $PML^{-/-}$ iPSCs, where a stop codon was introduced in exon 3, or correct the *ELANE*-I60F mutation. In short, $2x10^6$ iPSCs were transfected by electroporation with 500 ng px330 (Cas9 plasmid, #42230 Addgene), containing a gene-specific guide RNA, and 1500 ng recombination template containing PML with a stop codon or *ELANE* wild-type sequence and a neomycin selection cassette, using the 4D-Nucleofector System (Lonza), program CA-137. G418 selection (50 µg/ml) started 48 hours after electroporation. Single clones were picked and screened for homozygous integration of the stop codon and absence of PML protein, or correct integration of the wild-type *ELANE* sequence in the *ELANE*-I60F mutant allele. All clones were checked for retainment of pluripotency.

Hematopoietic induction

HPCs ($CD34^+CD45^+$) were produced with the STEMdiff Hematopoietic Kit (STEMCELL Technologies) according to the manufacturer's protocol. Suspension cells were harvested at day 12 of the protocol and used for further downstream analysis.

Neutrophil differentiation

To expand myeloid progenitors and subsequently differentiate them into mature neutrophils, suspension cells, harvested at day 12 of the hematopoietic induction protocol, were treated

as described previously.[21] In short, 10^5 cells/ml were plated in a nontissue culture-treated plate in IMDM (Life Technologies) complemented with 10% defined FBS (Hyclone), 10ng/ml IL3 (R&D systems), 10ng/ml GM-CSF (Peprotech), 50ng/ml SCF (CellGenix GmbH) and 50ng/ml CSF3 (Filgastrim, Zarzio). After 4 days medium was switched to IMDM complemented with 10% defined FBS and 50ng/ml CSF3. Cells were harvested 5 days later and used for subsequent FACS analysis with the EuroFlow AML tube 1 as described previously.[22,23]

MACS purification and immunofluorescence stainings

Suspension cells expressing CD45 were enriched using CD45 Microbeads (Miltenyi Biotec) and subsequent MACS separation according to the manufacturer's protocol. Cells were attached to glass slides with Cytospin 4 and fixed in 4% paraformaldehyde (PFA, Polysciences) on ice for 20 minutes. Cells were washed with PBS and the primary antibodies (PML 1:1000 #M041-3 MBL and NRF2 1:200 #ab31163 Abcam) were incubated overnight at 4°C in 0.05% Saponin (Merck, diluted in PBS). After washing 3x 5 minutes in 0.05% Saponin, cells were incubated with the secondary antibodies (goat anti mouse Alexa Fluor 488 1:200 Life or donkey anti rabbit Cy3 1:800 Bio-Connect) for 1 hour at 37°C. Cells were then washed 3x 5 minutes in 0.05% Saponin and 2x 5 minutes in PBS after which Hoechst 34580 (1:3000, Merck) was added for 10 minutes. Slides were mounted with ProLong Diamond Antifade Mountant (Merck) and imaged on a SP5 or SP8 confocal microscope (Leica). Quantifications were performed using Fiji software.[24]

Seahorse assay

The Agilent Seahorse XFe24 Cell Culture microplate (Agilent) was coated with 22.4 µg/ml Cell-Tak Cell and Tissue Adhesive (Corning) for 20 minutes at room temperature. Suspension cells, obtained after 12 days of hematopoietic induction, were harvested and subsequently live cells were sorted using 7AAD. Sorted live cells ($1.25x10^5$ per well) were added to the coated microplate and centrifuged for 5 minutes at 200g to form a monolayer of cells at the bottom of the well. Cell numbers and oligomycin, FCCP and antimycin concentrations (all 1.0 µM) were determined after optimalization. Per condition, 5 wells were used for the Seahorse Mitochondrial Stress Test, which was performed according to the manufacterer's instructions and measured on a XFe24 analyzer. Data were analyzed with the Seahorse Wave Desktop Software (Agilent).

CFU assays

ELANE-I60F patient bone marrow cells ($4x10^4$/ml) or bone marrow cells derived from a healthy control were seeded in triplo for colony formation in methylcellulose (H4230, STEMCELL Technologies) with increasing concentrations of CSF3 (0, 1, 3.33, 10, 33.3, 100 ng/ml). Colonies were counted after 14 days of culture. A similar protocol was used for the

iPSC-derived HPCs, where suspension cells were harvested after 12 days of hematopoietic differentiation and seeded ($1x10^4$/ml) in colony cultures with CSF3 concentrations as described above.

RNA isolation and RNA sequencing

RNA was isolated from $CD34^+CD45^+$ HPCs using TRIzol (Thermo Fisher Scientific) and GenElute-LPA (Sigma) according to the manufacturer's protocol. cDNA was generated with version 4 of the SMARTer Ultra Low Input RNA kit for sequencing (Clontech). Sequencing libraries were generated using the TruSeq Nano DNA Sample Preparation kit (Illumina), according to the low sample protocol and run on HiSeq 2500 or Novaseq 6000 instruments (Illumina).

Bioinformatics and statistics

Demultiplexing was performed using the CASAVA software (Illumina) allowing for one mismatch in the bar-codes. Subsequently, SMARTer adapters and poly-A tails were removed (fqtrim; https://ccb.jhu.edu/software/fqtrim/) and quality metrics were estimated (FastQC, Babraham bioinformatics & MultiQC, http://multiqc.info) for all of the resulting fastq files. Reads were then aligned against the Human Transcriptome (Gencode v19)/Genome (hg19) using the STAR aligner.[25] Abundance estimation was performed using Cufflinks (refSeq[26]), and raw counts were measured with the HTSeq-count software set in union mode.[27] Next, the measured raw counts were used to create clustering and principal component plots and to perform differential expression analysis using a combination of DESeq2[28] and R (https://www.r-project.org/). Finally, gene set enrichment analysis on the curated gene sets C2 and the hallmark pathways H was done using the GSEA software based on the pre-ranked ASHR log2 fold change, where a false discovery rate (FDR) <0.05 was considered significant.[29,30] Transcripts per million (TPM) were calculated using StringTie.[31]

Quantification and statistical analysis

Data are presented as mean ± SEM. Comparison of two groups was performed using unpaired t-test. Statistical analyses were performed using GraphPad Prism 8.0 (GraphPad Software Inc.) or DESeq2. A p-value <0.05 was considered significant.

Data sharing statement

For original data, please contact i.touw@erasmusmc.nl.

Results

Elevated ROS levels and activation of the NRF2 antioxidant pathway in SCN-iPSC-derived HPCs

Both mutations in *ELANE* and *HAX1* have been reported to cause increased ROS levels in promyelocytes,[3,7,10,11,32] but whether more immature myeloid precursors of patients with SCN already experience oxidative stress because of elevated ROS has not previously been addressed. CellROX Deep Red analysis of HPCs derived from SCN-iPSCs with different mutations (*ELANE*-R103L (NC_000019.10:g.853345G>T), *ELANE*-I60F (NC_000019.10:g.852986A>T), and *HAX1*-W44X (NC_000001.11:g.154273412_154273413insA) showed higher levels of ROS in SCN-HPCs compared to normal control HPCs (Figure 1a). Indicative of elevated ROS levels, NRF2, the master redox regulator,[33] was translocated to the nucleus and subsequently upregulated *GSR*, encoding the antioxidant enzyme gluthatione reductase (Figure 1b, c).

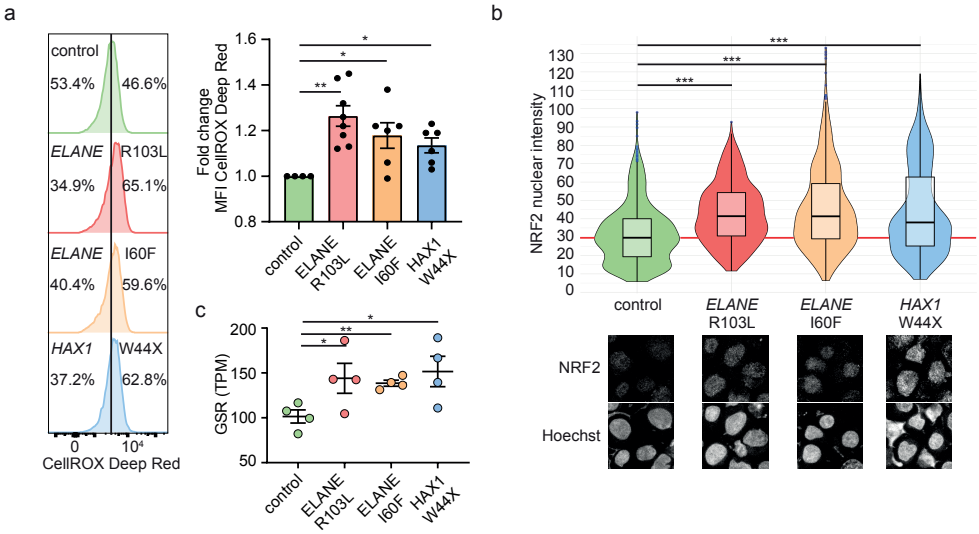

Figure 1: SCN-iPSC-derived CD34+CD45+ cells show elevated ROS levels and increased nuclear translocation of NRF2

*(a) Representative FACS histograms and quantifications of mean fluorescent intensities (MFI) showing increased levels of CellROX Deep Red in SCN HPCs. Data are from 3 independent experiments on 2 clones per genotype. (b) Quantification of the nuclear translocation of NRF2 by immunofluorescence stainings of HPCs showing increased nuclear NRF2 levels in SCN HPCs. The red line indicates the median NRF2 nuclear intensity for the control HPCs. Data are pooled from 2 independent clones and 5 independent experiments. Total cells analyzed: control n=765, ELANE-R103L n=721, ELANE-I60F n=677, HAX1-W44X n=574. (c) Expression of the antioxidant glutathione reductase (GSR) in transcript per million (TPM) obtained from 2 different iPSC clones and 2 independent experiments. *=p<0.05, **=p<0.01, ***=p<0.001.*

Accumulation of PML-NBs in ELANE-SCN HPCs with predicted NE-misfolding mutations

PML-NBs are formed upon acute generation of excessive oxidative stress to neutralize the effects of ROS that are not being coped with by the NRF2 antioxidant pathway.[19] Accordingly, the number of PML-NBs significantly increased after incubation of control HPCs with arsenic trioxide (As_2O_3), which induces excessive oxidative stress (Figures S1a,b). In *ELANE*-I60F HPCs, higher numbers of PML-NBs were found relative to controls in the absence of As_2O_3, which was not seen in *ELANE*-R103L or *HAX1*-W44X HPCs (Figure 2a). Incubation with the antioxidant N-acetylcysteine (NAC) significantly reduced ROS levels and the number of PML-NBs in *ELANE*-I60F cells, corroborating that in *ELANE*-I60F HPCs, PML-NBs were elevated by endogenous oxidative stress (Figures S1c,d). Comparison of the predicted structural alterations (https://www3.cmbi.umcn.nl/hope/)[34] caused by the *ELANE* mutations showed that the *ELANE*-R103L mutation alters a positively charged amino acid (R) into a smaller neutral amino acid (L) at the surface of the protein, thereby possibly affecting interactions with other molecules (Figure 2b). In contrast, the *ELANE*-I60F alteration causes a structural change in the core of the protein, by introducing a bulky amino acid, that predicts protein misfolding (Figure 2b). To exclude that the increased numbers of PML-NBs was a feature of iPSC-derived, rather than *bona fide* BM-derived HPCs, we quantified PML-NBs in $CD34^+$ cells from primary SCN bone marrow samples. These analyses confirmed that PML-NBs are increased in *ELANE*-I60F HPCs relative to controls (Figure 2c). Importantly, this was also seen in HPCs from a second patient with SCN with a misfolding mutation (p.P139L NC_000019.10:g. 855614C>T), but not in HPCs from 2 patients with ELANE-SCN patients that have mutations (p.I120T NC_000019.10:g. 853396T>C, p.S204TfsX11 NC_000019.10:g. 855962_855969dup) not predicting NE misfolding (Figure 2d).

PML knockout induces NRF2 nuclear translocation in ELANE-I60F HPCs

Because NRF2 and PML-NBs both neutralize ROS levels, we wondered to what extent deletion of PML in the *ELANE*-I60F and control HPCs affected NRF2 activation. Disruption of PML expression by introducing a stop codon in exon 3 (Figures S2a,b) resulted in the complete absence of PML-NBs (Figure 3a), while not affecting the generation of HPCs (Figure S2c,d). *ELANE*-I60F $PML^{-/-}$ HPCs showed significantly increased nuclear translocation of NRF2, confirming that PML-NBs reduced ROS levels, leading to lower NRF2 activation (Figure 3b). No major differences in total ROS levels were seen between PML proficient and deficient *ELANE*-I60F HPCs, indicating that NRF2, possibly in combination with other antioxidant pathways, compensated for the loss of PML (Figure 3c). In addition, As_2O_3 treatment of *ELANE*-R103L cells, which previously did not show increased numbers of PML-NBs but did show increased ROS levels and NRF2 translocation (Figures 1 and 2a), resulted in increased numbers of PML-NBs but not in increased ROS levels (Figures S1e,f), further strengthening the observation that both PML-NBs and NRF2 control ROS levels. No significant differences

in nuclear NRF2 were seen between PML proficient and deficient control HPCs, consistent with earlier work showing that, under physiological ROS conditions, PML-NBs do not play a major role in governing antioxidant responses (Figure 3d).[19]

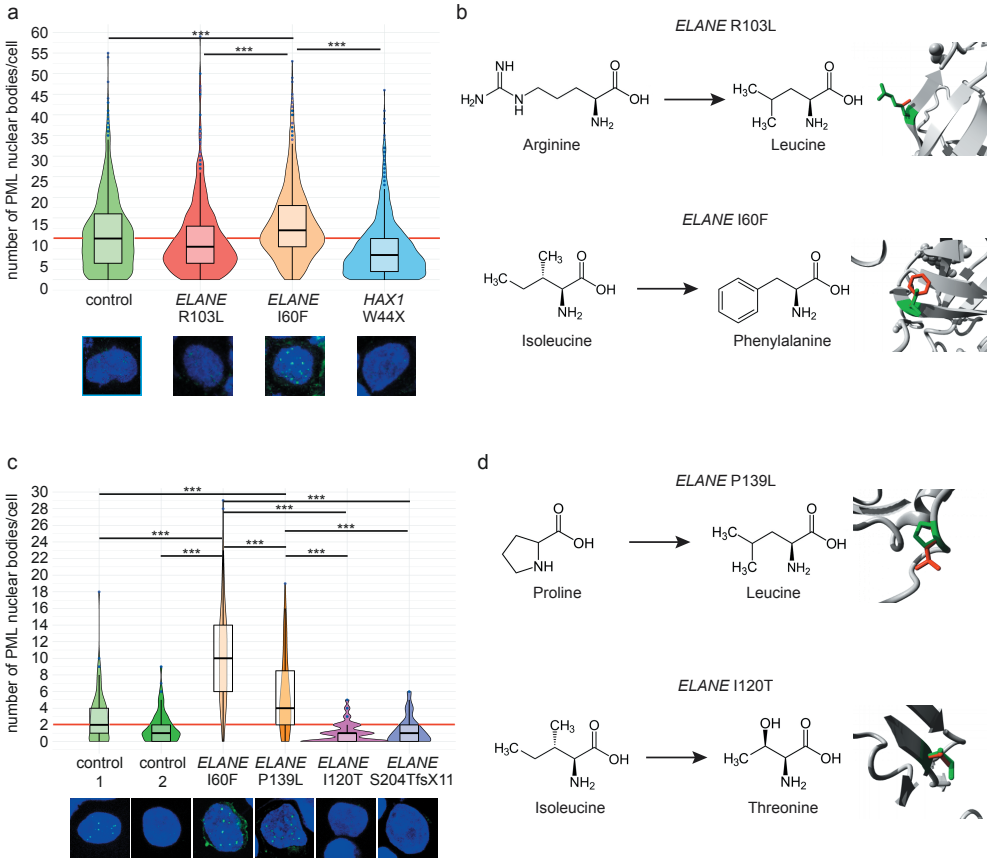

Figure 2: Increased numbers of PML-NBs in ELANE¬-SCN HPCs with predicted NE-misfolding mutations

*(a) Quantifications of the number of PML nuclear bodies (PML-NBs) per cell, by immunofluorescence stainings, shows increased numbers of PML-NBs in ELANE-I60F derived HPCs (data are pooled from 2 independent clones, 5 independent experiments and 2 different stainings resulting in; control n=1119, ELANE-R103L n=720, ELANE-I60F n=732, HAX1-W44X n=914, where n=the number of cells). The red line indicates the median number of PML-NBs/cell for the control HPCs. (b) Amino acid alterations of the ELANE-R103L and -I60F mutations, with a close-up of the mutation in ribbon-presentation. The wild type amino acid is depicted in green and the mutant in red. (c) Quantifications of the number of PML-NBs in CD34+ bone marrow cells, showing increased numbers of PML-NBs in ELANE-mutant HPCs with predicted NE misfolding (I60F and P139L). The red line indicates the median number of PML-NBs/cell for the control HPCs. Cells analysed: control 1 n=89, control 2 n=127, ELANE-I60F n=79, ELANE-P139L n=63, ELANE-I120T n=103 and ELANE-S204TfsX11 n=74. (d) Amino acid alterations of the ELANE-P139L and -I120T mutations, depicted as outlined under (b). ***=p<0.001.*

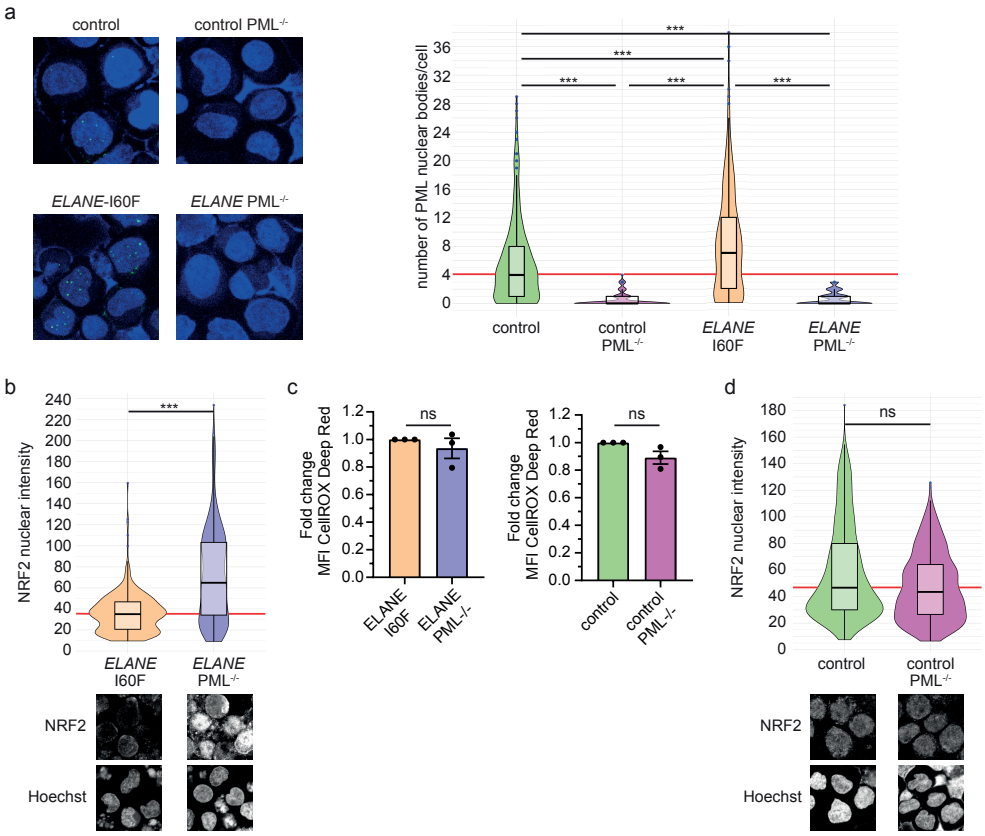

Figure 3: PML acts as a ROS sensor in ELANE-I60F HPCs

*(a) Representative immunofluorescent image showing complete loss of PML-NBs after introduction of a STOP-codon in exon 3 of the PML gene and subsequent PML-NB quantification. The red line indicates the median number of PML-NBs/cell for the control HPCs. Number of cells analysed (n): control n=441, control PML-/- n=175, ELANE-I60F n=353, ELANE-I60F PML-/-n=172. (b+d) Quantifications of immunofluorescent images showing (b) increased nuclear NRF2 levels in ELANE-I60F PML deficient HPCs, but not in control (d). Data are pooled from 3 independent experiments (ELANE-I60F: n=365; ELANE(-I60F) PML-/-: n=370; control: n=631; control PML-/-: n=644, where n= the number of cells). The red line indicates the median number of NRF2 nuclear intensity for the PML proficient HPCs. Microscope settings (laser power) differed between figures. (c) Relative quantification of the mean fluorescent intensity (MFI) showing no increased CellROX Deep Red levels after PML knockout, where PML proficient cells (ELANE-I60F or control) were used as baseline. Data are from 3 independent experiments. ***=p<0.001.*

SCN mutations result in distinct transcriptional profiles in HPCs

To further study how *ELANE* and *HAX1* mutations affect cellular responses of HPCs, we performed RNA sequencing on FACS purified $CD34^{+}CD45^{+}$ cells derived from 2 different iPSC clones, stemming from 2 independent hematopoietic induction experiments for each genotype. Principal component analysis of these transcriptome data showed distinct clustering for each SCN subtype and controls (Figure S3a). The homozygous *HAX1*-W44X mutation is predicted to activate nonsense-mediated mRNA decay (NMD).[35] This was confirmed by gene set enrichment analysis (GSEA), which showed strongly elevated NMD-related transcripts in these *HAX1* mutant HPCs, but not in the *ELANE* mutant subtypes (Figure S3b and data not shown). In line with the fact that loss of HAX1 results in mitochondrial leakage,[3] MitoTracker Red CM-H2XRos and TMRM stainings showed reduced mitochondrial membrane potential in *HAX1* mutant HPCs (Figure S3c). Surprisingly, no upregulation of transcripts linked to the canonical unfolded protein response (UPR) pathway in *ELANE*-I60F HPCs was seen, as would be predicted from a mutation leading to protein misfolding (Figures S3d,e). Transcriptome analysis on more mature myeloid cells derived from these HPCs, by culturing the cells in the presence of CSF3, did not show upregulation of classical UPR-related genes and pathways (Figures S3f-h). Because PML-NBs have also been shown to control degradation of misfolded proteins, independent of the canonical UPR[18], these data suggest that a PML-dependent mechanism, rather than the classical UPR, controlled levels of misfolded NE in the *ELANE*-I60F HPCs.

PML activates metabolic pathways in ELANE-I60F HPCs

To assess which additional intracellular processes are controlled by PML, we compared the transcriptomes from HPCs generated from PML proficient and deficient *ELANE*-I60F and control iPSC lines. Deletion of PML reduced MYC and mTORC1-induced transcription in HPCs from *ELANE*-I60F, but not control HPCs, suggesting that PML drives metabolic pathways in these *ELANE* mutant HPCs (Figure 4a). Oxygen consumption assays showed that PML enhanced basal- and maximal respiration as well as ATP production in *ELANE*-I60F, which was not seen in control HPCs (Figure 4b). In addition, transcriptional signatures indicated that PML activated cell cycling of *ELANE*-I60F HPCs, which translated into a moderately elevated fraction of cells in S-phase, while this was not seen in control HPCs (Figures S4a,b).

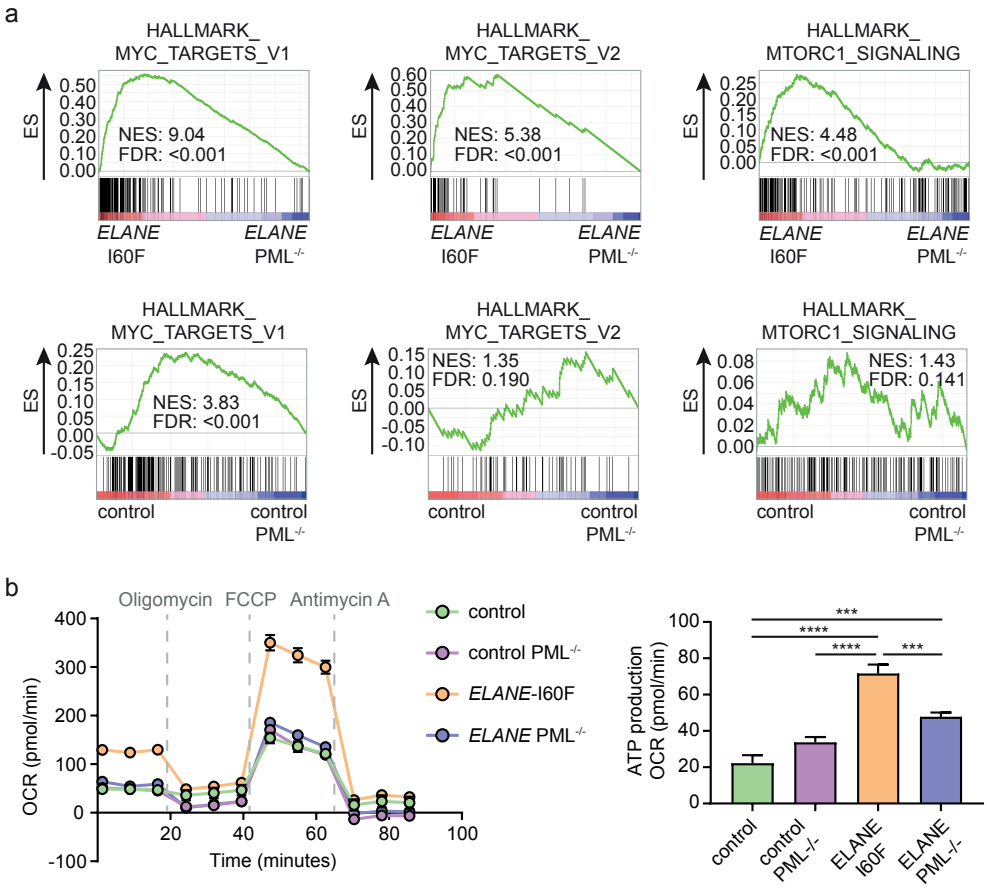

Figure 4: PML activates metabolic pathways in ELANE-I60F HPCs

*(a) GSEA comparing PML proficient and deficient cells showing that PML induces MYC and mTORC1 signalling in ELANE-I60F, but not in control HPCs. Data are derived from 3 independent experiments. (b) Oxygen consumption rate (OCR) measured with the Seahorse mitochondrial stress test (Agilent) showing PML dependent increases in basal respiration, ATP production and maximum respiration in ELANE-I60F cells (n=5). NES: normalized enrichment score, FDR: false discovery rate. ***=p<0.001, ****=p<0.0001.*

PML induces expression of ELANE-I60F

Transcriptome analysis further showed that *ELANE* was highly expressed in *ELANE*-I60F HPCs, relative to controls, whereas this increase in transcript levels was not observed in *ELANE*-R103L and *HAX1*-W44X HPCs (Figure 5a). Both wild-type and mutant transcripts could be detected in an approximately equal ratio in *ELANE*-I60F HPCs (Figure S5a). PML knockout significantly reduced transcription of both the normal and mutant alleles in the *ELANE*-I60F HPCs (Figures 5b and S5b), implying that PML drives the expression of *ELANE*-I60F and thereby exacerbates the disease phenotype. Extending this observation to protein levels, neutrophil elastase (NE) was detected at significantly higher levels in *ELANE*-I60F HPCs cells compared to control (Figure 5c). In both *ELANE*-I60F and control $PML^{-/-}$ HPCs, NE levels were strongly reduced, thus confirming the critical role of PML in *ELANE* expression in HPCs (Figure 5c). To exclude that this was a unique feature of the *ELANE*-I60F mutation in iPSC-derived HPCs, we analysed NE expression in the $CD34^{+}$ HPCs from the primary BM samples shown in Figure 2c. In addition to the elevated formation of PML-NBs, NE protein levels were higher in the HPCs from patients with SCN with the NE- misfolding mutations (I60F and P139L) than in those from patients with other *ELANE* mutations or control HPCs (Figure 5d).

Correction of the ELANE-I60F mutation reverses the PML-mediated phenotype

To exclude that the increased formation of PML-NBs and higher expression of NE resulted from variations between the iPSC lines related to, e.g., reprogramming or differences in (epi-) genetic states of the lines, we corrected the *ELANE*-I60F mutation by CRISPR-Cas9 mediated genome editing in a fully isogenic setting (Figures S6). Immunofluorescent stainings showed that the numbers of PML-NBs in the corrected HPCs returned to basal levels (Figure 5e). Similarly, immunoblot analysis of 2 independent corrected clones showed that the increased NE levels in *ELANE*-I60F HPCs were reduced to control levels in corrected HPCs (Figure 5f). In line with PML-induced expression of metabolic and cell cycle-related pathways, GSEA showed significantly reduced expression of MYC targets, mTORC1 signalling, E2F targets and G2M checkpoint in *ELANE*-I60F corrected lines (Figure 5g). These data establish that both the increase in PML-NB formation, NE expression, and metabolic/cell cycle-related transcripts in *ELANE*-I60F HPCs were solely caused by the I60F amino acid alteration.

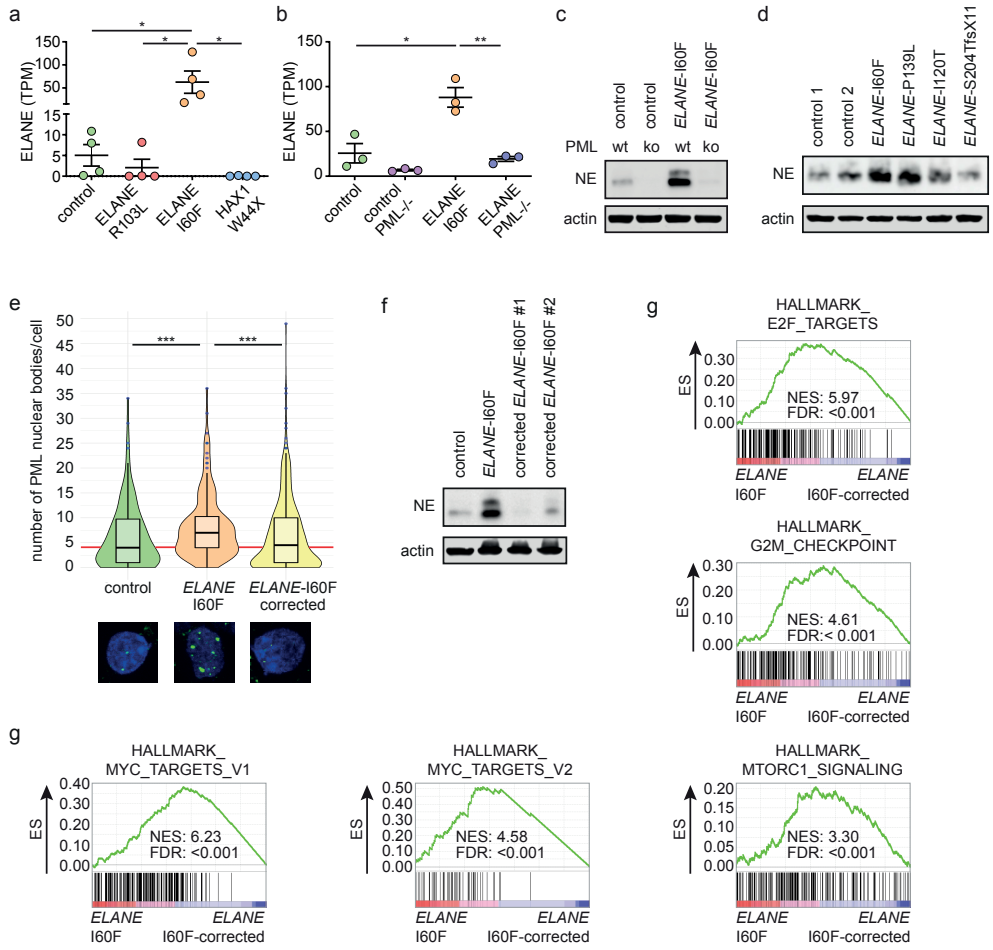

Figure 5: PML induces expression of ELANE-I60F

(a+b) Expression of ELANE in transcripts per million (TPM) showing (a) upregulated expression in ELANE-I60F, but not ELANE-R103L and HAX1-W44X (data are derived from 2 independent clones and 2 independent experiments), and (b) increased levels of ELANE mRNA in ELANE-I60F HPCs, which is reduced to control levels when PML is absent (n=3 independent experiments). (c) Immunoblot showing PML dependent neutrophil elastase (NE) protein abundance, with increased levels in ELANE-I60F cells. d) Immunblot of patient BM cells showing increased NE protein abundance in ELANE-mutant cells with predicted NE misfolding (I60F and P139L) but not others (I120T and S204TfsX11). (e) Quantification of immunofluorescence images showing increased, ELANE-I60F driven, numbers of PML-NBs. Data are pooled from 3 independent experiments and 3 independent ELANE-I60F corrected clones resulting in; control: n=126; ELANE-I60F: n=144; ELANE-I60F corrected n=442, where n= the number of cells. The red line indicates the median number of PML-NBs/cell for the control HPCs. (f) Immunoblot showing increased NE protein abundance in ELANE-I60F cells, which is reduced to control levels upon correction of the mutation, as shown in 2 independent clones. (g) GSEA comparing ELANE-I60F HPCs with corrected ELANE-I60F HPCs (2 independent experiments and 3 independent corrected clones) showing increased

*MYC, mTORC1 and cell cycle-related signatures in ELANE-I60F HPCs. ELANE PML-/- = ELANE-I60F PML-/-, NES: normalized enrichment score, FDR: false discovery rate, *=p<0.05, **=p<0.01, ***=p<0.001.*

PML inhibits the CSF3 response of ELANE-I60F myeloid progenitors

The patient with SCN from whom the *ELANE*-I60F iPSC line was derived showed a poor clinical response to CSF3, where treatment with an excessive dosage of 60-70µg/kg CSF3 resulted in only a modest increase in mature granulocytes. This was confirmed in CFU-G colony assays with titrated dosages of CSF3, showing that, while bone marrow cells from the patient with *HAX1*-W44X SCN and 2 healthy controls show a dosage dependent increase in colony formation, the *ELANE*-I60F CFUs did not respond to CSF3 dosages exceeding 100 ng/ml (Figure 6a). Notably, colony formation in the presence of a myeloid cytokine cocktail consisting of IL-3, GM-CSF and CSF3 was within the normal range, (i.e., 127 colonies per 10^5 Ficoll-purified BM cells plated, where the normal reference of control BM cells in our laboratory is between 90-800 colonies per 10^5 cells). Thus, the lack of CSF3 response was not caused by a loss of myeloid progenitors *per se*. Similar CSF3 titration experiments showed that *ELANE*-I60F iPSC-derived HPCs were hyporesponsive to increasing dosages of CSF3 in CFU-G assays, which was restored after correction of the mutation (Figure 6b). A comparable restoration of the CSF3 response was seen in PML-deficient *ELANE*-I60F HPCs. Flow cytometric analysis of CD11b expression, a marker for myeloid differentiation, showed that *ELANE*-I60F HPCs produced significantly less $CD11b^+$ cells relative to control, upon switching to CSF3-containing suspension cultures, consistent with a reduced response to CSF3. In agreement with the inhibitory effects of PML seen in colony assays, PML deletion almost completely restored the percentage of cells expressing CD11b (Figure 6c left panel). Additionally, although significantly increased numbers of $CD117^+$ immature myeloid cells (myeloblasts/promyelocytes) remained present in the *ELANE*-I60F cultures compared with control cells, this fraction decreased upon deletion of PML (Figure 6c right panel). Corroborating these findings, cytologic analysis showed that *ELANE* $PML^{-/-}$ and *ELANE*-I60F gene-corrected cells differentiated towards mature neutrophils in these cultures, whereas *ELANE*-I60F cells mainly accumulated in more immature stages of myeloid differentiation (Figure 6d). Taken together, these data imply that PML contributes to the poor CSF3 response and decreased neutrophil differentiation seen in this patient with SCN.

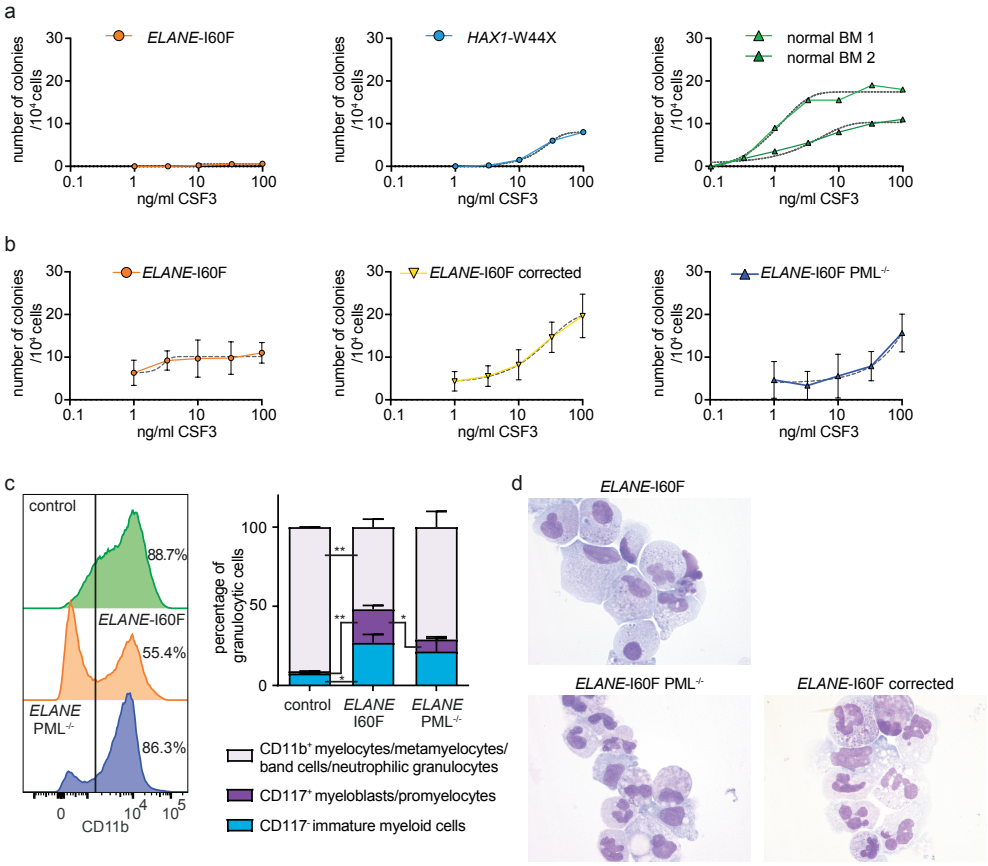

Figure 6: PML inhibits the CSF3 response of ELANE-I60F HPCs

*(a) CFU-G assays on ELANE-I60F bone marrow cells showing a very limited CSF3 response with increasing dosages of CSF3, where HAX1-W44X and normal bone marrow cells show a CSF3-induced increase in colony formation. (b) CFU-G assays on iPSC-derived HPCs showing a similar hyporesponsiveness in ELANE-I60F cells, which is restored upon correction of the mutation and partly restored by the removal of PML (data are pooled from 3 independent experiments performed in triplicate). Dashed line indicates a non-linear fitted curve. (c) Representative FACS histogram depicting CD11b expression (left panel) and subsequent quantifications of the myeloid cells present in CSF3-containing liquid culture (right panel, n=3) showing an elevated ratio of immature versus mature myeloid cells in ELANE-I60F cells relative to controls, which was partly reverted to normal after PML knockout (ELANE PML-/- = ELANE-I60F PML-/-). *=p<0.05, **=p<0.01. (d) Representative May Grünwald-Giemsa stained images of parental, PML deficient and corrected ELANE-I60F cells.*

Discussion

By generating iPSC models, we addressed how $CD34^{+}CD45^{+}$ HPCs from patients with SCN are affected by mutations in *ELANE* or *HAX1*, with emphasis on the levels of oxidative stress. We showed that, although elevated ROS levels and activation of the NRF2 antioxidant pathway were detectable in all cases tested, increased PML-NB formation was seen in a subgroup of *ELANE*-SCN patients with mutations leading to NE protein misfolding. Elevated PML-NB formation is a characteristic of cells undergoing acute and more excessive oxidative stress than cells under more physiological conditions.[19] The focus of this study was to unravel the function of PML in these cases.

Previous studies have shown that *ELANE* mutations evoke "classical" UPR responses in both mouse and human SCN models, likely caused by NE misfolding.[11,36] However, in a more recent study, mutant *ELANE* failed to induce an UPR, even though the mutation predicted NE misfolding.[37] A possible explanation for this discrepancy is that the wide spectrum of *ELANE*-mutations in patients with SCN differentially affect NE protein structure and folding.[9,10] It is therefore not inconceivable that different structural changes might result in variable degrees of NE misfolding and consequently activate different (i.e., canonical versus PML-mediated, UPR reponses).

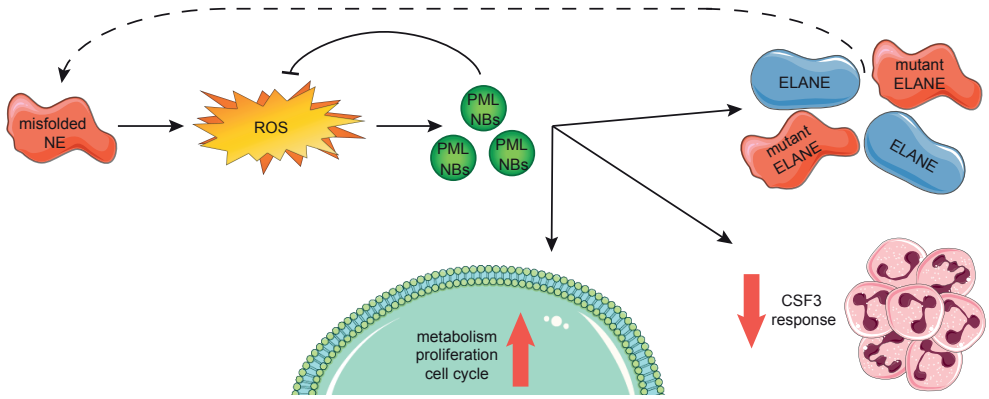

Figure 7: Graphical representation of the PML-mediated responses in ELANE-I60F HPCs

ELANE-mutations with predicted NE misfolding result in excessive doses of ROS, inducing the formation of PML-NBs. PML-NBs are important for reducing ROS levels, while also inducing metabolism, proliferation and cell cycling. In addition, PML reduces the response to CSF3 and induces the transcription of (mutant) ELANE, providing a feed-forward mechanism.

Our findings fit into a model (Figure 7) in which *ELANE* mutations that result in NE protein misfolding, e.g., by insertion of a bulky amino acid in the core of the protein, induce an

increased level of oxidative stress in $CD34^+CD45^+$ HPCs. As a consequence, PML-NBs are being formed, which not only act to reduce excessive ROS levels, but also stimulate metabolism and, to a lesser extent, proliferation of the HPCs. In addition, PML dampened the CSF3 responsiveness of *ELANE*-I60F HPCs *in vitro*, providing a possible explanation for the ineffective clinical CSF3 response in this patient. Finally, transcription of (mutant) *ELANE* and NE protein expression strongly depended on PML, suggestive of a PML-driven feed-forward loop aggravating the consequences of the NE misfolding mutation.

Even though a confirmation of the *ELANE*-I60F iPSC-derived data was obtained in primary $CD34^+$ cells from this patient with SCN, as well as in a SCN patient with an other predicted misfolding mutation (*ELANE*-P139L), it still needs to be addressed to what extent cases of SCN with NE misfolding mutations other than *ELANE*-I60F and *ELANE*-P139L fit into the model shown in Figure 7. Keeping in mind that a large number of different *ELANE* mutations have been reported in both SCN and cyclic neutropenia (CyN), some of which overlap between the two conditions[9], additional unknown host factors must have an impact on disease characteristics, i.e., determining (i) cyclic versus severe neutropenia, (ii) risk of leukemic transformation and (iii) response to CSF3 treatment and variations in dosaging.

Despite these limitations, we propose that SCN cases in which $CD34^+$ cells accumulate increased numbers of PML-NBs due to specific *ELANE* mutations predicting NE-misfolding represent a distinct subgroup of patients with specific clinical features. First of all, as increased ROS levels lead to more severe oxidative damage, these patients may face a higher risk to develop MDS or AML than patients with lower levels of oxidative stress in their HPCs. This is in line with the fact that patients with SCN who do not respond well to CSF3 treatment have a much higher chance to progress to MDS or AML than good responders.[5,6,38]

The finding that PML enhanced MYC and mTORC1 signaling in *ELANE*-I60F HPCs, leading to increased metabolic and proliferative activity, supports the notion of increased potential for progression to leukemia.[39,40] This appears in contrast with earlier studies showing that PML represses the AKT/mTOR pathway under hypoxic conditions in, for example, models of neoangiogenesis.[41,42] Potential explanations for this discrepancy might relate to the fact that PML functions can be divergent depending on the oxidative state of cells (i.e., hypoxic versus hyperoxic) or depend on the cell type or developmental stage of cells. In line with this, although PML has well-documented tumor suppressive functions, more recent evidence suggests that, depending on the cellular context, PML also has oncogenic properties.[43,44] Further studies are needed to resolve this issue and also to elucidate how PML and upregulation of mTORC1 signaling are transcriptionally connected.

Finally, the observation that expression of NE levels in the *ELANE*-I60F HPCs strongly depended on PML is intriguing. RNA-sequencing data indicated that transcription of both wild-type and mutant *ELANE* alleles fully depended on the presence of PML. PML ChIP sequencing data from the PML-RARα zinc-inducible U937 cell line (UPR9) showed that PML binds to the promoter/enhancer region of *ELANE,*[45] which could suggest that PML directly controls its transcription. Although suggestive of a PML-mediated feed-forward loop as illustrated by the dashed arrow in Figure 7, the possibility that mutant NE is, at least partly, degraded by a PML-driven mechanism should be taken into account, similar to the mechanism shown in a model of neurodegeneration.[18]

In summary, this study sheds further light on the complex and heterogeneous natural history of SCN and identified a subset of patients with *ELANE*-SCN characterized by the activation of PML-mediated responses of hematopoietic progenitors, which may ultimately help to design new strategies for disease management for these cases.

Acknowledgements

This work was supported by grants from KWF Kankerbestrijding (EMCR 2013-5755 and EMCR 2014-6780), and the Cancer Genome Editing Center of the Erasmus MC Cancer Institute funded by the Daniel den Hoed foundation. We thank Drs Tom Cupedo and Rebekka K. Schneider for valuable comments on the manuscript.

Authorship Contributions

Conceptualization, P.A.O. and I.P.T.; Methodology, P.A.O., D.A.B. and H.W.J.d.L.; Formal Analysis, P.A.O. and R.M.H.; Investigation, P.A.O., D.A.B., O.R., P.M.H.v.S., H.W.J.d.L., S.B., V.H.J.v.d.V and E.M.J.B.; Resources, M.G.; Data Curation, R.M.H.; Writing – Original Draft, P.A.O. and I.P.T.; Writing – Reviewing & Editing, P.G.M., E.M.J.B., E.M.d.P.; Visualization, P.A.O.; Supervision, I.P.T.; Funding Acquisition, I.P.T.

Disclosure of Conflicts of Interest

The authors have no potential conflict of interest to disclose.

References

1. Skokowa J, Dale DC, Touw IP, Zeidler C, Welte K. Severe congenital neutropenias. *Nat Rev Dis Primers.* 2017;3:17032.
2. Dale DC, Person RE, Bolyard AA, et al. Mutations in the gene encoding neutrophil elastase in congenital and cyclic neutropenia. *Blood.* 2000;96(7):2317-2322.
3. Klein C, Grudzien M, Appaswamy G, et al. HAX1 deficiency causes autosomal recessive severe congenital neutropenia (Kostmann disease). *Nat Genet.* 2007;39(1):86-92.
4. Dale DC, Bonilla MA, Davis MW, et al. A randomized controlled phase III trial of recombinant human granulocyte colony-stimulating factor (filgrastim) for treatment of severe chronic neutropenia. *Blood.* 1993;81(10):2496-2502.
5. Rosenberg PS, Alter BP, Bolyard AA, et al. The incidence of leukemia and mortality from sepsis in patients with severe congenital neutropenia receiving long-term G-CSF therapy. *Blood.* 2006;107(12):4628-4635.
6. Rosenberg PS, Zeidler C, Bolyard AA, et al. Stable long-term risk of leukaemia in patients with severe congenital neutropenia maintained on G-CSF therapy. *Br J Haematol.* 2010;150(2):196-199.
7. Glaubach T, Minella AC, Corey SJ. Cellular stress pathways in pediatric bone marrow failure syndromes: many roads lead to neutropenia. *Pediatr Res.* 2014;75(1-2):189-195.
8. Grenda DS, Johnson SE, Mayer JR, et al. Mice expressing a neutrophil elastase mutation derived from patients with severe congenital neutropenia have normal granulopoiesis. *Blood.* 2002;100(9):3221-3228.
9. Germeshausen M, Deerberg S, Peter Y, Reimer C, Kratz CP, Ballmaier M. The spectrum of ELANE mutations and their implications in severe congenital and cyclic neutropenia. *Hum Mutat.* 2013;34(6):905-914.
10. Horwitz MS, Duan Z, Korkmaz B, Lee HH, Mealiffe ME, Salipante SJ. Neutrophil elastase in cyclic and severe congenital neutropenia. *Blood.* 2007;109(5):1817-1824.
11. Kollner I, Sodeik B, Schreek S, et al. Mutations in neutrophil elastase causing congenital neutropenia lead to cytoplasmic protein accumulation and induction of the unfolded protein response. *Blood.* 2006;108(2):493-500.
12. Bernardi R, Pandolfi PP. Structure, dynamics and functions of promyelocytic leukaemia nuclear bodies. *Nat Rev Mol Cell Biol.* 2007;8(12):1006-1016.
13. Chang HR, Munkhjargal A, Kim MJ, et al. The functional roles of PML nuclear bodies in genome maintenance. *Mutat Res.* 2018;809:99-107.
14. Maarifi G, Chelbi-Alix MK, Nisole S. PML control of cytokine signaling. *Cytokine Growth Factor Rev.* 2014;25(5):551-561.

15. Niwa-Kawakita M, Wu HC, The H, Lallemand-Breitenbach V. PML nuclear bodies, membrane-less domains acting as ROS sensors? *Semin Cell Dev Biol.* 2018;80:29-34.
16. Sahin U, de The H, Lallemand-Breitenbach V. PML nuclear bodies: assembly and oxidative stress-sensitive sumoylation. *Nucleus.* 2014;5(6):499-507.
17. Tessier S, Martin-Martin N, de The H, Carracedo A, Lallemand-Breitenbach V. Promyelocytic Leukemia Protein, a Protein at the Crossroad of Oxidative Stress and Metabolism. *Antioxid Redox Signal.* 2017;26(9):432-444.
18. Guo L, Giasson BI, Glavis-Bloom A, et al. A cellular system that degrades misfolded proteins and protects against neurodegeneration. *Mol Cell.* 2014;55(1):15-30.
19. Niwa-Kawakita M, Ferhi O, Soilihi H, Le Bras M, Lallemand-Breitenbach V, de The H. PML is a ROS sensor activating p53 upon oxidative stress. *J Exp Med.* 2017;214(11):3197-3206.
20. Warlich E, Kuehle J, Cantz T, et al. Lentiviral vector design and imaging approaches to visualize the early stages of cellular reprogramming. *Mol Ther.* 2011;19(4):782-789.
21. Nayak RC, Trump LR, Aronow BJ, et al. Pathogenesis of ELANE-mutant severe neutropenia revealed by induced pluripotent stem cells. *J Clin Invest.* 2015;125(8):3103-3116.
22. van Dongen JJ, Lhermitte L, Bottcher S, et al. EuroFlow antibody panels for standardized n-dimensional flow cytometric immunophenotyping of normal, reactive and malignant leukocytes. *Leukemia.* 2012;26(9):1908-1975.
23. Olofsen PA, Touw IP. Chapter 5 - Modeling severe congenital neutropenia in induced pluripotent stem cells. In: Birbrair A, ed. *Recent Advances in iPSC Disease Modeling, Volume 1*: Academic Press; 2020:85-101.
24. Schindelin J, Arganda-Carreras I, Frise E, et al. Fiji: an open-source platform for biological-image analysis. *Nat Methods.* 2012;9(7):676-682.
25. Dobin A, Davis CA, Schlesinger F, et al. STAR: ultrafast universal RNA-seq aligner. *Bioinformatics.* 2013;29(1):15-21.
26. Trapnell C, Williams BA, Pertea G, et al. Transcript assembly and quantification by RNA-Seq reveals unannotated transcripts and isoform switching during cell differentiation. *Nat Biotechnol.* 2010;28(5):511-515.
27. Anders S, Pyl PT, Huber W. HTSeq--a Python framework to work with high-throughput sequencing data. *Bioinformatics.* 2015;31(2):166-169.
28. Love MI, Huber W, Anders S. Moderated estimation of fold change and dispersion for RNA-seq data with DESeq2. *Genome Biol.* 2014;15(12):550.

29. Mootha VK, Lindgren CM, Eriksson KF, et al. PGC-1alpha-responsive genes involved in oxidative phosphorylation are coordinately downregulated in human diabetes. *Nat Genet.* 2003;34(3):267-273.
30. Subramanian A, Tamayo P, Mootha VK, et al. Gene set enrichment analysis: a knowledge-based approach for interpreting genome-wide expression profiles. *Proc Natl Acad Sci U S A.* 2005;102(43):15545-15550.
31. Pertea M, Kim D, Pertea GM, Leek JT, Salzberg SL. Transcript-level expression analysis of RNA-seq experiments with HISAT, StringTie and Ballgown. *Nat Protoc.* 2016;11(9):1650-1667.
32. Xia J, Link DC. Severe congenital neutropenia and the unfolded protein response. *Curr Opin Hematol.* 2008;15(1):1-7.
33. Ishii T, Itoh K, Takahashi S, et al. Transcription factor Nrf2 coordinately regulates a group of oxidative stress-inducible genes in macrophages. *J Biol Chem.* 2000;275(21):16023-16029.
34. Venselaar H, Te Beek TA, Kuipers RK, Hekkelman ML, Vriend G. Protein structure analysis of mutations causing inheritable diseases. An e-Science approach with life scientist friendly interfaces. *BMC Bioinformatics.* 2010;11:548.
35. Nagy E, Maquat LE. A rule for termination-codon position within intron-containing genes: when nonsense affects RNA abundance. *Trends Biochem Sci.* 1998;23(6):198-199.
36. Grenda DS, Murakami M, Ghatak J, et al. Mutations of the ELA2 gene found in patients with severe congenital neutropenia induce the unfolded protein response and cellular apoptosis. *Blood.* 2007;110(13):4179-4187.
37. Garg B, Mehta HM, Wang B, Kamel R, Horwitz MS, Corey SJ. Inducible expression of a disease-associated ELANE mutation impairs granulocytic differentiation, without eliciting an unfolded protein response. *J Biol Chem.* 2020;295(21):7492-7500.
38. Cross CE, Halliwell B, Borish ET, et al. Oxygen radicals and human disease. *Ann Intern Med.* 1987;107(4):526-545.
39. Ben-Sahra I, Manning BD. mTORC1 signaling and the metabolic control of cell growth. *Curr Opin Cell Biol.* 2017;45:72-82.
40. Stine ZE, Walton ZE, Altman BJ, Hsieh AL, Dang CV. MYC, Metabolism, and Cancer. *Cancer Discov.* 2015;5(10):1024-1039.
41. Trotman LC, Alimonti A, Scaglioni PP, Koutcher JA, Cordon-Cardo C, Pandolfi PP. Identification of a tumour suppressor network opposing nuclear Akt function. *Nature.* 2006;441(7092):523-527.
42. Bernardi R, Guernah I, Jin D, et al. PML inhibits HIF-1alpha translation and neoangiogenesis through repression of mTOR. *Nature.* 2006;442(7104):779-785.

43. Mazza M, Pelicci PG. Is PML a Tumor Suppressor? *Front Oncol.* 2013;3:174.
44. Chung YL, Wu ML. Dual oncogenic and tumor suppressor roles of the promyelocytic leukemia gene in hepatocarcinogenesis associated with hepatitis B virus surface antigen. *Oncotarget.* 2016;7(19):28393-28407.
45. Martens JH, Brinkman AB, Simmer F, et al. PML-RARalpha/RXR Alters the Epigenetic Landscape in Acute Promyelocytic Leukemia. *Cancer Cell.* 2010;17(2):173-185.

Supplemental information

Materials and Methods

FACS analysis and cell sorting

SSEA4-PE (#330406, BioLegend, Amsterdam, the Netherlands) and Tra-1-60 Alexa Fluor 647 (AF647, #560122, BD Biosciences, San Jose, CA, USA) were used for regular pluripotency screenings of the iPSCs. Hematopoietic induction of iPSC was assessed using CD34-PE (#345802, BD Biosciences), CD34-Alexa Fluor 700 (#343525, BioLegend), CD45-APC (#555485, BD Biosciences) and/or CD45-FITC (#A07782, Beckman Coulter, Woerden, the Netherlands) antibodies. Cytoplasmic oxidative stress levels were measured with CellROX Deep Red, while mitochondrial membrane potential was measured using MitoTracker Red CM-H2XRos and TMRM (all Thermo Scientific). Dead cells were excluded using 7-aminoactinomycin-D (7AAD, Life Technologies) or 4',6-Diamidino-2-Phenylindole (DAPI, Thermo Fisher Scientific). Cell cycle analysis were performed with the BrdU flow kit (BD Pharmingen) according to the manufacturer's instructions. Flow cytometry was performed using a BD LSRII flow cytometer (BD Biosciences). Cell sorting was done using a FACSAria instrument (BD Biosciences). Analysis of FACS data was performed using FlowJo (TreeStar).

SDS-PAGE/Immunoblotting

Lysates were prepared, and immunoblot analyses performed as previously described[1]. The primary antibody (#ab131260, Abcam) was used to detect NE protein levels. Goat anti-rabbit HRP (#A16116, Life Technologies) was used as secondary antibody, after which the SuperSignal West Pico Plus Chemiluminescent Substrate (Thermo Fisher Scientific) was used to detect the signal on an Amersham Imager 600 instrument. A β-actin antibody (Sigma) was used as loading control, followed by incubation with the secondary IRdyes donkey anti-mouse 680LT antibody (Licor, Homburg, Germany) to detect the signal on an Odyssey instrument (Licor).

Arsenic trioxide and N-acetylcysteine treatment

Cells in suspension were harvested at day 12 of the hematopoietic induction and treated for 1 hour at 37°C with 1μM Arsenic trioxide (As_2O_3) or 2mM N-acetylcysteine (NAC, Sigma). Subsequently, cells were used for immunofluorescence stainings or CellROX Deep Red flow cytometry.

References

1. Palande KK, Beekman R, van der Meeren LE, Beverloo HB, Valk PJ, Touw IP. The antioxidant protein peroxiredoxin 4 is epigenetically down regulated in acute promyelocytic leukemia. PLoS One. 2011;6(1):e16340.

Supplemental Figures

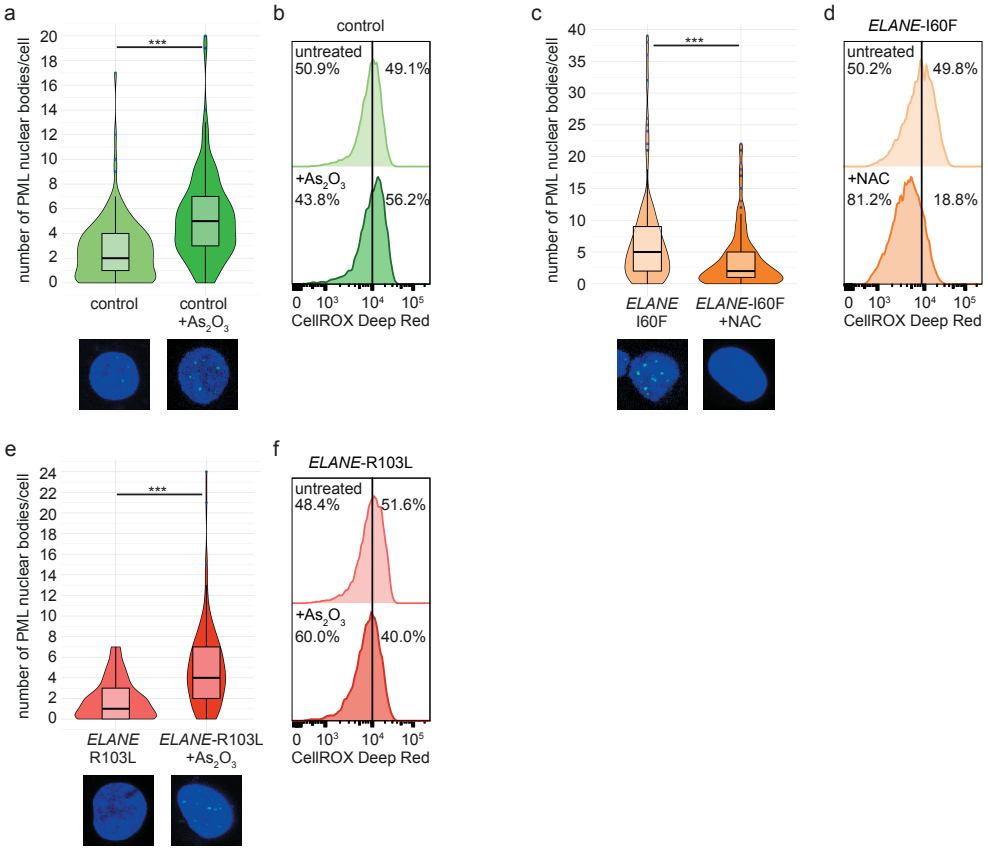

Figure S1: PML-NB formation can be induced with As_2O_3 and reduced with NAC treatment

*(a,c,e) Quantifications of the number of PML nuclear bodies (PML-NBs) per cell, by immunofluorescence stainings, showing (a) increased numbers of PML-NBs in control cells treated with arsenic trioxide (As_2O_3, 1µM for 1 hour), (c) reduced numbers of PML-NBs upon treatment with the antioxidant N-acetylcysteine (NAC, 2mM for 1 hour) in ELANE-I60F cells and (e) increased numbers of PML-NBs in ELANE-R103L cells treated with As_2O_3 (1µM for 1 hour). Total cells analyzed: control n=151, control+ As_2O_3 n=169, ELANE-I60F n=134, ELANE-I60F+NAC n=190, ELANE-R103L n=156, ELANE-R103L+ As_2O_3 n=126. (b,d,f) A representative FACS histogram showing CellROX Deep Red levels which are (b) increased upon treatment with As_2O_3 in control HPCs, (d) reduced upon treatment with NAC in ELANE-I60F HPCs, and (f) not significantly altered in ELANE-R103L HPCs upon treatment with As_2O_3. ***=p<0.001.*

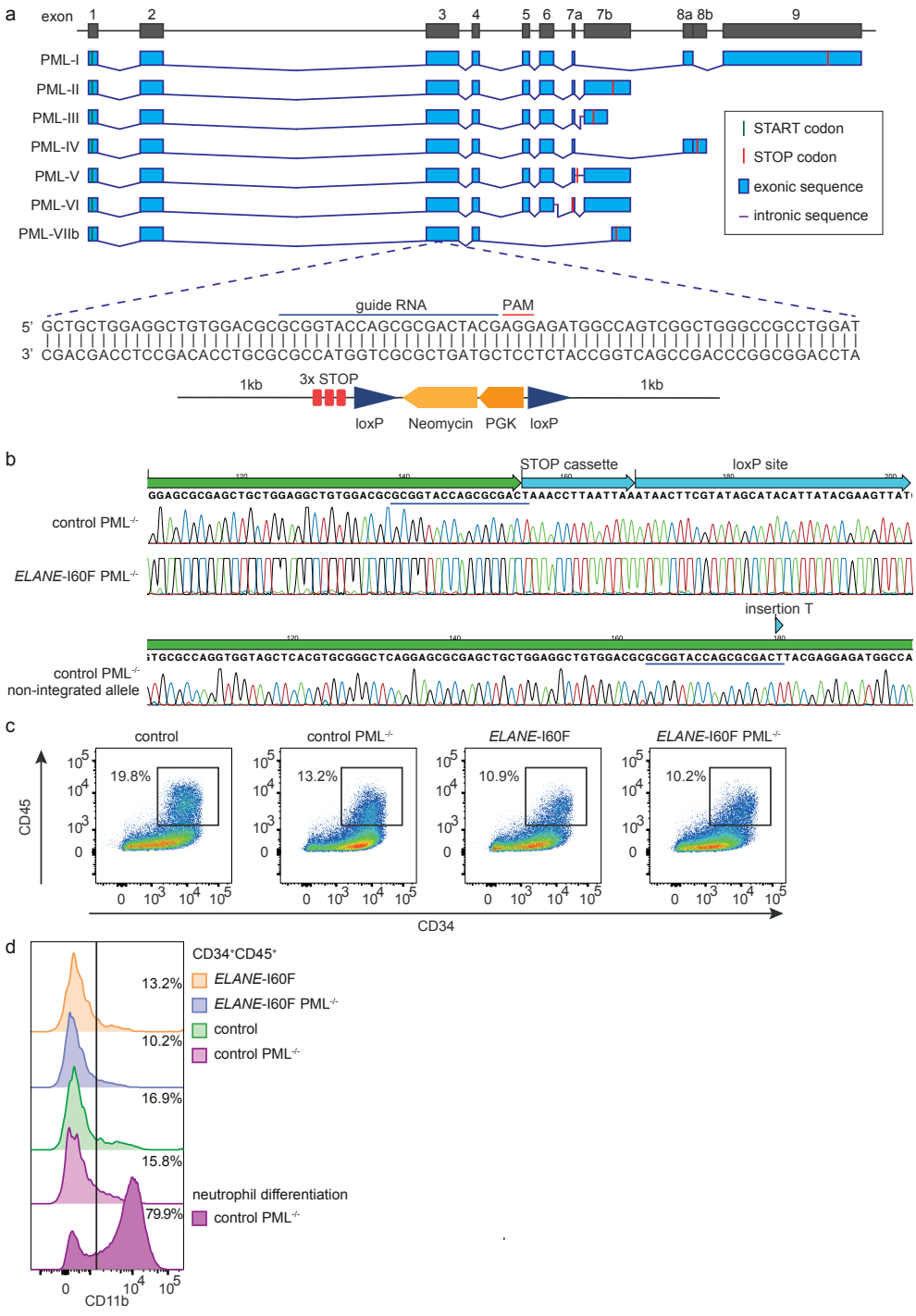
a
exon 1 2 3 4 5 6 7a 7b 8a 8b 9
PML-I
PML-II
PML-III
PML-IV
PML-V
PML-VI
PML-VIIb
START codon
STOP codon
exonic sequence
intronic sequence
guide RNA
PAM
5' GCTGCTGGAGGCTGTGGACGCGCGGTACCAGCGCGACTACGAGGAGATGGCCAGTCGGCTGGGCCGCCTGGAT
3' CGACGACCTCCGACACCTGCGCGCCATGGTCGCGCTGATGCTCCTCTACCGGTCAGCCGACCCGGCGGACCTA
1kb
3x STOP
1kb
loxP
Neomycin
PGK
loxP
b
STOP cassette
loxP site
GGAGCGCGAGCTGCTGGAGGCTGTGGACGCGCGGTACCAGCGCGACTAAACCTTAATTAATAACTTCGTATAGCATACATTATACGAAGTTAT
control PML-/-
ELANE-I60F PML-/-
insertion T
GTGCGCCAGGTGGTAGCTCACGTGCGGGCTCAGGAGCGCGAGCTGCTGGAGGCTGTGGACGCGCGGTACCAGCGCGACTTACGAGGAGATGGCCA
control PML-/-
non-integrated allele
c
control
control PML-/-
ELANE-I60F
ELANE-I60F PML-/-
19.8%
13.2%
10.9%
10.2%
CD45
CD34
d
CD34+CD45+
ELANE-I60F
ELANE-I60F PML-/-
control
control PML-/-
13.2%
10.2%
16.9%
15.8%
79.9%
neutrophil differentiation
control PML-/-
CD11b

Figure S2: CRISPR-Cas9 mediated genome editing of PML

(a) A guide RNA targeting exon 3 of PML, which is shared by all isoforms, was used to introduce 3 STOP codons, and a neomycin selection cassette, into the PML coding sequence. (b) Sanger sequencing data showing homozygous integration of the recombination template in ELANE-I60F PML$^{-/-}$, while the control PML$^{-/-}$ cells have a heterozygous integration and a frameshift mutation, resulting in a premature stop codon, in the allele that shows no integration of the recombination template. The blue line indicates part of the guide RNA. (c) FACS plots showing the floating cells at day 12 of the hematopoietic induction protocol. The percentages of CD34^{+}CD45^{+} HPCs differ between experiments (ranging from 10-50%), but no significant alterations are observed after CRISPR-Cas9 genome editing. (d) FACS histogram showing the CD11b expression of CD34^{+}CD45^{+} of the floating cells at day 12 of the hematopoietic induction protocol (light colors) and at the end of the neutrophil differentiation protocol (dark color). A small percentage of CD34^{+}CD45^{+} HPCs express CD11b, but no significant differences are observed between lines. At the end of the neutrophil differentiation protocol a clear induction of CD11b expression can be observed.

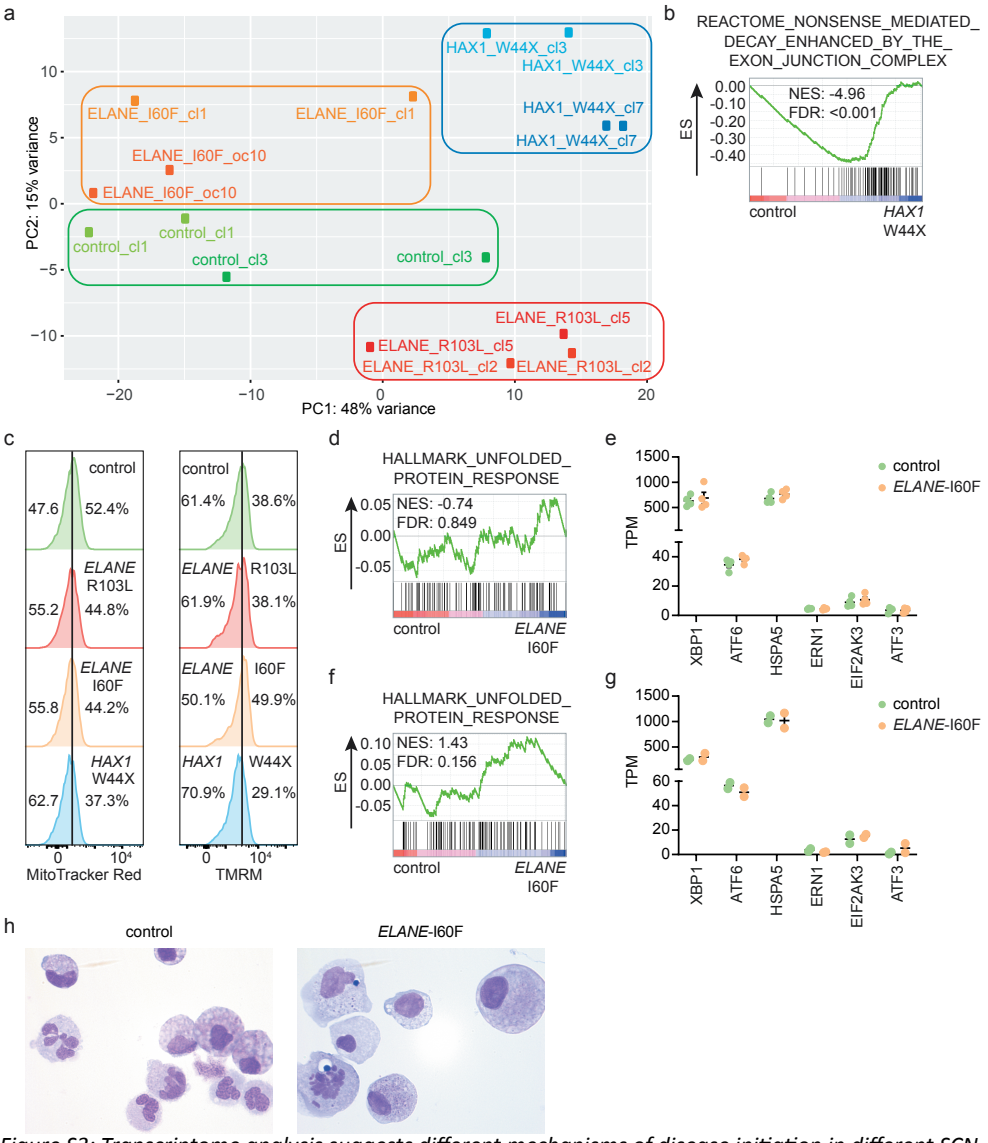

Figure S3: Transcriptome analysis suggests different mechanisms of disease initiation in different SCN patients

(a) Principal component analysis (PCA) showing separate clustering of HPCs derived from different SCN-patients (n=2 different clones and 2 independent experiments). (b) Gene set enrichment analysis (GSEA) showing upregulation of transcripts associated with the reactome 'nonsense mediated decay enhanced by the exon junction complex' in HAX1-W44X derived HPCs compared to control. (c) Representative FACS histogram showing reduced MitoTracker Red and TMRM levels, indicative of reduced mitochondrial membrane potential, in HAX1-W44X derived HPCs. (d) GSEA indicating lack of transcript expression associated with the canonical unfolded protein response pathway in ELANE-I60F derived HPCs. (e) Expression of various UPR-related genes (in TPM) showing no differences between control and ELANE-I60F HPCs (n=2 different clones and 2 independent experiments). (f) GSEA indicating

no induction of the canonical unfolded protein response pathway in more mature granulocytic cells from ELANE-I60F. (g) Expression of various UPR-related genes (in TPM) showing no differences between control and ELANE-I60F derived granulocytic cells (n=2 independent experiments). (h) Representative May Grünwald-Giemsa-stained images of more mature myeloid cells used for RNA sequencing 7 days after the start of the neutrophil differentiation protocol.
NES: normalized enrichment score, FDR: false discovery rate, TPM: transcripts per million.

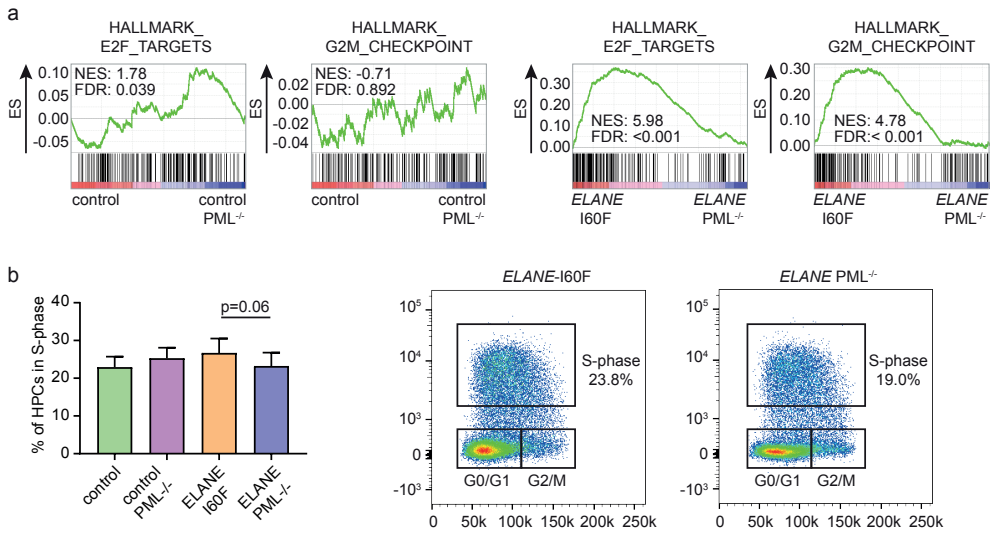

Figure S4: PML activates cell cycling in ELANE-I60F HPCs

(a) GSEA comparing PML proficient and deficient cells, which shows that PML does not influence E2F targets and G2M checkpoint related transcripts in control HPCs, while inducing expression of these transcripts in ELANE-I60F (data derived from 3 independent experiments). (b) BrdU analysis showing a moderately increased fraction of S-phase cells in PML proficient ELANE-I60F HPCs, compared to PML deficient ELANE-I60F HPCs (data combined from 3 independent experiments). NES: normalized enrichment score, FDR: false discovery rate. ELANE PML$^{-/-}$ = ELANE-I60F PML$^{-/-}$.

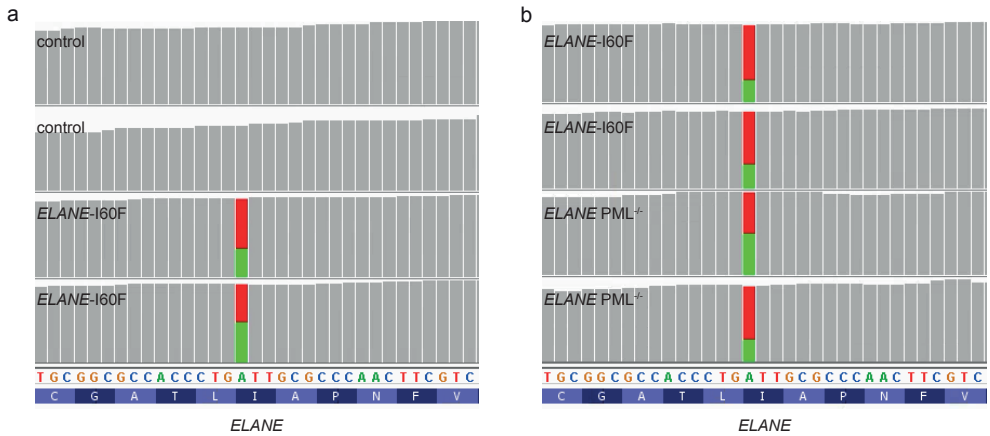

Figure S5: ELANE expression

(a+b) IGV snapshot showing approximately equal expression of the ELANE-I60F wildtype (A, in green) and mutant (T, in red) allele in RNA sequencing data of (a) control and ELANE-I60F HPCs as shown in Figure 5a and (b) ELANE-I60F and ELANE PML-/- HPCs as shown in Figure 5b.

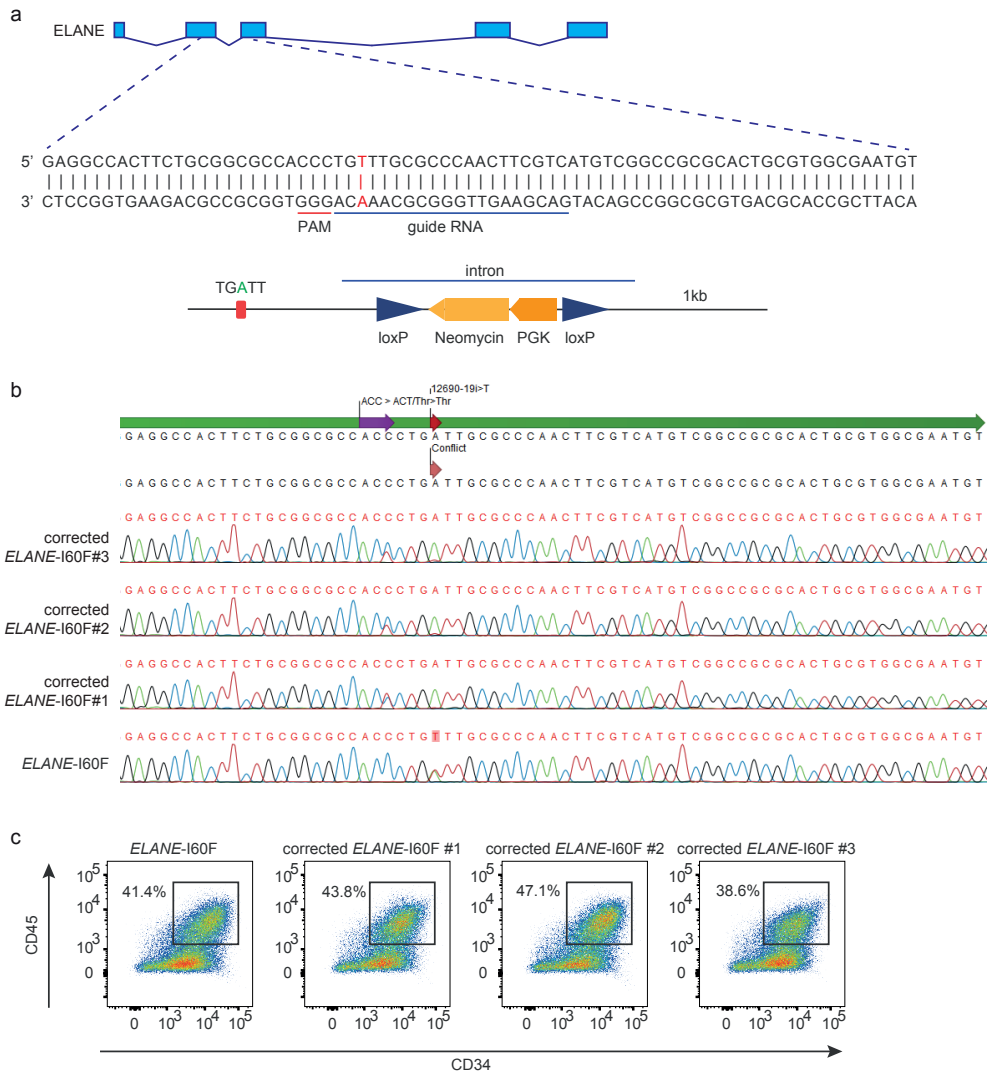

Figure S6: CRISPR-Cas9 mediated correction of ELANE-I60F mutation

(a) CRISPR-Cas9 strategy to correct the ELANE-I60F mutation, where the guide RNA overlaps the mutation, thereby increasing the probability of targeting the mutant allele. The correct sequence was introduced with a recombination template containing a neomycin selection cassette, located in the next intron, to be able to select for the recombined clones. (b) Sanger sequencing data showing correction of the ELANE-I60F mutation, and heterozygous introduction of the PAM mutation present in the recombination template, in the corrected ELANE-I60F lines. (c) FACS plots showing the floating cells at day 12 of the hematopoietic induction protocol. The percentages of $CD34^{+}CD45^{+}$ HPCs differ between experiments (ranging from 10-50%), but no significant alterations are observed after CRISPR-Cas9 genome editing.

Chapter 4

Truncated CSF3 receptors induce pro-inflammatory responses in severe congenital neutropenia

Patricia A. Olofsen[1], Dennis A. Bosch[1], Hans W.J. de Looper[1], Paulina M.H. van Strien[1], Remco M. Hoogenboezem[1], Onno Roovers[1], Vincent H.J. van der Velden[2], Eric M.J. Bindels[1], Emma. M. de Pater[1], Ivo P. Touw[1]

[1] Department of Hematology, Erasmus University Medical Center, Rotterdam 3015 CN, the Netherlands
[2] Department of Immunology, Erasmus University Medical Center, Rotterdam 3015 CN, the Netherlands

Short title: CSF3R mutant function in SCN

Manuscript under review

Abstract

Severe congenital neutropenia (SCN) patients are prone to develop myelodysplastic syndrome (MDS) or acute myeloid leukemia (AML). Leukemic progression of SCN is associated with the acquisition of *CSF3R* mutations in hematopoietic progenitor cells (HPCs), which truncate the colony-stimulating factor 3 receptor (CSF3R). These mutant clones may arise years before MDS/AML becomes overt. Introduction and activation of CSF3R truncation mutants in normal HPCs causes a clonally dominant myeloproliferative state in mice treated with CSF3. Paradoxically, in SCN patients receiving CSF3 therapy, clonal dominance of CSF3R mutant clones usually occurs only after the acquisition of additional mutations shortly before frank MDS or AML is diagnosed. To seek an explanation for this discrepancy, we introduced a patient-derived CSF3R-truncating mutation in ELANE-SCN and HAX1-SCN derived and control induced pluripotent stem cells (iPSCs) and compared the CSF3 responses of HPCs generated from these lines. In contrast to *CSF3R*-mutant control HPCs, *CSF3R*-mutant HPCs from SCN patients do not show increased proliferation but display elevated levels of inflammatory signaling. Thus, activation of the truncated CSF3R in SCN-HPCs does not evoke clonal outgrowth but causes a sustained pro-inflammatory state, which has ramifications for how these CSF3R mutants contribute to leukemic transformation of SCN.

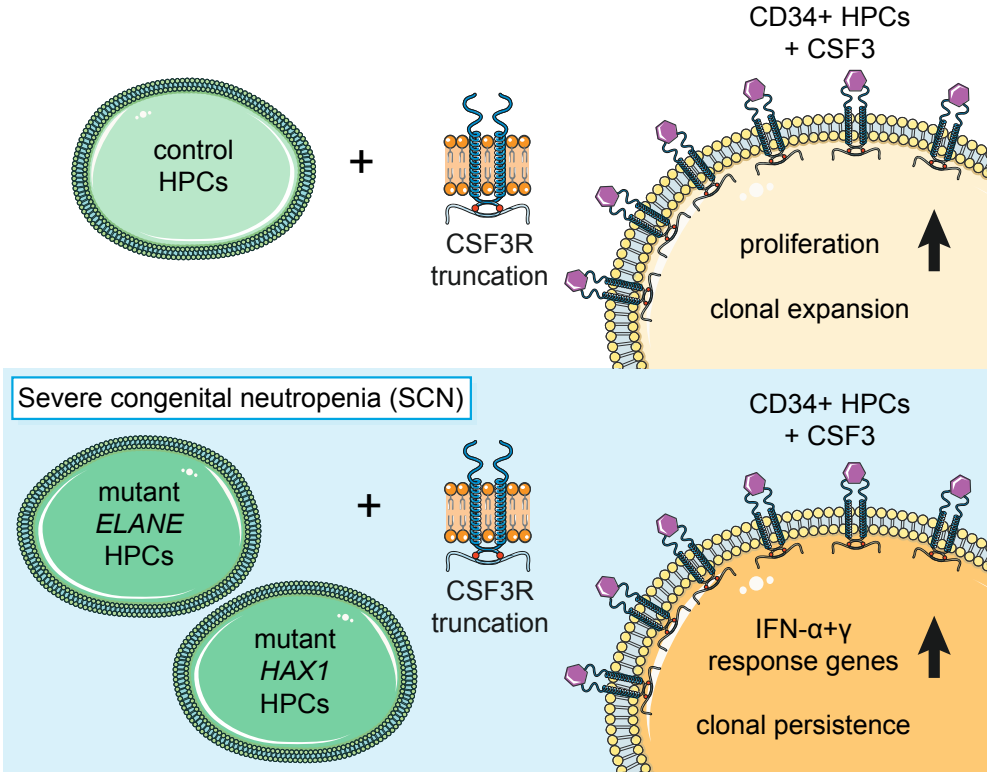

Introduction

Severe congenital neutropenia (SCN) is a genetically heterogeneous disease characterized by a promyelocyte maturation arrest and absolute peripheral neutrophil counts below $0.5x10^9$/L.[1] Most SCN patients present with autosomal dominant mutations in *ELANE*, encoding the granule protein neutrophil elastase (NE), or autosomal recessive mutations in *HAX1*, encoding a multifunctional protein involved in mitochondrial integrity.[2,3] Treatment with colony stimulating factor 3 (CSF3), also known as G-CSF, alleviates the neutropenia in most (>90%) SCN patients.[4]

Apart from being susceptible to life-threatening bacterial infections, SCN patients also face an increased risk to develop myelodysplastic syndrome (MDS) or acute myeloid leukemia (AML).[5] Leukemic progression correlates with somatic mutations in *CSF3R*, resulting in a truncated CSF3 receptor. These *CSF3R* mutations appear during the neutropenic phase of the disease in one or multiple clones, often years before MDS/AML becomes overt.[6] Previous work in mice and cell lines showed that CSF3R-truncation mutants function abnormally due to defective internalization and lysosomal degradation.[7,8] Consequently, myeloid progenitors showed increased CSF3-induced colony formation and reduced myeloid differentiation.[9-11]

How CSF3R-truncating mutants function in SCN-derived hematopoietic progenitor cells (HPCs) is unknown. Studies addressing this were hampered by the lack of suitable models, mainly because *ELANE*- or *HAX1*-mutant mice don't develop neutropenia.[11-13] To overcome this limitation, we generated patient-derived induced pluripotent stem cells (iPSCs), engineered to express a patient specific *CSF3R*-Q739* mutation, causing a truncation at amino acid 715 of the mature CSF3R protein (hereafter named CSF3R-d715). HPCs derived from these lines showed markedly different CSF3 responses compared to normal HPCs.

Methods

iPSC and patient details

Generation, genome editing and hematopoietic induction of iPSCs was described previously.[11] More details can be found in the supplement. The study was performed under the permission of the Institutional Review Boards of the Erasmus MC, the Netherlands.

CFU assays

Suspension cells were harvested 12 days after hematopoietic induction and seeded ($1x10^4$/ml) in methylcellulose (H4230, STEMCELL Technologies) with the addition of 200 ng/ml CSF3. Colonies were counted after 14 days of culture.

RNA isolation and sequencing

RNA was isolated from FACS sorted $CD34^+CD45^+$ HPCs using TRIzol (Thermo Fisher Scientific) and GenElute-LPA (Sigma), according to the manufacturer's protocol. The SMARTer Ultra Low Input RNA kit for sequencing (Clontech, version 4) was used to generate cDNA. Sequencing libraries were generated using the TruSeq Nano DNA Sample Preparation kit (Illumina), according to the low sample protocol and run on HiSeq 2500 or Novaseq 6000 instruments (Illumina).

Statistics

Data are presented as mean ± SEM. Comparison of two groups was performed using unpaired t-test. DESeq2 was used to determine significance based on normalized count data of the RNA-sequencing experiments. A p-value or false discovery rate (FDR) <0.05 was considered significant. More information on the bioinformatic analysis can be found in the supplemental methods section.

Data sharing statement

The RNA sequencing data is available at ArrayExpress: E-MTAB-10288. For additional original data, please contact i.touw@erasmusmc.nl.

Results and Discussion

The *CSF3R*-d715 mutation was introduced in iPSCs from a healthy control and SCN patients with an *ELANE*-R103L, *HAX1*-W44X, or *ELANE*-I60F mutation (Figure S1).[11] *ELANE*-R103L and *HAX1*-W44X patients responded favorably to CSF3 treatment, with dosages of 5-10μg/kg/day being sufficient to alleviate neutropenia (hereafter referred to as CSF3-normoresponsive). The *ELANE*-I60F patient was hyporesponsive to CSF3, with dosages of 60-70μg/kg/day leading to a modest increment in neutrophil counts.

Activation of CSF3R-d715 causes a hyperproliferative response and compromises myeloid differentiation in control- but not in SCN-HPCs

Transcriptome analysis showed that activation of CSF3R-d715 in control HPCs elevates proliferation (e.g., enhanced E2F- and MYC-targets and G2M checkpoint genes) relative to CSF3R-wt control HPCs, while this was not seen in SCN-HPCs (Figure S2a-b). Matching the studies in mice[9-11], CSF3-induced colony formation from CSF3R-d715 control HPCs is significantly increased relative to CSF3R-wt control HPCs, which is again lacking in CSF3-normoresponsive *ELANE*-R103L and *HAX1*-W44X CSF3R-d715 cells (Figure 1a). In line with previous studies in murine cell lines showing reduced neutrophilic differentiation in response to CSF3[9,14,15], activation of CSF3R-d715 in control HPCs induced the expression of various genes associated with immature hematopoietic cells, e.g., *CD34* and *CD164*, while genes associated with more advanced stages of myeloid differentiation, e.g., *C/EBPε, MNDA, SRGN* and *AZU1* are expressed at lower levels compared with CSF3R-wt control HPCs (Figures 1b-c). Additionally, gene sets associated with immature hematopoietic cells are upregulated in CSF3R-d715 control-HPCs (e.g., "IVANOVA_HEMATOPOIESIS_EARLY_PROGENITORS" and "RAMALHO_STEMNESS_UP), while myeloid differentiation gene sets are downregulated (e.g., "REACTOME_TRANSCRIPTIONAL_REGULATION_OF_GRANULOPOIESIS" and "KAMIKUBO_MYELOID_CEBPA_NETWORK", Figure S3a). In contrast, transcriptomes of CSF3R-d715 SCN-HPCs are suggestive of a myeloid bias within the HPC compartment, where both myeloid gene sets and myeloid genes are increased compared with CSF3R-wt SCN-HPCs (Figures 1b-c, S3b). Interestingly, *ELANE* expression is also significantly elevated upon CSF3R-d715 activation in both R103L and I60F *ELANE*-mutant HPCs, which involves both wildtype and mutant alleles (Figures 1c, S3c). In full agreement with the transcriptome data, NE protein levels were increased in CSF3R-d715 *ELANE*-R103L and -I60F cells, reduced in control and absent in the *HAX1*-W44X mutant cells compared to cells expressing CSF3R-wt (Figure 1d). These findings suggest that activation of CSF3R-d715 may affect SCN-HPCs by increasing mutant NE levels, thereby possibly aggravating the SCN phenotype. Upon transferring the CSF3-d715 HPCs to CSF3-containing suspension cultures, no gross differences in neutrophil differentiation between control- and CSF3-normoresponsive SCN-derived HPCs are seen

(Figure S3d). This is not surprising, given that SCN patients mostly respond well to CSF3 therapy, effectively alleviating the differentiation block, even when major CSF3R mutant clones are present.[16,17]

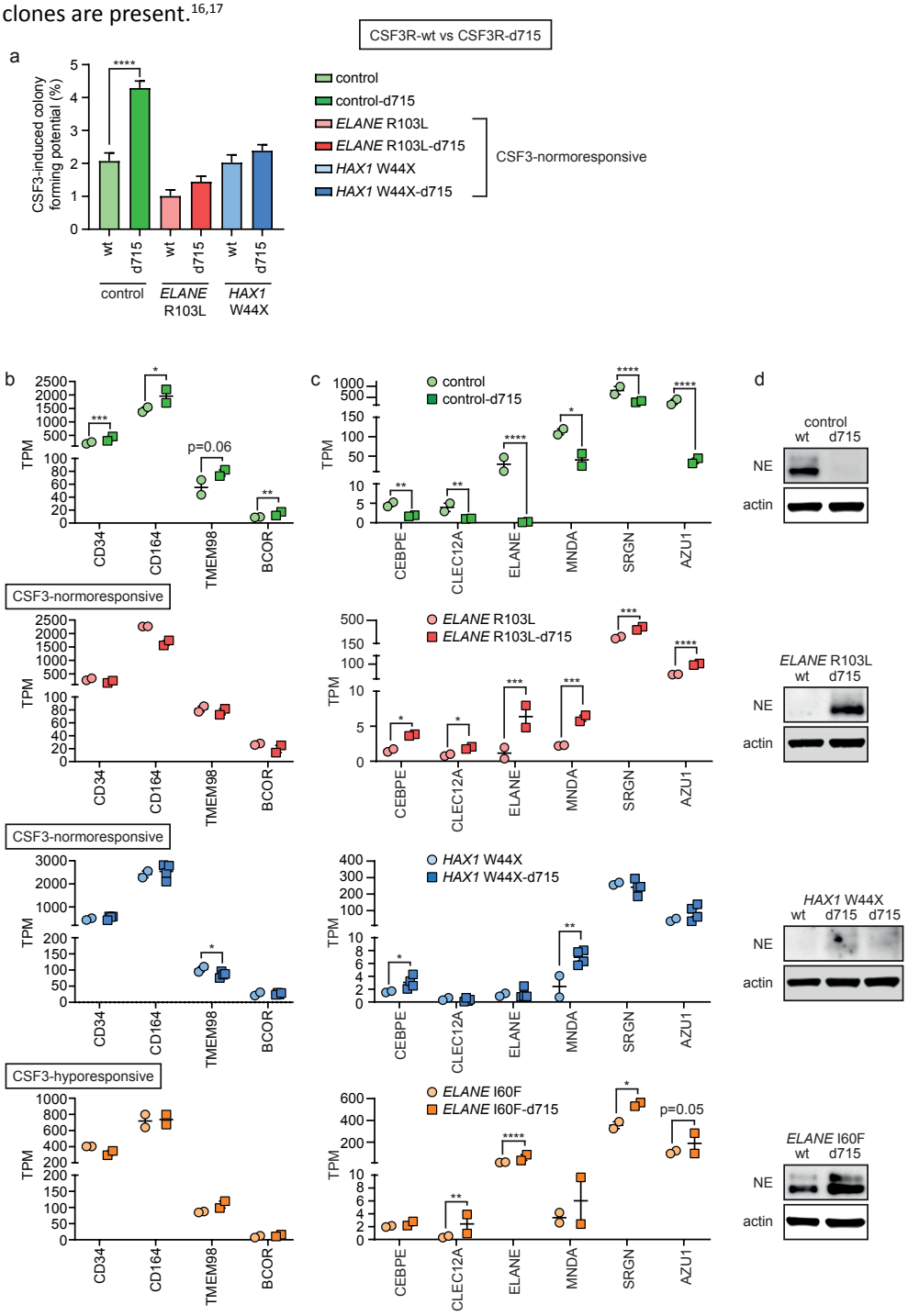

Figure 1: Activation of CSF3R-d715 results in hyperproliferation and reduced differentiation in control, but not SCN-HPCs

(a) CSF3-induced colony formation is significantly increased after introduction of the CSF3R-d715 in control, but not SCN-HPCs. Data are from 3 independent experiments (biological replicates), performed in triplicate (technical replicates), derived from 2 independent CSF3R-d715 control clones, 2 independent CSF3R-d715 HAX1-W44X clones and 1 CSF3R-d715 ELANE-R103L clone. (b) Gene expression, in transcript per million (TPM), of transcripts associated with more immature hematopoietic stem and progenitor cell stages are upregulated in CSF3R-d715 control HPCs compared with CSF3R-wt control HPCs. (c) Genes expressed at more advanced stages of myeloid differentiation are downregulated in CSF3R-d715 control HPCs, and upregulated in CSF3R-d715 SCN-HPCs compared to their isogenic control. Datapoints represent biological replicates. Additionally, CSF3R-d715 HAX1-W44X data are derived from 2 independent clones and 2 independent experiments. (d) Immunoblots showing neutrophil elastase (NE) protein abundance, which is increased in CSF3R-d715 ELANE-R103L and -I60F HPCs, decreased in CSF3R-d715 control HPCs, and absent in HAX1-W44X HPCs, compared to their isogenic control. Actin was used as loading control.

*TPM: transcript per million. P-values are determined with DESeq2 based on the normalized count data; *=p<0.05, **=p<0.01, ***=p<0.001, ****=p<0.0001. CSF3-normoresponsive: patient who responds good to relatively low dosages of CSF3, CSF3-hyporesponsive: patient who responds poorly to high CSF3-dosages.*

CSF3R-d715 exacerbates an inflammatory state of SCN-HPCs

Chronic inflammatory states of HSPCs have recently been linked to myeloid malignancy, in particular myeloproliferative neoplasms and MDS, where inflammation has been shown to be responsible for the competitive advantage of mutant clones.[18-21] How inflammation contributes to the neutropenic state in SCN, expansion of CSF3R mutant clones, and development of myeloid malignancy is unknown. Upon progression to MDS/AML, most SCN patients acquire *RUNX1* mutations in clones already harboring *CSF3R* mutations.[17] Leukemic progression of SCN in a *Csf3r*-d715/*RUNX1* mutant mouse model revealed increased pro-inflammatory signaling in HPCs, which was further aggravated by the downregulation of TET2.[11] We recently reported that non-leukemic HSPCs from an ELANE-SCN patient who progressed to AML already showed upregulation of interferon (IFN)-response genes before leukemic transformation.[22] In line with a potentially important role for inflammatory signaling in leukemic transformation, activation of the CSF3R-d715 in iPSC-derived cells enhances the expression of IFN-response genes of normo-responsive SCN-HPCs, but not of control HPCs (Figure 2a). IFN-response genes upregulated by CSF3R-d715 in SCN-HPCs include *IRF7*, *IRF9* and *MX1* (Figure 2b). Interestingly, IFN-response genes were also induced, albeit less strongly, in CSF3R-d715 SCN-HPCs derived from the hyporesponsive *ELANE*-I60F

patient (Figures 2a-b), suggesting that this may occur irrespective of a favorable response to CSF3 treatment. Thus, SCN-HPCs that are already rewired towards an inflammatory state endure a further increase in inflammatory signaling upon acquisition of a CSF3R mutation. How CSF3R-d715 and the SCN-causing mutations in *ELANE* or *HAX1* cooperate in enhancing IFN responses, rather than proliferation of HPCs, is not yet clear, but it explains why a strong dominance of CSF3R mutant clones does not occur in patients undergoing CSF3 treatment.[16,23] A possible explanation could be that the increased oxidative stress levels observed in SCN-HPCs play a role in CSF3R-d715 signaling, but this merits further studies.[24]

In conclusion, data presented here combined with previous studies fit into a scenario where increased inflammation of HPCs accompanies disease progression of SCN, creating a vulnerability for mutations leading to malignant transformation (Figure 2c). This differs from how CSF3R truncation mutants function in HPCs without SCN mutations, where their activation merely resulted in a hyper-proliferative response and more immature HPCs (Figure 1).[9-11] In SCN-HPCs, activation of the truncated CSF3R aggravates the inflammatory state initiated by the disease-causing mutation[22], as characterized by the increased expression of IFN-α and IFN-γ response genes (Figure 2). When the HPCs undergo transformation to AML, additional inflammatory pathways (e.g., characterized by upregulation of TNF-α/NF-κB and interleukin-6 response genes) are activated, fueled by the loss of TET2 activity.[11] Because wild-type RUNX1 also inhibits inflammatory cytokine production by neutrophils, *RUNX1* mutations may further enhance the inflamed state of SCN-HPCs, possibly via a feed-back loop involving the more mature progeny of these HPCs.[25]

Figure 2: Activation of CSF3R-d715 induces interferon responses in SCN-HPCs

*(a) Gene set enrichment analysis (GSEA) showing expression of interferon-α and -γ response genes which are unaltered in CSF3R-d715 control HPCs, but induced in CSF3R-d715 SCN-HPCs. Data from 2 independent experiments are combined. Additionally, CSF3R-d715 HAX1-W44X data are derived from 2 independent clones and 2 independent experiments. NES: normalized enrichment score, FDR: false discovery rate. (b) Expression of various interferon-α and -γ response genes in transcript per million (TPM). Datapoints represent biological replicates. Additionally, CSF3R-d715 HAX1-W44X data are derived from 2 independent clones and 2 independent experiments. P-values are determined with DESeq2 based on the normalized count data; *=p<0.05, **=p<0.01, ***=p<0.001, ****=p<0.0001. CSF3-normoresponsive: patient who responds good to relatively low dosages of CSF3, CSF3-hyporesponsive: patient who responds poorly to high CSF3-dosages.*

(c) Schematic overview of the proposed model based on data presented here combined with previous studies.[11,22]

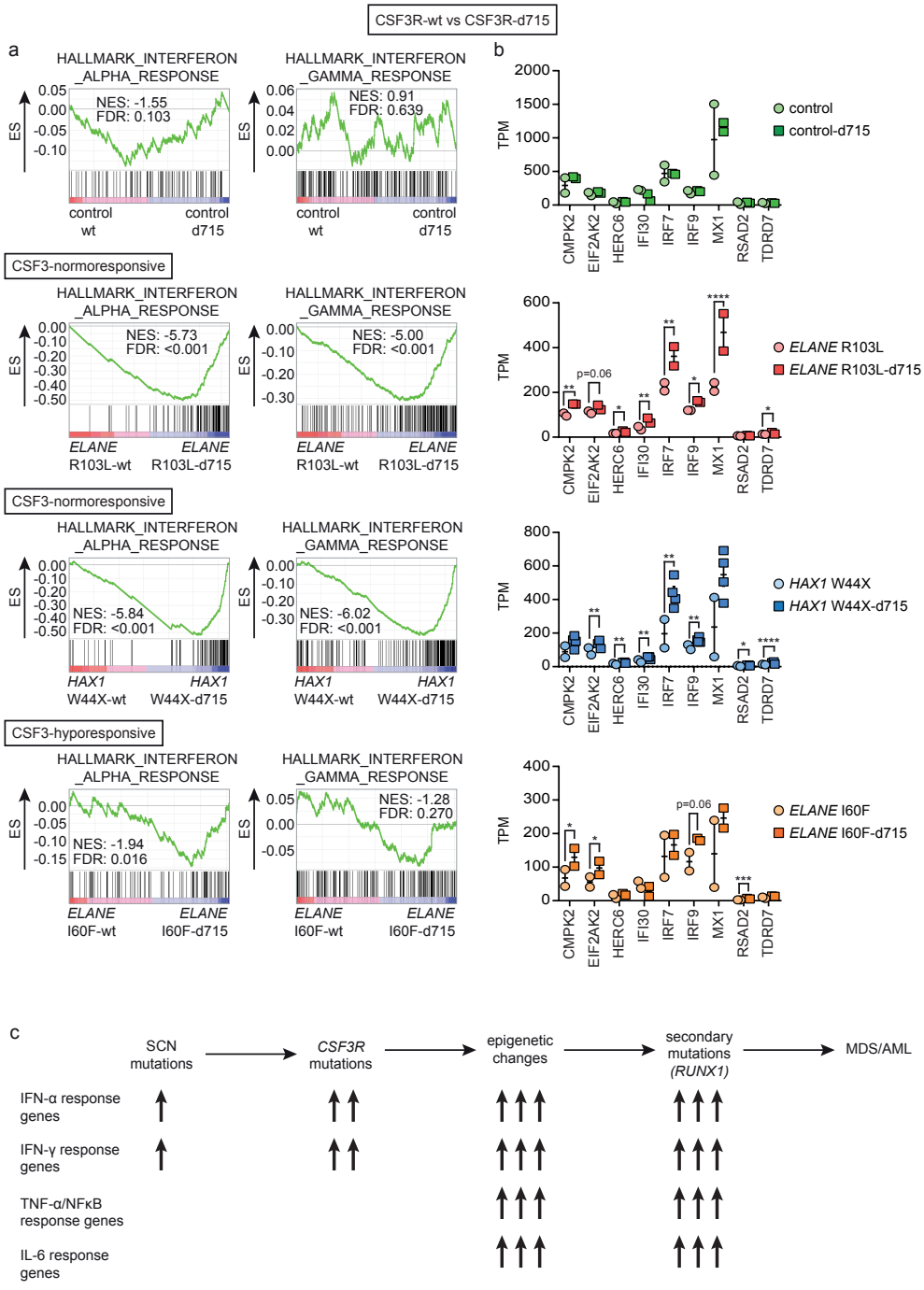
CSF3R-wt vs CSF3R-d715
a
HALLMARK_INTERFERON_ALPHA_RESPONSE
NES: -1.55
FDR: 0.103
HALLMARK_INTERFERON_GAMMA_RESPONSE
NES: 0.91
FDR: 0.639
control wt
control d715
b
TPM
control
control-d715
CSF3-normoresponsive
NES: -5.73
FDR: <0.001
NES: -5.00
FDR: <0.001
ELANE R103L-wt
ELANE R103L-d715
ELANE R103L
ELANE R103L-d715
p=0.06
CSF3-normoresponsive
NES: -5.84
FDR: <0.001
NES: -6.02
FDR: <0.001
HAX1 W44X-wt
HAX1 W44X-d715
HAX1 W44X
HAX1 W44X-d715
CSF3-hyporesponsive
NES: -1.94
FDR: 0.016
NES: -1.28
FDR: 0.270
ELANE I60F-wt
ELANE I60F-d715
ELANE I60F
ELANE I60F-d715
p=0.06
CMPK2
EIF2AK2
HERC6
IFI30
IRF7
IRF9
MX1
RSAD2
TDRD7
c
SCN mutations
CSF3R mutations
epigenetic changes
secondary mutations (RUNX1)
MDS/AML
IFN-α response genes
IFN-γ response genes
TNF-α/NFκB response genes
IL-6 response genes

Acknowledgements

This work was supported by grants from KWF Kankerbestrijding (EMCR 2013-6080 and EMCR 2014-6780), and the Cancer Genome Editing Center of the Erasmus MC Cancer Institute funded by the Daniel den Hoed foundation. The authors thank Mehrnaz Ghazvini for generation of the iPSCs.

Authorship Contributions

Conceptualization, P.A.O. and I.P.T.; Methodology, P.A.O. and H.W.J.d.L.; Formal Analysis, P.A.O. and R.M.H.; Investigation, P.A.O., D.A.B., H.W.J.d.L., P.M.H.v.S., O.R., V.H.J.v.d.V and E.M.J.B.; Data Curation, R.M.H.; Writing – Original Draft, P.A.O. and I.P.T.; Writing – Reviewing & Editing, E.M.J.B., E.M.d.P.; Visualization, P.A.O.; Supervision, I.P.T.; Funding Acquisition, I.P.T.

Disclosure of Conflicts of Interest

The authors have no potential conflict of interest to disclose.

References

1. Skokowa J, Dale DC, Touw IP, Zeidler C, Welte K. Severe congenital neutropenias. *Nat Rev Dis Primers*. 2017;3:17032.
2. Dale DC, Person RE, Bolyard AA, et al. Mutations in the gene encoding neutrophil elastase in congenital and cyclic neutropenia. *Blood*. 2000;96(7):2317-2322.
3. Klein C, Grudzien M, Appaswamy G, et al. HAX1 deficiency causes autosomal recessive severe congenital neutropenia (Kostmann disease). *Nat Genet*. 2007;39(1):86-92.
4. Dale DC, Bonilla MA, Davis MW, et al. A randomized controlled phase III trial of recombinant human granulocyte colony-stimulating factor (filgrastim) for treatment of severe chronic neutropenia. *Blood*. 1993;81(10):2496-2502.
5. Rosenberg PS, Zeidler C, Bolyard AA, et al. Stable long-term risk of leukaemia in patients with severe congenital neutropenia maintained on G-CSF therapy. *Br J Haematol*. 2010;150(2):196-199.
6. Beekman R, Valkhof MG, Sanders MA, et al. Sequential gain of mutations in severe congenital neutropenia progressing to acute myeloid leukemia. *Blood*. 2012;119(22):5071-5077.
7. Ward AC, van Aesch YM, Schelen AM, Touw IP. Defective internalization and sustained activation of truncated granulocyte colony-stimulating factor receptor found in severe congenital neutropenia/acute myeloid leukemia. *Blood*. 1999;93(2):447-458.
8. Irandoust MI, Aarts LH, Roovers O, et al. Suppressor of cytokine signaling 3 controls lysosomal routing of G-CSF receptor. *EMBO J*. 2007;26(7):1782-1793.
9. Dong F, van Buitenen C, Pouwels K, et al. Distinct cytoplasmic regions of the human granulocyte colony-stimulating factor receptor involved in induction of proliferation and maturation. *Mol Cell Biol*. 1993;13(12):7774-7781.
10. Ward AC, Smith L, de Koning JP, van Aesch Y, Touw IP. Multiple signals mediate proliferation, differentiation, and survival from the granulocyte colony-stimulating factor receptor in myeloid 32D cells. *J Biol Chem*. 1999;274(21):14956-14962.
11. Olofsen PA, Fatrai S, van Strien PMH, et al. Malignant Transformation Involving CXXC4 Mutations Identified in a Leukemic Progression Model of Severe Congenital Neutropenia. *Cell Reports Medicine*. 2020;1(5):100074.
12. Chao JR, Parganas E, Boyd K, Hong CY, Opferman JT, Ihle JN. Hax1-mediated processing of HtrA2 by Parl allows survival of lymphocytes and neurons. *Nature*. 2008;452(7183):98-102.
13. Grenda DS, Johnson SE, Mayer JR, et al. Mice expressing a neutrophil elastase mutation derived from patients with severe congenital neutropenia have normal granulopoiesis. *Blood*. 2002;100(9):3221-3228.

14. Dong F, Brynes RK, Tidow N, Welte K, Lowenberg B, Touw IP. Mutations in the gene for the granulocyte colony-stimulating-factor receptor in patients with acute myeloid leukemia preceded by severe congenital neutropenia. *N Engl J Med*. 1995;333(8):487-493.
15. Fukunaga R, Ishizaka-Ikeda E, Nagata S. Growth and differentiation signals mediated by different regions in the cytoplasmic domain of granulocyte colony-stimulating factor receptor. *Cell*. 1993;74(6):1079-1087.
16. Germeshausen M, Ballmaier M, Welte K. Incidence of CSF3R mutations in severe congenital neutropenia and relevance for leukemogenesis: Results of a long-term survey. *Blood*. 2007;109(1):93-99.
17. Skokowa J, Steinemann D, Katsman-Kuipers JE, et al. Cooperativity of RUNX1 and CSF3R mutations in severe congenital neutropenia: a unique pathway in myeloid leukemogenesis. *Blood*. 2014;123(14):2229-2237.
18. Muto T, Walker CS, Choi K, et al. Adaptive response to inflammation contributes to sustained myelopoiesis and confers a competitive advantage in myelodysplastic syndrome HSCs. *Nat Immunol*. 2020;21(5):535-545.
19. Barreyro L, Chlon TM, Starczynowski DT. Chronic immune response dysregulation in MDS pathogenesis. *Blood*. 2018;132(15):1553-1560.
20. Hasselbalch HC. Chronic inflammation as a promotor of mutagenesis in essential thrombocythemia, polycythemia vera and myelofibrosis. A human inflammation model for cancer development? *Leuk Res*. 2013;37(2):214-220.
21. Hasselbalch HC. Perspectives on chronic inflammation in essential thrombocythemia, polycythemia vera, and myelofibrosis: is chronic inflammation a trigger and driver of clonal evolution and development of accelerated atherosclerosis and second cancer? *Blood.* 2012;119(14):3219-3225.
22. Schmied L, Olofsen PA, Lundberg P, et al. Secondary CNL after SAA reveals insights in leukemic transformation of bone marrow failure syndromes. *Blood Adv*. 2020;4(21):5540-5546.
23. Klimiankou M, Uenalan M, Kandabarau S, et al. Ultra-Sensitive CSF3R Deep Sequencing in Patients With Severe Congenital Neutropenia. *Front Immunol*. 2019;10:116.
24. Olofsen PA, Bosch DA, Roovers O, et al. PML-controlled responses in severe congenital neutropenia with ELANE-misfolding mutations. *Blood Adv*. 2021;5(3):775-786.
25. Bellissimo DC, Chen CH, Zhu Q, et al. Runx1 negatively regulates inflammatory cytokine production by neutrophils in response to Toll-like receptor signaling. *Blood Adv.* 2020;4(6):1145-1158.

Supplemental information

Methods

Generation of iPSC

Bone marrow fibroblasts cultured from SCN patients harboring *ELANE* mutation p.I60F (NC_000019.10:g.852986A>T), *ELANE* mutation p.R103L (NC_000019.10:g.853345G>T), or *HAX1* mutation p.W44X (NC_000001.11:g.154273412_154273413insA), and from a healthy control bone marrow were reprogrammed as described previously.[1] Introduction of the *CSF3R*-d715 mutation (Q739*, NC_000001.11:g.36466653C>T) was done using CRISPR-Cas9 mediated genome editing as described previously.[2] The iPSC lines used showed homozygous (control, ELANE-R103L, HAX1-W44X) or heterozygous (ELANE-I60F, HAX1-W44X) integration of the recombination template. If applicable, the wildtype allele was sequenced to determine the lack of possible additional alterations. Introduction of CSF3R-d715 did not affect the potential of the iPSCs to generate CD34+CD45+ HPCs. Cells were cultured in mTeSR™1 (STEMCELL Technologies) on Geltrex™ LDEV-Free Reduced Growth Factor Basement Membrane Matrix (Thermo Fisher Scientific) and were regularly checked for pluripotency, correct karyotype (using Global Screening Array)[3] and their ability to generate hematopoietic progenitor cells and mature neutrophils.

Sanger sequencing and primers

To determine correct integration of the *CSF3R*-d715 mutation and recombination template, an integration PCR was performed followed by sanger sequencing using the following primers; integration PCR: forward 5'-ACCCCACCCAAAGGATGCTGATTTT-3', reverse 5'-TGGCTGGACGTAAACTCCTC-3', sanger sequencing: forward 5'-ACGCCACCCATCACCAAGCT-3', reverse 5'-TGGCTGGACGTAAACTCCTC-3'.

Hematopoietic induction

Hematopoietic Progenitor cells (HPCs, $CD34^{+}CD45^{+}$) were produced with the STEMdiff™ Hematopoietic Kit (STEMCELL Technologies) according to the manufacturer's protocol. Suspension cells were harvested at day 12 of the protocol and used for further downstream analysis.

Flow cytometry and cell sorting

Hematopoietic induction of iPSCs was assessed using CD34-PE (#345802, BD Biosciences) and CD45-FITC (#A07782, Beckman Coulter) antibodies. Dead cells were excluded using 7-aminoactinomycin-D (7AAD, Life Technologies). Flow cytometry was performed using a

LSRII flow cytometer (BD Biosciences). Cell sorting was done using a FACSAria instrument (BD Biosciences). Analysis were performed using FlowJo (TreeStar).

Neutrophil differentiation

To expand myeloid progenitors and subsequently differentiate them into mature neutrophils, $2x10^5$ suspension cells/ml were plated in a non-tissue culture treated plate in IMDM (Life Technologies) complemented with 10% defined FBS (HyClone), 10ng/ml IL3 (R&D systems), 10ng/ml GM-CSF (PeproTech), 50ng/ml SCF (CellGenix GmbH) and 50ng/ml CSF3 (Filgastrim, Zarzio) as described previously.[4] After 4 days, medium was switched to IMDM complemented with 10% defined FBS and 50ng/ml CSF3. Cells were harvested 5 days later and used for subsequent FACS analysis with the EuroFlow AML tube 1.[5,6]

Bioinformatics

Demultiplexing was performed using the CASAVA software (Illumina) allowing for one mismatch in the barcodes. Subsequently, SMARTer adapters and poly-A tails were removed (fqtrim; https://ccb.jhu.edu/software/fqtrim/) and quality metrics were estimated (FastQC, Babraham bioinformatics & MultiQC, http://multiqc.info) for all of the resulting fastq files. Reads were then aligned against the Human Transcriptome (Gencode v19)/Genome (hg19) using the STAR aligner,[7] and visualized with the Integrative Genomics Viewer (IGV; https://software.broadinstitute.org/software/igv/).[8] Abundance estimation was performed using Cufflinks (refSeq9), and raw counts were measured with the HTSeq-count software set in union mode.10 Next, the measured raw counts were used to create clustering and principal component plots and to perform differential expression analysis using a combination of DESeq211 and R (https://www.r-project.org/). Gene set enrichment analysis on the curated gene sets C2 and the hallmark pathways H was done using the GSEA software (https://www.gsea-msigdb.org/gsea/msigdb/genesets.jsp) based on the pre-ranked ASHR log2 fold change, where a false discovery rate (FDR) <0.05 was considered significant.[12,13] Transcripts per million (TPM) were calculated using StringTie.[14]

References

1. Warlich E, Kuehle J, Cantz T, et al. Lentiviral vector design and imaging approaches to visualize the early stages of cellular reprogramming. *Mol Ther*. 2011;19(4):782-789.
2. Olofsen PA, Fatrai S, van Strien PMH, et al. Malignant Transformation Involving CXXC4 Mutations Identified in a Leukemic Progression Model of Severe Congenital Neutropenia. *Cell Reports Medicine*. 2020;1(5):100074.
3. Wang K, Li M, Hadley D, et al. PennCNV: an integrated hidden Markov model designed for high-resolution copy number variation detection in whole-genome SNP genotyping data. *Genome Res*. 2007;17(11):1665-1674.
4. Nayak RC, Trump LR, Aronow BJ, et al. Pathogenesis of ELANE-mutant severe neutropenia revealed by induced pluripotent stem cells. *J Clin Invest*. 2015;125(8):3103-3116.
5. van Dongen JJ, Lhermitte L, Bottcher S, et al. EuroFlow antibody panels for standardized n-dimensional flow cytometric immunophenotyping of normal, reactive and malignant leukocytes. *Leukemia*. 2012;26(9):1908-1975.
6. Olofsen PA, Touw IP. Chapter 5 - Modeling severe congenital neutropenia in induced pluripotent stem cells. In: Birbrair A, ed. *Recent Advances in iPSC Disease Modeling, Volume 1*. Academic Press; 2020:85-101.
7. Dobin A, Davis CA, Schlesinger F, et al. STAR: ultrafast universal RNA-seq aligner. *Bioinformatics.* 2013;29(1):15-21.
8. Robinson JT, Thorvaldsdottir H, Winckler W, et al. Integrative genomics viewer. *Nat Biotechnol.* 2011;29(1):24-26.
9. Trapnell C, Williams BA, Pertea G, et al. Transcript assembly and quantification by RNA-Seq reveals unannotated transcripts and isoform switching during cell differentiation. *Nat Biotechnol.* 2010;28(5):511-515.
10. Anders S, Pyl PT, Huber W. HTSeq--a Python framework to work with high-throughput sequencing data. *Bioinformatics.* 2015;31(2):166-169.
11. Love MI, Huber W, Anders S. Moderated estimation of fold change and dispersion for RNA-seq data with DESeq2. *Genome Biol.* 2014;15(12):550.
12. Mootha VK, Lindgren CM, Eriksson KF, et al. PGC-1alpha-responsive genes involved in oxidative phosphorylation are coordinately downregulated in human diabetes. *Nat Genet.* 2003;34(3):267-273.
13. Subramanian A, Tamayo P, Mootha VK, et al. Gene set enrichment analysis: a knowledge-based approach for interpreting genome-wide expression profiles. *Proc Natl Acad Sci U S A.* 2005;102(43):15545-15550.
14. Pertea M, Kim D, Pertea GM, et al. Transcript-level expression analysis of RNA-seq experiments with HISAT, StringTie and Ballgown. *Nat Protoc*. 2016;11(9):1650-1667.

Supplemental Figures

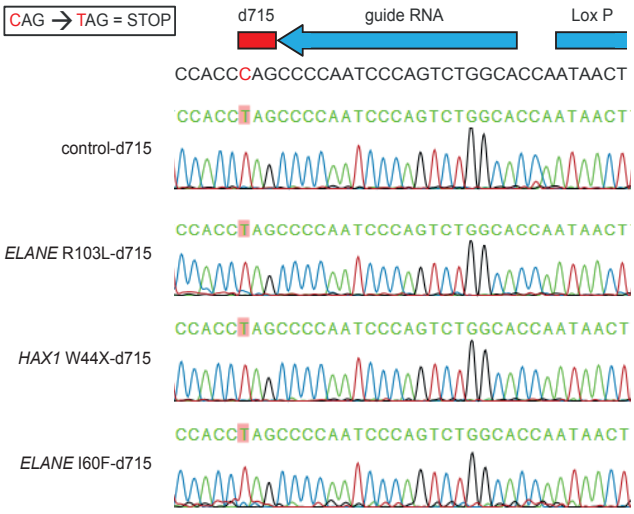

Figure S1: Introduction of CSF3R-d715 (Q739) in iPSC lines*

Sanger sequencing data showing the introduction of the C>T mutation, resulting in a premature stop codon, and the correct integration of the recombination template.[2]

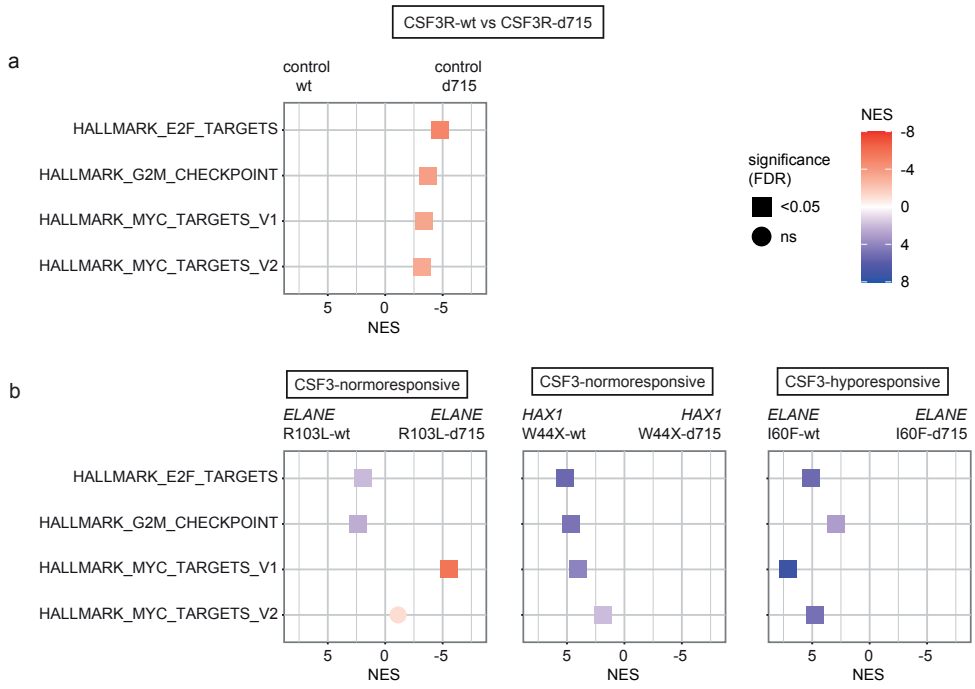

Figure S2: Cell cycle and proliferation associated pathways are upregulated in control-d715 HPCs
Gene set enrichment analysis (GSEA) hallmark pathways showing the expression of E2F targets, G2M checkpoint and MYC targets which are (a) induced in CSF3R-d715 control HPCs compared to their CSF3R-wt counterpart, and (b) reduced or not consistently altered in CSF3R-d715 SCN-HPCs compared to their isogenic control. Data are combined from 2 independent experiments. Additionally, CSF3R-d715 HAX1-W44X data are derived from 2 independent clones and 2 independent experiments. NES: normalized enrichment score, FDR: false discovery rate, ns: not significant. CSF3-normoresponsive: patient responding favorably to relatively low (5 to 10 µg per kg body weight per day) dosages of CSF3, CSF3-hyporesponsive: patient responding poorly, even to high CSF3-dosages.

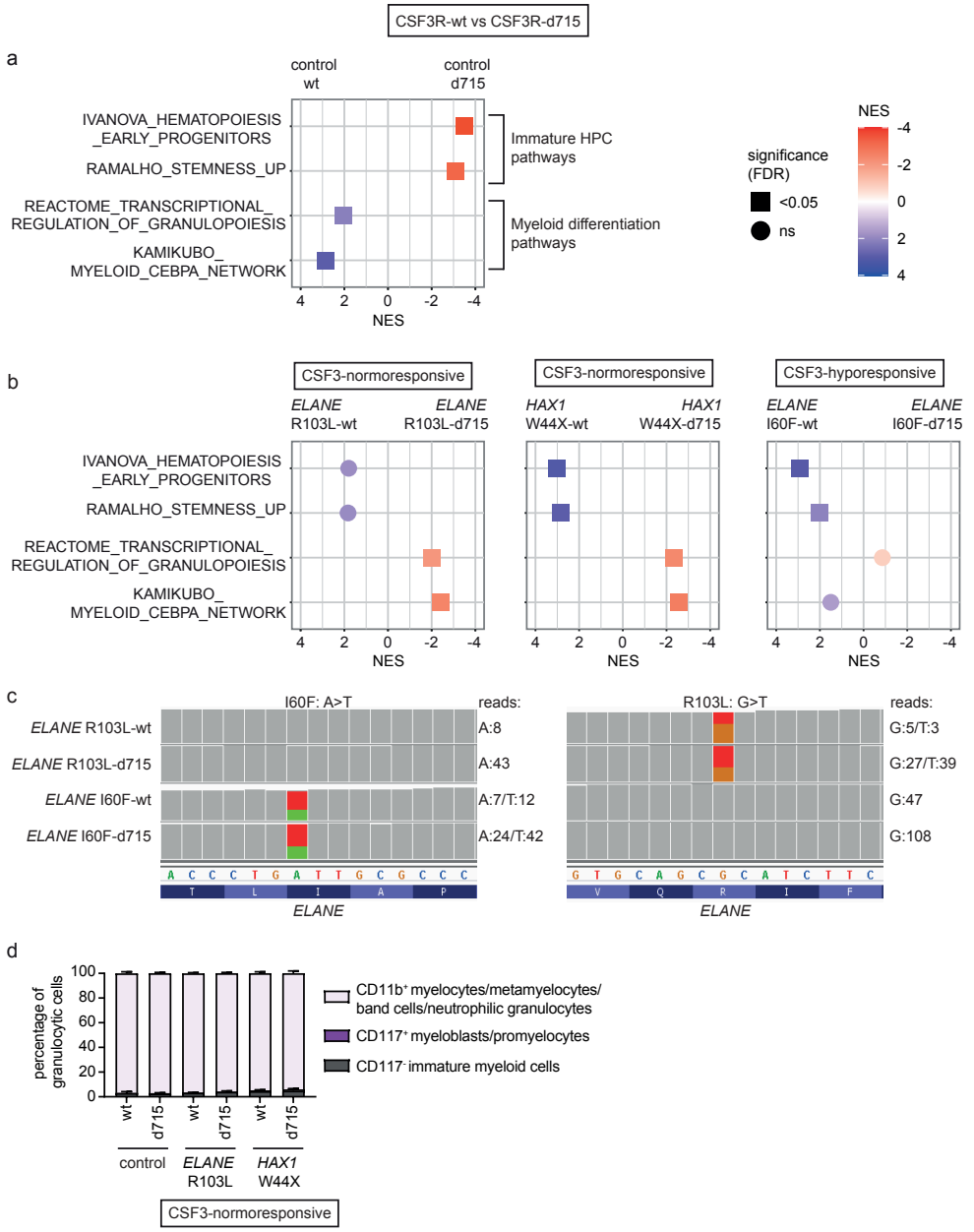

Figure S3: Increased expression of myeloid pathways and genes in SCN-d715 HPCs

(a+b) GSEA showing the expression of more immature HPC pathways, e.g., early hematopoietic progenitors and stemness, and mature myeloid pathways, e.g., C/EBPα network and transcriptional regulation of granulopoiesis. Data are combined from 2 independent experiments and depict the comparison of CSF3R-wt and CSF3R-d715 HPCs. Additionally, CSF3R-d715 HAX1-W44X data are derived from 2 independent clones and 2 independent experiments. NES: normalized enrichment score, FDR:

false discovery rate, ns: not significant. (a) CSF3R-d715 control HPCs show expression of more immature HPC pathways, while expression of myeloid differentiation pathways is reduced. (b) CSF3R-d715 SCN-HPCs express more myeloid differentiation related pathway genes, while immature HPC pathways are downregulated. (c) Integrated genome viewer (IGV) snapshot depicting the expression of wildtype and mutant ELANE before and after introduction of the CSF3R-d715. ELANE-I60F: A (green) > T (red), ELANE-R103L: G (orange) > T (red). Numbers represent the number of reads for the depicted nucleotide. (d) Quantifications of the myeloid cells present in CSF3-containing liquid culture which show no differences after introducing the CSF3R-d715, consistent with the CSF3-normoresponsiveness of the ELANE-R103L and HAX1-W44X patient. Data are from 3 independent experiments (biological replicates).
CSF3-normoresponsive: patient responding favorably to relatively low (5 to 10 µg per kg body weight per day) dosages of CSF3; CSF3-hyporesponsive: patient responding poorly, even to high CSF3-dosages.

Chapter 5

RUNX1 mutations in the leukemic progression of severe congenital neutropenia

Patricia A. Olofsen[1] and Ivo P. Touw[1]

[1] Department of Hematology, Erasmus University Medical Center, Rotterdam 3015 CN, the Netherlands

Mol Cells. 2020 Feb 29;43(2):139-144

Abstract

Somatic *RUNX1* mutations are found in approximately 10% of patients with *de novo* acute myeloid leukemia (AML), but are more common in secondary forms of myelodysplastic syndrome (MDS) or AML. Particularly, this applies to MDS/AML developing from certain types of leukemia-prone inherited bone marrow failure syndromes. How these *RUNX1* mutations contribute to the pathobiology of secondary MDS/AML is still unknown. This mini-review focusses on the role of RUNX1 mutations as the most common secondary leukemogenic hit in MDS/AML evolving from severe congenital neutropenia (SCN).

Introduction

The occurrence and frequency of *RUNX1* mutations in a variety of hematological malignancies has been well-documented[1]. Originally identified as a chromosomal translocation partner in the so-called core-binding factor (CBF) leukemias, somatic *RUNX1* mutations were also found in myeloid malignancies, particularly in myelodysplastic syndrome (MDS) and acute myeloid leukemia (AML)[2-10]. Somatic mutations in RUNX1 cluster mostly within the N-terminal Runt homology domain (RHD) whereas mutations disrupting the C-terminal transactivation domain (TAD) occur less frequently[4,8,10,11]. Importantly, mutations in *RUNX1* were identified as the cause of familial platelet disorder, in which patients show a predisposition to develop MDS or AML (FPDMM or FPD/AML)[12]. These germline mutations are similar to those acquired in MDS/AML[12]. Finally, it has become clear that somatic *RUNX1* mutations are particularly prevalent in MDS/AML secondary to inherited bone marrow failure syndromes (iBMFs) such as Fanconi anemia and severe congenital neutropenia (SCN), and in radiation-associated MDS/AML[13-15]. These forms of secondary MDS/AML (sMDS/AML) are characterized by an adverse prognosis due to refractoriness to treatment. Why secondary *RUNX1* mutations are associated with sMDS/AML and how they contribute to the pathogenesis of these conditions remains largely unclear. Here, we will discuss the current insights and ideas regarding mutant *RUNX1* in the context of malignant transformation of iBMFs, taking SCN as the leading example. Specifically, we will briefly summarize and discuss our most recent insights into these issues based on observations in patients, mouse- and induced pluripotent stem cell (iPSC)-models.

Severe congenital neutropenia

SCN is an iBMF characterized by severely reduced neutrophil counts, leading to life-threatening bacterial infections[16]. Autosomal dominant mutations in *ELANE*, the gene encoding neutrophil elastase, are the most frequently observed genetic defects in SCN patients. How these mutations give rise to severe neutropenia is still largely unknown[16]. Life-long administration of colony stimulating factor 3 (CSF3), also known as granulocyte colony-stimulating factor (G-CSF), successfully alleviates the neutropenia in the majority of SCN patients[17]. Importantly, SCN patients have a high risk of developing MDS or AML, with a median incidence of 21%, 15 years after initiation of CSF3 treatment[18,19]. The majority of SCN patients with leukemic progression show the appearance of hematopoietic clones with somatic mutations in *CSF3R*, resulting in a truncated form of CSF3R with defective internalization and aberrant signaling properties[20]. These clones may persist for months or even years before MDS or AML becomes overt[21], raising the question how these CSF3R mutants contribute to the malignant transformation of SCN. Activation of oxidative stress

through enhanced production of reactive oxygen species (ROS) and sustained activation of signal transducer and activator of transcription STAT5 have been put forward as candidate mechanisms by which activation of truncated CSF3R drive clonal expansion of myeloid progenitors [22,23].

RUNX1 mutations in SCN-MDS/AML patients

Like for numerous other disease conditions, the introduction of massive parallel ("next generation") sequencing has greatly advanced our insights into the genomic defects associated with the leukemic progression of SCN. A retrospective analysis in an ELANE-SCN patient, who continuously received CSF3 therapy for 15 years and during which period serial BM sampling was done, showed that after the occurrence of multiple CSF3R mutant clones 2 years after the start of CSF3 treatment, no additional mutations were detected until MDS/AML became clinically overt[24]. At that fully transformed stage, a limited number of clonal mutations in regulatory genes, including *RUNX1*, *SUZ12*, *ASXL1* and *EP300,* were present[24]. This pattern of leukemic evolution was confirmed in a follow-up study involving 31 SCN-MDS/AML cases[15]. Importantly, this study revealed that mutations in *RUNX1* are by far the most frequent somatic secondary mutations in SCN-MDS/AML and preferentially occurred in *CSF3R* mutation clones. In SCN-MDS/AML, mainly *RUNX1* mutations disrupting the runt homology domain (RHD), essential for DNA binding and for interaction with the regulatory protein core-binding factor β, were found[15,24]. In view of these characteristics, the molecular pathogenesis of SCN/AML serves as an attractive model to investigate the role of secondary RUNX1 mutations in a molecularly well-defined process of leukemic progression.

Mouse model to study the impact of *Csf3r* and *RUNX1* mutations in conjunction with CSF3-treatment

The impact of Runx1 and mutants on hematopoietic cell development has been investigated in a variety of mouse models and has been the subject of several recent reviews[1,25-27]. Notwithstanding some contradictory results, possibly related to discrepancies in the immune-phenotyping based classification of stem cell subpopulations, it is generally accepted that wild type Runx1 has no major impact on the production and function of long-term hematopoietic stem cells (LT-HSCs) in mice, both under homeostatic conditions and under conditions of proliferative stress[28]. More relevant in the context of RUNX1 mutations in SCN-MDS/AML are the mouse models with RUNX1-RHD mutations equivalent to those recurrently found in patients[5]. Watanabe-Okochi and colleagues studied the effects of such a mutant in transplantation experiments, in which donor bone marrow (BM) cells were transduced with a murine leukemia virus (MLV)-derived vector to express the most common RUNX1 mutant D171N and reported that this resulted in MDS and MDS/AML [29]. However,

integration of the MLV-based vector in the *Mecom* (*Evi1*) locus caused overexpression of Evi1 in these mice[29]. Because the combination of *RUNX1* mutations and high EVI1 expression is rarely seen in MDS/AML, and because high Evi1 expression can be leukemogenic by itself, the contribution of RUNX1-RHD in MDS/AML development in more general could not be accurately deduced from this model[29,30]. In fact, expression of mutant D171N in human cord blood cells had marginal effects on the rate of proliferation and differentiation capacity of $CD34^+$ cells in *in vitro* suspension culture relative to empty vector control cells, suggesting that isolated RUNX-RHD mutations are only weakly leukemogenic[31].

To study the role of RUNX1-D171N in a context relevant to SCN-MDS/AML, we used a mouse model expressing a truncated Csf3r (Csf3r-d715) identical to the mutant CSF3R form in SCN patients[32,33]. To avoid the tropism of MLV-based vectors for oncogenic enhancers, we generated a lentiviral expression vector to express RUNX1 mutant D171N[31] in conjunction with enhanced green fluorescent protein (eGFP) in Csf3r-d715 BM cells, which were subsequently serially transplanted in wild type recipients. Recipients were treated either 3x a week with CSF3 or with PBS (solvent control). Transcriptome analysis and whole exome sequencing on FACS purified $eGFP^+Lin^-c\text{-}Kit^+$ (LK) populations were done to identify molecular pathways associated with leukemic progression. Sequential $CD34^+$ cell samples from a SCN/AML patient with identical *CSF3R* and *RUNX1* mutations[24] and whole genome sequencing data from diagnostic AML samples were used for clinical comparisons[34].

CSF3 treatment of primary recipients transplanted with *Csf3r-RUNX1* mutant BM cells resulted in sustained (30+ weeks) presence of $eGFP^+$LK cells in the peripheral blood (PB), which had the morphological appearance of myeloblasts. The PB also contained $eGFP^+$ neutrophils, indicating that myeloid differentiation was not completely blocked. Importantly, none of these primary recipient mice succumbed to symptoms of AML, suggesting that the elevated myeloblasts in the PB reflected a pre-leukemic rather than a fully transformed state. However, upon transplantation in secondary and tertiary recipients, mice developed *Csf3r-RUNX1* mutant AML that was no longer dependent on CSF3 administration. Transcriptome profiles of purified $eGFP^+$LK cells sorted before transplantation, showed that expression of *RUNX1* mutant protein in *Csf3r* mutant cells resulted in elevated proliferative/metabolic signatures characterized by elevated MYC and mTORC1 signaling relative to empty vector controls. Strikingly, at the sequential steps of leukemic transformation in the mouse model, these signatures declined while TNFα-, interferon- and interleukin-6-driven inflammatory responses were increasingly upregulated. Whole exome sequencing performed on the LK- cells from these stages revealed that an internal tandem duplication (ITD) in *Cxxc4* was acquired. In the secondary and tertiary recipients all AML cells harbored the *Csf3r*, *RUNX1* and heterozygous *Cxxc4* mutations, while the primary recipient showed a subclonal *Cxxc4* mutation (VAF: 0.27). The mutation resulted in a 7-fold higher expression of CXXC4 protein. CXXC4 was previously shown to inhibit TET2 protein levels[35,36] and in agreement with this,

TET2 levels were strongly reduced in the CXXC4 mutant/overexpressing leukemic samples. Intriguingly, *CXXC4* mutations have also been detected in human AML cases, including the ITD mutations identified in our mouse model[34]. These observations in mice fit into a model in which the activation of a truncated Csf3r by the sustained administration of CSF3 and the presence of RUNX1-RHD mutant D171N give rise to a premalignant state, characterized by the accumulation of LK cells in the PB and elevated activation of proliferative signalling (Figure 1). An additional clonal mutation that reduces the levels of TET2 drives the full transformation to AML, at which stage the leukemia-initiating cells have lost their need for CSF3 for propagation *in vivo* and the AML blasts have adopted an inflammatory signature identical to that of SCN/AML cells with identical mutations in *CSF3R* and *RUNX1* (Figure 1)[24,37]. Although CXXC4 mutations have thus far not been reported in clinical SCN/AML samples, mutations potentially affecting TET2 levels and/or function, such as mutations in polycomb repressor complex-2 genes (EZH2, SUZ12) are recurrently present[15,24].

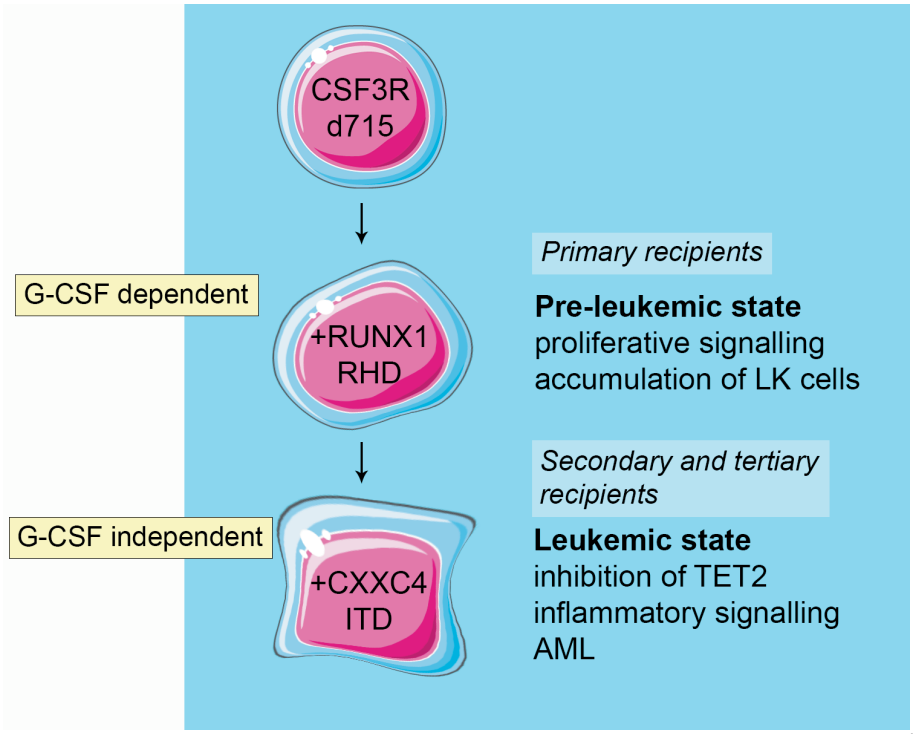

Figure 1: Model of leukemic progression in mice based on serial transplantation of Csf3r-d715/RUNX1-RHD mutant BM cells.

In primary recipients, the combination of Csf3r-d715 and RUNX1-D171N gives rise to accumulation of immature LK cells. This occurs only when mice are treated with G-CSF (CSF3) and mice do not succumb to symptoms of leukemia. Upon secondary and subsequent transplantations of these LK cells, a G-CSF independent AML develops, which is characterized by elevated inflammatory responses and reduced TET2 protein levels.

Studies in induced pluripotent stem cell (iPSC) models

The use of patient-derived iPSC lines has created new possibilities to model diseases, including myeloid malignancies[38]. In the context of *RUNX1*, these studies have mainly dealt with FPD/AML, characterized by germline *RUNX1* mutations[39-41]. Key features of these iPSC lines are (i) their reduced ability to generate $CD34^+CD45^+$ hematopoietic stem and progenitor cells (HSPCs) and (ii) their affected ability of megakaryocyte (Mk) production and pro-platelet formation, thus explaining the platelet defects observed in patients. The reduced production of HSPCs from FPD-derived iPSCs is consistent with a role of RUNX1 in hematopoietic development from pluripotent stem cells[42]. As mentioned above, in SCN patients who develop MDS or AML, *RUNX1* mutations are most often acquired in *CSF3R* mutant HSPC clones. Hence, it is important in this context to assess the consequences of somatic *RUNX1* mutations in HSPCs cells that already harbor a *CSF3R* nonsense mutation. To achieve this, a CRISPR/Cas9-based strategy was used to introduce a patient-derived *CSF3R* nonsense mutation into iPSCs. After switching the cells to hematopoietic culture conditions (STEMdiff Hematopoietic Kit from STEMCELL Technologies), $CD34^+CD45^+$ cells were lentivirally transduced to express the *RUNX1-RHD* D171N mutant. These experiments showed that the combined presence of *CSF3R* and *RUNX1* mutations had a moderate effect on myeloid differentiation, characterized by a relative abundance of immature neutrophilic differentiation stages, but not by an absolute differentiation block (Figure 2). As such, these findings corroborate the findings in the mouse model described above and further suggest that secondary *RUNX1* mutations in clones with CSF3R mutations do not confer a fully transformed, i.e., MDS/AML like phenotype. In agreement with this, transcriptome analysis showed that the *CSF3R-RUNX1* mutant cells had elevated proliferative signatures but did not show the inflammatory profiles seen in the SCN/AML patient and the mouse AML cells. A key question that remains to be addressed is how mutations in *ELANE*, *HAX1* and other SCN-causing mutations contribute to leukemic progression in conjunction with *CSF3R* and *RUNX1* mutations. Preliminary data from these models suggest that *ELANE* and *HAX1* mutations cause elevated levels of reactive oxygen species (ROS) in $CD34^+CD45^+$ HSPCs generated from SCN-iPSCs, resulting in the upregulation of anti-oxidant pathways[43] (and Olofsen PA et al., manuscript submitted). Future work should clarify whether and to what extent the oxidative damage caused by ROS and the adaptive anti-oxidant protection mechanisms contribute to malignant transformation.

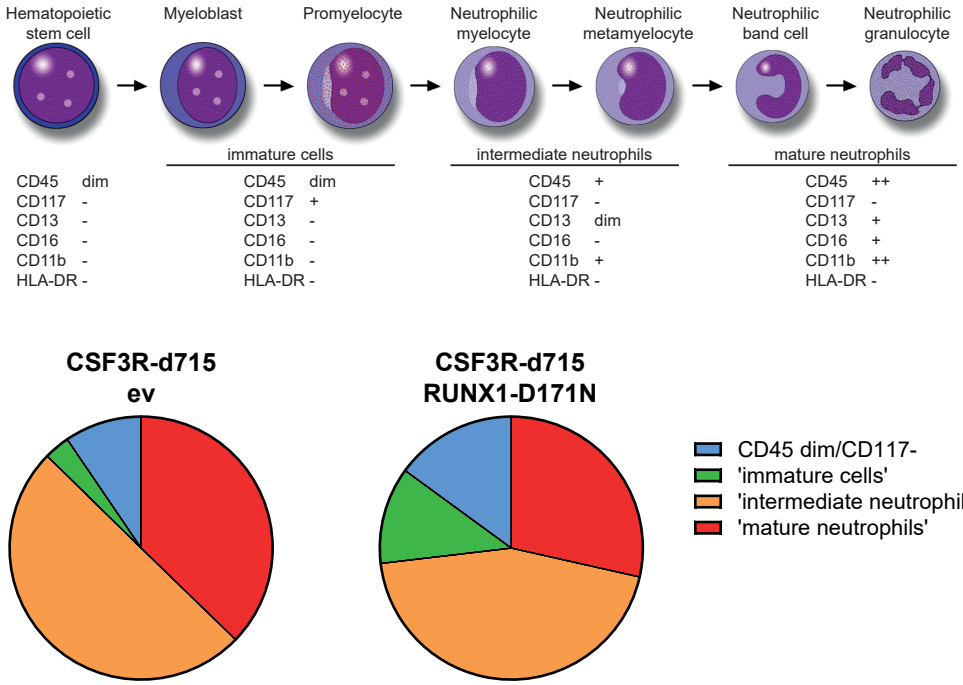

Figure 2: Myeloid differentiation of iPSC-derived $CD34^{\pm}CD45^{\pm}$ cells, genome-edited to express a truncated form (d715) of CSF3R and transduced with RUNX1-D171N lentiviral expression vector or empty vector (ev) control.

Cells were cultured in suspension for a total of 9 days in medium supplemented with myeloid growth factors, i.e., a cocktail of IL3, SCF, GM-CSF and G-CSF for the first 4 days, followed by G-CSF as the single growth factor for the next 5 days.

Conclusions and outlook

The role of RUNX1 mutations in the development of MDS and AML remains incompletely understood. Studies in mouse-, patient- and iPSC-models, addressing the role of a recurrent *RUNX1* mutation (D171N) in combination with the most frequent *CSF3R* mutation in the leukemic progression of SCN (CSF3R-d715), showed that RUNX1-D171N enhanced the activation of proliferative signaling pathways but only mildly affected myeloid differentiation, leading to a relative accumulation of immature cells but not to an absolute differentiation block. Furthermore, the studies in mice showed that the combination of these two mutations is not enough for leukemic progression, even when the mice were subjected to sustained G-CSF (CSF3) treatment. These findings established that additional events, one of which affecting TET2 levels, are necessary for full leukemic transformation. Leukemic progression in all models was also associated with enhanced interferon-γ, interleukin-6 and TNFα/NFκB

signaling, suggesting that inflammation is a major additional component in the development of myeloid malignancy involving RUNX1 mutations. How this interplay between mutant CSF3R signaling, aberrant transcriptional control by mutant RUNX1, loss of TET2 function and inflammatory responses contributes to leukemic transformation and what the exact causal relationships between these mechanisms are remains to be addressed. Detailed insights into this complex network of events may help to discover biomarkers for early detection of leukemic progression of SCN and possibly other forms of iBMFs and may provide leads for novel forms of therapeutic intervention to avoid full malignant transformation of these conditions.

Acknowledgement

This work was financially supported by grants from the Dutch Cancer Society “KWF-kankerbestrijding”.

References

1. Sood R, Kamikubo Y, Liu P. Role of RUNX1 in hematological malignancies. *Blood*. 2017;129(15):2070-2082.
2. Chen CY, Lin LI, Tang JL, et al. RUNX1 gene mutation in primary myelodysplastic syndrome--the mutation can be detected early at diagnosis or acquired during disease progression and is associated with poor outcome. *Br J Haematol*. 2007;139(3):405-414.
3. Christiansen DH, Andersen MK, Pedersen-Bjergaard J. Mutations of AML1 are common in therapy-related myelodysplasia following therapy with alkylating agents and are significantly associated with deletion or loss of chromosome arm 7q and with subsequent leukemic transformation. *Blood*. 2004;104(5):1474-1481.
4. Gaidzik VI, Bullinger L, Schlenk RF, et al. RUNX1 mutations in acute myeloid leukemia: results from a comprehensive genetic and clinical analysis from the AML study group. *J Clin Oncol*. 2011;29(10):1364-1372.
5. Harada H, Harada Y, Niimi H, Kyo T, Kimura A, Inaba T. High incidence of somatic mutations in the AML1/RUNX1 gene in myelodysplastic syndrome and low blast percentage myeloid leukemia with myelodysplasia. *Blood*. 2004;103(6):2316-2324.
6. Mangan JK, Speck NA. RUNX1 mutations in clonal myeloid disorders: from conventional cytogenetics to next generation sequencing, a story 40 years in the making. *Crit Rev Oncog*. 2011;16(1-2):77-91.
7. Osato M. Point mutations in the RUNX1/AML1 gene: another actor in RUNX leukemia. *Oncogene*. 2004;23(24):4284-4296.
8. Schnittger S, Dicker F, Kern W, et al. RUNX1 mutations are frequent in de novo AML with noncomplex karyotype and confer an unfavorable prognosis. *Blood*. 2011;117(8):2348-2357.
9. Steensma DP, Gibbons RJ, Mesa RA, Tefferi A, Higgs DR. Somatic point mutations in RUNX1/CBFA2/AML1 are common in high-risk myelodysplastic syndrome, but not in myelofibrosis with myeloid metaplasia. *Eur J Haematol*. 2005;74(1):47-53.
10. Tang JL, Hou HA, Chen CY, et al. AML1/RUNX1 mutations in 470 adult patients with de novo acute myeloid leukemia: prognostic implication and interaction with other gene alterations. *Blood*. 2009;114(26):5352-5361.
11. Preudhomme C, Warot-Loze D, Roumier C, et al. High incidence of biallelic point mutations in the Runt domain of the AML1/PEBP2 alpha B gene in Mo acute myeloid leukemia and in myeloid malignancies with acquired trisomy 21. *Blood*. 2000;96(8):2862-2869.
12. Song WJ, Sullivan MG, Legare RD, et al. Haploinsufficiency of CBFA2 causes familial thrombocytopenia with propensity to develop acute myelogenous leukaemia. *Nat Genet*. 1999;23(2):166-175.

13. Harada H, Harada Y, Tanaka H, Kimura A, Inaba T. Implications of somatic mutations in the AML1 gene in radiation-associated and therapy-related myelodysplastic syndrome/acute myeloid leukemia. *Blood*. 2003;101(2):673-680.
14. Quentin S, Cuccuini W, Ceccaldi R, et al. Myelodysplasia and leukemia of Fanconi anemia are associated with a specific pattern of genomic abnormalities that includes cryptic RUNX1/AML1 lesions. *Blood*. 2011;117(15):e161-170.
15. Skokowa J, Steinemann D, Katsman-Kuipers JE, et al. Cooperativity of RUNX1 and CSF3R mutations in severe congenital neutropenia: a unique pathway in myeloid leukemogenesis. *Blood*. 2014;123(14):2229-2237.
16. Skokowa J, Dale DC, Touw IP, Zeidler C, Welte K. Severe congenital neutropenias. *Nat Rev Dis Primers*. 2017;3:17032.
17. Dale DC, Bonilla MA, Davis MW, et al. A randomized controlled phase III trial of recombinant human granulocyte colony-stimulating factor (filgrastim) for treatment of severe chronic neutropenia. *Blood*. 1993;81(10):2496-2502.
18. Rosenberg PS, Alter BP, Bolyard AA, et al. The incidence of leukemia and mortality from sepsis in patients with severe congenital neutropenia receiving long-term G-CSF therapy. *Blood*. 2006;107(12):4628-4635.
19. Rosenberg PS, Zeidler C, Bolyard AA, et al. Stable long-term risk of leukaemia in patients with severe congenital neutropenia maintained on G-CSF therapy. *Br J Haematol*. 2010;150(2):196-199.
20. Touw IP. Game of clones: the genomic evolution of severe congenital neutropenia. *Hematology Am Soc Hematol Educ Program*. 2015;2015:1-7.
21. Germeshausen M, Ballmaier M, Welte K. Incidence of CSF3R mutations in severe congenital neutropenia and relevance for leukemogenesis: Results of a long-term survey. *Blood*. 2007;109(1):93-99.
22. Liu F, Kunter G, Krem MM, et al. Csf3r mutations in mice confer a strong clonal HSC advantage via activation of Stat5. *J Clin Invest*. 2008;118(3):946-955.
23. Zhu QS, Xia L, Mills GB, Lowell CA, Touw IP, Corey SJ. G-CSF induced reactive oxygen species involves Lyn-PI3-kinase-Akt and contributes to myeloid cell growth. *Blood*. 2006;107(5):1847-1856.
24. Beekman R, Valkhof MG, Sanders MA, et al. Sequential gain of mutations in severe congenital neutropenia progressing to acute myeloid leukemia. *Blood*. 2012;119(22):5071-5077.
25. Bellissimo DC, Speck NA. RUNX1 Mutations in Inherited and Sporadic Leukemia. *Front Cell Dev Biol*. 2017;5:111.
26. Chin DW, Watanabe-Okochi N, Wang CQ, Tergaonkar V, Osato M. Mouse models for core binding factor leukemia. *Leukemia*. 2015;29(10):1970-1980.

27. Harada Y, Harada H. Molecular pathways mediating MDS/AML with focus on AML1/RUNX1 point mutations. *J Cell Physiol*. 2009;220(1):16-20.
28. Cai X, Gaudet JJ, Mangan JK, et al. Runx1 loss minimally impacts long-term hematopoietic stem cells. *PLoS One*. 2011;6(12):e28430.
29. Watanabe-Okochi N, Kitaura J, Ono R, et al. AML1 mutations induced MDS and MDS/AML in a mouse BMT model. *Blood*. 2008;111(8):4297-4308.
30. Harada Y, Inoue D, Ding Y, et al. RUNX1/AML1 mutant collaborates with BMI1 overexpression in the development of human and murine myelodysplastic syndromes. *Blood*. 2013;121(17):3434-3446.
31. Goyama S, Schibler J, Cunningham L, et al. Transcription factor RUNX1 promotes survival of acute myeloid leukemia cells. *J Clin Invest*. 2013;123(9):3876-3888.
32. Hermans MH, Antonissen C, Ward AC, Mayen AE, Ploemacher RE, Touw IP. Sustained receptor activation and hyperproliferation in response to granulocyte colony-stimulating factor (G-CSF) in mice with a severe congenital neutropenia/acute myeloid leukemia-derived mutation in the G-CSF receptor gene. *J Exp Med*. 1999;189(4):683-692.
33. Hermans MH, Ward AC, Antonissen C, Karis A, Lowenberg B, Touw IP. Perturbed granulopoiesis in mice with a targeted mutation in the granulocyte colony-stimulating factor receptor gene associated with severe chronic neutropenia. *Blood*. 1998;92(1):32-39.
34. Olofsen PA, Fatrai S, van Strien PMH, et al. Malignant Transformation Involving CXXC4 Mutations Identified in a Leukemic Progression Model of Severe Congenital Neutropenia. *Cell Reports Medicine*. 2020;1(5):100074.
35. Ko M, An J, Bandukwala HS, et al. Modulation of TET2 expression and 5-methylcytosine oxidation by the CXXC domain protein IDAX. *Nature*. 2013;497(7447):122-126.
36. Hino S, Kishida S, Michiue T, et al. Inhibition of the Wnt signaling pathway by Idax, a novel Dvl-binding protein. *Mol Cell Biol*. 2001;21(1):330-342.
37. Schmied L, Olofsen PA, Lundberg P, et al. Secondary CNL after SAA reveals insights in leukemic transformation of bone marrow failure syndromes. *Blood Adv*. 2020;4(21):5540-5546.
38. Papapetrou EP. Modeling myeloid malignancies with patient-derived iPSCs. *Exp Hematol*. 2019;71:77-84.
39. Antony-Debre I, Manchev VT, Balayn N, et al. Level of RUNX1 activity is critical for leukemic predisposition but not for thrombocytopenia. *Blood*. 2015;125(6):930-940.
40. Connelly JP, Kwon EM, Gao Y, et al. Targeted correction of RUNX1 mutation in FPD patient-specific induced pluripotent stem cells rescues megakaryopoietic defects. *Blood*. 2014;124(12):1926-1930.

41. Sakurai M, Kunimoto H, Watanabe N, et al. Impaired hematopoietic differentiation of RUNX1-mutated induced pluripotent stem cells derived from FPD/AML patients. *Leukemia*. 2014;28(12):2344-2354.
42. Yzaguirre AD, de Bruijn MF, Speck NA. The Role of Runx1 in Embryonic Blood Cell Formation. *Adv Exp Med Biol*. 2017;962:47-64.
43. Olofsen PA ea. PML Plays a Key Role in Severe Congenital Neutropenia with Mutant ELANE Causing Neutrophil Elastase Protein Misfolding. *Blood*. 2019;134:213.

Chapter 6

Malignant Transformation Involving *CXXC4* Mutations Identified In A Leukemic Progression Model Of Severe Congenital Neutropenia

Patricia A. Olofsen[1], Szabolcs Fatrai[1], Paulina M.H. van Strien[1], Julia C. Obenauer[1], Hans W.J. de Looper[1], Remco M. Hoogenboezem[1], Claudia A.J. Erpelinck-Verschueren[1], Michael P.W.M. Vermeulen[1], Onno Roovers[1], Torsten Haferlach[2], Joop H. Jansen[3], Mehrnaz Ghazvini[4], Eric M.J. Bindels[1], Rebekka K. Schneider[1], Emma M. de Pater[1], Ivo P. Touw[1]

[1] Department of Hematology, Erasmus University Medical Center, Rotterdam 3015 CN, the Netherlands
[2] Munich Leukemia Laboratory (MLL), Munich 81377, Germany
[3] Department of Laboratory Medicine, Radboud University Medical Center, Nijmegen 6525 GA, the Netherlands
[4] Department of Developmental Biology, iPS Core Facility, Erasmus University Medical Center, Rotterdam 3015 CN, the Netherlands

Short title: CXXC4 and leukemic progression

Cell Reports Medicine. 2020 Aug 25; 1(5): 100074

Abstract

Severe congenital neutropenia (SCN) patients treated with CSF3/G-CSF to alleviate neutropenia frequently develop acute myeloid leukemia (AML). A common pattern of leukemic transformation involves the appearance of hematopoietic clones with CSF3 receptor (*CSF3R*) mutations in the neutropenic phase, followed by mutations in *RUNX1* before AML becomes overt. To investigate how the combination of CSF3 therapy and *CSF3R* and *RUNX1* mutations contributes to AML development, we make use of mouse models, SCN-derived induced pluripotent stem cells (iPSCs), and SCN and SCN-AML patient samples. CSF3 provokes a hyper-proliferative state in *CSF3R*/*RUNX1* mutant hematopoietic progenitors but does not cause overt AML. Intriguingly, an additional acquired driver mutation in *Cxxc4* causes elevated CXXC4 and reduced TET2 protein levels in murine AML samples. Expression of multiple pro-inflammatory pathways is elevated in mouse AML and human SCN-AML, suggesting that inflammation driven by downregulation of TET2 activity is a critical step in the malignant transformation of SCN.

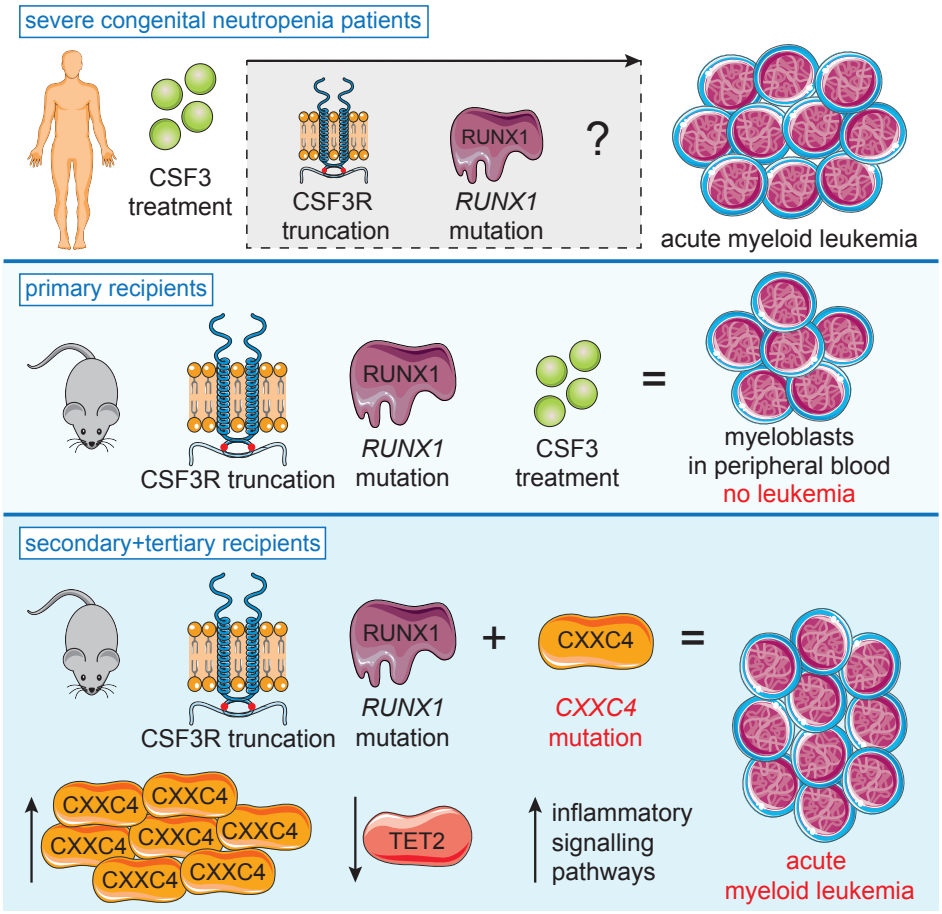

Introduction

Severe congenital neutropenia (SCN) is an inherited bone marrow failure syndrome characterized by an almost complete lack of neutrophils, leading to life-threatening bacterial infections.[1] SCN is most often caused by autosomal dominant mutations in *ELANE*, the gene encoding neutrophil elastase, but how these mutations give rise to severe neutropenia is still largely unknown.[1] In the majority of SCN patients, neutropenia is successfully alleviated by life-long administration of colony-stimulating factor 3 (CSF3), also known as granulocyte CSF (G-CSF).[2] SCN patients are at risk of developing high-risk myelodysplastic syndrome (MDS) or acute myeloid leukemia (AML), with a reported median incidence of 21%, 15 years after initiation of CSF3 treatment.[3,4] Leukemic progression correlates with the appearance of hematopoietic clones with somatic mutations in *CSF3R*, resulting in a truncated form of CSF3R with defective internalization and aberrant signaling properties.[5] These mutant clones arise before MDS or AML becomes clinically overt, indicating that additional defects are needed for malignant transformation.

Mutations in *RUNX1* are the most prevalent mutations (64.5%) acquired during leukemic transformation of SCN and typically occur in clones already harboring somatic *CSF3R* mutations (85%).[6] RUNX1 is a member of the runt transcription factor family and is essential for fetal hematopoiesis.[7,8] RUNX proteins share the highly conserved runt homology domain (RHD) involved in DNA binding and in the interaction with the regulatory protein core-binding factor β.[9] In SCN-MDS/AML, mainly *RUNX1* missense mutations in the RHD were found in combination with the *CSF3R*-truncating mutations.[6,10] Although recurrent mutations in other genes (e.g., encoding the epigenetic modifiers *ASXL1* and *SUZ12*) were also found, these were far less frequent. How truncated *CSF3R* mutants and *RUNX1* mutations in conjunction with disease-causing *ELANE* mutations contribute to AML development in SCN is unknown. To address this question, we used a combination of *in vivo* mouse models and *in vitro* patient-derived induced pluripotent stem cell (iPSC) models, engineered to express patient-specific *CSF3R* and *RUNX1* mutations.

Results

CSF3R and RUNX1 mutations elevate CSF3 induced proliferation of LK progenitor cells

We first investigated how a *RUNX1* mutation affects CSF3 responses of mouse hematopoietic stem and progenitor cells (HSPCs) *in vitro*. The patient-specific truncated CSF3R, *Csf3r*-d715, or wild type (WT) lineage-depleted bone marrow (BM) cells expressing the patient-specific *RUNX1*-D171N (RHD) mutation (Figures S1A,B) or an empty vector (ev) control were cultured in stem cell expansion medium with or without CSF3 (Figures 1A and 1B). In the absence of CSF3, no differences in absolute cell numbers between any of the conditions were seen (Figure 1A), whereas addition of CSF3 induced a strong and sustained hyperproliferative response in *Csf3r*-d715 cells that was slightly, but not significantly, extended by mutant RUNX1 (Figure 1B). *Csf3r*-d715 cells expressing RUNX1-RHD (d715-RHD cells) cultured in CSF3 medium showed selective expansion of lineage-negative, Sca1-negative, c-Kit-expressing (LK) cells relative to d715-ev control cells, which showed a more equal distribution between LK and more primitive LSK (Lineage$^-$, Sca1$^+$, c-Kit$^+$) cells (Figure 1C). Notably, d715-RHD cell cultures consistently showed a higher number of LK cells and reduced numbers of differentiated cells relative to the ev controls from day 5 onward (Figure 1D). d715-RHD cells also displayed a moderate ability of secondary and tertiary replating in CSF3-containing colony cultures, whereas d715-ev or WT-RHD cells lacked this capability (Figure 1E). Comparative transcriptome analysis and subsequent single-sample gene set enrichment analysis (ssGSEA) of LK cells from CSF3-supplemented cultures purified by fluorescence-activated cell sorting (FACS) on days 2, 5 and 9 showed higher activation of hallmark pathways of cell proliferation (E2F, G2M checkpoint, and MYC) and metabolism (mTORC1) in d715-RHD cells relative to d715-ev cells (Figure 1F). In summary, these results show that mutations in *Csf3r* and *RUNX1* have additive effects on proliferation of myeloid cells, leading to expansion of LK cells and reduced production of more mature myeloid cells.

In vivo expansion of Csf3r-d715/RUNX1-RHD mutant HSPCs induced by sustained CSF3 administration

To address how the *Csf3r* and *RUNX1* mutations in combination with CSF3 administration affected hematopoiesis *in vivo*, we performed transplantation experiments using lentivirally transduced lineage-negative *Csfr*-d715 BM cells (Figure S1C). Western blot analysis confirmed the presence of human RUNX1-D171N protein (Figure S1D). Transduction efficiency, analyzed by flow cytometry based on the presence of the IRES-GFP cassette in the lentiviral vector (Figure S1C), was approximately 40%-50% in lineage-negative BM cells (Figure S1E) and 65% in d715-RHD or d715-ev LSK cells (Figure S1F). These cells were transplanted into lethally irradiated WT recipients. Starting 4 weeks after transplantation, mice were treated three times per week with CSF3 or PBS (n=9 per group; Figure 1G).

GFP$^+$ cells in the peripheral blood (PB) within each group varied between mice (Figure 1H). Overall, mice transplanted with d715-RHD BM cells and treated with CSF3 showed the highest level of long-term chimerism; i.e., exceeding 16 weeks following transplantation and 12 weeks after initiation of CSF3 administration (Figure 1H). Fluctuations in GFP$^+$ PB cell percentages in individual mice over time suggest that CSF3 propagated the persistence rather than a dominant outgrowth of d715-RHD clones. Strikingly, CSF3-treated d715-RHD mice had significant percentages (16.5% average, SEM 7%) of GFP$^+$ LK cells in PB, which was not seen in the other experimental groups (Figure 1I; <1%). These cells were characterized as myeloblasts by morphology (Figure 1J) and comprised 1%-2% myeloid colony-forming cells (Figure 1K; 50-100 colonies/5000 cells), equivalent to the observations of *in vitro* cultures (Figures 1C-1E). Although more than 5% myeloblasts in the PB are a characteristic of AML, none of the CSF3-treated d715-RHD mice showed acute symptoms of AML, such as bleeding or anemia. In addition, no defect in myeloid differentiation was observed as percentages of GFP$^+$CD11b$^+$GR1$^+$ neutrophils in PB were comparable between groups (Figure S1G). At the time of sacrifice, no excessive GFP$^+$ blasts in the BM were seen, with the exception of mouse 29 (Figure 2A). On the other hand, increased numbers of GFP$^+$ cells were detected in the spleens of d715-RHD CSF3-treated mice (Figure 2B). These findings suggest that the CSF3-treated d715-RHD mice display a pre-malignant phenotype characterized by cellular but no symptomatic features of overt AML.

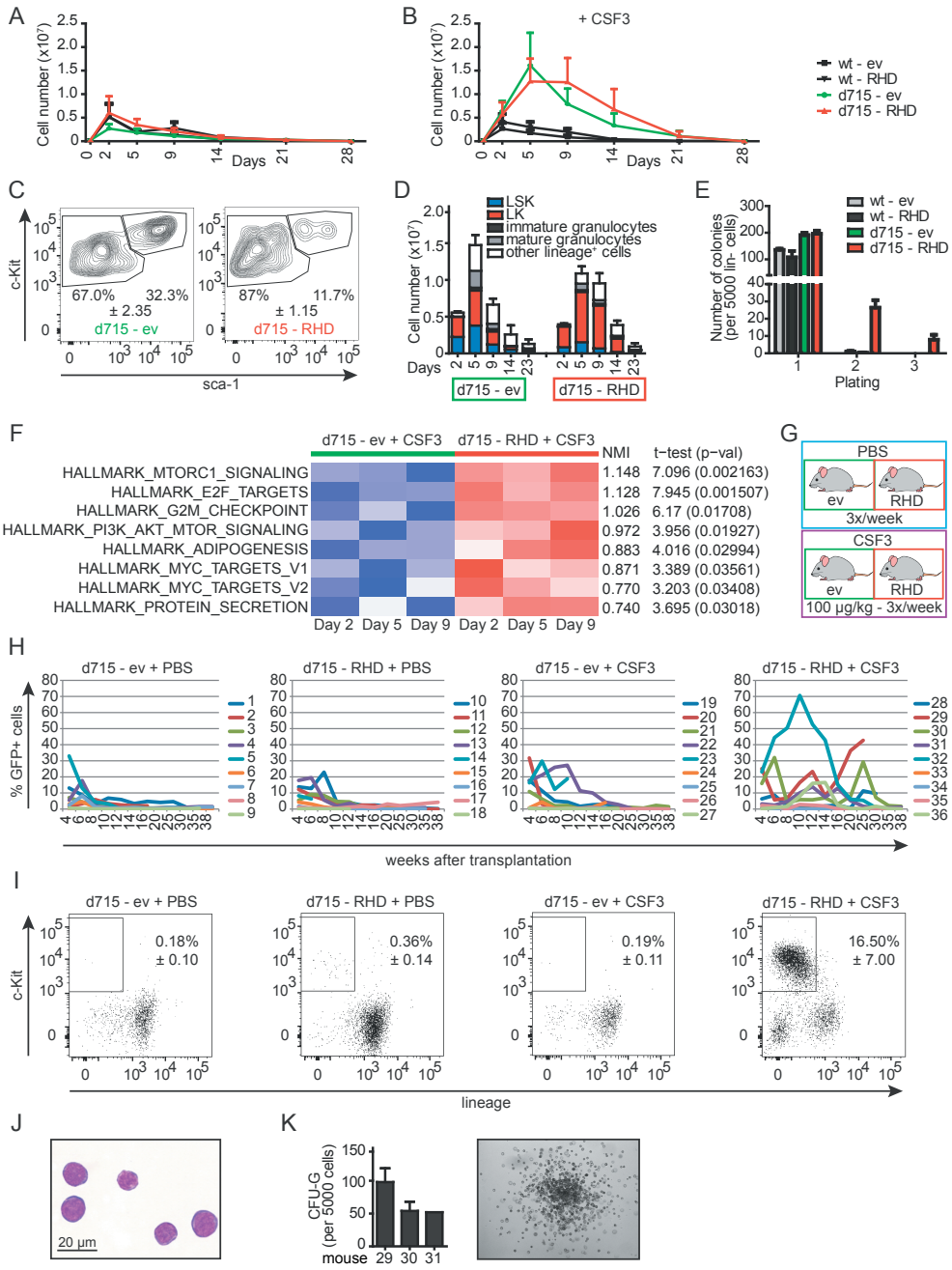

Figure 1: Csf3r-d715 and RUNX1-RHD in conjunction with CSF3 treatment causes the expansion of LK cells

(A-B) Proliferation of empty vector (ev)- or RUNX1-RHD virus-transduced cells in stem cell expansion medium (A) without CSF3 and (B) with 50 ng/ml CSF3. Error bars show one-sided standard error of the mean (SEM) of 3 independent experiments (biological replicates). (C) Representative FACS contour plots

showing LK/LSK distribution of d715-ev (left panel) and d715-RHD (right panel) in CSF3-supplemented cultures (day 9), with ± indicating the SEM. (D) Distribution of immature and differentiated cell types in CSF3-containing cultures spanning 23 days. Error bars show one-sided standard error of the mean (SEM) of 3 independent experiments (biological replicates). (E) CSF3-induced colony formation in primary colony assays and in secondary and tertiary replating cultures (n=3 independent experiments [biological replicates] in triplicate [technical replicates]). (F) Comparative transcriptome profiles of CSF3-stimulated d715-ev and d715-RHD LK cells on days 2, 5, and 9 of culture (n=1 sample per timepoint). (G) Experimental setup. CSF3/PBS administration started 4 weeks after transplantation. (H) Longitudinal analysis of GFP expressing cells in the PB (n=9 mice per experimental group, biological replicates). (I) Accumulation of GFP-expressing LK cells in PB of CSF3-treated d715-RHD-transplanted mice but not in other groups. Data are from PB samples taken 14 and 16 weeks after transplantation (n=11 or 12 per group) with ± indicating the SEM. (J) Myeloblast morphology of FACS-purified PB LK cells. The scale bar indicates 20 μm. (K) CSF3 induced colony formation of PB LK cells (mice 29, 30, and 31) and representative example of the colony (n=1 experiment in triplicate [technical replicates]). See also Figure S1.

Premalignant Csf3r/RUNX1 mutant BM cells progress to AML in secondary recipients

The ability to engraft in secondary recipients is a hallmark of murine leukemia models. To determine to what extent this applied to the pre-malignant nature of d715-RHD BM cells from CSF3-treated mice, we transplanted BM cells from mouse 29, which presented with the highest level of engraftment 25 weeks after primary transplantation, in sub-lethally irradiated secondary recipients that were subsequently treated with CSF3 (n=6; Figures 2C and 2D). $GFP^+c\text{-}Kit^+$ cells were detectable in the blood 4 weeks after transplantation and could be detected untill the end of the experiment (Figures 2E and 2F). Contrary to the LK cells expanding in primary recipients, these cells weakly co-expressed the myeloid marker CD11b, suggestive of a myeloid bias within the LK compartment (Figure 2G). High percentages of $GFP^+c\text{-}Kit^+$ cells were present in the BM, spleen, and liver (Figure 2H). Prior to sacrifice, mice were severely anemic because of an erythroid differentiation block at the $CD71^+Ter119^+$ basophilic and early chromatophilic erythroblasts (RII) stage in the BM and spleen (Figures S2A and S2B). Histological analysis showed a normo- to hypercellular BM with more than 90% myeloid blast infiltration with significant nuclear atypia and atypical mitoses and apoptosis (Figure 2I), consistent with the diagnosis of AML.

Outgrowth of d715-RHD AML without CSF3 administration

To interrogate whether the d715-RHD-derived AML was still dependent on CSF3 administration, we transplanted leukemic cells into tertiary recipients that were subsequently treated with PBS or CSF3 (n=4 per group; Figure 2J). GFP^+ cells in the PB were detectable from 10 weeks untill the end of the experiment and increased over time in PBS- and CSF3-treated groups with similar kinetics (Figures 2K and 2L).

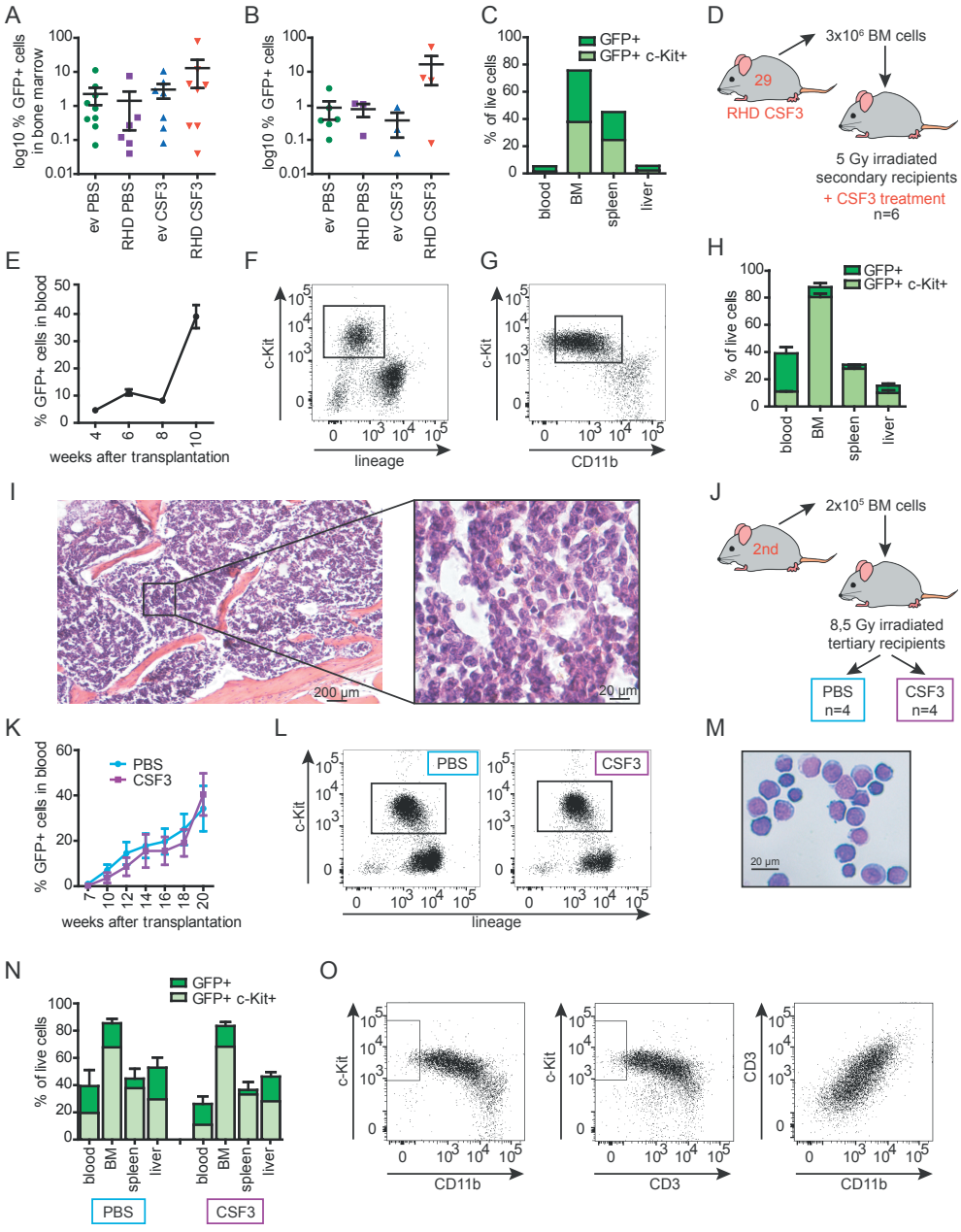

Figure 2: Spleen infiltration and CSF3-independent leukemogenic properties of d715-RHD cells

(A and B) Distribution of GFP-expressing cells in (A) BM and (B) spleen in primary recipients, showing enhanced spleen infiltration in CSF3-treated d175-RHD mice. (C) Relative distributions of total GFP⁺ and GFP⁺c-Kit⁺ cells in various organs of mouse 29. (D) Secondary transplant setup; cells from mouse 29 were transplanted into 6 recipients. (E-G) Expansion of GFP⁺ cells in PB of 6 secondary recipients (E, biological replicates), with (F) the c-Kit⁺ immuno-phenotype and (G) Intermediate CD11b expression on

c-Kit$^+$ cells. (H) Organ distribution of GFP$^+$ and GFP$^+$c-Kit$^+$ cells. (I) H&E staining of the spine, showing a hypercellular BM with more than 90% myeloblast infiltration. The scale bars indicates 200 and 20 μm, respectively. (J) Tertiary transplantation setup. (K) Equal expansion of GFP$^+$ cells in PB of CSF3-treated (n=4) or PBS-treated (n=4) mice (biological replicate). (L) The c-Kit$^+$ phenotype of PB GFP$^+$ cells in CSF3- and PBS-treated mice. (M) Blast morphology of FACS-purified c-Kit$^+$ PB cells. (N) Organ distribution of GFP$^+$ and GFP$^+$c-Kit$^+$ cells in PBS- or CSF3-treated mice (n=4 per group). (O) FACS analysis showing an immature (c-Kit$^+$) mixed myeloid (CD11b$^+$) and T-cell (CD3$^+$) immuno-phenotype of AML blasts; the boxes indicate c-Kit$^+$CD11b$^-$CD3$^-$. Error bars represent SEM. See also Figure S2.

c-Kit$^+$ AML cells weakly expressed lineage markers (Figure 2L) but retained their myeloblast morphology (Figure 2M). The BM, spleen, and liver contained equivalent numbers of GFP$^+$ cells independent of CSF3 treatment (Figure 2N), confirming that the outgrowth of AML no longer depended on CSF3 administration. Immuno-phenotyping revealed that, in addition to CD11b, the leukemic blasts co-expressed CD3, suggestive of a mixed myeloid/T-lymphoid phenotype (Figure 2O). As expected, all mice developed symptoms of AML, including severe anemia and a block of erythropoiesis in the BM and spleen (Figures S2C-S2E; data not shown). Although significant numbers of GFP$^-$ CD71$^{intermediate/loWT}$er119$^+$ poly/ortho-chromatophilic erythroblasts and enucleated erythrocytes (RIII/RIV) were found in the liver, these cells did not compensate for the anemia (Figures S2C, S2F, and S2G).

Leukemic progression in d715-RHD mice is accompanied by elevated pro-inflammatory cytokine responses

To determine which signaling pathways changed during the sequential steps of transformation, we performed transcriptome profiling on FACS-purified BM- or PB-derived LK cells (1) prior to transplantation, (2) from d715-RHD CSF3 treated primary recipients (pre-leukemic) and (3) c-Kit$^+$ cells from leukemic (secondary and tertiary recipient) mice (because these cells co-express lineage markers). Unsupervised clustering based on gene sets derived from GSEA-defined hallmark pathways revealed that LK cells from non-leukemic (t=0, red), pre-leukemic (primary recipients, blue) and the c-Kit$^+$ cells from the leukemic (secondary and tertiary recipients, green) mice clustered based on interferon γ (IFN-γ)- (Figure 3A), inflammatory- (Figure 3B), and tumor necrosis factor alpha (TNFα)/nuclear factor κB (NFκB)-responses (data not shown), which increased with progressive stages of transformation.

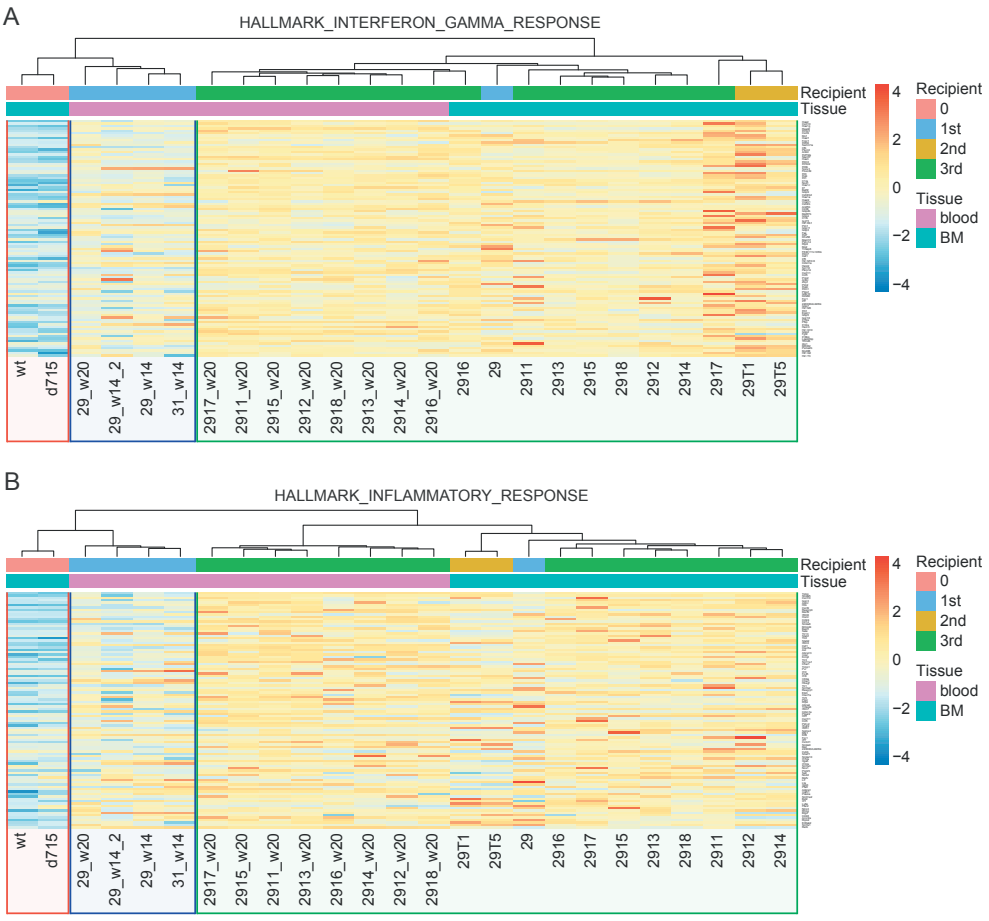

Figure 3: Elevated inflammatory transcriptomes associated with leukemic progression in d715-RHD mouse models

(A and B) Heatmap showing unsupervised clustering and expression of the top 100 differentially expressed transcripts in BM and PB samples of control, pre-leukemic, and leukemic LK/c-Kit⁺ cells (A) associated with IFN-γ signaling and (B) inflammatory response.

Comparison of the mouse model to clinical SCN-AML

To determine whether the gene expression changes in the mouse model mimic the clinical progression of SCN to AML, we took advantage of bio-banked samples of a previously reported *ELANE* mutant-SCN patient who received life-long CSF3 therapy and acquired *CSF3R* (d715) and *RUNX1* (D171N) mutations identical to our mouse model.[10] GSEA comparisons in the mouse showed that activation of inflammation-associated pathways TNFα via NFκB signaling, IFN-γ, inflammatory response, and interleukin-6 (IL-6)/JAK/STAT3 signalling were significantly elevated in leukemia samples relative to non-leukemic LK populations (the

expression data of WT and *Csf3r*-d715 were combined and compared with the combined data of the eight tertiary transplant recipients; Figure 4A). On the other hand, canonical proliferative hallmark signatures (E2F, G2M checkpoint, and MYC) initially upregulated in the premalignant state conferred by the activated CSF3R-d715 and RUNX1-RHD (Figure 1F), were significantly blunted in the leukemic samples (Figure 4B).

Transcriptome analysis of FACS-purified $CD34^+$ cells from the neutropenic phase (SCN 1992) and the AML phase (SCN-AML 2007) showed markedly similar hallmark signature patterns compared with the mouse model: upregulation of TNFα via NFκB signaling, IFN-γ and inflammatory responses, and IL6/JAK/STAT3 signaling pathways (Figure 4C) and down regulation of the proliferation signatures E2F, G2M checkpoint, and MYC (Figure 4D). GSEA comparing the $CD34^+$ cells of the SCN-AML phase with 3 healthy controls showed the same transcriptional alterations (Figures S3A and S3B).

In addition, we found 55 of 241 significantly ($p<0.05$) upregulated transcripts in SCN-AML samples overlapping with significantly ($q<0.05$) upregulated transcripts in mouse AML samples (Table S1), whereas 53 of the 188 downregulated transcripts were overlapping (Table S2). These data furnish a rich substrate for further studies into the critical downstream mechanisms contributing to leukemic progression. For instance, *ANXA2*, *CDKN1A*, *CISH*, *DUSP1*, *FOS*, and *IL10RA* are prominent inflammatory genes that were commonly upregulated in mouse AML and patient SCN-AML samples (Table S1). Similarly, genes that are downregulated merit further study in the context of inflammation-driven leukemogenesis (Table S2).

Whole exome sequencing identifies a mutation in Cxxc4 as a somatic clonal driver for progression to AML

Because we discriminated a pre-leukemic stage in our mouse model, we asked whether leukemic progression was caused by acquisition of additional driver mutations. To address this, we performed whole-exome sequencing on AML cells from one secondary recipient (29T1) and eight tertiary recipients (2911-2918). These leukemic mice harbored a relatively small number of newly acquired somatic mutations that were mostly subclonal and varied between individual mice (data not shown). The single mutation present in all leukemic mice was a clonal heterozygous abnormality (VAF: 0.52±0.06) characterized by a 6 nucleotide (GGCGGC) internal tandem duplication (ITD) in *Cxxc4*/*Idax*, introducing 2 glycine residues at amino acid position 158 of the WT protein (Figure 5A). This mutation already appeared in a subclone (VAF: 0.27) in primary recipient mouse 29 and expanded in the secondary and tertiary recipients, in which all AML cells harbored the *Csf3r*-d715, *RUNX1*-RHD, and *Cxxc4*-ITD mutations (Figure 5B). Notably, *Csf3r*-d715 donor BM samples did not contain any detectable reads with *Cxxc4*-ITD mutations, indicating that the mutation was acquired *de novo* as a somatic driver mutation during leukemic transformation (Figure 5B).

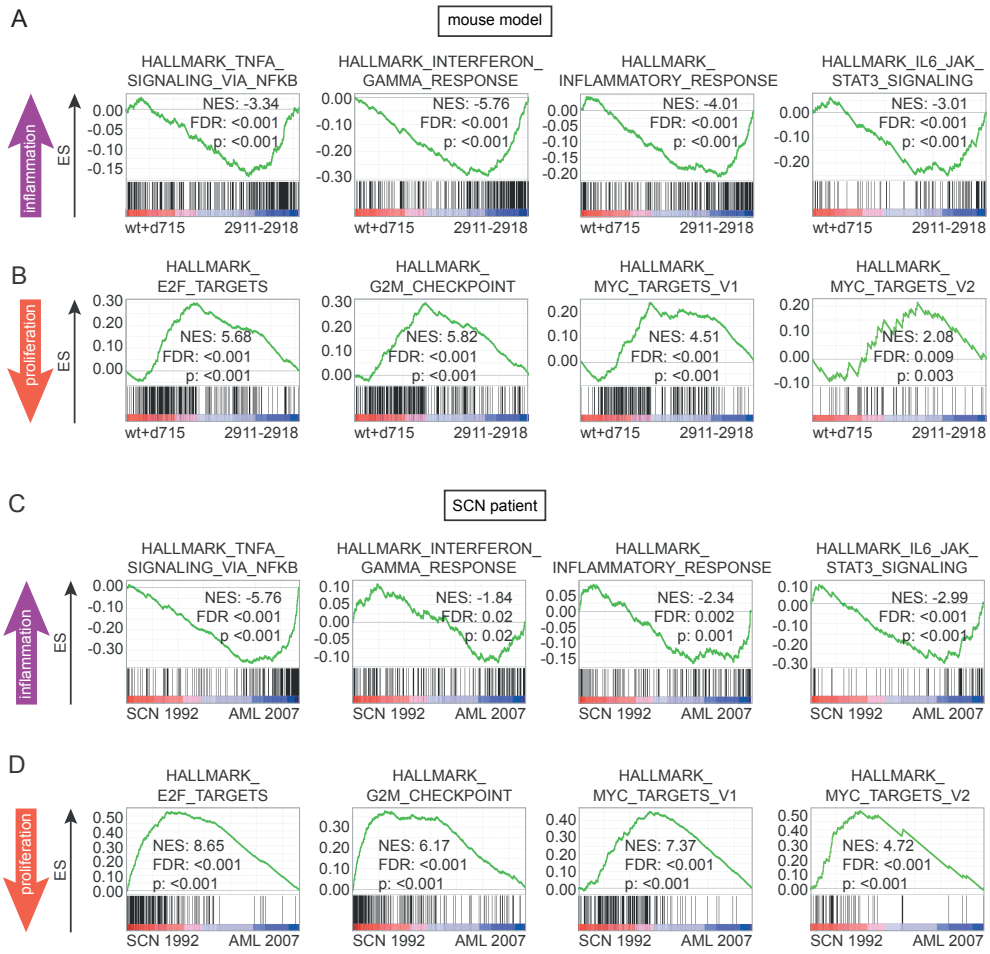

Figure 4: Leukemic progression of d715-RHD mouse model and SCN (SCN-AML) is associated with increased inflammatory and decreased proliferative signaling

(A and B) GSEA analyses comparing control (WT and d715 transcriptional data combined, n=2) versus leukemic (tertiary recipients 2911-2918, n=8) LK/c-Kit$^+$ cells showing (A) upregulation of inflammatory signaling and (B) downregulation of proliferative pathways in the leukemic mice. GSEA comparing CD34$^+$ cells from the SCN-phase (1992) and the SCN-AML phase (2007), showing (C) increased inflammatory pathways and (D) down-regulated proliferation signatures. NES = normalized enrichment score, FDR = false discovery rate. See also Figure S3 and Tables S1 and S2.

The Cxxc4-ITD mutation correlates with elevated CXXC4 and reduced TET2 protein levels

To assess the effects of the *Cxxc4* mutation, we first determined its effect on protein expression. The predicted molecular weight of WT mouse CXXC4 is 36.4 kDa. Immunoblotting confirmed the presence of this CXXC4 isoform in *Csf3r*-d715 BM cells (Figure 5C) and showed 7-fold higher expression levels (7.25 ±0.64) in pre-leukemic and leukemic samples

harboring the *Cxxc4* mutation. *CXXC4*/*IDAX* is genetically closely linked to *TET2* and was originally encoded within the ancestral *TET2* gene before it became a separate gene during evolution.[11] CXXC4 is an inhibitor of Wnt/β-catenin signaling.[12] Suggestive of elevated CXXC4 activity, transcriptome analysis using GSEA showed reduced Wnt/β-catenin signaling in *Cxxc4*-ITD-expressing leukemia samples (2911-2918) relative to WT *Cxxc4* BM LK cells (data not shown). More striking in the context of leukemic progression, it was shown that CXXC4 activates proteolytic degradation of TET2 through a mechanism involving caspases 3 and 8.[11] Indeed, we found that TET2 protein levels were severely reduced in leukemic relative to normal samples (0.20 ±0.08), whereas reduced expression of *Tet2* was not observed on transcriptional level (Figure 5C; data not shown). Quantification of TET2/CXXC4 ratios illustrates the strong inverse relationship between TET2 and CXXC4(ITD) protein levels (Figure 5D).

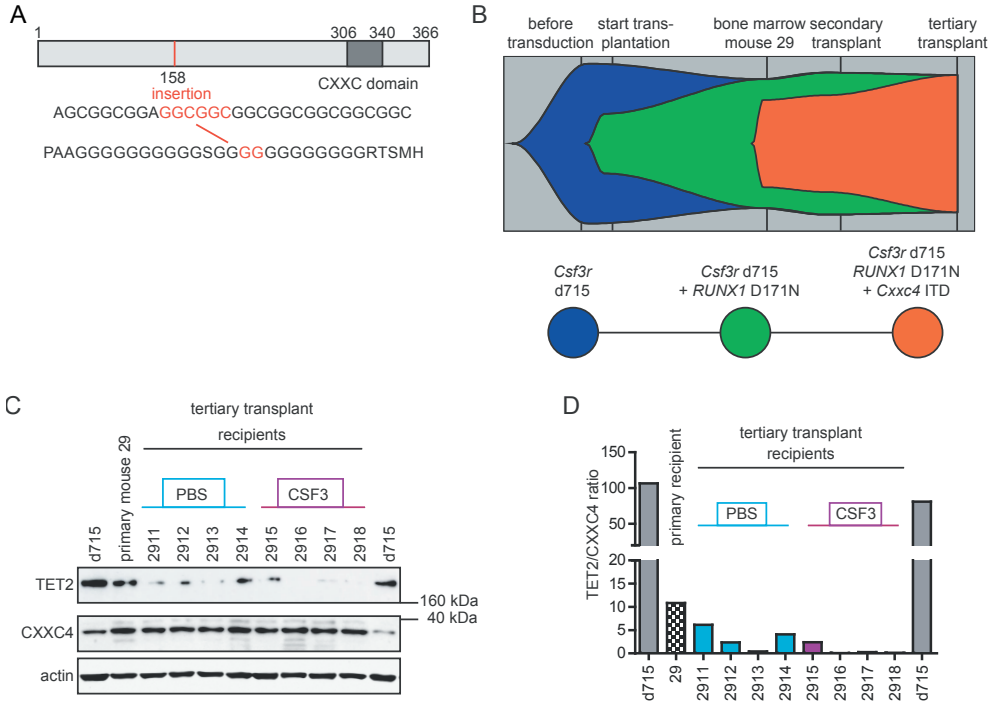

Figure 5: Cxxc4 mutations and expression of CXXC4 and TET2 proteins in AML cells

(A) Schematic overview of the CXXC4 gene showing acquisition of a Cxxc4-ITD in mouse leukemic cells. (B) Fish plot illustrating the clonal pattern of leukemia development. (C) Immunoblot showing elevated CXXC4 protein levels (36.44 kDa) and reduced TET2 protein levels (212.13 kDa) in pre-leukemic and leukemic samples derived from primary recipient 29 (biological replicates). (D) Quantification of TET2/CXXC4 ratios. See also Figure S4.

CXXC4 mutations in human AML

To determine whether *CXXC4*-ITD mutations similar to those identified in the mouse model are relevant for human disease, we analyzed whole-genome sequencing data from 591 AML patients generated at the Munich Leukemia Laboratory (MLL), complemented by targeted sequencing of 87 consecutive AML patients from the HOVON102 clinical trial. The CXXC4 protein shows high homology between mouse and human (Figure S4). In total, 6 *CXXC4*-ITD mutations were found (Figure 6A). Interestingly, the insertion of 2 glycine residues caused by the ITD in our mouse model was also found in 2 *de novo* AML patients. Besides the tandem glycine insertions, smaller insertions comprising 1 glycine residue or larger ITDs comprising 6 glycine residues were found. Cross-referencing with the gnomAD database (v.2.1.1), which contains sequences from 141,456 unrelated individuals (https://gnomad.broadinstitute.org/), showed that the *CXXC4*-ITD was absent or detected in 10 to 140-fold lower frequencies than in our cohort. This suggests that some *CXXC4*-ITD mutations may be somatic, whereas others may be present in the germline and predispose to leukemia. The fact that these insertions were all located in or around the glycine repeats suggests that this region is important for protein expression and/or stability.

CXXC4-ITD reduces TET2 levels and has a prolonged half-life relative to wild type CXXC4 protein

To determine how a patient-specific *CXXC4*-ITD (Gly160_165dup) exerts its enhanced effect on reducing TET2 levels relative to WT CXXC4, we lentivirally introduced both forms in K562 and HEK293T cells. Ectopic overexpression of WT CXXC4 as well as the CXXC4-ITD resulted in a significant reduction in TET2 protein levels (Figure 6B), confirming the observations of Ko et al.[11] Because we observed increased CXXC4 protein levels in murine *Cxxc4*-ITD leukemic cell samples (Figure 5C), we wondered whether elevated protein levels are the result of prolonged protein stability of the CXXC4-ITD protein. Indeed, translation inhibition by cycloheximide to block *de novo* protein synthesis showed that the CXXC4-ITD was maintained at higher levels than WT CXXC4 (Figure 6C), providing a plausible explanation for its elevated abundance in the mouse leukemia cells.

CSF3R-d715 RUNX1-RHD increases proliferative signaling in CD34$^+$CD45$^+$ cells derived from control iPSCs while inducing inflammatory pathways in SCN iPSC

A limitation of the mouse transplantation model is that it lacks the disease-causing mutation of *ELANE*-SCN. However, *Elane* mutations equivalent to those found in SCN patients do not cause neutropenia in murine models,[13] precluding the possibility to analyze the additional effect of *ELANE* mutations in murine models. To model leukemic progression in human SCN, we introduced the *CSF3R*-d715 mutation by CRISPR-Cas9-mediated genome editing and the *RUNX1*-D171N mutation by lentiviral transduction (containing IRES-GFP; Figure S1C) in iPSCs

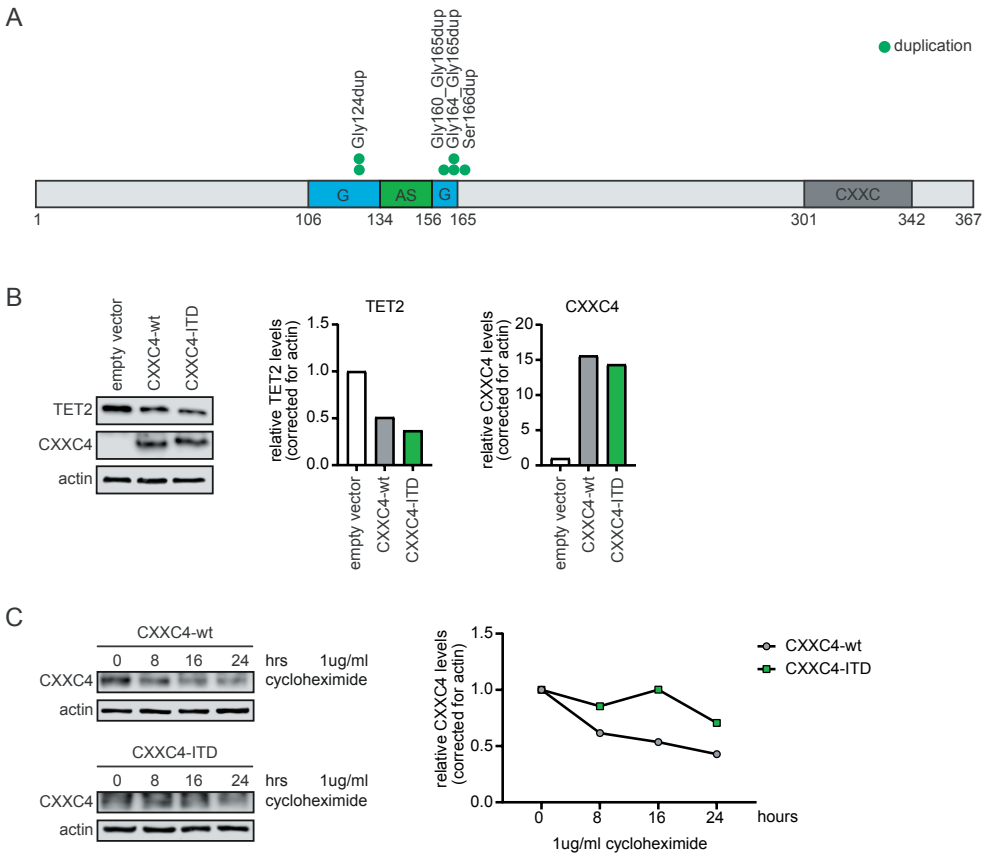

Figure 6: Human CXXC4-ITD mutation result in a more stable CXXC4 protein and reduced TET2 levels
(A) Schematic overview of the human CXXC4 gene showing CXXC4-ITD mutations in de novo AML. (B) Overexpression of wildtype (WT) or CXXC4-ITD (duplication of Glycines 160-165) in K562 cells shows a subsequent reduction in TET2 protein levels by immunoblot. (C) Representative image and quantification of an immunoblot, showing increased stability of the CXXC4-ITD protein upon prolonged treatment with 1 µg/ml cycloheximide. See also Figure S4.

from an *ELANE* mutant-SCN patient (Figures S5A-S5C) and performed RNA sequencing on GFP$^+$CD34$^+$CD45$^+$ hematopoietic progenitor cells (HPCs) derived from two independent experiments. First we checked, in control iPSCs, whether the GFP$^+$ *CSF3R*-d715 mutant HPCs recapitulated the findings of *in vitro* mouse experiments (Figure 1F). When comparing RUNX1-RHD cells with ev control cells, the expression pattern corroborated the mouse experiments; e.g., increased proliferation-related signaling (compare Figure S6A with Figure 1F; the leukemic mice shown in Figure 3 acquired an additional mutation in *CXXC4,* altering the transcriptome). In addition, we observed reduced inflammatory signaling, establishing that *RUNX1* mutations *per se* do not cause inflammatory signaling but, instead, are involved in gaining a proliferative advantage (Figure S6A).

In contrast, in *RUNX1* mutant-expressing cells derived from an *ELANE* mutant patient a slight increase in inflammatory responses (e.g., IFN-γ signaling) was observed compared with ev controls, which was associated with leukemic progression in the mouse model and SCN-AML patient (compare Figure S6B with Figures 1F and 4). In line with the data from control cells and the *in vitro* mouse data, the proliferation-related signatures G2M checkpoint and E2F targets were enriched upon expression of the RUNX1-RHD mutant in an *ELANE* mutant, *CSF3R*-d715 background (Figure S6B). However, MYC targets were not induced, and even inhibited, in *ELANE* mutant cells (Figure S6B). These data suggest that the SCN background already primes for leukemic progression, where the combination of *ELANE, CSF3R,* and *RUNX1* mutations already shows signs of tipping the balance between inflammatory and proliferative signaling as seen during the leukemic progression in the mouse model and SCN patient.

Analysis of 5mC/5hmC levels in mouse leukemia samples

Several recent studies have linked TET2 to inflammatory responses and connected loss of TET2 to inflammation-driven clonal hematopoiesis, pre-leukemia, and MDS.[14-19] The effects of TET2 on repressing inflammation have been assigned to its methylcytosine dioxygenase activity but also to its ability to recruit histone deacetylase (HDAC)-mediated repressor activity to pro-inflammatory genes.[17,19] To investigate whether the *Cxxc4*-ITD and subsequent reduction in TET2 levels altered the 5-hydroxymethylcytosine (5hmC) and 5-methylcytosine (5mC) levels of the DNA, we performed quantitative mass spectrometry experiments on the LK cells derived from the leukemic mice.[20] Surprisingly, we did not observe major alterations in the proportion of 5mC and 5hmC nucleotides compared with LK cells from WT or d715 mice (Figure S7A), suggesting that the reduction of TET2 levels did not alter the methylcytosine dioxygenase activity. This might either be due to technical limitations, a redundancy with other methylcytosine dioxygenases,[21] or to the fact that reduced TET2 levels were not restrictive for its enzymatic activity. On the other hand, this could suggest that a noncanonical function of TET2, such as its ability to recruit HDAC activity to chromatin, rather than its enzymatic activity was mainly affected by the *Cxxc4*-ITD.

CSF3R-d715 RUNX1-RHD cells switch transcriptional signatures from proliferative to inflammatory upon HDAC inhibition in human iPSC models

We next aimed to functionally validate the findings from leukemic mice in a human SCN-derived iPSC model expressing the truncated *CSF3R*-d715 and the *RUNX1*-RHD mutant. An obvious experiment would be to introduce the *CXXC4*-ITD in these cells by CRISPR-Cas9-mediated genome editing, but this was technically infeasible because of the high GC-repeat content in the target region. Instead, to discriminate between the two functions of TET2 proposed above, we wanted to find out how inhibition of its enzymatic activity by

administration of octyl-(R)-2hydroxyglutarate (2HG) and its ability to recruit HDAC activity by administration of the HDAC inhibitor MS275 (Entinostat) affected the transcriptional profile of *CSF3R*-d715 *RUNX1*-RHD expressing SCN-iPSC-derived CD34⁺CD45⁺ HPCs. In line with the unaltered 5hmC levels in mouse AML cells, hallmark analyses showed that 2HG did not induce an inflammatory profile as observed in *Cxxc4* mutant mouse AML cells (Figure S7B). In contrast, HDAC inhibition with MS275 ignited inflammatory signaling while inhibiting the proliferative signatures in control and *ELANE* mutant cells, recapitulating the signaling profiles of *Cxxc4* mutant mouse AML cells and SCN-AML patient material (Figures 7A ans 7B; data not shown). Although HDAC inhibition may also affect pathways independent of TET2, these data fit into a model of leukemic progression in which TET2 represses inflammatory signaling through its ability to recruit HDACs to pro-inflammatory genes,[17,19] whereas DNA hydroxyl-methylation had little or no effect. This model may apply specifically to the context of leukemic progression of SCN involving acquisition of *CSF3R* and *RUNX1* mutations but could also be relevant to other forms of AML (e.g., with RUNX1 mutations and/or secondary to BM failure syndromes other than SCN).

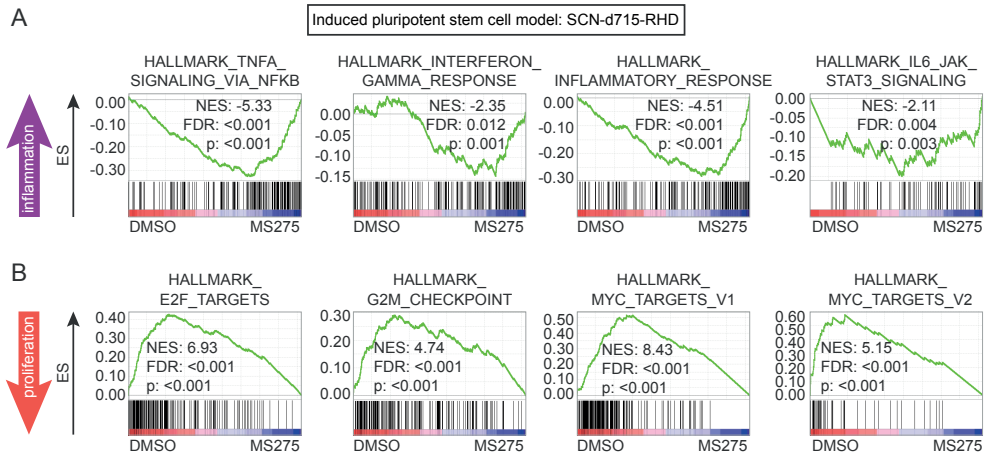

Figure 7: HDAC-inhibitor MS275 induces inflammatory signatures in SCN iPSC-derived CD34±CD45± cells

(*A and B) GSEAs comparing CD34⁺CD45⁺ CSF3R-d715 RUNX1-RHD cells from ELANE mutant SCN cells treated with DMSO or the HDAC inhibitor MS275, derived from two independent experiments (biological replicates), showing (A) induced inflammatory signaling and (B) reduced proliferative signatures in MS275 treated cells. NES = normalized enrichment score, FDR = false discovery rate. See also Figure S5.*

Discussion

In this study, we investigated how mutations in *CSF3R* and *RUNX1*, frequently associated with leukemic progression of SCN in conjunction with CSF3 treatment,[1] contribute to AML development. By developing a mouse model with the most recurrent *CSF3R* and *RUNX1* mutations, we found that this combination resulted in the accumulation of myeloblasts and myeloid colony-forming progenitors in PB, which persisted for 25+ weeks while on sustained CSF3 treatment. Although myeloblasts were found in PB, mice did not reveal signs of overt AML. These findings agree with clinical observations in an *ELANE* mutant SCN patient with *CSF3R* and *RUNX1* mutations (in the absence of other somatic defects) who showed CSF3-dependent expansion of a *CSF3R/RUNX1* mutant myeloblast clone that spontaneously disappeared after CSF3 treatment was stopped.[6] These findings heralded that full malignant transformation of SCN to AML requires additional defects. This was confirmed in serial transplantation experiments in which we identified a clonal mutation in *Cxxc4* as a driver of AML development. This mutation resulted in increased levels of CXXC4 protein. CXXC4 has been recently shown to control caspase-mediated degradation of TET2,[11] and, in agreement with this, TET2 levels were severely reduced in AML cells.

CXXC4 mutations were also found in a minority of *de novo* AML patients. At what frequencies *CXXC4* mutations are present in SCN-AML or other forms of secondary AML and whether they coincide with acquisition of other mutations (e.g., in *RUNX1*) is currently under study. The possibility that mutations in other genes affecting the TET2 pathway will have similar consequences for development of SCN-AML must be considered in this context. In agreement with this, mutations in *SUZ12*, a component of EZH2-containing polycomb repressor complex 2 (PRC2), which inhibits CXXC4 expression,[22] have been detected in the SCN-AML patient used for this study and others.[6,10] Mutations in *ASXL1*, also recurrent in SCN-AML, may have similar effects and have recently been functionally connected to leukemic transformation in conjunction with *RUNX1* mutations.[23,24] These findings are consistent with the concept that reduced TET2 levels contribute to leukemic progression of SCN.

Another key finding that emerged from our study concerns the connection between inflammation, clonal expansion, and leukemic progression of SCN. A role for inflammation in regulating hematopoietic stem cell fate in normal and several disease-related conditions, including MDS, has been suggested previously.[15] Some studies showed that pro-inflammatory cytokines initially activate stem cells to exit from a dormant state but, when chronically active, cause a loss of stem cell fitness, which eventually results in age-related BM failure.[25-27] Importantly, TET2 has been shown to repress pro-inflammatory cytokine genes in macrophages and dendritic cells, in part by recruitment of HDAC2,[19] whereas,

inversely, loss of *Tet2* fosters an inflammatory state characterized by upregulation of IL-6 and TNF-α.[16,28,29] More recent studies in *Tet2*-deficient mice showed that inflammation drives clonal expansion of pre-leukemic myeloid precursors.[14,17,30] Taken together, these findings fit into a model where reduction of TET2 levels through gene disruption or downregulation of expression induces an inflamed state. Acquisition of a *RUNX1* mutation would then stimulate outgrowth of a malignant clone that evolves into AML.

Although the transcriptome analysis of mouse AML cells, the SCN-AML patient sample, and HDAC inhibitor-treated SCN iPSC-derived $CD34^+CD45^+$ cells showed elevated IL-6-, IFN-γ- and TNF-α-mediated inflammatory responses, increased transcription of these cytokine genes themselves was not seen (data not shown). This could suggest that the inflammatory responses were activated by a cell-extrinsic, rather than a cell-intrinsic (autocrine) stimulus. Because these studies were done on immature $CD34^+$ or c-Kit^+ fractions, it is possible that affected macrophages and/or dendritic cells derived from these cells and/or environmental cells, e.g., endothelial cells, produced elevated levels of pro-inflammatory cytokines, inducing an inflammatory state in immature progenitor populations in a paracrine manner. An alternative possibility is that the genomic damage underlying SCN itself activates inflammatory signaling, e.g., IFN-γ-induced pathways, which is aggravated when TET2 levels are reduced. For instance, increased IFN-γ signaling has been reported in the context of DNA double-strand breaks induced by etoposide treatment or X-ray irradiation of cells.[31,32]

In conclusion, this study provides insights into sequential steps in leukemic progression of SCN and identifies pro-inflammatory mechanisms as important mediators of this process. Questions that still need to be addressed are how mutant neutrophil elastase proteins shape the “fertile ground” for the acquisition of *CSF3R* mutations and how CSF3 treatment contributes to reshaping this into the cellular state in which elevated inflammatory responses are induced and tolerated and *RUNX1* mutations can be acquired, resulting in progression to AML. Resolving these issues holds promise for clinical management of SCN, and possibly other leukemia predisposition syndromes, with the objective to avoid or interfere early in the malignant transformation of these conditions.

Limitations of Study

Although *CSF3R/RUNX1/CXXC4* mutant cells could repopulate and form AML in multiple secondary (n=6) and teriary (n=8) recipients, the *CXXC4*-ITD mutation originally arose in a single primary recipient (1/9), who acted as a donor for subsequent retransplantation

studies.

Hence, rather than being frequently involved in the leukemic progression of SCN, the *CXXC4*-ITD mutation should be taken as evidence that downregulation of TET2 and the associated upregulation of inflammatory signaling contribute to malignant transformation in conjuction with the *CSF3R* and *RUNX1* mutations. Supporting a role of *CXXC4* mutations in human disease, *CXXC4*-ITD mutations very similar to those detected in the mouse model were found in a subset of *de novo* AML patients, some but not all of which are found in the healthy population, but at much lower frequencies. Further studies are needed to address wether *CXXC4* mutations in human AML are somatic or germline. Studies to unravel co-occurrence with other mutations in, e.g., *RUNX1* or *TET2* could provide further insight in the pathogenic mechanism of *CXXC4* alterations. Inhibition of HDAC-recruiting function of TET2 with the HDAC inhibitor MS275 provides a possible mechanism of how reduced TET2 levels can induce inflammatory signaling, but this inhibitor may also affect pathways independent of TET2. How TET2 regulates inflammation at specific gene targets and how *RUNX1* mutations affect this process (e.g., by enabling pre-leukemic cells to escape from inflammation-mediated exhaustion) merits further study.

Acknowledgments

This work was supported by grants from KWF Kankerbestrijding (EMCR 2013-5755 and EMCR 2014-6780), the KiKa foundation (project 152) and the Cancer Genome Editing Center of the Erasmus MC Cancer Institute funded by the Daniel den Hoed foundation. We thank Inge A.M Snoeren for technical assistance, Drs Tom Cupedo and Mathijs Sanders for valuable comments on the manuscript, and Dr Peter Valk for providing access to clinical samples.

Author Contributions

Conceptualization, P.A.O., S.F., J.C.O. and I.P.T.; Methodology, P.A.O., S.F., P.M.H.v.S., J.C.O. and H.W.J.d.L.; Formal Analysis, P.A.O. and R.M.H.; Investigation, P.A.O., S.F., P.M.H.v.S., J.C.O., H.W.J.d.L., C.A.J.E., P.W.M.V., O.R., J.H.J., E.M.J.B. and R.K.S.; Resources, T.H. and M.G.; Data Curation, R.M.H.; Writing – Original Draft, P.A.O. and I.P.T.; Writing – Review & Editing, E.M.J.B., R.K.S. and E.d.P.; Visualization, P.A.O.; Supervision, I.P.T.; Funding Acquisition, I.P.T.

Declaration of Interests

The authors declare no competing interests.

STAR methods

RESOURCE AVAILABILITY

Lead contact

Further information and requests for resources and reagents should be directed to and will be fulfilled by the Lead Contact, Ivo P. Touw (i.touw@erasmusmc.nl).

Materials Availability

Viral constructs and iPSC lines generated in this study will be made available on request, but we may require a payment and/or a completed Materials Transfer Agreement if there is potential for commercial application.

Data and Code Availability

The RNA sequencing dataset comparing the effect of the introduction of RUNX1-D171N (RHD) in Csf3r-d715 mice bone marrow cells generated during this study, as shown in Figure 1, is available at ArrayExpress: E-MTAB-9373.

The RNA sequencing dataset comparing different stages of leukemic progression in a mouse model of SCN generated during this study, as shown in Figures 3 and 4 and Tables S1 and S2, is available at ArrayExpress: E-MTAB-9377.

The RNA sequencing dataset comparing the transcriptome of a SCN patient who progressed to AML (SCN-AML) with the SCN phase and healthy controls generated during this study, as shown in Figures 4 and S3 and Tables S1 and S2, is available at ArrayExpress: E-MTAB-9381.

The DNA sequencing dataset comparing different stages of leukemic progression generated during this study, as shown in Figure 5, is available at ArrayExpress: E-MTAB-9376.

The RNA sequencing dataset comparing the effect of the introduction of RUNX1-D171N (RHD) in control- or SCN -CSF3R-d715 hematopoietic progenitor cells (HPCs) generated during this study, as shown in Figure S6, is available at ArrayExpress: E-MTAB-9375.

The RNA sequencing dataset comparing SCN CSF3R-d715 RUNX1-D171N (RHD) HPCs treated with the HDAC inhibitor MS275, octyl-(R)-2hydroxyglutarate (2HG) or solvent control (DMSO) generated during this study, as shown in Figures 7 and S7, is available at ArrayExpress: E-MTAB-9374.

EXPERIMENTAL MODEL AND SUBJECT DETAILS

Mice

All animals were kept according to Erasmus MC guidelines and experiments were performed under CCD license EMCAVD101002017869. FVB/n Csf3r-d715 knock-in mice,[33] were bred at the Erasmus MC animal facility under specific pathogen free conditions and the mice were genotyped by PCR. FVB/n wild-type (WT) control mice were purchased from Envigo, Horst,

the Netherlands. All animals used were male, single housed, 10-12 weeks old at the start of the experiment, and randomly assigned to experimental groups.
Lentivirally transduced *CSF3R*-d715 lineage negative bone marrow cells were transplanted 72 hours after the first transduction. GFP expression was determined by flow cytometry and $1x10^5$ GFP positive cells were transplanted, together with their GFP negative counterparts and $1x10^5$ spleen cells, into 8.5 Gy irradiated (Cesium-137, GammaCell GC40) FVB/n wildtype (WT) recipients. Secondary transplant FVB/n WT recipients received 5 Gy irradiation and $3x10^6$ total bone marrow cells together with $1x10^5$ spleen cells. The tertiary FVB/n WT recipients were irradiated with 8.5 Gy (IBL637 Cs-137) and received $2x10^5$ total bone marrow cells together with $1x10^5$ spleen cells.
Mice were injected subcutaneously three times a week with 100 µg/kg CSF3 (Filgrastrim, Zarzio) or vehicle control (PBS). Treatment was started five weeks after transplantation in the primary recipients. The secondary recipients started CSF3 treatment four weeks after transplantation, while the tertiary transplant recipients received CSF3 or PBS treatment two weeks after transplantation. The tertiary recipients received a higher dose of CSF3 (200 µg/kg). From the start of the experiment, all mice received 50 µg/ml of Ciprofloxacin in the drinking water.

Patient samples

Ficoll-gradient separated bone marrow and blood cells were obtained and frozen according to established procedures for viable cell cryopreservation. The study was performed under the permission of the Institutional Review Boards of the Erasmus MC, the Netherlands (registration number MEC-2008-387 for biobanking and MEC-2012-030 for the genetic analysis of leukemic progression in SCN patients).

Generation of iPSC

Bone marrow fibroblasts cultured from a healthy control (22 year old female) and a SCN patient (3 months old female) harboring *ELANE* mutation (chr19:852986A>T) I60F were reprogrammed at the iPSC core facility of the Erasmus MC using a previously described protocol.[34] Cells were cultured in mTeSR™1 (STEMCELL Technologies) on Geltrex™ LDEV-Free Reduced GroWTh Factor Basement Membrane Matrix (Thermo Fisher Scientific) at 37°C and 5% CO_2, and were regularly checked for pluripotency and correct karyotype (Supplemental Figure 5a).

METHOD DETAILS

Bone marrow isolation and lineage depletion

Bone marrow (BM) was isolated from femurs, tibias and sternum of the mice. Cells were harvested by crushing bones in a mortar, and the harvested marrow depleted from

erythrocytes by Stem-Kit lysing solution (Beckman Coulter). The early stem and progenitor compartment was enriched using the Biotin Mouse Hematopoietic Progenitor (Stem) Enrichment Set (Thermo Fisher Scientific), according to the manufacturer's protocol.

Viral expression constructs, virus production and transduction of BM cells

pMY-RUNX1 retroviral vectors[35] were obtained from Gang Huang (Cincinnati Children's Hospital, Cincinnati). RUNX1b mutant 4518 (D171N, RHD mutant) insert was subsequently cloned into the pBabe vector[36] and used in *in vitro* mouse studies. For the *in vivo* and iPSC studies, the RUNX1 mutant was inserted into the lentiviral CSI vector (kind gift from Brian Duncan, University College London). The lentiviral CSI vector was also used to express CXXC4-wildtype and CXXC4-ITD (Glycine 160-165 duplication). All constructs were tested for correct introduction of inserts by enzymatic digestion and Sanger sequencing. Retroviral supernatants were harvested from HEK293T cells 48 hours after transfection with 5 µg of pBabe RUNX1 RHD mutant or empty vector (EV), together with 5 µg pCL-eco[37] and 30 µl TransIt transfection reagent (Mirus). Lentiviral supernatants were obtained from HEK293T cells 48 hours after transfection with 4 µg of the CSI vector, 3 µg pSPAX2, 1 µg pMD2.G and 25 µl FuGENE HD (Promega). Viral supernatant and $1x10^6$ lineage depleted BM cells were incubated in RPMI medium (Gibco) supplemented with 10 ng/ml each of murine interleukin-3 (IL-3), interleukin-6 (IL-6, Tebu-bio), stem cell factor (SCF, Preprotech) and granulocyte macrophage colony-stimulating factor (GM-CSF, Tebu-bio) on retronectin coated dishes (TaKaRa). Fresh virus supernatant was again added after 24 hours and transduced BM cells harvested another 48hours later (72 hours after the first transduction).

SDS-PAGE/Immunoblotting

RUNX1 expression was determined using a RUNX1 antibody directed to human AML1 (4334, Cell Signaling Technology) or an antibody that recognized both human and mouse AML1 (8529, Cell Signaling Technology). CXXC4 (NBP1-76491, Novus Bio) and TET2 (ab94580, Abcam) antibodies were used to determine both mouse and human protein levels. Preparation of lysates, and Western blot analyses were performed as previously described.[38]

Murine colony assays

Lineage negative bone marrow cells from FVB/n mice harboring either a WT or a truncated CSF3R were isolated, and retrovirally transduced with either RUNX1 RHD mutant or an empty vector control. Cells were then seeded for colony formation ($4x10^4$/ml) in methylcellulose (M3234, STEMCELL Technologies) with 50 ng/ml CSF3. Colonies were counted after 7 to 9 days of culture and replated if applicable.

Suspension cultures

$1x10^5$ lineage depleted bone marrow cells per ml were plated after transduction into LODISH stem cell expansion medium. LODISH medium consisted of CellGro GMP serum-free stem cell groWTh medium (SCGM, CellGenix, Freiburg, Germany) supplemented with 10 ng/ml each of SCF, thrombopoietin (TPO, Preprotech), insuline-like groWTh factor (IGF, R&D systems), fibroblast groWTh factor (FGF, Preprotech) and with or without 50 ng/ml CSF3. Angiopoietin was harvested as conditioned medium of transfected HEK293T cells, and added to the culture medium in a 1:5 dilution.

Flow cytometry and cell sorting

Cellular composition of the liquid cultures and *in vivo* tissues were analyzed using flow cytometry. The following antibodies and recombinant proteins were used: Sca1-Pacific blue (PB), CD34-Phycoerythrin (PE), CD48-PE, CD150-PE.Cy7, Ter119 Allophycocyanin (APC) (all Biolegend), CD117-APC, CD16/32-APC.Cy7, CD11b-PE, Gr1-APC, CD3-PE.Cy7, CD71 PE (all BD Biosciences), CD19 Alexa Fluor 700 (AF700, Life) and CD117 PerCpCy5.5 (SONY). Lineage positive cells were detected using the murine lineage detection kit (BD Biosciences) subsequently stained with streptavidin-pacific orange (PO, Fisher Scientific).
SSEA4-PE (Biolegend) and Tra-1-60 Alexa Fluor 647 (AF647, BD Biosciences) were used for regular pluripotency screenings of the iPSCs. Hematopoietic induction of iPSC was assessed using CD34-PE and CD45-BV421 antibodies (both BD Biosciences). Dead cells were excluded by using 7-aminoactinomycin-D (7AAD, Life) or 4',6-Diamidino-2-Phenylindole (DAPI, Fisher Scientific). Flow cytometry was performed using a BD LSRII flow cytometer (BD Biosciences). For subsequent cell sorting a FACSAria (BD Biosciences) was used. Analysis of FACS data was performed using FlowJo (TreeStar).

Blood, bone marrow, spleen and liver isolation from mice

Peripheral blood was obtained by cheek puncture. Upon sacrifice, bone marrow was isolated from femurs and tibias of the mice. Cells were harvested by flushing the bones and subsequently filtered. Cells from spleen and liver were obtained by mashing parts of the organs through a filter.

Histological and morphological analyses

Mouse organs were fixed in 4% formaldehyde overnight, dehydrated and prepared for paraffin embedding, after which they were stained with Haemotoxylin and Eosin (H&E).
Cells were attached to glass slides using a Cytospin 4 (Thermo Scientific) according to the manufacturer's protocol and stained with May-Grünwald Giemsa staining. Stainings were performed according to routine protocols.

Introduction of CXXC4 in K562/HeLa and protein stability assays

Lentiviral supernatant containing either an empty vector control, CXXC4-wildtype or the CXXC4-ITD (duplication of Glycines 160-165) was added to K562 and HeLa cells. Transduced cells were sorted for GFP^+ expression and subsequently used. To test protein stability of CXXC4-wildtype or -ITD, we added 1ug/ml of the translation inhibitor cycloheximide (Merck) and harvested the cells 0, 8, 16 or 24 hours after the start of the treatment.

Targeted sequencing of CXXC4

Custom CXXC4 amplicon sequencing was performed on patients of the HOVON102 trial using the Illumina PCR-based Custom Amplicon Library Preparation workflow. Forward primer AGGGGATAAGGTGGAGAGGA and reverse primer CCCCTGGAACTGCGACAA were used to amplify the Glycine repeat region of CXXC4. Libraries were paired-end sequenced with the MiSeq V2 Nano kit (Illumina) on the Illumina MiSeq. Bioinformatic analysis was performed as previously described.[39]

CRISPR/Cas9-mediated genome editing

To introduce the *CSF3R*-d715 mutation in iPSCs, $2x10^6$ cells were electroporated with 500 ng px330[40] (Cas9 plasmid, Addgene plasmid #42230) and 1500 ng recombination template containing the d715 mutation and a puromycin selection cassette (Supplemental Figure 4b), using the 4D-Nucleofector System (Lonza), program CA-137. Puromycin selection (300 ng/ml) started 48 hrs after electroporation. Single clones were picked and screened for correct and heterozygous integration of the CSF3R mutation and pluripotency (Supplemental Figures 5a,b).

Hematopoietic induction and colony assays from iPSC

Hematopoietic Stem and Progenitor cells (HSPCs) were produced with the STEMdiff™ Hematopoietic Kit (STEMCELL Technologies) according to the manufacturer's protocol. Floating cells were harvested at Day 12 of the protocol.

Lentiviral production and transduction of iPSC

Lentiviral supernatant was harvested at 24 and 48 hours after transfection of HEK293T cells with 4 µg of the CSI vector, 3 µg pSPAX2, 1 µg pMD2.G, and 25 µl FuGENE HD (Promega). Viral particles were 100x concentrated by ultracentrifugation (Optima XPN-80, Beckman Coulter) for 2 hours at 20.000g and 4°C. Virus (25 ul/ml) and hexadimethrine bromide (polybrene, 4 ug/ml, Sigma) were added to the hematopoietic induction cultures 60 hours before harvesting the floating cells.

TET inhibitor experiments

DMSO (solvent control), 0.1 mM Octyl-(R)-2HG (Sigma-Aldrich) or 2 μM MS275 (Santa Cruz) was added for 16 hours to the hematopoietic induction cultures before harvesting the floating cells.

RNA isolation and RNA sequencing

RNA was isolated from FACS purified mouse LK or c-Kit$^+$ cells, human CD34$^+$ cells from the bone marrow (SCN phase, 1992) or blood (AML phase, 2007) or CD34$^+$CD45$^+$ hematopoietic stem and progenitor cells derived from the iPSCs using TRIzol (Thermo Fisher Scientific) according to the manufacturer's protocol. For the *in vitro* mouse experiments cDNA was generated with the SMARTer Ultra Low Input RNA kit for sequencing (version 3, Clontech), while version 4 of the SMARTer Ultra Low Input RNA kit for sequencing (Clontech) was used for the other samples. Sequencing libraries were generated using TruSeq Nano DNA Sample Preparation kits (Illumina), according to the low sample protocol and run on HiSeq 2500 or Novaseq 6000 instruments (Illumina).

Whole exome sequencing

100 ng genomic DNA was fragmented using enzymatic fragmentation and sample libraries were constructed following the SeqCap EZ HyperPlusCap workflow User's Guide version 1.0 (Roche). Unique, dual index adapters (Integrated DNA technologies) were used for ligation. After ligation of adapters and an amplification step, exome target sequences were captured using in-solution oligonucleotide baits (SeqCap EZ Developer Library mm9_exome_L2R_D02). Amplified captured sample libraries were paired-end sequenced (2x100 cycles) on the HiSeq 2500 platform (Illumina).

Bioinformatics and statistics

Demultiplexing was performed using the CASAVA software (Illumina) allowing for one mismatch in the barcodes. Subsequently quality metrics were estimated (FastQC, Babraham bioinformatics & MultiQC, http://multiqc.info) for all of the resulting fastq files. Afterwards reads were aligned against the Mouse Transcriptome (Gencode m12)/Genome (mm10) or Human Transcriptome (Gencode v19)/Genome (hg19) using the STAR aligner.[41] Abundance estimation was performed using Cufflinks[42] (refSeq), and raw counts were measured with the HTSeq-count software set in union mode.[43] Next the measured raw counts were used to create clustering and principle component plots and perform differential expression analysis both using DESeq2 and R[44] (https://www.r-project.org/). Finally gene set enrichment analysis, with the hallmark pathways H, was done using the GSEA software[45,46] (https://www.gsea-msigdb.org/gsea/msigdb/genesets.jsp?collection=H).

QUANTIFICATION AND STATISTICAL ANALYSIS

Data are presented as mean ± SEM. Comparison of two groups was performed using unpaired t-test. Statistical analyses were performed using GraphPad Prism 5.0c (GraphPad Software Inc., San Diego, CA) or DESeq2. A p-value <0.05 was considered significant.

References

1. Skokowa J, Dale DC, Touw IP, Zeidler C, Welte K. (2017). Severe congenital neutropenias. Nat Rev Dis Primers;3:17032.
2. Dale DC, Bonilla MA, Davis MW, Nakanishi AM, Hammond WP, Kurtzberg J, Wang W, Jakubowski A, Winton E, Lalezari P, et al. (1993). A randomized controlled phase III trial of recombinant human granulocyte colony-stimulating factor (filgrastim) for treatment of severe chronic neutropenia. Blood;81(10):2496-502.
3. Rosenberg PS, Alter BP, Bolyard AA, Bonilla MA, Boxer LA, Cham B, Fier C, Freedman M, Kannourakis G, Kinsey S, et al. (2006). The incidence of leukemia and mortality from sepsis in patients with severe congenital neutropenia receiving long-term G-CSF therapy. Blood;107(12):4628-35.
4. Rosenberg PS, Zeidler C, Bolyard AA, Alter BP, Bonilla MA, Boxer LA, Dror Y, Kinsey S, Link DC, Newburger PE, et al. (2010). Stable long-term risk of leukaemia in patients with severe congenital neutropenia maintained on G-CSF therapy. Br J Haematol;150(2):196-9.
5. Touw IP. (2015). Game of clones: the genomic evolution of severe congenital neutropenia. Hematology Am Soc Hematol Educ Program;2015:1-7.
6. Skokowa J, Steinemann D, Katsman-Kuipers JE, Zeidler C, Klimenkova O, Klimiankou M, Unalan M, Kandabarau S, Makaryan V, Beekman R, et al. (2014). Cooperativity of RUNX1 and CSF3R mutations in severe congenital neutropenia: a unique pathway in myeloid leukemogenesis. Blood;123(14):2229-37.
7. Sroczynska P, Lancrin C, Kouskoff V, Lacaud G. (2009). The differential activities of Runx1 promoters define milestones during embryonic hematopoiesis. Blood;114(26):5279-89.
8. Bee T, Liddiard K, Swiers G, Bickley SR, Vink CS, Jarratt A, Hughes JR, Medvinsky A, de Bruijn MF. (2009). Alternative Runx1 promoter usage in mouse developmental hematopoiesis. Blood Cells Mol Dis;43(1):35-42.
9. Miyoshi H, Ohira M, Shimizu K, Mitani K, Hirai H, Imai T, Yokoyama K, Soeda E, Ohki M. (1995). Alternative splicing and genomic structure of the AML1 gene involved in acute myeloid leukemia. Nucleic Acids Res;23(14):2762-9.
10. Beekman R, Valkhof MG, Sanders MA, van Strien PM, Haanstra JR, Broeders L, Geertsma-Kleinekoort WM, Veerman AJ, Valk PJ, Verhaak RG, et al. (2012). Sequential gain of mutations in severe congenital neutropenia progressing to acute myeloid leukemia. Blood;119(22):5071-7.
11. Ko M, An J, Bandukwala HS, Chavez L, Aijo T, Pastor WA, Segal MF, Li H, Koh KP, Lahdesmaki H, et al. (2013). Modulation of TET2 expression and 5-methylcytosine oxidation by the CXXC domain protein IDAX. Nature;497(7447):122-6.

12. Hino S, Kishida S, Michiue T, Fukui A, Sakamoto I, Takada S, Asashima M, Kikuchi A. (2001). Inhibition of the Wnt signaling pathway by Idax, a novel Dvl-binding protein. Mol Cell Biol;21(1):330-42.
13. Grenda DS, Johnson SE, Mayer JR, McLemore ML, Benson KF, Horwitz M, Link DC. (2002). Mice expressing a neutrophil elastase mutation derived from patients with severe congenital neutropenia have normal granulopoiesis. Blood;100(9):3221-8.
14. Abegunde SO, Buckstein R, Wells RA, Rauh MJ. (2018). An inflammatory environment containing TNFalpha favors Tet2-mutant clonal hematopoiesis. Exp Hematol;59:60-5.
15. Barreyro L, Chlon TM, Starczynowski DT. (2018). Chronic immune response dysregulation in MDS pathogenesis. Blood;132(15):1553-60.
16. Cull AH, Snetsinger B, Buckstein R, Wells RA, Rauh MJ. (2017). Tet2 restrains inflammatory gene expression in macrophages. Exp Hematol;55:56-70 e13.
17. Meisel M, Hinterleitner R, Pacis A, Chen L, Earley ZM, Mayassi T, Pierre JF, Ernest JD, Galipeau HJ, Thuille N, et al. (2018). Microbial signals drive pre-leukaemic myeloproliferation in a Tet2-deficient host. Nature;557(7706):580-4.
18. Shen Q, Zhang Q, Shi Y, Shi Q, Jiang Y, Gu Y, Li Z, Li X, Zhao K, Wang C, et al. (2018). Tet2 promotes pathogen infection-induced myelopoiesis through mRNA oxidation. Nature;554(7690):123-7.
19. Zhang Q, Zhao K, Shen Q, Han Y, Gu Y, Li X, Zhao D, Liu Y, Wang C, Zhang X, et al. (2015). Tet2 is required to resolve inflammation by recruiting Hdac2 to specifically repress IL-6. Nature;525(7569):389-93.
20. Kroeze LI, Aslanyan MG, van Rooij A, Koorenhof-Scheele TN, Massop M, Carell T, Boezeman JB, Marie JP, Halkes CJ, de Witte T, et al. (2014). Characterization of acute myeloid leukemia based on levels of global hydroxymethylation. Blood;124(7):1110-8.
21. An J, Rao A, Ko M. (2017). TET family dioxygenases and DNA demethylation in stem cells and cancers. Exp Mol Med;49(4):e323.
22. Lu H, Sun J, Wang F, Feng L, Ma Y, Shen Q, Jiang Z, Sun X, Wang X, Jin H. (2013). Enhancer of zeste homolog 2 activates wnt signaling through downregulating CXXC finger protein 4. Cell Death Dis;4:e776.
23. Gelsi-Boyer V, Brecqueville M, Devillier R, Murati A, Mozziconacci MJ, Birnbaum D. (2012). Mutations in ASXL1 are associated with poor prognosis across the spectrum of malignant myeloid diseases. J Hematol Oncol;5:12.
24. Nagase R, Inoue D, Pastore A, Fujino T, Hou HA, Yamasaki N, Goyama S, Saika M, Kanai A, Sera Y, et al. (2018). Expression of mutant Asxl1 perturbs hematopoiesis and promotes susceptibility to leukemic transformation. J Exp Med;215(6):1729-47.

25. Essers MA, Offner S, Blanco-Bose WE, Waibler Z, Kalinke U, Duchosal MA, Trumpp A. (2009). IFNalpha activates dormant haematopoietic stem cells in vivo. Nature;458(7240):904-8.
26. Pietras EM. (2017). Inflammation: a key regulator of hematopoietic stem cell fate in health and disease. Blood;130(15):1693-8.
27. Walter D, Lier A, Geiselhart A, Thalheimer FB, Huntscha S, Sobotta MC, Moehrle B, Brocks D, Bayindir I, Kaschutnig P, et al. (2015). Exit from dormancy provokes DNA-damage-induced attrition in haematopoietic stem cells. Nature;520(7548):549-52.
28. Hemmati S, Haque T, Gritsman K. (2017). Inflammatory Signaling Pathways in Preleukemic and Leukemic Stem Cells. Front Oncol;7:265.
29. Leoni C, Montagner S, Rinaldi A, Bertoni F, Polletti S, Balestrieri C, Monticelli S. (2017). Dnmt3a restrains mast cell inflammatory responses. Proc Natl Acad Sci U S A;114(8):E1490-E9.
30. Cai Z, Kotzin JJ, Ramdas B, Chen S, Nelanuthala S, Palam LR, Pandey R, Mali RS, Liu Y, Kelley MR, et al. (2018). Inhibition of Inflammatory Signaling in Tet2 Mutant Preleukemic Cells Mitigates Stress-Induced Abnormalities and Clonal Hematopoiesis. Cell Stem Cell;23(6):833-49 e5.
31. Erdal E, Haider S, Rehwinkel J, Harris AL, McHugh PJ. (2017). A prosurvival DNA damage-induced cytoplasmic interferon response is mediated by end resection factors and is limited by Trex1. Genes Dev;31(4):353-69.
32. Brzostek-Racine S, Gordon C, Van Scoy S, Reich NC. (2011). The DNA damage response induces IFN. J Immunol;187(10):5336-45.
33. Hermans MH, Ward AC, Antonissen C, Karis A, Lowenberg B, Touw IP. (1998). Perturbed granulopoiesis in mice with a targeted mutation in the granulocyte colony-stimulating factor receptor gene associated with severe chronic neutropenia. Blood;92(1):32-9.
34. Warlich E, Kuehle J, Cantz T, Brugman MH, Maetzig T, Galla M, Filipczyk AA, Halle S, Klump H, Scholer HR, et al. (2011). Lentiviral vector design and imaging approaches to visualize the early stages of cellular reprogramming. Mol Ther;19(4):782-9.
35. Goyama S, Schibler J, Cunningham L, Zhang Y, Rao Y, Nishimoto N, Nakagawa M, Olsson A, Wunderlich M, Link KA, et al. (2013). Transcription factor RUNX1 promotes survival of acute myeloid leukemia cells. J Clin Invest;123(9):3876-88.
36. Morgenstern JP, Land H. (1990). Advanced mammalian gene transfer: high titre retroviral vectors with multiple drug selection markers and a complementary helper-free packaging cell line. Nucleic Acids Res;18(12):3587-96.
37. Naviaux RK, Costanzi E, Haas M, Verma IM. (1996). The pCL vector system: rapid production of helper-free, high-titer, recombinant retroviruses. J Virol;70(8):5701-5.

38. Palande KK, Beekman R, van der Meeren LE, Beverloo HB, Valk PJ, Touw IP. (2011). The antioxidant protein peroxiredoxin 4 is epigenetically down regulated in acute promyelocytic leukemia. PLoS One;6(1):e16340.
39. Jongen-Lavrencic M, Grob T, Hanekamp D, Kavelaars FG, Al Hinai A, Zeilemaker A, Erpelinck-Verschueren CAJ, Gradowska PL, Meijer R, Cloos J, et al. (2018). Molecular Minimal Residual Disease in Acute Myeloid Leukemia. N Engl J Med;378(13):1189-99.
40. Cong L, Ran FA, Cox D, Lin S, Barretto R, Habib N, Hsu PD, Wu X, Jiang W, Marraffini LA, et al. (2013). Multiplex genome engineering using CRISPR/Cas systems. Science;339(6121):819-23.
41. Dobin A, Davis CA, Schlesinger F, Drenkow J, Zaleski C, Jha S, Batut P, Chaisson M, Gingeras TR. (2013). STAR: ultrafast universal RNA-seq aligner. Bioinformatics;29(1):15-21.
42. Trapnell C, Williams BA, Pertea G, Mortazavi A, Kwan G, van Baren MJ, Salzberg SL, Wold BJ, Pachter L. (2010). Transcript assembly and quantification by RNA-Seq reveals unannotated transcripts and isoform switching during cell differentiation. Nat Biotechnol;28(5):511-5.
43. Anders S, Pyl PT, Huber W. (2015). HTSeq--a Python framework to work with high-throughput sequencing data. Bioinformatics;31(2):166-9.
44. Love MI, Huber W, Anders S. (2014). Moderated estimation of fold change and dispersion for RNA-seq data with DESeq2. Genome Biol;15(12):550.
45. Mootha VK, Lindgren CM, Eriksson KF, Subramanian A, Sihag S, Lehar J, Puigserver P, Carlsson E, Ridderstrale M, Laurila E, et al. (2003). PGC-1alpha-responsive genes involved in oxidative phosphorylation are coordinately downregulated in human diabetes. Nat Genet;34(3):267-73.
46. Subramanian A, Tamayo P, Mootha VK, Mukherjee S, Ebert BL, Gillette MA, Paulovich A, Pomeroy SL, Golub TR, Lander ES, et al. (2005). Gene set enrichment analysis: a knowledge-based approach for interpreting genome-wide expression profiles. Proc Natl Acad Sci U S A;102(43):15545-50.

Supplemental Figures

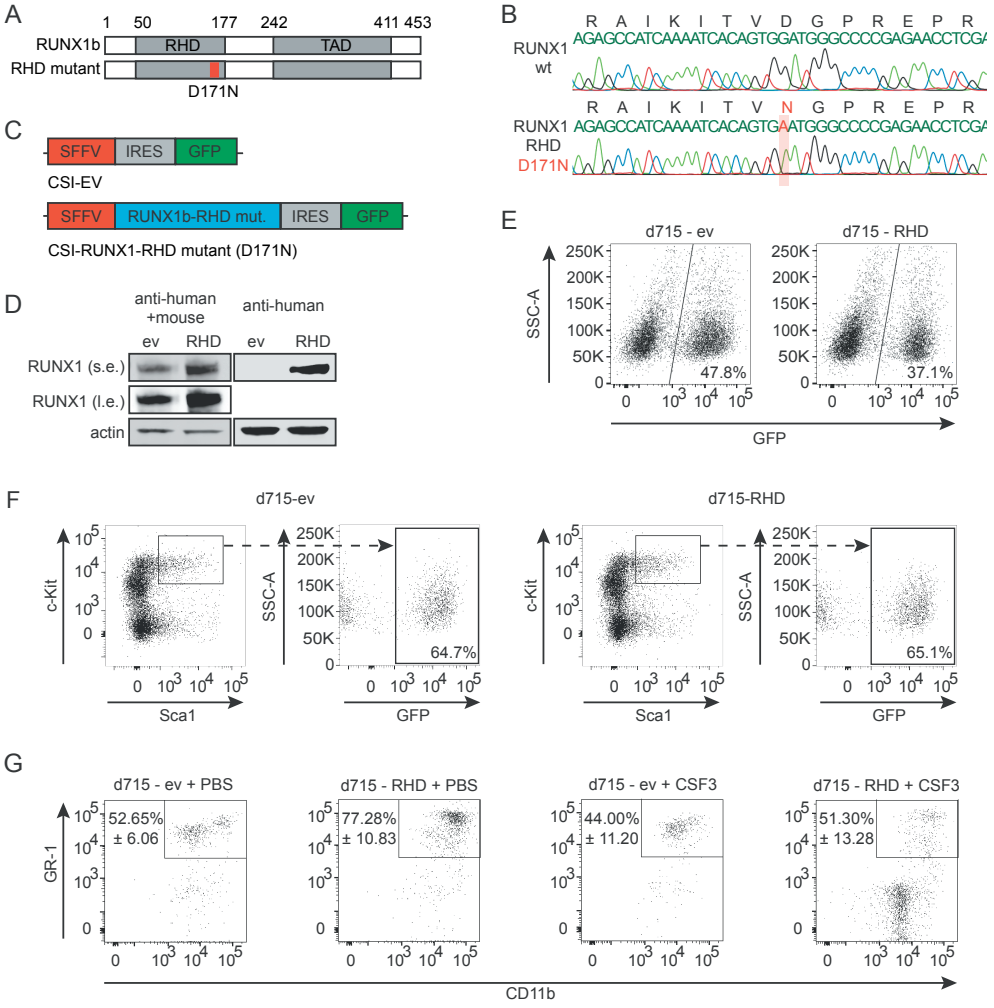

Figure S1: Lentiviral transduction of mouse bone marrow cells (related to Figure 1)

(A,B): Position of the G-to-A missense mutation shown by Sanger sequencing, resulting in D171N amino acid change in RUNX1b (wild type) protein. (C): Lentiviral expression constructs used for transplantation experiments. (D): Expression of mutant RUNX1 protein in lentivirus-transduced lineage depleted hematopoietic progenitors; immunoblot stained with Ab8529 (left panel), detecting both mouse and human RUNX1 after short (s.e.) and long (l.e.) exposure; and with Ab4334 (right panel), specific for human RUNX1. (E): FACS dot plots showing GFP expression in lineage negative cells before transplantation. (F): FACS dot plots showing GFP expression in ~ 65% of LSK cells. (G): Representative FACS dot plots showing GFP+CD11b+GR-1+ neutrophils in the PB. Data are from samples taken 14 and 16 weeks after transplantation (n=11 or 12 per group).

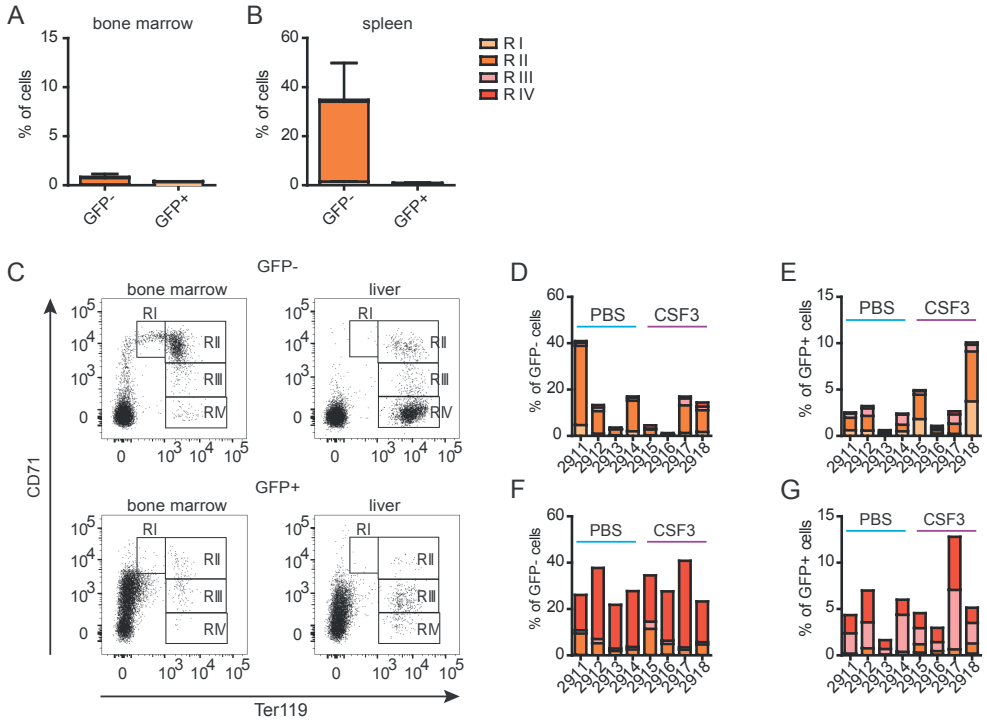

Figure S2: Analysis of erythroid cell populations (related to Figure 2)

(A-G): CD71 and Ter119 staining is used to discriminate between the 4 stages of erythropoiesis with FACS. RI: CD71highTer119-, RII: CD71highTer119+, RIII: CD71intermediateTer119+, RIV: CD71-Ter119+. (A): erythroid cells observed in the bone marrow of the secondary recipients and (B): in the spleen. (C): Representative FACS dot plot showing the different stages of erythroid development based on CD71 and Ter119 in the bone marrow or liver of tertiary recipients. (D): histogram showing erythropoiesis of the GFP- cells in the bone marrow of the tertiary recipients and (E): the GFP+ erythroid cells in the BM. (F): GFP- erythroid cells in the liver and (G): GFP+ erythroid cells in the liver.

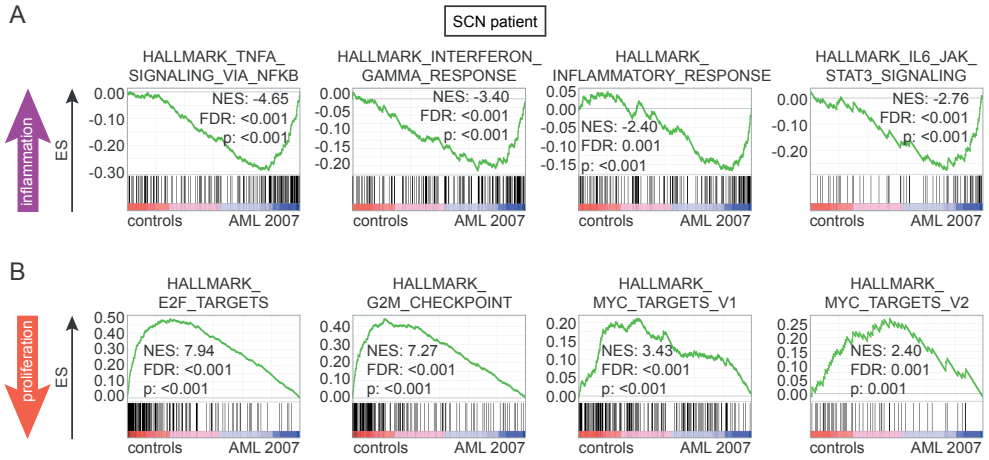

Figure S3: Leukemic progression of SCN (SCN-AML) is associated with increased inflammatory and decreased proliferative signaling (related to Figure 4)

GSEA comparing CD34+ cells from 3 healthy controls with the SCN-AML phase (2007) showing (A): increased inflammatory pathways and (B): down-regulated proliferation signatures. ES = enrichment score, NES = normalized enrichment score, FDR = false discovery rate.

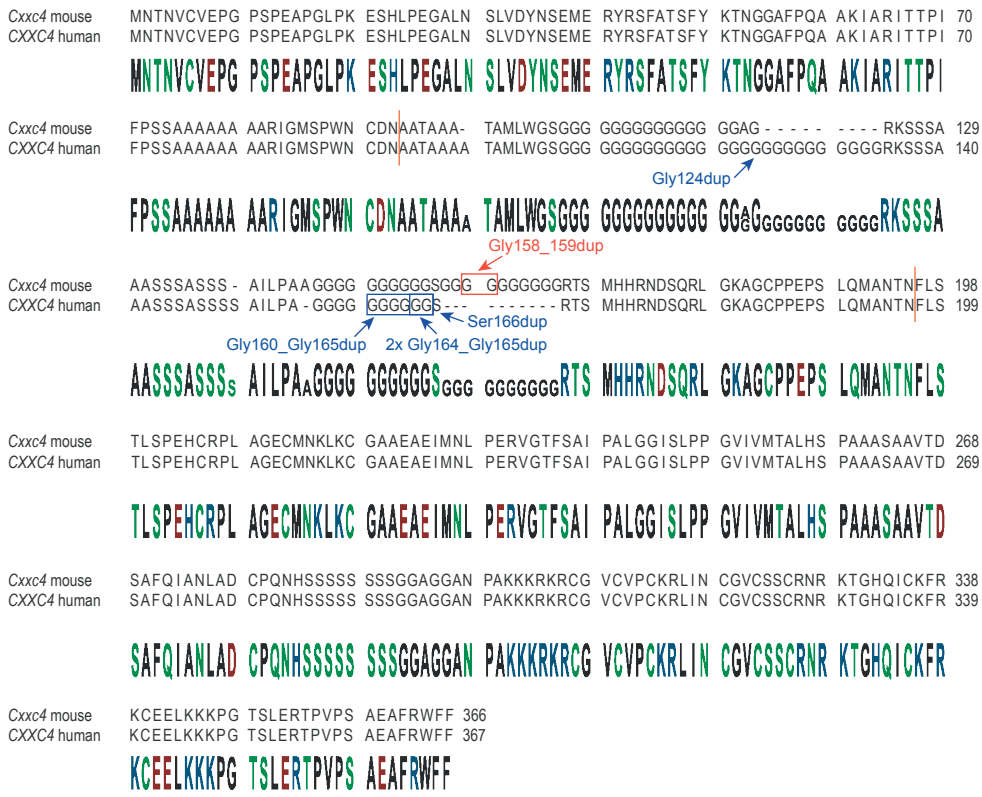

Figure S4: Alignment of mouse and human CXXC4 protein sequences and positioning of mutations in human AML (related to Figures 5 and 6)

Mutations marked in blue indicate alterations found in human AML; the mutation marked in red indicates the CXXC4 alteration found in the murine AML cells. Orange and red bars indicate start and finish of the 2 amplicons used for targeted sequencing.

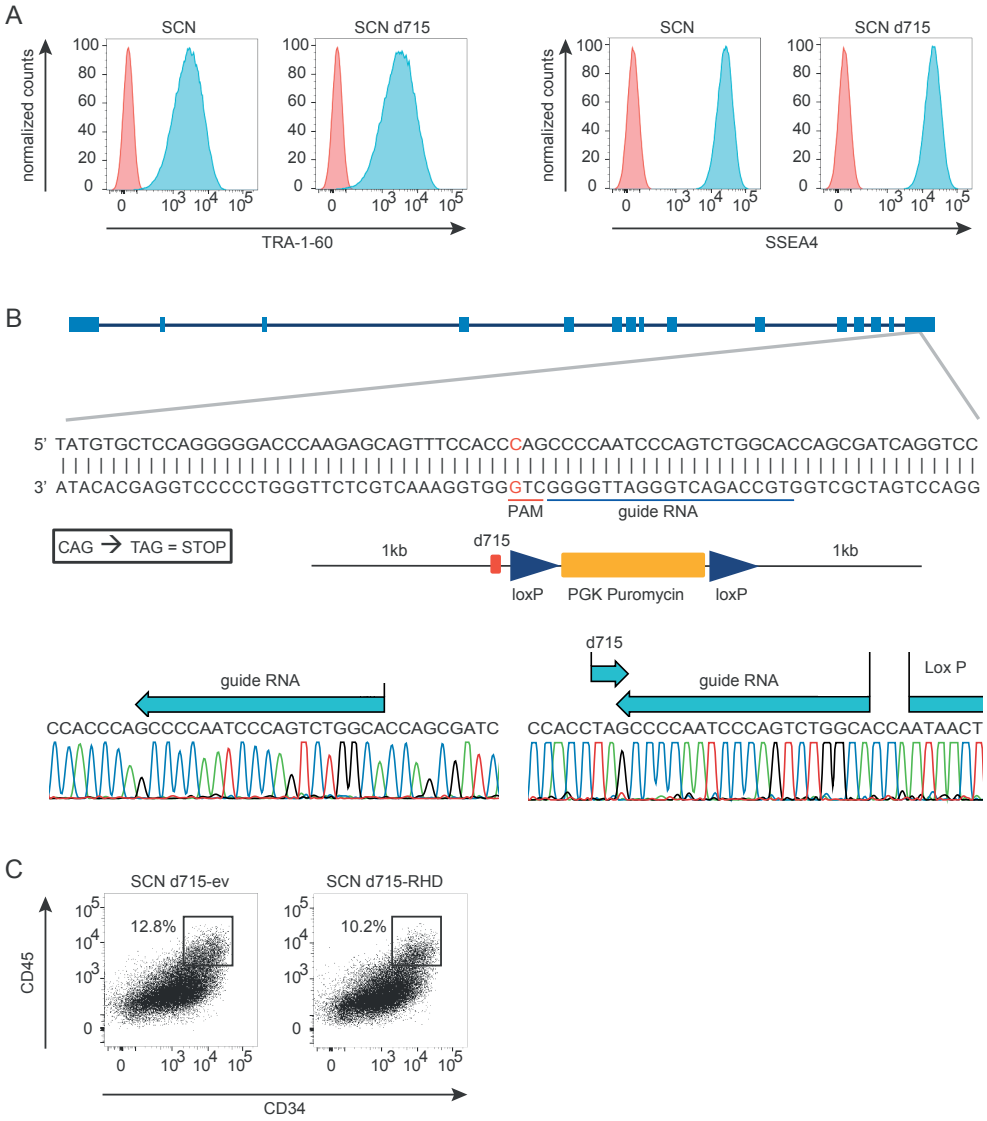

Figure S5: Characterization of pluripotency and the introduction of CSF3R mutation in iPSCs (related to Figures 7, S6, S7 and STAR Methods)

(A): FACS histograms (blue) showing TRA-1-60 and SSEA4 expression in SCN-iPSC and SCN-iPSC with the CRISPR-Cas9 targeted CSF3R-d715 mutation. Red histograms are from unstained cells. (B): Schematic overview of the recombination template used to introduce the CSF3R-d715 mutation with CRISPR-Cas9 and Sanger sequencing data showing the heterozygous integration of the recombination template. (C): FACS dot plot showing CD34 and CD45 expression of floating cells harvest at Day 12 of hematopoietic induction with the STEMdiff Hematopoietic kit.

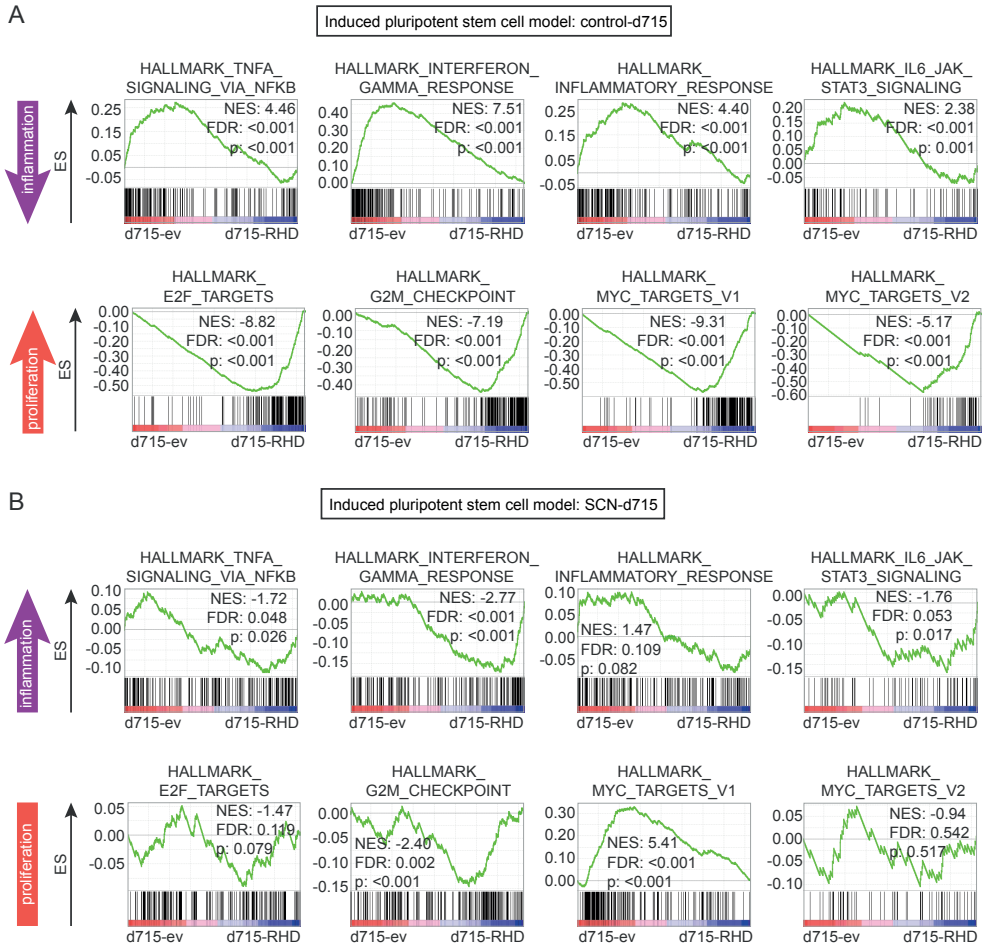

Figure S6: Transcriptome analysis in control and SCN iPSC-derived CD34+CD45+ cells with truncated CSF3R: the SCN background alters the inflammation/ proliferation balance (related to Figures 1, S5)

GSEA analyses comparing CD34+CD45+ cells from CSF3R-d715 transduced with either empty vector or RUNX1-RHD in (A): control cells showing reduced inflammatory signaling and increased proliferative signatures, and in (B): ELANE-mutant SCN cells showing slightly increased inflammatory signaling, while the proliferation induction is less pronounced. Data shown is derived from 2 independent experiments. ES = enrichment score, NES = normalized enrichment score, FDR = false discovery rate.

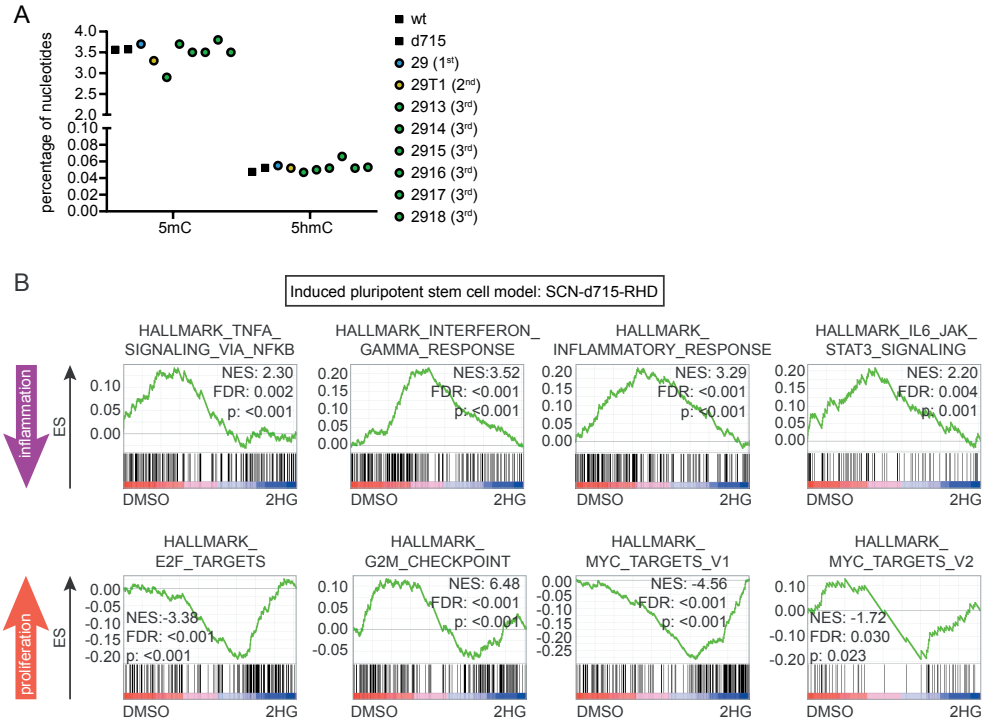

Figure S7: Inhibition of TET2 activity does not mimic the expression signatures observed in AML (related to Figures 4, 7)

(A): Dot plot showing no differences between the percentage of 5mC or 5hmC modified nucleotides in control, primary-, secondary-, and tertiary-transplant recipient mice. Inflammatory and proliferation related GSEA comparing (B): DMSO or 2HG treated, CSF3R-d715, RUNX1-RHD CD34+CD45+ cells derived from ELANE-mutant SCN-iPSC (two independent experiments).

Table S1: Upregulated transcripts in mouse AML and SCN-AML samples (related to Figures 3 and 7)

	wt+d715 (TPM)		2911-2918 (TPM)				SCN	SCN-AML	
Transcripts	Mean	SEM	Mean	SEM	p-value	q-value	(TPM)	(TPM)	p-value
ADAP1	**76.610**	7.734	**112.078**	3.714	0.000	0.000	**3.123**	**107.222**	0.007
AKAP12	**1.174**	0.495	**8.178**	0.717	0.000	0.000	**0.125**	**9.114**	0.019
ALDOC	**4.566**	0.518	**20.833**	2.173	0.000	0.000	**4.085**	**66.011**	0.034
ANXA2	**98.767**	2.025	**170.653**	17.325	0.002	0.005	**148.538**	**1166.104**	0.030
ARID3B	**6.817**	0.057	**10.026**	0.784	0.003	0.008	**4.991**	**48.246**	0.040
C2	**0.000**	0.000	**3.416**	0.473	0.000	0.000	**0.000**	**1.029**	0.000
CASS4	**0.989**	0.989	**3.595**	0.339	0.005	0.015	**0.045**	**28.485**	0.002
CDKN1A	**32.308**	4.833	**95.238**	4.043	0.000	0.000	**12.338**	**150.233**	0.022
CISH	**20.392**	0.286	**56.367**	6.222	0.000	0.000	**10.556**	**143.478**	0.022
CSF3R	**81.353**	6.397	**116.220**	6.645	0.000	0.001	**86.063**	**568.637**	0.032
CXCL2	**0.000**	0.000	**1.235**	0.424	0.001	0.004	**92.786**	**1003.455**	0.019
CYTH4	**92.696**	13.180	**142.309**	10.530	0.000	0.000	**8.796**	**127.143**	0.016
DGAT2	**4.360**	0.969	**15.291**	2.522	0.000	0.000	**0.060**	**44.868**	0.001
DUSP1	**74.312**	1.299	**337.066**	110.876	0.018	0.041	**387.031**	**2744.965**	0.035
DUSP2	**129.095**	30.487	**277.417**	46.648	0.019	0.043	**62.289**	**808.883**	0.013
ECHDC2	**0.951**	0.110	**3.173**	0.599	0.014	0.033	**2.398**	**59.611**	0.023
EFNA1	**2.406**	1.089	**8.496**	1.225	0.000	0.001	**2.614**	**66.791**	0.020
ESAM	**37.701**	1.076	**111.813**	12.971	0.000	0.000	**17.079**	**129.748**	0.048
F13A1	**47.495**	8.898	**510.433**	86.608	0.000	0.000	**17.280**	**705.205**	0.003
FAM49A	**10.927**	0.263	**14.803**	0.993	0.004	0.012	**0.093**	**52.449**	0.000
FGD5	**2.089**	0.546	**14.054**	1.059	0.000	0.000	**0.595**	**26.595**	0.008
FOS	**41.011**	16.634	**457.660**	181.649	0.004	0.011	**436.335**	**6789.652**	0.010
GDPD5	**0.224**	0.224	**4.420**	0.626	0.000	0.000	**0.000**	**61.903**	0.000
GNG11	**32.207**	4.152	**43.629**	2.385	0.004	0.011	**51.361**	**489.900**	0.028
HCK	**0.672**	0.518	**32.154**	3.692	0.000	0.000	**19.422**	**341.296**	0.012
HIP1	**2.020**	0.294	**14.266**	0.459	0.000	0.000	**2.172**	**19.226**	0.047
ICAM1	**44.452**	10.317	**84.731**	3.274	0.000	0.000	**14.345**	**154.835**	0.027
IER2	**273.214**	19.229	**847.096**	137.990	0.000	0.002	**344.232**	**3173.270**	0.023
IL10RA	**9.567**	5.397	**23.257**	3.637	0.012	0.030	**22.399**	**275.262**	0.018
KCNK6	**2.574**	1.785	**9.410**	0.902	0.000	0.000	**0.965**	**37.293**	0.009
KLF2	**2.028**	0.239	**19.443**	9.241	0.007	0.017	**14.971**	**128.116**	0.036
MAP3K1	**1.557**	0.415	**4.109**	0.262	0.000	0.000	**0.352**	**11.187**	0.028
MIR22HG	**0.000**	0.000	**3.166**	0.754	0.000	0.000	**4.310**	**11.151**	0.040
MYRF	**0.000**	0.000	**1.503**	0.311	0.000	0.000	**0.000**	**17.450**	0.001
PARP8	**29.957**	11.253	**50.302**	3.074	0.000	0.002	**1.413**	**25.464**	0.022
PDE2A	**17.286**	1.015	**40.984**	4.261	0.000	0.000	**0.051**	**63.809**	0.000
PEAK1	**0.876**	0.174	**4.056**	0.247	0.000	0.000	**0.172**	**11.633**	0.011
PELI2	**4.112**	0.100	**5.844**	0.292	0.002	0.007	**1.817**	**27.706**	0.028
PLK2	**1.958**	0.831	**4.445**	0.598	0.011	0.027	**0.000**	**37.952**	0.001
PMAIP1	**1.514**	0.463	**181.861**	9.115	0.000	0.000	**112.887**	**667.623**	0.047
POU2F2	**5.479**	0.488	**10.329**	0.980	0.001	0.003	**0.894**	**14.981**	0.047
PPAP2A	**4.018**	2.135	**7.460**	0.526	0.013	0.030	**0.040**	**109.365**	0.001
PTGIR	**2.619**	0.815	**9.546**	0.698	0.000	0.000	**14.987**	**193.512**	0.020

	wt+d715 (TPM)		**2911-2918 (TPM)**				**SCN**	**SCN-AML**	
Transcripts	Mean	SEM	Mean	SEM	p-value	q-value	**(TPM)**	**(TPM)**	p-value
RBPMS	**73.450**	12.444	**159.384**	11.375	0.000	0.000	**22.089**	**243.656**	0.018
RHOB	**7.714**	0.559	**24.352**	4.253	0.000	0.000	**7.875**	**75.929**	0.044
RXFP1	**0.000**	0.000	**2.603**	0.242	0.000	0.000	**2.255**	**218.103**	0.002
S100A16	**0.101**	0.101	**15.640**	3.291	0.000	0.000	**0.450**	**201.869**	0.000
SGCE	**15.925**	0.527	**41.888**	2.877	0.000	0.000	**0.848**	**81.740**	0.012
SORT1	**17.619**	1.869	**31.723**	1.231	0.000	0.000	**1.734**	**49.372**	0.008
SPARC	**1.000**	0.918	**15.064**	1.596	0.000	0.000	**137.496**	**772.904**	0.049
SPP1	**5.969**	2.560	**98.210**	6.977	0.000	0.000	**4.538**	**98.258**	0.022
TNNT1	**2.163**	0.091	**37.240**	2.072	0.000	0.000	**0.000**	**63.938**	0.001
VNN1	**1.068**	1.068	**5.946**	0.614	0.000	0.000	**19.620**	**148.520**	0.039
YES1	**0.469**	0.263	**1.798**	0.292	0.002	0.006	**1.096**	**70.475**	0.003
ZFP36	**62.796**	9.864	**341.485**	84.642	0.001	0.003	**372.547**	**2042.670**	0.049

Table S2: Downregulated transcripts in mouse AML and SCN-AML samples (related to Figures 3 and 7)

	wt+d715 (TPM)		**2911-2918 (TPM)**				**SCN**	**SCN-AML**	
Transcripts	Mean	SEM	Mean	SEM	p-value	q-value	**(TPM)**	**(TPM)**	p-value
ABLIM1	**3.135**	2.449	**0.443**	0.180	0.003	0.008	**17.242**	**0.000**	0.000
ALDH1A1	**40.810**	18.173	**2.811**	0.750	0.000	0.000	**267.785**	**1.687**	0.001
APOE	**1457.806**	75.156	**139.495**	26.103	0.000	0.000	**151.051**	**10.498**	0.039
BLNK	**8.679**	2.850	**0.087**	0.041	0.000	0.000	**71.718**	**5.069**	0.042
BLVRB	**124.042**	8.566	**34.675**	6.532	0.000	0.000	**348.949**	**30.415**	0.035
CEP152	**21.006**	1.614	**10.996**	0.601	0.000	0.000	**46.303**	**3.988**	0.038
CHST2	**0.732**	0.250	**0.116**	0.036	0.010	0.024	**45.965**	**0.026**	0.000
CKAP2L	**158.325**	12.128	**69.921**	3.530	0.000	0.000	**38.703**	**3.558**	0.047
DEPDC1B	**90.213**	13.161	**41.690**	2.524	0.000	0.000	**127.093**	**12.717**	0.041
DHX32	**47.015**	10.050	**14.669**	1.364	0.000	0.000	**72.522**	**4.681**	0.034
DTL	**150.428**	0.056	**59.978**	2.771	0.000	0.000	**109.663**	**14.026**	0.049
DYNLT3	**133.093**	10.515	**63.246**	2.294	0.000	0.000	**50.740**	**0.000**	0.001
EPOR	**103.405**	2.778	**23.938**	5.811	0.001	0.004	**100.145**	**1.177**	0.005
FAM178B	**1.034**	0.402	**0.000**	0.000	0.000	0.001	**183.409**	**0.364**	0.002
FRMD6	**14.164**	2.754	**8.098**	0.623	0.009	0.023	**25.186**	**0.000**	0.001
FZD3	**1.105**	0.460	**0.190**	0.027	0.000	0.000	**6.719**	**0.002**	0.002
GATA1	**370.954**	32.021	**48.081**	15.706	0.003	0.008	**427.197**	**4.972**	0.002
GNG2	**32.650**	0.353	**10.757**	1.946	0.000	0.001	**65.696**	**4.499**	0.027
GPR183	**6.159**	1.352	**0.850**	0.260	0.000	0.000	**74.745**	**4.742**	0.042
HMMR	**71.704**	8.790	**42.926**	3.632	0.005	0.014	**118.365**	**4.299**	0.015
HNRNPLL	**178.291**	2.327	**19.761**	4.419	0.000	0.000	**48.831**	**0.697**	0.005
IGLL1	**18.724**	1.757	**0.063**	0.063	0.000	0.000	**937.323**	**55.152**	0.015
IL1B	**3.883**	0.750	**0.142**	0.079	0.000	0.002	**263.481**	**27.556**	0.040
KCNH2	**1.367**	0.451	**0.268**	0.098	0.022	0.048	**219.696**	**0.744**	0.001
KIF15	**43.094**	0.878	**26.427**	1.275	0.000	0.000	**52.337**	**3.100**	0.024
KLF1	**454.940**	39.636	**52.026**	20.291	0.006	0.015	**700.309**	**4.974**	0.001
LEF1	**3.373**	1.681	**0.032**	0.024	0.000	0.000	**66.537**	**0.022**	0.001
LTBP1	**4.494**	1.367	**0.084**	0.024	0.000	0.000	**41.812**	**2.023**	0.018
MMRN1	**35.972**	0.586	**6.478**	1.504	0.000	0.001	**55.165**	**2.381**	0.015
MS4A2	**49.546**	3.729	**8.008**	3.627	0.000	0.000	**34.475**	**1.267**	0.023
MYCT1	**38.009**	6.315	**23.830**	1.273	0.006	0.015	**28.496**	**0.000**	0.001
NDN	**12.449**	2.148	**0.119**	0.063	0.000	0.000	**52.644**	**1.734**	0.023
NHLRC1	**17.069**	1.609	**9.799**	0.890	0.005	0.014	**67.709**	**2.740**	0.021
NMNAT3	**56.707**	0.478	**29.187**	1.108	0.000	0.000	**126.918**	**3.366**	0.007
NUDT12	**22.107**	1.271	**6.863**	0.514	0.000	0.000	**23.473**	**1.334**	0.046
OAT	**314.230**	18.419	**178.851**	6.536	0.000	0.000	**290.159**	**40.190**	0.046
PDZD8	**26.334**	1.826	**17.264**	1.248	0.004	0.011	**62.318**	**5.040**	0.026
PTPN22	**46.281**	8.276	**12.565**	1.787	0.000	0.000	**43.349**	**1.812**	0.025
REC8	**3.687**	0.059	**1.097**	0.234	0.007	0.018	**291.910**	**3.809**	0.003
SLAIN1	**65.971**	2.351	**32.809**	3.312	0.000	0.001	**61.145**	**0.036**	0.000
SLC14A1	**298.487**	11.272	**10.699**	3.687	0.000	0.000	**22.432**	**1.285**	0.046
SLC18A2	**122.849**	1.763	**28.599**	5.559	0.001	0.002	**20.948**	**0.013**	0.018
SLC44A1	**9.040**	1.376	**0.812**	0.230	0.000	0.000	**28.705**	**2.720**	0.039

	wt+d715 (TPM)		2911-2918 (TPM)				SCN	SCN-AML	
Transcripts	Mean	SEM	Mean	SEM	p-value	q-value	(TPM)	(TPM)	p-value
SNX9	**106.569**	2.147	**37.675**	1.870	0.000	0.000	**35.243**	**1.191**	0.015
STEAP3	**40.553**	1.689	**13.375**	1.970	0.000	0.000	**40.457**	**3.494**	0.047
TGM2	**19.927**	6.583	**3.418**	0.704	0.000	0.000	**59.561**	**1.928**	0.011
TMEM246	**14.893**	0.026	**0.842**	0.120	0.000	0.000	**64.100**	**0.051**	0.000
TOP2A	**187.231**	10.462	**75.674**	4.452	0.000	0.000	**117.467**	**15.956**	0.049
TRIB2	**236.288**	7.422	**11.866**	4.045	0.000	0.001	**84.766**	**4.264**	0.015
TSPYL5	**0.766**	0.766	**0.000**	0.000	0.022	0.049	**32.012**	**0.000**	0.000
TTK	**54.824**	12.176	**31.376**	2.024	0.003	0.010	**52.528**	**3.994**	0.038
WEE1	**137.495**	0.252	**59.770**	1.893	0.000	0.000	**183.638**	**22.740**	0.045
XK	**30.586**	1.902	**14.624**	1.372	0.000	0.000	**32.481**	**0.042**	0.001

Chapter 7

Internal tandem duplications, deletions and missense mutations in *CXXC4* in human myeloid malignancies

P.A. Olofsen[1], H.W.J. de Looper[1], P.M.H. van Strien[1], Tim Grob[1], R.M. Hoogenboezem[1], P.L. Gradowska[2], D.A. Bosch[1], O. Roovers[1], C.A.J. Erpelinck-Verschueren[1], B. Löwenberg[1], G.J. Ossenkoppele[3], T. Haferlach[4], P.J.M. Valk[1], M.A. Sanders[1], E.J. Bindels[1], E.M. de Pater[1], I.P. Touw[1]

[1] Department of Hematology, Erasmus University Medical Center, Rotterdam, the Netherlands
[2] HOVON Data Center, Department of Hematology, Erasmus University Medical Center, Rotterdam, the Netherlands
[3] Department of Hematology, VU University Medical Center, Amsterdam, the Netherlands
[4] MLL Munich Leukemia Laboratory, Munich, Germany

Short title: CXXC4 in human myeloid malignancies

Manuscript in preparation

Abstract

We recently identified an acquired internal tandem duplication (ITD) in *Cxxc4* as an additional driver in a murine leukemic progression model of severe congenital neutropenia. This ITD duplicates two glycine residues in a glycine-repeat, resulting in a more stable and abundant CXXC4 protein, which was associated with decreased TET2 protein levels and increased inflammatory signaling. To investigate whether similar ITDs are present in human acute myeloid leukemia (AML) or myelodysplastic syndrome (MDS) we performed targeted amplicon sequencing in 1706 patients enrolled in multiple clinical trials. Additionally, whole genome sequenced data from independent AML, MDS or myeloproliferative neoplasm (MPN) patients were added. We find that glycine-repeat alterations in *CXXC4* are rare and detectable in the germline, and significantly more frequent in MDS, MPN and C/EBPα-silenced AML than in other AML or control cohorts. Hence, although infrequent and not generally predisposing to *de novo* AML, CXXC4 glycine-repeat alterations may contribute to myeloid malignancies with a natural history involving inflammatory signaling, such as high-risk MDS and MPN.

Introduction

The ten-eleven translocation (TET) family of enzymes comprises 3 members (TET 1-3) that catalyze the stepwise oxidation of 5-methylcytosine (5mC) in DNA to 5-hydroxymethylcytosine (5hmC), eventually resulting in demethylation of cytosines.[1,2] DNA-binding of TETs is mediated by CXXC domains, which, in case of TET1 and TET3 are encoded by the respective genes themselves.[3] In case of *TET2*, a chromosomal inversion splits the catalytic- and CXXC-domain into adjacent but separate genes (*TET2* and *CXXC4*) transcribed in opposite direction.[4] In addition to its enzymatic activity, TET2 has also been shown to be able to recruit histone deacetylase-2 (HDAC2) to the gene encoding interleukin-6 (IL-6), thereby reducing IL-6 mediated inflammation.[5] Upon DNA binding, CXXC4 recruits TET2 and induces its caspase mediated degradation, thereby regulating TET2 protein abundance.[6,7]
We recently identified an acquired internal tandem duplication (ITD) in *Cxxc4* in *Csf3r/RUNX1* mutant cells of a murine leukemic progression model of severe congenital neutropenia (SCN).[7] The ITD duplicated 2 glycines in a glycine-repeat region (GRR), resulting in a more stable CXXC4 protein, increased CXXC4 protein abundance and decreased TET2 protein levels in *Csf3r/RUNX1/Cxxc4* mutant acute myeloid leukemia (AML) cells.[7]

The human CXXC4 protein, also known as IDAX (for inhibition of the Dvl and Axin complex), contains 2 GRRs of respectively 28 (GRR-1) and 10 glycine residues (GRR-2), which are separated by 21 amino acids consisting of mainly alanine and serine residues. Because these GRRs are encoded by GC-rich DNA stretches, they are prone to insertions or deletions (indels) caused by slipped strand mispairing (SSM) during DNA replication.[8] Because high GC content leads to inefficient nucleotide sequencing, The Cancer Genome Atlas (TCGA) and Genome Aggregation (gnomAD) databases[9] lack coverage of especially GRR-1, preventing to obtain proper insights in the frequency of mutations in this region. Here, we used a targeted amplicon sequencing approach to screen patients with high-risk myelodysplastic syndrome (MDS) or AML, from various HOVON clinical trials, for mutations in amino acids 103-168, encompassing GRR-1 and GRR-2 of CXXC4. In addition, we investigated the clinical, cytogenetic and molecular characteristics of the *CXXC4* mutant patients in comparison to patients without mutations in the glycine-repeat region of CXXC4. We extended this cohort with whole genome sequenced (WGS) data from AML, MDS or MPN patients generated at the Munich Leukemia Laboratory (MLL).

Methods

Patients

Patients were treated according to the clinical protocol of either the Dutch–Belgian Cooperative Trial Group for Hematology–Oncology (HOVON) or the Swiss Group for Clinical Cancer Research (SAKK). Treatment protocols and patient eligibility criteria have been described previously.[10-14] All patients provided written informed consent.

DNA sequencing

Custom amplicon sequencing was performed, using the Illumina PCR-based Custom Amplicon Library Preparation workflow, to amplify the GRR of CXXC4 while using the following primers; amplicon 1: forward 5'-AGGGGATAAGGTGGAGAGGA-3' and reverse 5'-CCCCTGGAACTGCGACAA-3', amplicon 2: forward 5'-CCCCATCTTCCCCAGCAG-3' and reverse 5'-GCGGGGGAATGCATGAACAAGC-3'. Libraries were paired-end sequenced with the MiSeq V3 Nano kit (Illumina) on the Illumina MiSeq.

The Illumina TruSight Myeloid panel (Illumina) was used to detect mutations in genes frequently associated with leukemia, and samples were paired-end sequenced (2x221bp) on an Illumina HiSeq 2500 System (Illumina) in rapid run mode. Variant calling was performed as described previously.[15] Variants with a minor allele frequency of <0.1% were automatically selected, and variants causing an amino acid change or splice site base change were reported.

Statistical analysis

Differences in categorical variables were tested with the Chi-squared test. Whenever expected frequencies were <5% in any one cell of a 2x2 contingency table, a Fisher's exact test was performed to obtain a p-value that does not rely on the approximation to the Chi-squared distribution. When more than 20% of the expected frequencies were <5% in a large contingency table, groups were combined to reduce the number of variables and to be able to perform statistical tests (either Chi-squared or Fisher's exact tests). A Mann-Whitney U test was performed on continuous variables. A two-sided p-value <0.05 was considered statistically significant.

Results and Discussion

Mutation detection

Targeted amplicon sequencing of the region of *CXXC4* encompassing GRR-1 and GRR-2 (Figure S1) was performed in 1706 patients with AML or refractory anemia with excess of blasts (RAEB) with an IPSS score >1.5 or an IPSS-R risk score >4.5, participating in HOVON clinical trials. Because acute promyelocytic leukemia forms a distinct disease entity, these patients were excluded from this analysis.[16,17] Of these 1706 patients, 46 showed an alteration in amino acids 103-168, hereafter referred to as the GRR, comprising GRR-1, GRR-2, the alanine/serine-rich region (ASR) separating these 2 repeats and 3 flanking amino acids (Figure S1). No significant differences between patients with (CXXC4+) or without (CXXC4-) alterations in the GRR were seen with regard to median age at diagnosis, gender, cytogenetics, complete remission and relapse rates (Table S1).

In addition to the ITD duplicating 2 glycine residues similar to that discovered in the mouse AML cells[7], ITDs spanning 1-6 glycines were found (Table 1). In total 10 patients with such ITDs could be detected, comprising 6 different alterations in both GRR-1 and GRR-2. Deletion of glycine residues were observed in 27 patients, comprising 11 different alterations resulting in the loss of 1-10 glycine residues (Table 1). Missense mutations resulting in the alteration of a glycine residue were found at 2 positions and in 3 patients (Table 1). Finally, alterations were observed in the alanine/serine-rich region separating the 2 GRRs; 1 missense mutation (in 2 patients), 1 duplication inserting additional ASSS residues (1 patient) and 1 deletion resulting in the loss of the ASSS residues (3 patients, Table 1). All indels and mutations were in-frame resulting in an intact CXXC domain.

CXXC4 mutations in remission and saliva samples

The majority of mutations in the GRR of *CXXC4* showed a variant allele frequency (VAF) of >0.3 (Table S2), suggestive of a heterozygous mutation in all or the vast majority of cells. To determine whether these mutations could be constitutive rather than acquired, we obtained saliva samples from 12 *CXXC4* mutant patients, and remission samples from an additional 5 patients. Targeted amplicon sequencing data of saliva/remission samples showed the presence of the mutations in these 17 patients with a similar VAF as in tumor material (Table S2). In addition, we used the gnomAD database (v3.1), comprising WGS data from 74,032 cancer-free individuals, to investigate whether the mutations could be detected in healthy individuals.[9] Although the WES data present in v2.1 of the gnomAD database do not cover the first glycine-repeat (GRR-1), we did check whether other variants were present here, since this dataset comprises >120,000 samples from cancer-free individuals, significantly increasing the sample power and possibility to detect rare variants. As depicted in Table 1, most mutations detected in our cohort are also found in the healthy population, albeit often

in lower frequencies, as indicated by fold changes >1. Three out of the 22 mutations were not previously described in the European, non-Finnish, population. Although the p111_112 duplication could not be detected in the gnomAD database, analysis of saliva did show the presence of the p111_112 duplication in the germline in this patient (Tables 1 and S2). Hence, in contrast to the previously described mouse model[7], the *CXXC4* mutations identified so far in human myeloid malignancies were of germline rather than somatic origin.

Table 1: Observed CXXC4 mutations in amino acids 103-168 in MDS/AML

Mutation	No	Region	gnomAD		Fold change			Saliva	Remission
				v3	v3 EU	v2*	v2 EU		
p111_112dup	1	Gly repeat 1	no	-	-	-	-	yes	
G115R	1	Gly repeat 1	no	-	-	-	-		
p115_121del	1	Gly repeat 1	yes	40.9	-	-	-		
p115_125del	1	Gly repeat 1	yes	4.85	3.88	-	-		
p121_125del	1	Gly repeat 1	yes	2.83	2.21	-	-	yes	
p123_125del	1	Gly repeat 1	yes	0.12	1.03	-	-	yes	
p124dup	2	Gly repeat 1	yes	0.71	0.82	-	-	yes[1]	
p124_125del	1	Gly repeat 1	yes	0.49	0.91	-	-		
p124_127del	15	Gly repeat 1	yes	1.15	0.71	-	-	yes[3]	yes[3]
p128_129dup	2	Gly repeat 1	yes	0.63	2.29	-	-	yes[1]	
p145_150del	3	Ala-Ser region	yes	4.06	3.62	5.23	2.74		
p146_149dup	1	Ala-Ser region	yes	6.64	9.00	23.7	10.2	yes	
S147A	2	Ala-Ser region	yes	7.01	4.97	13.4	30.9		
p159_165del	2	Gly repeat 2	yes	5.00	3.74	5.21	15.1		
G160S	2	Gly repeat 2	yes	0.80	0.60	0.51	0.35	yes[1]	
p160_165del	1	Gly repeat 2	yes	1.18	1.70	1.53	1.62		
p160_165dup	1	Gly repeat 2	yes	8.50	6.23	-	-		
p162_165del	1	Gly repeat 2	yes	6.07	4.68	-	-		
p163_165del	2	Gly repeat 2	yes	1.37	7.48	1.68	3.23		yes
p164_165dup	3	Gly repeat 2	yes	0.47	2.34	1.35	2.95	yes[2]	
p163_166del	1	Gly repeat 2	yes	-	-	19.4	12.5		
p165dup	1	Gly repeat 2	yes	0.31	0.69	0.32	0.53		yes

***** *The WES data from gnomAD v2 does not show coverage of the 1st glycine repeat*

Mutations in the GRR of CXXC4 are more frequent in high-risk MDS and MPN than in de novo AML

Leukemic transformation of the murine *Cxxc4/Csf3r/RUNX1* mutant cells was preceded by a pre-leukemic stage, characterized by the presence of blasts in the peripheral blood upon CSF3 treatment. These mutant cells did not cause overt leukemia until the *Cxxc4*-ITD was present as well.[7] Interestingly, when dividing the HOVON patients in 2 categories; AML encompassing the patients with the French-American-British (FAB) classification subtypes

M0-M2 and M4-M7, and MDS, encompassing patients with RAEB/RAEB-t with an IPSS score >1.5 or an IPSS-R risk score >4.5 and patients with prior-MDS, a significant difference can be observed, where CXXC4+ patients more often present with MDS (p=0.0056, Table 2). The frequency of *CXXC4* mutations is more than 2-fold higher in high-risk MDS patients than in patients with AML, where 5.26% of the MDS patients present with an alteration in CXXC4 (12/228), in contrast to 2.00% of the AML patients (40/1998). Because patients included in the HOVON clinical trials were all high-risk MDS patients, we wondered whether *CXXC4* mutations can also be found in lower-risk MDS patients. WGS data generated at the MLL Munich showed the presence of mutations in the glycine-repeat region in 12/701 patients (1.71%, Table 2). Alterations included duplications, deletions and missense mutations in the 2 glycine-repeats as well as in the alanine/serine-rich region (Table S3). Chronic inflammatory states have been linked to the clonal expansion of MDS.[18,19] Interestingly, we observed upregulation of inflammatory signaling pathways upon acquisition of the *Cxxc4* mutation in the leukemic mouse model[7], suggesting that mutations in *CXXC4* might be able to provide this permissive condition for the clonal expansion of MDS, possibly explaining the higher frequency of *CXXC4* mutations in high-risk MDS than in low-risk MDS or *de novo* AML. The myeloproliferative neoplasms (MPN) represent another hematologic condition in which a chronic inflammatory state has been implicated in disease initiation and progression.[20,21] In line with a potential role for *CXXC4* mutations in providing an inflammatory milieu, *CXXC4* mutations could be detected in 3.11% (10/322) WGS MPN patients, 1.5-fold higher than observed in *de novo* AML patients (Tables 2 and S3). In sum, these data show that *CXXC4* mutations are overrepresented in both high risk MDS and MPN, when compared to *de novo* AML and normal cohort databases.

Table 2: Occurrence of mutations in amino acids 103-168 (GRR) of CXXC4 in hematological malignancies (patients from HOVON clinical trials and MLL Munich)

Cancer type	**Abbreviation**	**Number of patients**	**Number of mutations**	**Frequency**
High-risk myelodysplastic syndrome	hr-MDS	228	Observed: 12 Expected: 5.19	5.26% 2.28%
Myelodysplastic syndrome	MDS	701	Observed: 12 Expected: 15.97	1.71% 2.28%
Myeloproliferative neoplasm	MPN	322	Observed: 10 Expected: 7.33	3.11% 2.28%
de novo Acute myeloid leukemia	AML	1998	Observed: 40 Expected: 45.51	2.00% 2.28%
Total		**3249**	**74**	**2.28%**
		χ^2= 0.008		

CXXC4 mutations are not mutually exclusive with mutations associated with clonal hematopoiesis of indeterminate potential (CHIP) but correlate with CEBPA silencing

To identify co-occurring or mutually exclusive mutations in CXXC4+ patients, we performed targeted NGS with the Illumina TruSight Myeloid Sequencing panel, comprising 54 genes associated with myeloid malignancies, e.g., MDS and AML. We first asked whether *CXXC4* mutations (anti-)correlated with mutations in *DNMT3A*, *TET2* or *ASXL1*, which often mark a history of CHIP without having a major impact on the AML/MDS disease course.[15] No significant differences in *TET2* (p=0.94), *DNMT3A* (p=0.72) and *ASXL1* (p=0.71) mutations could be observed between CXXC4+ and CXXC4- patients (Table 3). Additionally, no significant differences were observed between CXXC4+ and CXXC4- patients when looking at mutations in *FLT3*, *NPM1*, *NRAS*, *KRAS*, *CEBPA*, *EVI1*, *KIT*, *IDH1*, *IDH2*, *WT1*, *TP53*, *RUNX1*, *SF3B1*, *JAK2*, *PTPN11* and *SRSF2* (data not shown). Only so-called C/EBPα-silenced AML cases, in which *CEBPA* expression is silenced by promoter/enhancer methylation, were significantly more represented in the CXXC4+ patient group (p=0.0083, Table 3). C/EBPα-silenced leukemia often presents with a mixed myeloid/T-lymphoid phenotype, illustrated by expression of T-lymphoid genes like *CD7*, *CD3* and *NOTCH1* and the presence of one or multiple T-cell related markers on the cell surface of myeloid blasts.[22] Strikingly, a similar mixed myeloid/T-lymphoid phenotype was seen in the *Cxxc4/Csf3r/RUNX1* mutant murine AML cells, with co-expression of the myeloid marker CD11b and the T-lymphoid marker CD3 on the cell surface of c-Kit+ AML blasts.[7] While the underlying explanation for this observation and the question whether this correlation holds in larger patient cohorts both merit further study, one possibility is that a reduced TET2 activity mediated by elevated CXXC4 protein levels may contribute to the deregulation of myeloid differentiation, leading to a differentiation block in a common myeloid/T cell precursor.

Table 3: CEBP/α-silenced AML[1]

CXXC4	Number of patients	Number of patients with CEBP/α-silenced AML	Frequency
pos	10	2	20.0%
neg	384	4	1.0%
	2-sided Fisher's exact test p= 0.0083		

[1] *Unknown in 1325 patients*

In conclusion, the findings reported here suggest that mutations in the GRR of *CXXC4*, previously identified in a mouse model of leukemic progression[7], are most often germ line mutations that are overrepresented in high risk MDS, MPN and CEBP/α-silenced AML. As such, these mutations may represent a vulnerability for these conditions, which will only become overt in a context in which reduced TET2 activity, caused by increased CXXC4 levels, becomes critical in addition to other driver events, such as JAK2 mutations in MPN and *CEBPA* gene silencing in AML.

References

1. Tahiliani M, Koh KP, Shen Y, et al. Conversion of 5-methylcytosine to 5-hydroxymethylcytosine in mammalian DNA by MLL partner TET1. *Science*. 2009;324(5929):930-935.
2. Ito S, D'Alessio AC, Taranova OV, Hong K, Sowers LC, Zhang Y. Role of Tet proteins in 5mC to 5hmC conversion, ES-cell self-renewal and inner cell mass specification. *Nature*. 2010;466(7310):1129-1133.
3. An J, Rao A, Ko M. TET family dioxygenases and DNA demethylation in stem cells and cancers. *Exp Mol Med*. 2017;49(4):e323.
4. Iyer LM, Tahiliani M, Rao A, Aravind L. Prediction of novel families of enzymes involved in oxidative and other complex modifications of bases in nucleic acids. *Cell Cycle*. 2009;8(11):1698-1710.
5. Zhang Q, Zhao K, Shen Q, et al. Tet2 is required to resolve inflammation by recruiting Hdac2 to specifically repress IL-6. *Nature*. 2015;525(7569):389-393.
6. Ko M, An J, Bandukwala HS, et al. Modulation of TET2 expression and 5-methylcytosine oxidation by the CXXC domain protein IDAX. *Nature*. 2013;497(7447):122-126.
7. Olofsen PA, Fatrai S, van Strien PMH, et al. Malignant Transformation Involving CXXC4 Mutations Identified in a Leukemic Progression Model of Severe Congenital Neutropenia. *Cell Reports Medicine*. 2020;1(5):100074.
8. Usdin K, House NCM, Freudenreich CH. Repeat instability during DNA repair: Insights from model systems. *Critical Reviews in Biochemistry and Molecular Biology*. 2015;50(2):142-167.
9. Karczewski KJ, Francioli LC, Tiao G, et al. The mutational constraint spectrum quantified from variation in 141,456 humans. *Nature*. 2020;581(7809):434-443.
10. Lowenberg B, Beck J, Graux C, et al. Gemtuzumab ozogamicin as postremission treatment in AML at 60 years of age or more: results of a multicenter phase 3 study. *Blood*. 2010;115(13):2586-2591.
11. Lowenberg B, Ossenkoppele GJ, van Putten W, et al. High-dose daunorubicin in older patients with acute myeloid leukemia. *N Engl J Med*. 2009;361(13):1235-1248.
12. Lowenberg B, Pabst T, Maertens J, et al. Therapeutic value of clofarabine in younger and middle-aged (18-65 years) adults with newly diagnosed AML. *Blood*. 2017;129(12):1636-1645.
13. Pabst T, Vellenga E, van Putten W, et al. Favorable effect of priming with granulocyte colony-stimulating factor in remission induction of acute myeloid leukemia restricted to dose escalation of cytarabine. *Blood*. 2012;119(23):5367-5373.
14. HOVON. Home page: Dutch-Belgian Cooperative Trial Group for Hematology-Oncology.

15. Jongen-Lavrencic M, Grob T, Hanekamp D, et al. Molecular Minimal Residual Disease in Acute Myeloid Leukemia. *N Engl J Med*. 2018;378(13):1189-1199.
16. Haferlach T, Gassmann W, Loffler H, et al. Clinical aspects of acute myeloid leukemias of the FAB types M3 and M4Eo. The AML Cooperative Group. *Ann Hematol*. 1993;66(4):165-170.
17. Douer D. The epidemiology of acute promyelocytic leukaemia. *Best Pract Res Clin Haematol*. 2003;16(3):357-367.
18. Muto T, Walker CS, Choi K, et al. Adaptive response to inflammation contributes to sustained myelopoiesis and confers a competitive advantage in myelodysplastic syndrome HSCs. *Nat Immunol*. 2020;21(5):535-545.
19. Barreyro L, Chlon TM, Starczynowski DT. Chronic immune response dysregulation in MDS pathogenesis. *Blood*. 2018;132(15):1553-1560.
20. Mendez Luque LF, Blackmon AL, Ramanathan G, Fleischman AG. Key Role of Inflammation in Myeloproliferative Neoplasms: Instigator of Disease Initiation, Progression. and Symptoms. *Curr Hematol Malig Rep*. 2019;14(3):145-153.
21. Gleitz HFE, Dugourd AJF, Leimkuhler NB, et al. Increased CXCL4 expression in hematopoietic cells links inflammation and progression of bone marrow fibrosis in MPN. *Blood*. 2020;136(18):2051-2064.
22. Wouters BJ, Jorda MA, Keeshan K, et al. Distinct gene expression profiles of acute myeloid/T-lymphoid leukemia with silenced CEBPA and mutations in NOTCH1. *Blood*. 2007;110(10):3706-3714.

Supplemental data

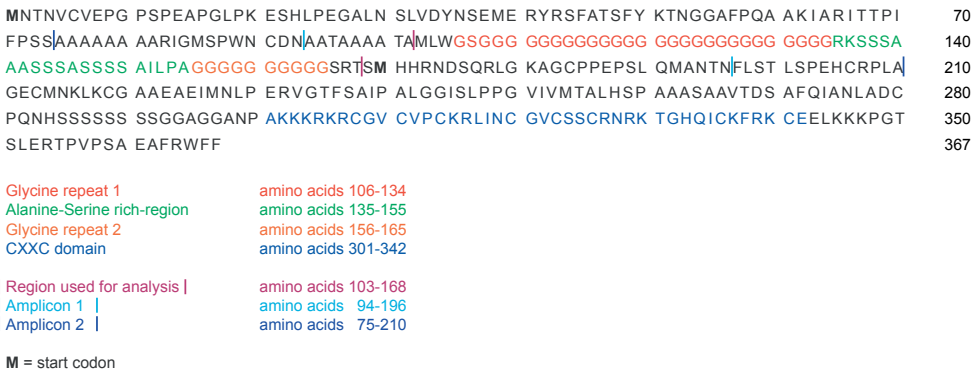

Figure S1: Targeted amplicon sequencing of the region of CXXC4 encompassing the two glycine-repeats

CXXC4 protein sequence depicting the various amplicons used to sequence the gene (indicated by the blue lines) and the glycine-repeat region (GRR) used for analysis (indicated by the purple lines). The GRR comprises GRR-1 (red), GRR-2 (orange), the alanine/serine-rich region (ASR, green) separating these 2 repeats and 3 flanking amino acids.

Table S1: Clinical characteristics HOVON sequenced patients

	CXXC4+	**CXXC4-**
Age at diagnosis – yr		
median	49.5	53
range	28-67	15-77
	p=0.6055	
Gender – no (%)		
male	43.5% (20/46)	55.2% (917/1660)
female	56.5% (26/46)	44.8% (743/1660)
	χ2= 0.1137	
Cytogenetic analysis – % (no/total no)[1]		
normal	44.4% (20/45)	50.7% (817/1612)
cytogenetic abnormal	40.0% (18/45)	27.1% (437/1612)
monosomal karyotype	6.7% (3/45)	10.5% (169/1612)
t(8;21)	4.4% (2/45)	6.0% (96/1612)
inv(16)	4.4% (2/45)	5.8% (93/1612)
	χ2= 0.4192	
Complete remission – % (no/total no)		
Yes (ever)	95.7% (44/46)	86.6% (1438/1660)
No (never)	4.3% (2/46)	13.4% (222/1660)
	χ2= 0.0738	
Relapse – % (no/total no)		
Yes	30.4% (14/46)	24.0% (398/1660)
No	69.6% (32/46)	76.0% (1262/1660)
	χ2= 0.3127	

[1] *Karyotyping failed in 49 patients*

Table S2: Variant allele frequencies (VAFs) of observed CXXC4 mutations in amino acids 103-168 in MDS/AML

Mutation	Region	VAF	Saliva VAF	Remission VAF
p111_112dup	Gly repeat 1	0.42	0.40	
G115R	Gly repeat 1	0.35		
p115_121del	Gly repeat 1	0.56		
p115_125del	Gly repeat 1	0.59		
p121_125del	Gly repeat 1	0.56	0.52	
p123_125del	Gly repeat 1	0.46	0.41	0.45
p124dup	Gly repeat 1	0.28		
p124dup	Gly repeat 1	0.30	0.33	
p124_125del	Gly repeat 1	0.45		
p124_127del	Gly repeat 1	0.43		
p124_127del	Gly repeat 1	0.45		
p124_127del	Gly repeat 1	0.46		
p124_127del	Gly repeat 1	0.45		
p124_127del	Gly repeat 1	0.46		
p124_127del	Gly repeat 1	0.46		
p124_127del	Gly repeat 1	0.43		
p124_127del	Gly repeat 1	0.46		0.44
p124_127del	Gly repeat 1	0.45		0.44
p124_127del	Gly repeat 1	0.43		0.42
p124_127del	Gly repeat 1	0.46		
p124_127del	Gly repeat 1	0.45		
p124_127del	Gly repeat 1	0.45	0.45	
p124_127del	Gly repeat 1	0.43	0.45	
p124_127del	Gly repeat 1	0.44	0.51	
p128_129dup	Gly repeat 1	0.33		
p128_129dup	Gly repeat 1	0.34	0.39	
p145_150del	Ala-Ser region	0.48		
p145_150del	Ala-Ser region	0.47		
p145_150del	Ala-Ser region	0.46		
p146_149dup	Ala-Ser region	0.17	0.12	
S147A	Ala-Ser region	0.96		
S147A	Ala-Ser region	0.48		
p159_165del	Gly repeat 2	0.58		
p159_165del	Gly repeat 2	0.58		
G160S	Gly repeat 2	0.43		
G160S	Gly repeat 2	0.36	0.37	
p160_165del	Gly repeat 2	0.56		
p160_165dup	Gly repeat 2	0.27		
p162_165del	Gly repeat 2	0.52		
p163_165del	Gly repeat 2	0.50		0.52
p163_165del	Gly repeat 2	0.39		
p164_165dup	Gly repeat 2	0.24		

Mutation	Region	VAF	Saliva VAF	Remission VAF
p164_165dup	Gly repeat 2	0.26	0.23	
p164_165dup	Gly repeat 2	0.26	0.22	
p163_166del	Gly repeat 2	0.55		
p165dup	Gly repeat 2	0.32		0.34

Table S3: Observed CXXC4 mutations in the GRR (amino acids 103-168) in hematological malignancies (MLL Munich)

Mutation	No	Malignancy	Region	gnomAD	HOVON
p115_121del	1	MPN	Gly repeat 1	yes	1
p117_120dup	1	MPN	Gly repeat 1	no	0
p123_125del	1	MDS	Gly repeat 1	yes	1
p124dup	3	AML, MDS, MPN	Gly repeat 1	yes	1
p124_125del	2	AML, MDS	Gly repeat 1	yes	1
p124_127del	6	AML[2], MDS, MPN[3]	Gly repeat 1	yes	14
S139A	1	MDS	Ala-Ser region	yes	0
S147A	1	MDS	Ala-Ser region	yes	2
L153R	3	AML, MDS, MPN	Ala-Ser region	no	0
G160S	4	AML[2], MDS[2]	Gly repeat 2	yes	2
p160_165del	1	MPN	Gly repeat 2	yes	1
p163_165dup	2	MDS[2]	Gly repeat 2	yes	0
p163_165del	1	MPN	Gly repeat 2	yes	2
p164_165dup	3	AML[2], MPN	Gly repeat 2	yes	3
p165dup	1	MDS	Gly repeat 2	yes	1
p166dup	1	AML		yes	0

Chapter 8

Secondary CNL after SAA reveals insights in leukemic transformation of bone marrow failure syndromes

Patricia A. Olofsen*[3], Laurent Schmied*[1,2], Pontus Lundberg[1], Alexander Tzankov[4], Martina Kleber[1,2], Jörg Halter[1], Mario Uhr[5], Peter J.M. Valk[3], Ivo P. Touw[3], Jakob Passweg[1] and Beatrice Drexler[1]

* L.S. and P.A.O. contributed equally to this study.
[1] University Hospital Basel, Division of Hematology, University Hospital, Basel, Switzerland
[2] University Hospital Basel, Division of Internal Medicine, Basel, Switzerland
[3] Erasmus University Medical Center, Department of Hematology, Rotterdam, the Netherlands
[4] University Hospital Basel, Division of Pathology, University Hospital, Basel, Switzerland
[5] Moncucco Hospital Lugano, Division of Hematology, Lugano, Switzerland

Blood Advances, 2020 Nov 10; 4(21):5540-5546.

Abstract

Acquired aplastic anemia and severe congenital neutropenia (SCN) are bone marrow (BM) failure syndromes of different origin, however, they share a common risk for secondary leukemic transformation. Here, we present a patient with severe aplastic anemia (SAA) evolving to secondary chronic neutrophilic leukemia (CNL; SAA-CNL). We show that SAA-CNL shares multiple somatic driver mutations in *CSF3R*, *RUNX1,* and *EZH2/SUZ12* with cases of SCN that transformed to myelodysplastic syndrome (MDS) or acute myeloid leukemia (AML). This molecular connection between SAA-CNL and SCN progressing to AML (SCN-AML) prompted us to perform a comparative transcriptome analysis on nonleukemic CD34^{high} hematopoietic stem and progenitor cells, which showed resembling transcriptional profiles indicative of interferon (IFN)-driven pro-inflammatory responses. These findings provide further insights in the mechanisms underlying leukemic transformation in bone marrow failure syndromes.

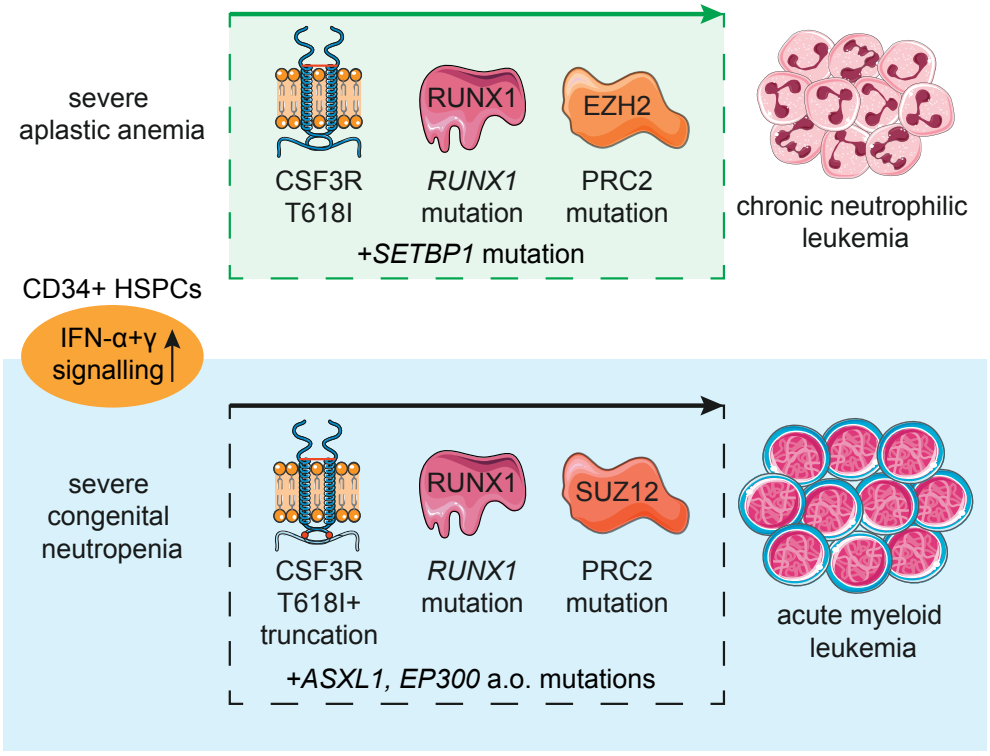

Introduction

We recently treated a patient with chronic neutrophilic leukemia (CNL) evolving from severe aplastic anemia (SAA). Both CNL and aplastic anemia (AA) are very rare hematological diseases. In western contries, the incidence of AA is 2-3 per 10^6 persons per year; however, only ~200 CNL cases have been reported in the first 15 years after its formal recognition in 2001 as a distinct entity in the classification system of the World Health Organization (WHO).[1,2] The genetic hallmark of CNL are mutations in the colony-stimulating factor 3 (CSF3) receptor-gene (*CSF3R*), which permit augmented and/or autonomous signaling and are detected in >80% of CNL patients.[3-5] These *CSF3R* mutations were recently integrated in the WHO classification.[5] The most commonly found *CSF3R* mutation in CNL is the *CSF3R*-T618I alteration, which provides autonomous signaling, supporting hyperproliferation of mature neutrophil progenitors.[5] Severe congenital neutropenia (SCN), a bone marrow failure with a high risk of progression to myelodysplastic syndrome (MDS) and acute myeloid leukemia (AML),[6,7] is another hematological entity in which *CSF3R* mutations are detected in 70%-80% of patients during the course of leukemic transformation. The *CSF3R* mutations found in SCN are mostly truncating the cytoplasmic tail of the receptor, which is critical for receptor endocytosis and lysosomal routing.[8] Interestingly, an autoactivating *CSF3R* mutation identical to those found in CNL patients was present in a case of SCN that progressed to AML (SCN-AML).[9] Moreover, combinations of truncating and autoactivating *CSF3R* mutations have also been reported in cases of CNL,[5] fueling the concept that CNL might be preceded by a premalignant state characterized by CSF3 hyporesponsiveness, which in analogy to SCN can be overcome by the acquisition of *CSF3R* mutations.[10] Given the molecular link between SCN-AML and CNL, we conducted a comparative analysis of the present patient with SAA evolving to secondary CNL (SAA-CNL) and the previously described SCN-AML patient,[9] aiming to interrogate clonal evolution and uncover possible common disease mechanisms underlying the malignant transformation of these cases.

Methods

Patient samples

Ficoll density gradient separated bone marrow (BM) and peripheral blood (PB) cells were obtained from healthy donors, the SCN-AML patient (SCN phase), and the SAA-CNL patient (CNL phase) and frozen according to established procedures for viable cell cryopreservation. BM aspirate smear samples served as the DNA source of the SAA phase in the SAA-CNL patient. The study was performed under the permission of the institutional review boards of the University Hospital Basel (Basel, Switzerland; registration number Req-2019-00126) and the Erasmus MC (Rotterdam, the Netherlands; registration number MEC-2008-387 for biobanking and MEC-2012-030 for the genetic analysis of leukemic progression in SCN patients).

Microscopy

BM aspirate and PB smears were fixed in formalin solution containing 4% paraformaldehyde followed by a subsequent May-Grünwald-Giemsa staining. Images were captured by a Leica DM4B widefield microscope (Leica Microsystems GmbH, Wetzlar, Germany) equipped with an Olympus UC90 camera (Olympus, Shinjuku, Tokyo, Japan). For acquisition, Olympus Cell sense Entry (Olympus, Shinjuku, Tokyo, Japan) software was used and images were annotated using ImageJ (ImageJ2, Fiji).[11]

Flow cytometry and cell sorting

Hematopoietic stem and progenitor cells (HSPCs) were stained using CD34-PE (clone 8G12, BD Biosciences), neutrophils using CD11b-BV510 (clone ICRF44, BioLegend), while dead cells were excluded by using 4',6-Diamidino-2-Phenylindole (DAPI, Fisher Scientific). The cells were sorted with a FACSAria cell sorter (BD Biosciences).

DNA isolation and DNA sequencing

DNA was extracted from BM samples using a QiaSymphony (Qiagen). Next-generation sequencing (NGS) libraries were prepared with the IonTorrent library kit using the Oncomine myeloid research gene panel (Supplementary Table 3) and sequenced with an IonGeneStudio S5 instrument (ThermoFischer). The coverage of the samples was >3000-fold with all exons being covered. The sequencing data were analyzed using the Oncomine workflow on an IonReporter server with a variant detection limit set to 5%. The Illumina TruSight Myeloid panel (Illumina, Supplementary Table 4) was used to detect mutations in the sorted populations, whereas BM failure-associated genes were analyzed by a custom designed Illumina panel focusing on genes indicating a predisposition for progression to leukemia when mutated (Supplementary Table 2). The Illumina NGS libraries were paired-

end sequenced (2x221bp) on an Illumina HiSeq 2500 System (Illumina, San Diego, CA) in rapid run mode and variant calling was performed as described previously.[12] Variants with a minor allele frequency of <0.1% were automatically selected, and variants causing an amino acid change or splice site base change were reported.

RNA isolation and RNA sequencing

RNA was isolated from sorted human CD34^{high} cells from the BM (SCN phase, 1992 and 3 healthy controls) or PB (SAA-CNL patient pre-transplant). cDNA was generated using the SMARTer Ultra Low Input RNA kit for sequencing (version 4, Clontech) and libraries were generated using the TruSeq Nano DNA Sample Preparation kit (Illumina), according to the low sample protocol, and run on a Novaseq 6000 instrument (Illumina). Demultiplexing was performed using the Casava software (Illumina) allowing for one mismatch in the bar-codes. Subsequently quality metrics were estimated for all of the resulting fastq files (FastQC, Babraham bioinformatics & MultiQC, http://multiqc.info). Afterwards trimmed reads were aligned against the Human Transcriptome (Gencode v19)/Genome (hg19) using the STAR aligner.[13] Abundance estimation was performed using Cufflinks (refSeq[14]) and raw counts were measured with the HTSeq-count software set in union mode.[15] Next the measured raw counts were used to create clustering and principle component plots and to perform differential expression analysis both using DESeq2 (after ASHR shrinkage) and R (https://www.r-project.org/).[16] Finally, gene set enrichment analysis with the hallmark pathways H (https://www.gsea-msigdb.org/gsea/msigdb/genesets.jsp?collection=H) was done using the GSEA software based on the pre-ranked log2 fold change ASHR shrunken DESeq2 data.[17-19]

Results

Case history

The SAA-CNL patient was referred to the clinic at the age of 42 years for evaluation of bone marrow (BM) transplantation. He was diagnosed with SAA at the age of 22 years, for which he was treated with intensive immunosuppressive therapy (IST; 2x anti-lymphocyte globulin and 1x anti-thymocyte globulin (ATG) together with cyclosporine-A (CsA)) over a period of 18 years with initial response to IST but subsequent relapse. The IST at the age of 23 years and 31 years resulted in partial remission for almost 9 and 3 years, respectively. After the third cycle at the age of 34 years, the patient depended on a maintenance therapy with CsA (350 mg/d) for 6 years. At the age of 41 years, that is, 19 years after the initial SAA diagnosis, increasing neutrophil counts up to 39 G/L were observed in peripheral blood (PB) in the absence of infection, inflammation, or solid tumor. BM examination revealed hypercellularity with excess mature neutrophils without an increase in myeloblasts (Figure 1A&B). Discrete reactive dysplastic changes were observed, which did not classify for diagnosis of MDS. Cytogenetic analysis showed a normal karyotype (46, XY) and a normal array comparative genomic hybridization (array-CGH) profile. Together with the findings in PB and BM, and the presence of a *CSF3R*-T618I mutation, the criteria of the WHO classification for the diagnosis of CNL were fulfilled (Table S1).

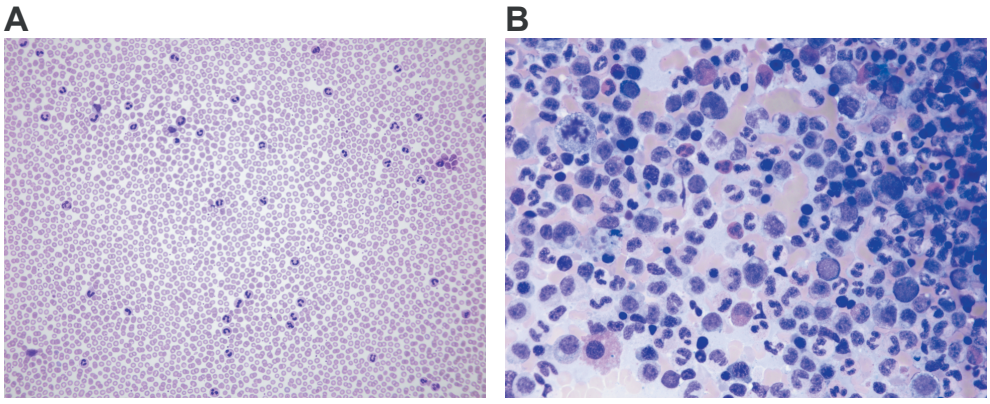

Figure 1. Microscopical analysis of PB and BM at CNL diagnosis.
(A) Neutrophilia in PB. (B) BM examination shows hypercellularity resulting from proliferation of the myeloid lineage without an increase in myeloblasts. The pictures were acquired by a Leica DM4B widefield microscope equipped with an Olympus UC90 camera: original magnification x20 (A) and x50 (B), respectively; Mäy-Grünwald-Giemsa stain. The images were taken at room temperature using immersion oil. For acquisition, Cell sense Entry software was used; the images were subsequently annotated using ImageJ.

Therapy with ruxolitinib was initiated based on previous data showing spontaneous JAK-mediated signaling in *CSF3R*-T618I mutants and the possible therapeutic potential of ruxolitinib in CNL.[5] Upon normalization of neutrophil counts, ruxolitinib was tapered after 4 months and stopped after 5 months due to progressive thrombocytopenia (Figure 2). Because thrombocytopenia and elevated neutrophil counts persisted (Figure 2), the patient underwent allogeneic hematopoietic stem cell transplantation from a 12 of 12 HLA identical unrelated donor after myeloablative conditioning with cyclophosphamide and pharmacokinetics-guided busulfan. Graft-versus-host disease (GvHD) prophylaxis consisted of ATG, methotrexate, and CsA. To date, almost 4 years post-transplant, the patient remains in complete hematological, morphological, and molecular remission with 100% donor chimerism in BM as well as in the $CD3^+$ and $CD66^+$ leukocyte fraction in PB. Mild chronic GvHD developed but immunosuppressive treatment could be stopped 1 year posttransplant.

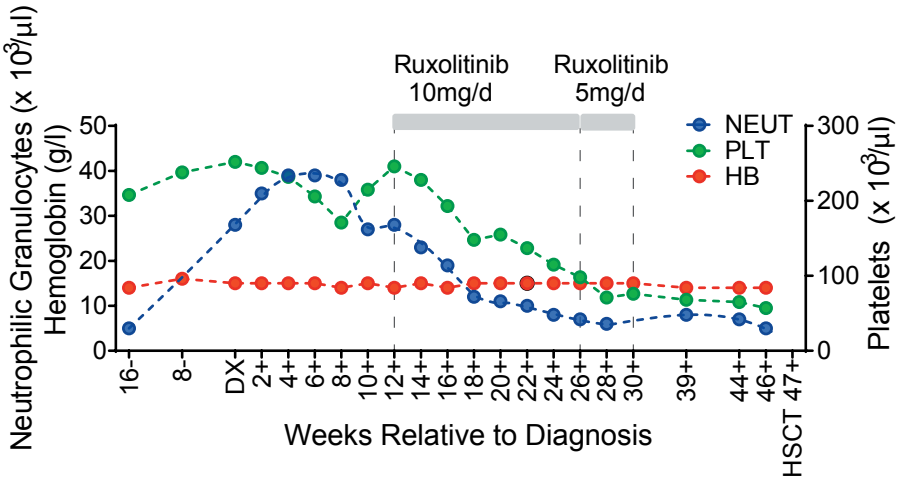

Figure 2. PB cell counts in relation to CNL diagnosis.

Hemoglobin levels (HB) and neutrophil granulocyte (NEUT) and platelet (PLT) cell counts are depicted before, during, and after treatment with ruxolitinib at the indicated dosage. DX, diagnosis; HSCT, hematopoietic stem cell transplantation.

Genetic analysis

Next generation sequencing (NGS) of BM cells from the SAA-CNL patient with the IonTorrent Oncomine Myeloid research gene panel uncovered, in addition to the *CSF3R*-T618I mutation (variant allele frequency (VAF): 29%), mutations in *SETBP1* (VAF: 42%), *EZH2* (VAF: 40%) and *RUNX1* (VAF: 5%) (Table S3 & Figure 3). The patient did not carry mutations in genes associated with BM failure syndromes, e.g., *ELANE*, *HAX1*, *SBDS*, *SRP54,* and *GATA2* (Table S2). Retrospective analysis of a BM sample taken 7 years before CNL diagnosis revealed no specific mutation, implying the acquisition of these mutations particularly during the last years of the disease course.

Flow cytometric analysis of a PB sample taken from the SAA-CNL patient just before transplantation showed the presence of $CD34^{high}$ cells, raising the possibility that a further evolution step toward a more blast-like phenotype might have been in progress. To further investigate the clonal cellular hierarchy at this stage, we performed Illumina TruSight myeloid panel sequencing (Table S4) on fluorescence-activated cell sorter (FACS)-purified $CD34^{high}CD11b^{-}$ hematopoietic stem and progenitor cells (HSPCs), $CD34^{dim}CD11b^{+}$ myeloid precursor cells, and $CD34^{-}CD11b^{-}$ cells from cryopreserved PB. This analysis revealed that the *SETBP1, EZH2*, *CSF3R* and *RUNX1* mutations were only present in the $CD34^{dim}CD11b^{+}$ myeloid progenitors cells with VAFs that were grossly similar to the noncryopreserved unsorted CNL sample (Table 1). On the other hand, none of these mutations were detected in the $CD34^{high}CD11b^{-}$ HSPC fraction, indicating that these phenotypically immature cells were not derived from a *SETBP1*/*EZH2*/*CSF3R*/*RUNX1* mutant ancestor, but represent SAA-derived nonleukemic progenitors.

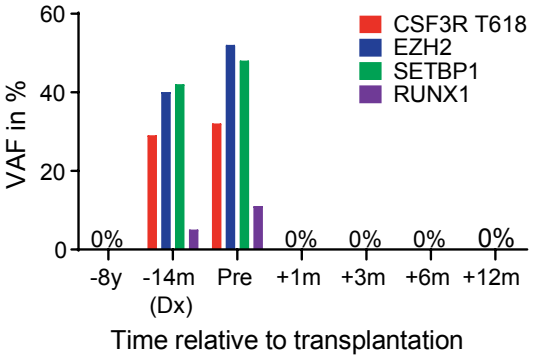

Figure 3. VAFs of mutations during evolution from SAA to CNL.

VAF 8 years before transplantation, at diagnosis of CNL, pretransplant, and 1, 3, 6, and 12 months after allogeneic hematopoietic stem cell transplantation.

Table 1: CSF3R, EZH2, SETBP1 and RUNX1 mutation status per sorted population

Gene	Mutation	Variant allele frequency (VAF)		
		$CD34^{dim}CD11b^{+}$	$CD34^{high}CD11b^{-}$	$CD34^{-}CD11b^{-}$
CSF3R	T618I	6.8%	-	-
EZH2	Y663C	38.8%	-	-
SETBP1	G870S	28.8%	-	-
RUNX1	V164fs	7.3%	-	-

-,0%; VAF, variant allele frequency

Comparative transcriptome analysis of SCN and SAA HSPCs

Based on the clonal evolution patterns that SCN-AML and SAA-CNL have in common, we asked if, and to what extent, comparable regulatory pathways might be affected in the nonleukemic CD34^{high} HSPCs in this SAA-CNL patient compared with SCN. To investigate this, we made use of material from a previously described *ELANE*-mutant SCN patient who later on progressed to AML.[9] As shown in Figure 4A, besides the *CSF3R*-T618I mutation, both patients show mutations in *RUNX1* and in *SUZ12* or *EZH2*, encoding proteins of the polycomb-repressive complex (PRC2), upon leukemic progression. We performed whole-transcriptome analysis on the CD34^{high} HSPCs from the pretransplant sample of the SAA-CNL patient that lacked *SETBP1*/*EZH2*/*CSF3R*/*RUNX1* mutations and compared these with CD34^{high} cells from healthy donors (n=3). The same analysis was done on CD34^{high} cells from the *ELANE* mutant SCN patient, which at the time of analysis during the neutropenic phase had a minor (<10%) clone with a *CSF3R*-truncating mutation.[9] Gene set enrichment analysis (GSEA) indicated upregulation of several overlapping pathways in both the SAA-CNL and the SCN patient compared with healthy controls, among which were induction of apoptosis, activation of the p53 pathway, mTORC1 signaling, and responses to reactive oxygen species (Figure S1). Most strikingly, the CD34^{high} HSPCs from the SAA-CNL and the SCN patient displayed transcriptional profiles characterized by upregulation of inflammatory-related signatures, in particular type I (IFN-α) and type II (IFN-γ) interferon responses (Figures 4B and C). A selection of IFN-response genes that were most strongly upregulated in both the SAA-CNL and SCN HSPCs is shown in Figure 4D and includes *PML* and *PARP9*, genes involved in oxidative stress and DNA-damage responses, respectively, possibly linking the induction of apoptosis- and reactive oxygen species-induced signatures to increased interferon signaling.[20,21] Taken together, these results suggest that IFN-driven proinflammatory responses represent a feature of SAA and SCN CD34^{high} HSPCs that may contribute to the preleukemic state of these cells.

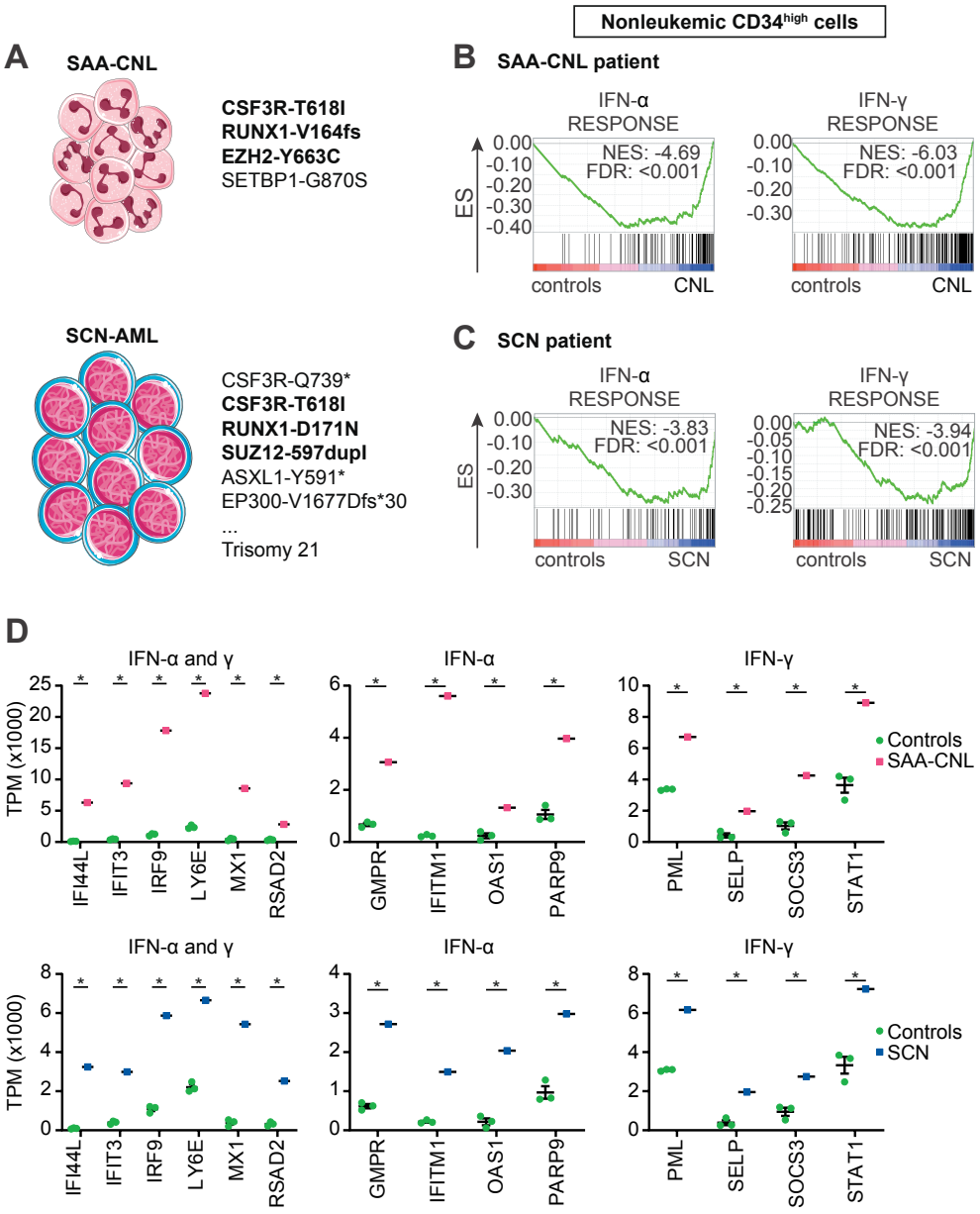

Figure 4. Comparative analysis between the SAA-CNL and SCN-AML patient regarding mutations and transcriptional profile.

(A) Mutational spectrum observed in the SCN-AML patient and the SAA-CNL patient. The bold genes are overlapping (SUZ12 and EZH2 together form the polycomb-repressive complex 2). (B-C) GSEA comparing nonleukemic CD34^{high} cells from (B) 3 healthy controls with CD34^{high} cells obtained from the SAA-CNL patient, (C) CD34^{high} cells from 3 healthy controls with CD34^{high} cells obtained from the SCN patient (SCN-phase before AML became clinically overt), both showing increased IFN-related

*signalling. (D) Expression levels (in transcript per million, TPM) of various IFN-inducable genes, which are significantly increased in both the SAA-CNL and the SCN stage. NES = normalized enrichment score, FDR = false discovery rate, TPM = transcript per million, * = p<0.05.*

Discussion

The low probability of an unrelated, sequential occurrence of CNL after SAA in the same patient prompted the question of a causal link and possible mechanisms underlying the leukemic transformation to CNL. Per se, the course of AA can be complicated by the development of clonal disorders such as MDS and AML, in particular after IST as it was repeatedly given to our reported SAA-CNL patient.[22-25] Recent analyses of myeloid precursor cells of AA patients demonstrated recurrent somatic mutations in a defined spectrum of genes with a low VAF and certain founder mutations with the potential to initiate the progression to MDS.[26,27]

In comparison with genetic alterations found in MDS or age-related clonal hematopoiesis, certain sets of mutations are overrepresented (*BCOR, BCORL1, PIGA*) in AA, whereas other mutations (*TET2, JAK2*) occur less frequently, suggesting distinct clonal selection mechanisms in the aplastic BM environment. Interestingly, *CSF3R* mutations have not been reported in AA so far, but are linked to leukemic transformation in SCN. Sequential myeloid colony assays during the development from SCN to secondary AML revealed that *CSF3R*-truncating mutations occur early and are disease driving[9] whereas *RUNX1* and *CSF3R*-T618I mutations appear shortly before MDS/AML becomes clinically overt.[28] The specific *CSF3R* mutation (T618I) in the present case was previously shown to enable myeloid colony formation in the absence of CSF3, thereby suggesting a constitutive ligand-independent activation of the receptor.[5]

A molecular connection between the pathogenesis of SCN-AML and CNL has been suggested before because HSPCs in these malignancies acquire truncating and/or autoactivating mutations in *CSF3R* at an increased frequency.[5,29] Although the exact time point at which *CSF3R* mutations are acquired during CNL development remains unknown, a possible explanation is that CNL is preceded by a CSF3-hyporesponsive preleukemic state, from which HSPC clones escape through the acquisition of *CSF3R* mutations.[29] The SAA-CNL patient reported here could serve as a unique clinical case to support this hypothesis. Comparative gene-expression analysis of the nonleukemic CD34^{high} HSPCs in the SCN and the SAA-CNL patient revealed strikingly similar transcriptional profiles, characterized by upregulation of type I (IFN-α) and type II (IFN-γ) interferon responses (Figure 4). These

results corroborate the important role of inflammatory signaling pathways in preleukemic stem cells, particularly in the context of secondary leukemia,[30,31] and may suggest that an inflammatory BM environment in which the SAA and SCN mutant CD34^{high} HSPCs reside contribute to a permissive condition for the development of leukemic cells.[32,33]

In summary, this patient with CNL evolving from SAA provides unique insights into potentially important mechanisms of leukemic transformation of BM failure syndromes. The molecular similarities with SCN and the resembling transcriptional profiles corroborate the role of inflammatory signaling pathways in preleukemic and leukemic stem cells, particularly in the context of secondary leukemia.

Acknowledgement

The authors thank Paulina M.H. van Strien and Remco M. Hoogenboezem for technical assistance, as well the Swiss Transplant Cohort Study for providing pretransplant sample of the SAA-CNL patient.
This work was supported by a grant from KWF Kankerbestrijding (EMCR 2013-5755).

Authorship

Contribution: L.S., P.A.O., P.L., I.P.T., and B.D. designed and performed the research, analyzed the data, and wrote the manuscript; A.T., M.K., J.H., M.U., P.J.M.V., and J.P. analyzed the data and wrote the manuscript.

Conflict-of-interest

The authors declare no competing financial interests.

References

1. Montane E, Ibanez L, Vidal X, et al. Epidemiology of aplastic anemia: a prospective multicenter study. *Haematologica*. 2008;93(4):518-523.
2. Gotlib J, Maxson JE, George TI, Tyner JW. The new genetics of chronic neutrophilic leukemia and atypical CML: implications for diagnosis and treatment. *Blood*. 2013;122(10):1707-1711.
3. Maxson JE, Tyner JW. Genomics of chronic neutrophilic leukemia. *Blood*. 2017;129(6):715-722.
4. Pardanani A, Lasho TL, Laborde RR, et al. CSF3R T618I is a highly prevalent and specific mutation in chronic neutrophilic leukemia. *Leukemia*. 2013;27(9):1870-1873.
5. Maxson JE, Gotlib J, Pollyea DA, et al. Oncogenic CSF3R mutations in chronic neutrophilic leukemia and atypical CML. *N Engl J Med*. 2013;368(19):1781-1790.
6. Dong F, Brynes RK, Tidow N, Welte K, Lowenberg B, Touw IP. Mutations in the gene for the granulocyte colony-stimulating-factor receptor in patients with acute myeloid leukemia preceded by severe congenital neutropenia. *N Engl J Med*. 1995;333(8):487-493.
7. Germeshausen M, Ballmaier M, Welte K. Incidence of CSF3R mutations in severe congenital neutropenia and relevance for leukemogenesis: Results of a long-term survey. *Blood*. 2007;109(1):93-99.
8. Aarts LH, Roovers O, Ward AC, Touw IP. Receptor activation and 2 distinct COOH-terminal motifs control G-CSF receptor distribution and internalization kinetics. *Blood*. 2004;103(2):571-579.
9. Beekman R, Valkhof MG, Sanders MA, et al. Sequential gain of mutations in severe congenital neutropenia progressing to acute myeloid leukemia. *Blood*. 2012;119(22):5071-5077.
10. Touw IP, Beekman R. Severe congenital neutropenia and chronic neutrophilic leukemia: an intriguing molecular connection unveiled by oncogenic mutations in CSF3R. *Haematologica*. 2013;98(10):1490-1492.
11. Schindelin J, Arganda-Carreras I, Frise E, et al. Fiji: an open-source platform for biological-image analysis. *Nat Methods*. 2012;9(7):676-682.
12. Jongen-Lavrencic M, Grob T, Hanekamp D, et al. Molecular Minimal Residual Disease in Acute Myeloid Leukemia. *N Engl J Med*. 2018;378(13):1189-1199.
13. Dobin A, Davis CA, Schlesinger F, et al. STAR: ultrafast universal RNA-seq aligner. *Bioinformatics*. 2013;29(1):15-21.
14. Trapnell C, Williams BA, Pertea G, et al. Transcript assembly and quantification by RNA-Seq reveals unannotated transcripts and isoform switching during cell differentiation. *Nat Biotechnol*. 2010;28(5):511-515.

15. Anders S, Pyl PT, Huber W. HTSeq--a Python framework to work with high-throughput sequencing data. *Bioinformatics*. 2015;31(2):166-169.
16. Love MI, Huber W, Anders S. Moderated estimation of fold change and dispersion for RNA-seq data with DESeq2. *Genome Biol*. 2014;15(12):550.
17. Mootha VK, Lindgren CM, Eriksson KF, et al. PGC-1alpha-responsive genes involved in oxidative phosphorylation are coordinately downregulated in human diabetes. *Nat Genet*. 2003;34(3):267-273.
18. Subramanian A, Tamayo P, Mootha VK, et al. Gene set enrichment analysis: a knowledge-based approach for interpreting genome-wide expression profiles. *Proc Natl Acad Sci U S A*. 2005;102(43):15545-15550.
19. Liberzon A, Birger C, Thorvaldsdottir H, Ghandi M, Mesirov JP, Tamayo P. The Molecular Signatures Database (MSigDB) hallmark gene set collection. *Cell Syst*. 2015;1(6):417-425.
20. Yan Q, Xu R, Zhu L, et al. BAL1 and its partner E3 ligase, BBAP, link Poly(ADP-ribose) activation, ubiquitylation, and double-strand DNA repair independent of ATM, MDC1, and RNF8. *Mol Cell Biol*. 2013;33(4):845-857.
21. Lallemand-Breitenbach V, de The H. PML nuclear bodies: from architecture to function. *Curr Opin Cell Biol*. 2018;52:154-161.
22. de Planque MM, Kluin-Nelemans HC, van Krieken HJ, et al. Evolution of acquired severe aplastic anaemia to myelodysplasia and subsequent leukaemia in adults. *Br J Haematol*. 1988;70(1):55-62.
23. Ogawa S. Clonal hematopoiesis in acquired aplastic anemia. *Blood*. 2016;128(3):337-347.
24. Socie G, Henry-Amar M, Bacigalupo A, et al. Malignant tumors occurring after treatment of aplastic anemia. European Bone Marrow Transplantation-Severe Aplastic Anaemia Working Party. *N Engl J Med*. 1993;329(16):1152-1157.
25. Maciejewski JP, Risitano A, Sloand EM, Nunez O, Young NS. Distinct clinical outcomes for cytogenetic abnormalities evolving from aplastic anemia. *Blood*. 2002;99(9):3129-3135.
26. Yoshizato T, Dumitriu B, Hosokawa K, et al. Somatic Mutations and Clonal Hematopoiesis in Aplastic Anemia. *N Engl J Med*. 2015;373(1):35-47.
27. Negoro E, Nagata Y, Clemente MJ, et al. Origins of myelodysplastic syndromes after aplastic anemia. *Blood*. 2017;130(17):1953-1957.
28. Skokowa J, Steinemann D, Katsman-Kuipers JE, et al. Cooperativity of RUNX1 and CSF3R mutations in severe congenital neutropenia: a unique pathway in myeloid leukemogenesis. *Blood*. 2014;123(14):2229-2237.
29. Touw IP. Game of clones: the genomic evolution of severe congenital neutropenia. *Hematology Am Soc Hematol Educ Program*. 2015;2015:1-7.

30. Hemmati S, Haque T, Gritsman K. Inflammatory Signaling Pathways in Preleukemic and Leukemic Stem Cells. *Front Oncol*. 2017;7:265.
31. Olofsen P, Fatrai S, van Strien P, et al. A Leukemic Progression Model of Severe Congenital Neutropenia Uncovers a Novel Mechanism of AML Development Involving Elevated Inflammatory Responses, Mutation of CXXC4 and Decreased TET2 Levels. *Blood*. 2018;132(Suppl 1):540-540.
32. Cai Z, Kotzin JJ, Ramdas B, et al. Inhibition of Inflammatory Signaling in Tet2 Mutant Preleukemic Cells Mitigates Stress-Induced Abnormalities and Clonal Hematopoiesis. *Cell Stem Cell*. 2018;23(6):833-849 e835.
33. Leimkuhler NB, Schneider RK. Inflammatory bone marrow microenvironment. *Hematology Am Soc Hematol Educ Program*. 2019;2019(1):294-302.

Supplemental Data

Table S1: Diagnostic criteria for CNL

WHO (2016) Diagnostic Criteria for CNL		Diagnostic Findings SAA-CNL
1. PB		
- WBC ≥25x10^9/L	✓	28.5 x 10^9/L
- Segmented neutrophils plus band forms ≥80% of WBCs	✓	88% of WBCs
- Neutrophil precursors (promyelocytes, myelocytes, metamyelocytes) <10% of WBC	✓	2.5% of WBC
- Myeloblasts rarely observed	✓	None observed
- Monocyte count <1x10^9/L	✓	0.64x10^9/L
- No dysgranulopoiesis	✓	Not observed
2. Hypercellular BM		
- Neutrophil granulocytes increased in percentage and number	✓	Hypercellular with markedly increased myelopoiesis
- Neutrophil maturation appears normal	✓	All maturation stages present
- Myeloblasts <5% of nucleated cells	✓	1% of nucleated cells
3. Not meeting WHO criteria for BCR-ABL1+ CML, PV, ET, or PMF	✓	Not meeting criteria
4. No rearrangement of PDGFRA, PDGFRB, FGFR1, or PCM1-JAK2	✓	No rearrangement
5. Presence of CSF3R T618I or other activating CSF3R mutation	✓	Present

Table S2: Bone marrow failure panel with a focus on genes indicating a predisposition for myeloid leukemia if mutated)

No	Gene	No	Gene	No	Gene
1	ACD	31	FANCL	62	RPL35A
2	ALAS2	32	FANCM	63	RPL5
3	ANKRD26	33	G6PC3	64	RPS10
4	ATG2B	34	GATA1	65	RPS17
5	ATM	35	GATA2	66	RPS19
6	BLM	36	GFI1	67	RPS24
7	BRCA1	37	GSKIP	68	RPS26
8	BRCA2	38	HAX1	69	RPS7
9	BRIP1	39	IKZF1	70	RTEL1
10	CBL	40	MLH1	71	RUNX1
11	CEBPA	42	MSH2	72	SAMD9
12	CHEK2	43	MSH6	73	SAMD9L
13	CSF3R	44	NAF1	74	SBDS
14	CTC1	45	NBN	75	SBF2
15	CXCR4	46	NF1	76	SLX4
16	DDX41	47	NHP2	77	SRP72
17	DKC1	48	NOP10	78	TERC
18	DNAJC21	49	PALB2	79	TERT
19	ELANE	50	PARN	80	TINF2
20	EPCAM	51	PAX5	81	TP53
21	ERCC4	52	PMS2	82	UBE2T
22	ETV6	53	POT1	83	USB1
23	FANCA	54	PTPN11	84	VPS45
24	FANCB	55	RAD51	85	WAS
25	FANCC	56	RAD51C	86	WRAP53
26	FANCD2	57	RBBP6		
27	FANCE	58	RBM8A		
28	FANCF	59	RPL11		
29	FANCG	60	RPL15		
30	FANCI	61	RPL26		

Table S3: IonTorrent Oncomine Myeloid research gene panel

No	Gene	No	Gene	No	Gene
1	ABL1	14	ETV6	27	PDGFRA
2	ASXL1	15	EZH2	28	PDGFRB
3	BCR	16	FLT3	29	PTPN11
4	BRAF	17	GATA2	30	RUNX1
5	CALR	18	IDH1	31	SETBP1
6	CBL	19	IDH2	32	SF3B1
7	CEBPA	20	JAK2	33	SH2B3
8	CHEK2	21	KIT	34	SRSF2
9	CSF3R	22	KRAS	35	TET2
10	DNMT3A	23	MPL	36	TP53
11	EGLN1	24	NF1	37	U2AF1
12	EPOR	25	NPM1	38	VHL
13	ETNK1	26	NRAS	39	ZRSR2

Table S4: TruSight Myeloid panel

No	Gene	No	Gene	No	Gene
1	ABL1	19	FLT3	37	NRAS
2	ASXL1	20	GATA1	38	PDGFRA
3	ATRX	21	GATA2	39	PHF6
4	BCOR	22	GNAS	40	PTEN
5	BCORL1	23	HRAS	41	PTPN11
6	BRAF	24	IDH1	42	RAD21
7	CALR	25	IDH2	43	RUNX1
8	CBL	26	IKZF1	44	SETBP1
9	CBLB	27	JAK2	45	SF3B1
10	CBLC	28	JAK3	46	SMC1A
11	CDKN2A	29	KDM6A	47	SMC3
12	CEBPA	30	KIT	48	SRSF2
13	CSF3R	31	KRAS	49	STAG2
14	CUX1	32	MLL	50	TET2
15	DNMT3A	33	MPL	51	TP53
16	ETV6/TEL	34	MYD88	51	U2AF1
17	EZH2	35	NOTCH1	53	WT1
18	FBXW7	36	NPM1	54	ZRSR2

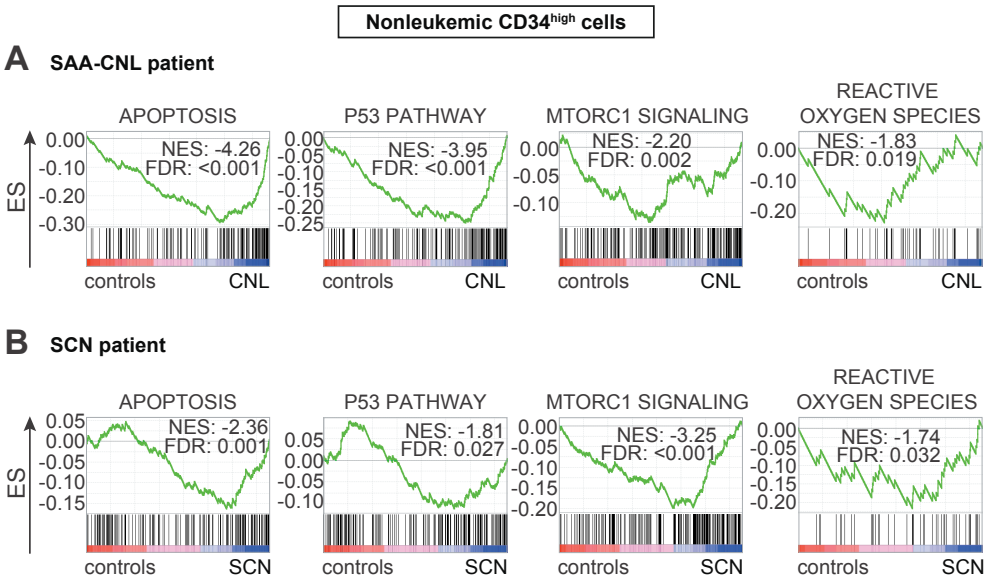

Figure S1. Comparative analysis between the transcriptional profiles of nonleukemic CD34^{high} cells from the SAA-CNL and SCN patient

(A-B) GSEA comparing nonleukemic CD34^{high} cells from (A) 3 healthy controls with CD34^{high} cells obtained from the SAA-CNL patient, (B) CD34^{high} cells from 3 healthy controls with CD34^{high} cells obtained from the SCN patient (SCN-phase before AML became clinically overt), both showing induction of apoptosis, activation of the p53 pathway, mTORC1 signaling, and responses to reactive oxygen species.

Chapter 9

Summary and General Discussion

9.1 Summary

Severe congenital neutropenia (SCN) is a bone marrow failure syndrome characterized by a neutrophil differentiation block at the promyelocyte stage. SCN patients are effectively treated by colony stimulating factor 3 (CSF3/G-CSF) administration, alleviating the neutropenia in >90% of patients. A major concern in treating SCN patients with CSF3 is the highly increased risk of developing myelodysplastic syndrome (MDS) or acute myeloid leukemia (AML). Progression to MDS/AML is associated with the appearance of hematopoietic clones with somatic mutations in the gene encoding the CSF3 receptor (*CSF3R*), resulting in a truncated form of CSF3R with defective internalization and aberrant signaling properties.[1-3] These clones can persist for months or years before MDS/AML, most frequently characterized by additional mutations in *RUNX1*, becomes clinically overt.[1,4] The work presented in this thesis focusses on the mechanisms involved in the leukemic progression of SCN by modelling the various sequential steps in induced pluripotent stem cells (iPSC) or mice.

Chapter 2 comprises a book chapter focusing on modeling SCN in iPSC. Since mouse models with patient specific mutations in *ELANE* and *HAX1* do not show signs of neutropenia[5,6], human models are needed to study the biology of SCN. Before the introduction of iPSC technology, attempts to model SCN in human cells have been mainly restricted to retroviral introduction of *ELANE* mutations in the promyelocytic leukemia cell line HL-60. The outcome of these experiments was mixed[7,8], and leukemic cell lines are now generally considered as less suitable for studying the biology of SCN. Since the introduction of iPSC technology[9,10], various SCN patient-derived iPSC have been generated and described. The development of CRISPR-Cas9 mediated genome editing made it feasible to precisely target modifications in iPSC, e.g., to repair disease causative gene defects in patient-derived lines or to introduce patient-derived mutations in normal controls.[11] By generating these so-called isogenic lines, it is possible to study phenotypic consequences of mutations without possible confounding factors, e.g., differences due to viral introduction/overexpression or differences between iPSC lines or clones.

In **Chapter 3** three new SCN patient-derived iPSC lines (*ELANE*-I60F, *ELANE*-R103L and *HAX1*-W44X) and one control iPSC line are described, which are employed to study the effect of *ELANE/HAX1* mutations on hematopoietic progenitor cells (HPCs). Increased oxidative stress levels, leading to activation of NRF2-mediated antioxidant responses, could be observed in SCN patient-derived HPCs. Additionally, in *ELANE*-SCN patients with a mutation that leads to misfolding of the neutrophil elastase (NE) protein, HPCs showed strongly increased numbers of promyelocytic leukemia protein nuclear bodies (PML-NBs). PML-NBs are a hallmark of more acute/excessive oxidative stress, but are also linked to a plethora of other processes

like metabolism, DNA damage response, and apoptosis.[12-18] In the case of *ELANE* mutations resulting in NE protein misfolding, PML enhanced the metabolic state of the HPCs, while also strongly elevating the expression of mutant *ELANE*, suggestive of a feed-forward mechanism of disease development. In addition, PML inhibited CSF3-induced outgrowth of neutrophil progenitors from these *ELANE*-mutant HPCs, implying an important role for PML in CSF3 therapy response and SCN-pathogenesis.

In **Chapter 4** CRISPR-Cas9 mediated genome editing is employed to introduce the patient-specific CSF3R-truncating mutation d715 (Q739X) in the previously described iPSC lines. RNA sequencing analyses indicate major differences between control and SCN-derived HPCs upon introduction of the truncated CSF3R. Where control-d715 HPCs mimic findings previously reported in cell lines and mouse models[19,20], the CSF3R-d715 in a SCN background does not induce proliferation but inflammation, while inducing differentiation instead of inhibiting neutrophil maturation. These findings might explain why in SCN patients *CSF3R*-mutant clones persist as minor clones for years before leukemia becomes clinically overt.[21,22] In addition, these data provide a possible explanation for the high frequency of *CSF3R* mutations found in the leukemic clone, since induction of pro-inflammatory signaling might induce the selection and outgrowth of clones that acquired additional mutations, making them more resistant to the inflammatory stimuli. Cells with loss of function mutations in, e.g., *RUNX1* and *TET2*, both frequently found mutated in AML, are described to be more resistant to an inflammatory environment, possibly explaining why *RUNX1* mutations are observed in the majority of *CSF3R* mutant SCN clones.[4,23,24]

Chapter 5 comprises a (p)review that discusses the role of *RUNX1* mutations in SCN, mainly focusing on the *Csf3r*-d715/*RUNX1*-D171N mouse model described in **Chapter 6**, which shows a selective expansion of immature lineage negative, c-Kit positive, Sca-1 negative (LK) myeloblasts, but no absolute neutrophil differentiation arrest, upon CSF3 treatment. In line with this, additional experiments in iPSC show a reduction in neutrophil maturation upon introduction of the patient specific *RUNX1*-D171N mutation in *CSF3R*-d715 cells derived from a healthy control.

Chapter 6 describes how the combination of CSF3 therapy, *CSF3R,* and *RUNX1* mutations contribute to AML development. CSF3-, but not PBS-, treated *Csf3r*/*RUNX1* mutant mice show a selective expansion of lineage negative, c-Kit positive, Sca-1 negative (LK) hematopoietic progenitors in the peripheral blood, but no overt AML. Intriguingly, one *Csf3r*/*RUNX1* mutant, CSF3-treated, mouse (1/9) acquired an additional mutation in *Cxxc4* which resulted in AML upon serial transplantations. The *Cxxc4* alteration, an insertion of 2 glycine residues in a glycine-repeat, causes increased CXXC4 protein stability resulting in

elevated CXXC4 levels and reduced TET2 protein levels. In addition, elevated expression of multiple pro-inflammatory pathways is observed in both mouse AML and human SCN-AML, which could be mimicked in iPSC by inhibiting (TET2's) HDAC recruitment function, suggesting that inflammation driven by down-regulation of TET2 activity is a critical step in the malignant transformation of SCN.

In **Chapter 7** we screened 1706 AML patients from various HOVON clinical trials for the presence of mutations in the glycine-repeat region of CXXC4, which we found altered in de leukemic mice. *CXXC4* insertions, deletions and missense mutations were observed in 46 AML patients. Saliva samples were available from 12 *CXXC4* mutant patients, which all showed the presence of this mutations in the germline. In addition, analyses of 5 follow-up samples of *CXXC4* mutant patients showed the presence of the *CXXC4* mutations upon reaching complete morphological remission. Although *CXXC4* mutations could be detected in the germline, incidences were significantly higher in pre-leukemic conditions in which inflammatory signaling plays an important role; high-risk MDS and myeloproliferative neoplasm, compared to AML and low-risk MDS (p=0.008). These data suggest that *CXXC4* mutations might contribute to, but are not sole drivers of, leukemic transformation by providing an inflammatory environment important for the clonal expansion of hematopoietic stem and progenitor cells (HSPCs). Leukemic transformation is then dependent on acquisition of additional mutations which are often proceeded by a more "benign" pre-leukemic stage like MDS.

In **Chapter 8** the first patient with severe aplastic anemia (SAA) evolving to secondary chronic neutrophilic leukemia (CNL) is described. Somatic driver mutations in *CSF3R*, *RUNX1* and a polycomb repressor complex 2 (PRC2) gene (*EZH2*) in this SAA-CNL patient are shared with the previously described SCN patient (mutation in PRC2 gene *SUZ12*) that transformed to AML.[1] Comparative transcriptome analysis on non-leukemic $CD34^{high}$ HSPCs of this SAA-CNL patient, or the SCN patient, with 3 healthy controls showed resembling transcriptional profiles indicative of interferon (IFN)-driven pro-inflammatory responses. These findings indicate the presence of a pro-inflammatory milieu in SAA and SCN, possibly contributing to the pre-leukemic state of these cells, thereby providing further insights in possible mechanisms underlying leukemic transformation in bone marrow failure syndromes.

In conclusion, this thesis reveals new mechanisms of how SCN mutations, and possibly other bone marrow failure syndromes like SAA, contribute to leukemic progression. We show that PML-NBs play an important role in *ELANE*-mutant patients with predicted NE-misfolding, while inflammatory signaling plays a critical step in the malignant transformation of SCN. In addition, we identified a mutation in *Cxxc4*, which can also be found in *de novo* AML, as an

additional driver for leukemic progression in a mouse model of SCN.

9.2 General discussion

Severe congenital neutropenia (SCN) is a family of genetic diseases associated with low neutrophil counts and an increased risk of leukemic transformation. To date, more than 20 distinct genes have been identified to be able to cause SCN.[25] In addition to the classical SCN, characterized by a promyelocyte differentiation arrest, the SCN family comprises various other bone marrow failure syndromes, e.g., glycogen storage disease Ib (mutation in *SLC37A4*), Shwachman-Diamond syndrome (mutation in *SBDS*), WHIM syndrome (mutation in *CXCR4*), GATA2 syndrome (mutation in *GATA2*) and Barth disease (mutation in *TAZ*).[26-30] Mutations in many of these genes result in additional defects in other organs. For example, Shwachman-Diamond syndrome patients present with abnormalities in the pancreas and bone, GATA2 mutant patients can present with lymphedema and deafness, while Barth disease patients present with cardiac abnormalities. The common denominator between SCN patients is the increased risk of infections due to the neutropenia, while also showing high risk of leukemic transformation. How mutations in these genes cause neutropenia and why they show such a highly increased risk of leukemic transformation remains an important point of study.

In this thesis we used SCN, more specifically patients with mutations in *ELANE* and *HAX1,* as model disease to study the sequential steps of leukemic transformation.

9.2.1 Increased oxidative stress as possible common denominator of CNs

As mentioned in **Chapter 1**, mutations in a plethora of genes have been shown to result in SCN, all affecting proteins with different cellular locations and functions, where *ELANE* encodes the primary granule protein neutrophil elastase (NE)[31,32], *HAX1* encodes a mitochondrial protein[33], *WAS* a cytoskeletal protein[34], *G6PC3* a metabolic enzyme[35], *VPS45* an endosomal membrane trafficking protein[36], *GFI1* a myeloid transcription factor[37], *JAGN1*[38] a transmembrane protein and *CSF3R* a cytokine receptor.[39] One of the remaining questions is how mutations in these very different genes can result in the same phenotype and can cause the same disease. We showed that, although the mutations in the 3 SCN patients used to generate iPSC are in different genes or are predicted to have different effects on the protein, they all result in increased oxidative stress levels in hematopoietic progenitor cells (HPCs). Excessive ROS has been observed in various other diseases like Alzheimer, Parkinson disease, and different types of cancer[40,41], and are extensively studied for their contribution in aging.[42] When not efficiently cleared, an excessive and toxic oxidative stress burden results in DNA, protein and lipid damage due to oxidation by free oxygen radicals present.[42] Whether increased oxidative stress levels in SCN patients result in these kind of damages needs to be further studied, and might give insights into which patients might have

an increased risk of acquiring additional mutations and potential leukemic transformation due to inefficient clearing of ROS. In line with this, a mouse model of Shwachman-Diamond syndrome showed increased oxidative stress levels in HSPCs which resulted in increased DNA damage and genotoxic stress.[43]

It remains to be answered whether increased oxidative stress levels are observed in SCN patients with mutations in other genes, e.g., *WAS, G6PC3* or *JAGN1*, and if all mutations result in similar increases in ROS levels. Our studies on the *ELANE*-I60F mutation would suggest differences between patients and mutations, since these cells, but not the other SCN-derived HPCs, showed increased numbers of promyelocytic leukemia nuclear bodies (PML-NBs), associated with more acute/excessive oxidative stress.[12] We could link the increased PML-NBs with *ELANE*-mutant cases with predicted NE misfolding (*ELANE*-I60F *and ELANE*-P139L), but more patients need to be screened to verify if this holds true for all predicted misfolding cases.

9.2.2 The promyelocytic leukemia protein PML as important player in SCN

9.2.2.1 PML and promyelocyte arrest

The PML protein has first been described in acute promyelocytic leukemia (APL), where it forms a fusion protein with retinoic acid receptor α (RARA), resulting in disorganized PML-NBs.[44] The PML-RARA fusion protein interferes with the function of wildtype PML protein[45], resulting in a promyelocyte arrest, similar as observed in SCN. This is especially interesting in the light of *ELANE*-mutant cases with predicted NE misfolding, since PML functions might be altered due to the increased need for clearing of excessive ROS and/or the misfolded protein. One of the possibilities could be that the SUMOylation status of important myeloid transcription factors is altered, rendering them less efficient in inducing transcription. Another option could be that transcription factors are trapped inside of PML-NBs preventing them from binding DNA. Suggestive of a role for PML and SUMOylation in differentiation is the fact that hematopoietic transcription factors c-MYB, MECOM and IKZF1 are differentially SUMOylated upon PML loss in the myeloid leukemia cell line K562 (data not shown). These observations merit a rich substrate for further studies which are needed to unravel the potential role of SUMOylation of these proteins on transcriptional activity and myeloid differentiation.

9.2.2.2 Canonical and PML-driven clearing of misfolded proteins

Studies on the effect of *ELANE* mutations have mainly focused on activation of the classical unfolded protein response (UPR). The first paper suggesting a possible involvement of the UPR in ELANE-SCN was published in 2006 by Köllner et al.[46] They showed that overexpression of mutant NE moderately increased expression of the UPR gene BiP (*HSPA5*) in U937 cells, although mainly after induction of apoptosis with camptothecin. Shortly thereafter,

Grenda et al. showed significant upregulation of BiP and the short isoform of XBP1 after overexpression of 4/5 *ELANE*-mutants in U937, providing more compelling evidence of the possible NE-misfolding and activation of the UPR in some of the *ELANE* mutant cases.[47] However, both studies involved overexpression of the various mutant NE proteins, hence studying the effects of *ELANE* mutations at nonphysiological levels. In addition, not all mutations seem to activate the UPR, indicating that various mutations can have different effects on the protein. This is not unexpected given that more than 200 different *ELANE* mutations have been described, spanning the whole *ELANE* gene including 3' UTR and various introns.[48-52] In line with this, several other mechanisms have been suggested as initiators of neutropenia, e.g., mislocalization of the mutant NE protein and an altered enzymatic activity.[46,51] However, when using mutation prediction programs, the majority of mutations in *ELANE* are predicted to result in protein misfolding.[53]

In addition, functional studies of the effect of *ELANE* mutations in iPSC generated from *ELANE*-SCN patients, studying the mutations at physiological levels, have mainly focused on activation of the UPR. Also here, evidence for a role of the canonical UPR is rather weak, as only the expression of less than a handful of UPR genes was measured and consistent differences could often not be observed when multiple UPR genes were analyzed.[54-56]

Another pathway that is described to be able to clear misfolded proteins involves PML.[57] We showed upregulation of PML-NBs in HPCs from *ELANE*-mutant cases with predicted NE misfolding (*ELANE*-I60F *and ELANE*-P139L), but no activation of the classical UPR pathway genes, not even in more differentiated granulocytic cells. The difficulty to properly and accurately define and study the promyelocyte stage might explain the variably outcomes reported in the various iPSC studies, where no clearly defined cell population is used to study the expression of various UPR genes and apoptosis. It would be interesting to see whether predicted misfolding mutations in other genes associated with SCN would cause the same upregulation of PML-NBs, or if this is specific for *ELANE*. In addition, whether PML is able to clear misfolded NE remains to be determined[57], since ELANE transcript levels are significantly reduced upon PML loss in *ELANE*-I60F iPSC-derived HPCs. One could think of performing peptide specific mass spectrometry to investigate the ratio of wildtype and mutant protein, but this is a tedious procedure which does not work for the majority of peptides due to limited enzymatic cut locations that yield the required peptide length.

9.2.3 Inflammatory signaling

In this thesis we describe inflammatory signaling as an important player in the leukemic progression of SCN (**Chapter 6**), while non-leukemic HSPCs in SCN and SAA-CNL already show upregulation of interferon-related signaling pathways (**Chapter 8**). In addition to SCN and SAA-CNL, an inflammatory bone marrow microenvironment has been described in aging and various other hematological malignancies, e.g., AML, MDS, and Shwachman-Diamond

syndrome, and it is believed that the presence of this inflammatory environment plays an important role in the progression of myeloid leukemias.[43,58-62] The majority of cytokines, including inflammatory cytokines, signal via downstream NF-κB and JAK-STAT molecules.[63] The dimerization of the different phosphorylated STAT proteins, and subsequent nuclear translocation and DNA binding, results in expression of various target genes depending on which STATs dimerize. In *CSF3R*-d715 SCN-HPCs an increase in inflammatory signaling pathways is observed compared to their wildtype counterparts, while proliferation-related pathways are decreased, which is in contrast to what is observed in control cells (**Chapter 4**). It would be interesting to see whether different STATs are activated depending on the cell's background, resulting in expression of different target genes. In addition, these studies might then provide new insights into possible new therapies by reducing the activation of inflammatory pathways.

The high overlap between the different pathways in downstream signaling makes it difficult to accurately verify activation of specific inflammatory pathways, besides looking at upregulation of target genes or presence of inflammatory cytokines themselves. However, inflammatory cytokines might not easily be detectable since there is increasing evidence that these cytokines might be produced by cells of the bone marrow microenvironment or more differentiated myeloid cells instead of the HSPCs, increasing the local cytokine level.[43,62] This local change makes it difficult to detect changes in cytokine levels globally, by, e.g., looking for cytokine levels in the peripheral blood.

9.2.4 The effect of *CSF3R* mutations and CSF3 treatment

Acquired *CSF3R* truncating mutations almost always appear in the context of an underlying SCN mutation and are not observed during leukemic transformation of other CNs.[64] Whether CSF3 treatment, which is prescribed to SCN patients but usually not to other CN patients[25], might play a role in the acquisition of *CSF3R* mutations and subsequent leukemic transformation remains unanswered. The observation that patients treated with higher dosages of CSF3 show an increased risk of leukemic transformation suggests a contributing role for CSF3 treatment, but whether these hyporesponsive patients acquire *CSF3R* mutations and whether CSF3 might contribute before and/or after acquisition of the truncated *CSF3R* is not known.[65] In line with a role for CSF3-treatment after acquisition of a truncating *CSF3R* mutation is the finding that lineage negative *Csf3r*-d715 murine bone marrow cells show a CSF3-induced hyperproliferative phenotype *in vitro*, while mice transplanted with *Csf3r*-d715 *RUNX1*-D171N bone marrow show a CSF3-dependent expansion of lineage$^-$ c-Kit$^+$ (LK) cells (**Chapter 6**). Additionally, CSF3R-d715 control HPCs show a significant increase in CSF3-induced colony forming potential (**Chapter 4**).

So far studies on the function of truncated CSF3R have only been performed in cell lines or mouse models lacking the underlying SCN mutation. Therefore, our studies in SCN patient

derived iPSC give valuable new information on how the truncated receptor functions in a disease relevant context. Surprisingly, CSF3-induced myeloid colony formation was not increased in SCN *CSF3R*-d715 cells compared to their wildtype counterparts, where a 1.5 to 2-fold increase is observed in *CSF3R*-d715 cells derived from control iPSCs and mouse bone marrow (**Chapters 4 and 6**). This finding was accompanied by RNA sequencing experiments which showed no increase, and even a decrease, in proliferative signatures in SCN-d715 HPCs, while control-d715 HPCs showed a significant induction of proliferative signaling pathways compared to their wildtype counterparts (**Chapter 4**). In addition, where control-d715 HPCs showed increased expression of pathways associated with hematopoietic stem/progenitor cells and a reduction in myeloid differentiation pathways, SCN-d715 HPCs showed the opposite suggesting induction of myeloid differentiation upon introduction of the truncated CSF3R (**Chapter 4**). These findings might explain why several minor *CSF3R* mutant clones can be present and persist in SCN patients receiving CSF3 therapy without becoming a major clone, unless additional mutations are acquired.[1]

Additional studies need to be done to investigate the downstream signaling alterations due to the truncated CSF3R in a SCN background in more detail, encompassing downstream signaling molecules like STAT3 and STAT5. Differences in activation of the STAT proteins between control and SCN mutant cells might explain the different effects observed on proliferation and differentiation.[66]

9.2.5 Overlap with chronic neutrophilic leukemia

The genetic hallmark of chronic neutrophilic leukemia (CNL) is an auto-activating mutation in the *CSF3R* (T618I), which is observed in >80% of patients. Some patients also present with truncating mutations, but this is often accompanied by the *CSF3R*-T618I mutation.[67] In addition, some SCN patients acquire the *CSF3R*-T618I mutation, often in the allele that also acquired the *CSF3R* truncating mutation.[1] These cases fuel the concept that CNL might be preceded by a premalignant state characterized by CSF3 hyporesponsiveness, just like in SCN, which can be overcome by the acquisition of *CSF3R* mutations.[64] In line with a possible pre-malignant state preceding CNL, we identified the acquisition of CNL in a severe aplastic anemia (SAA) patient (**Chapter 8**). RNA sequencing of non-leukemic $CD34^+$ hematopoietic stem and progenitor cells (HSPCs) indicate upregulation of interferon (IFN)-α and -γ signaling pathways in both the SCN patient and the SAA-CNL patient (**Chapter 8**). These data suggest that the SCN and SAA HSPCs reside in an inflammatory bone marrow microenvironment, which might contribute to a permissive condition for the development of leukemic cells.[68,69]

9.2.6 The effect of *RUNX1* mutations

Acquired mutations in the hematopoietic transcription factor *RUNX1* are frequently found in SCN patients who progress to MDS or AML (64.5%).[4] In contrast to truncating *CSF3R* mutations, mutations in *RUNX1* are also observed in various other hematological malignancies like *de novo* AML and acute lymphocytic leukemia (ALL).[70] Mutations in *RUNX1* include deletions, missense mutations, splicing alterations, frameshift and nonsense mutations and these alterations can result in a truncated protein lacking/perturbing the transactivation domain (TAD), and sometimes also the DNA binding runt-homology domain (RHD), or a RUNX1 protein that show disrupted DNA binding due to missense mutations in the RHD.[71-73] In addition, various chromosomal translocations, e.g., t(8;21) and t(12;21), involve the *RUNX1* gene and generate RUNX1-RUNX1T1 and ETV6-RUNX1 fusion proteins, respectively.[74-79] Germline mono-allelic *RUNX1* mutations are also described and cause familial platelet disorder with predisposition to AML (FDP/AML).[80]

Since *RUNX1* mutations are found throughout the protein, different mutations might have different effects on myeloid differentiation and leukemic transformation. In line with this, the SCN-patient-specific mutation *RUNX1*-S291fsX9, resulting in a premature termination codon and a truncated protein lacking part of the transactivation domain (TAD), results in a selective expansion of lineage-negative, c-Kit-positive, Sca-1-positive (LSK, in contrast to LK cells in the *RUNX1*-D171N (RHD) mutant) cells in *in vitro* Csf3r-d715 mouse bone marrow cells (Figure 1). Data from these *in vitro* experiments, in combination with our observations *in vivo,* indicate that mutations in *RUNX1* result in selective expansion of immature cells but not an absolute differentiation arrest.

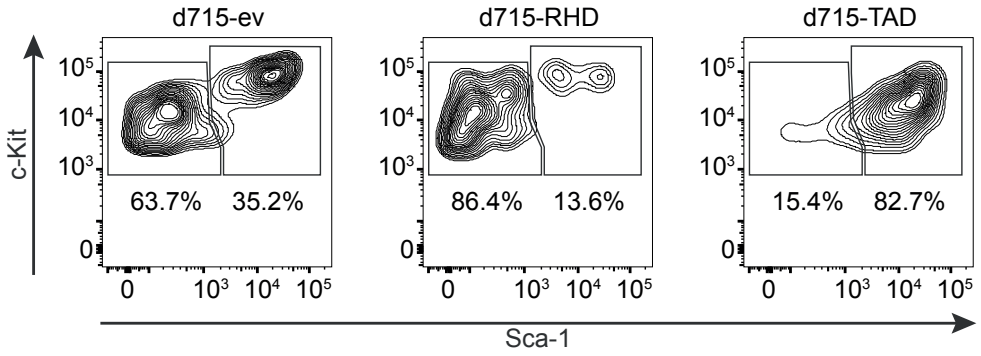

Figure 1: LK/LSK distribution is differently affected upon introduction of various RUNX1-mutations
Representative FACS contour plots showing LK/LSK distribution of d715-ev (left panel), d715-RHD (middle), and d715-TAD (right panel) in CSF3-supplemented cultures (day 9).

In addition to an effect on myeloid differentiation, *RUNX1* mutations have also been described to result in defective DNA repair[81,82], possibly by dysregulated expression or activity of important DNA repair proteins, as has been described for the RUNX1-RUNX1T1 (AML1-ETO) fusion protein.[83-86] *RUNX1* mutations may also promote the survival of HSPCs, since *Runx1* deficient HSPCs show lower p53 protein levels and a decreased percentage of apoptotic cells.[87-89] Additionally, wildtype RUNX1 inhibits inflammatory cytokine production by neutrophils, suggesting that loss-of-function mutations in *RUNX1* increase inflammation.[90] However, various studies showed a decrease in long-term HSCs in *Runx1*-mutant mice, indicating that *Runx1* mutations do not give a proliferative- or competitive-advantage and might even result in stem cell exhaustion.[87,91,92] These data combined suggest that *RUNX1* mutations might provide a favorable environment for the acquisition and survival of mutant HSPCs, but additional mutations are needed to provide a competitive advantage.[23]

9.2.6.1 Modeling *RUNX1* mutations *in vitro*

Lentiviral introduction of mutant RUNX1 results in overexpression at possible non-physiological levels if not controlled properly. In addition, viral transductions induce an inflammatory response in the cells, making it impossible to study changes in inflammatory signaling pathways shortly after transduction. Therefore, taking along the proper controls to be able to correct for this transduction effect is essential. Transduction with wildtype RUNX1 would be the best control, but overexpression of wildtype RUNX1 results in apoptosis and can therefore not be used (data not shown).[93,94] To correct for changes due to viral transduction we used an empty vector control.

Another option would be to introduce RUNX1 mutations with genome editing strategies, making it possible to study the effect of the mutation under physiological conditions. However, CRISPR-Cas9 mediated genome editing of RUNX1 results in the absence/severe reduction of HPCs derived from iPSC, making it impossible for downstream applications (Figure 2). This finding is in line with published studies on iPSC from familial platelet syndrome (FPD) patients who have a germline *RUNX1* mutation and also show severely reduced numbers of HPCs.[95] Another alternative would be to generate an inducible model with CRISPR-Cas9 mediated genome editing, inducing the mutation in RUNX1 after the generation of hematopoietic progenitor cells. However, besides the challenges of generating such a model, the recombination efficiency will be low and a good screening mechanism is needed. In addition, overexpression of RUNX1 has been observed in SCN-AML cases, while also trisomy 21 (containing the *RUNX1* gene) is frequently observed, making the overexpression model (if the levels remain physiological) the best available option to date.[4]

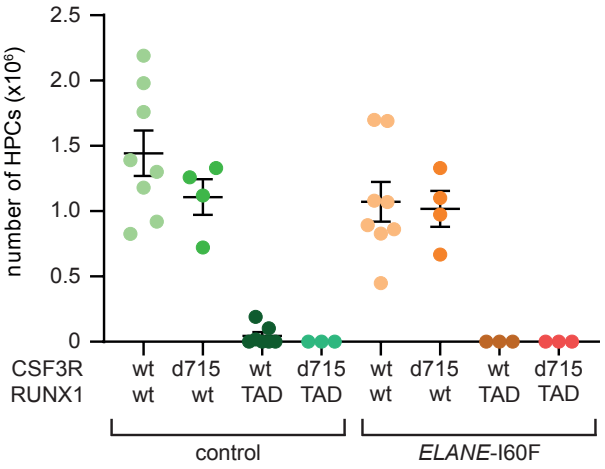

Figure 2: RUNX1-TAD mutation affects production of HPCs from control and ELANE-I60F mutant iPSCs
Quantification of number of HPCs upon hematopoietic induction of various CRISPR-Cas9 genome edited iPSC lines.

9.2.7 Hierarchical acquisition of mutations

A remaining unanswered question concerns the order of acquired mutations during leukemic transformation. Various *CSF3R* mutant clones can be detected in SCN patients, years before a potential leukemia becomes clinically overt, indicating that these types of mutations are the "second hit" towards leukemic transformation, when counting the SCN mutation as being first. The majority of *CSF3R* mutant clones acquire a *RUNX1* mutation relatively shortly before leukemia becomes clinically overt. However, lack of sequential sampling of SCN patients progressing to AML makes it impossible to accurately determine when *RUNX1* mutations are acquired.[1,4] The question if the combination of these 3 mutations (SCN/*CSF3R/RUNX1*) is enough for the leukemic progression remains unanswered. In our mouse model, lacking the SCN mutation, the combination of a *Csf3r* and *RUNX1* mutation resulted in a pre-leukemic condition but not overt AML. However, when an additional mutation in *Cxxc4* was acquired mice progressed to a CSF3-independent AML, showing a severe reduction in TET2 levels and upregulation of inflammatory signaling pathways. Whether mutations in *CXXC4* occur in SCN patients is unknown, because the majority of patients nowadays undergo bone marrow transplantation before they progress to leukemia, making material very scarce. Mutations in other epigenetic genes, e.g., *SUZ12, EZH2, ASXL1* or *EP300,* are described to be present in SCN-AML and might provide a similar function as mutant *CXXC4*.[1,4] In line with this, EZH2, which together with SUZ12 forms the polycomb repressive complex 2 (PRC2), regulates CXXC4 protein level.[96] It would be interesting to determine if *EZH2,* and possibly also *SUZ12,* mutations observed in SCN-AML result in increased CXXC4 protein abundance

and a reduction of TET2 levels. Another option would be that all epigenetic regulators are able to induce the transcription of genes important for inflammatory signaling, as is seen upon iPSC treatment with the HDAC inhibitor MS275, and that this phenomenon is the missing "fourth step" in leukemic transformation. However, it might still be possible that the combination of *CSF3R* and *RUNX1* mutations is sufficient for leukemic transformation in a SCN mutant background. Therefore, the field would benefit greatly if it would be feasible to generate long-term hematopoietic stem cells (LT-HSCs) from iPSC, making it possible to transplant SCN patient derived cells into mice.

9.2.8 Conclusions and Outlook

In conclusion, this thesis provides various mechanistical insights into SCN and its leukemic progression. Further studies into these mechanisms are needed and might provide new/better treatment options for CSF3-hyporesponsive (*ELANE*-mutant) SCN patients by, e.g., reducing oxidative stress levels, thereby preventing the increased formation of PML-NBs. Whether PML-NBs play an important role in other types of SCN, and/or all CSF3-hyporesponsive patients remains to be determined. Additionally, lowering inflammatory signaling might decrease the possibility of acquiring additional (*RUNX1*) mutations, thereby preventing the leukemic transformation of SCN. Investigating the downstream signaling cascade upon activation of the CSF3R-d715 in SCN-HPCs might provide leads for a more targeted therapy approach, e.g., by specifically preventing the phosphorylation or dimerization of specific STAT molecules.

References

1. Beekman R, Valkhof MG, Sanders MA, et al. Sequential gain of mutations in severe congenital neutropenia progressing to acute myeloid leukemia. *Blood*. 2012;119(22):5071-5077.
2. Dong F, Brynes RK, Tidow N, Welte K, Lowenberg B, Touw IP. Mutations in the gene for the granulocyte colony-stimulating-factor receptor in patients with acute myeloid leukemia preceded by severe congenital neutropenia. *N Engl J Med*. 1995;333(8):487-493.
3. Touw IP. Game of clones: the genomic evolution of severe congenital neutropenia. *Hematology Am Soc Hematol Educ Program*. 2015;2015:1-7.
4. Skokowa J, Steinemann D, Katsman-Kuipers JE, et al. Cooperativity of RUNX1 and CSF3R mutations in severe congenital neutropenia: a unique pathway in myeloid leukemogenesis. *Blood*. 2014;123(14):2229-2237.
5. Chao JR, Parganas E, Boyd K, Hong CY, Opferman JT, Ihle JN. Hax1-mediated processing of HtrA2 by Parl allows survival of lymphocytes and neurons. *Nature*. 2008;452(7183):98-102.
6. Grenda DS, Johnson SE, Mayer JR, et al. Mice expressing a neutrophil elastase mutation derived from patients with severe congenital neutropenia have normal granulopoiesis. *Blood*. 2002;100(9):3221-3228.
7. Makaryan V, Kelley ML, Fletcher B, Bolyard AA, Aprikyan AA, Dale DC. Elastase inhibitors as potential therapies for ELANE-associated neutropenia. *J Leukoc Biol*. 2017;102(4):1143-1151.
8. Massullo P, Druhan LJ, Bunnell BA, et al. Aberrant subcellular targeting of the G185R neutrophil elastase mutant associated with severe congenital neutropenia induces premature apoptosis of differentiating promyelocytes. *Blood*. 2005;105(9):3397-3404.
9. Takahashi K, Tanabe K, Ohnuki M, et al. Induction of pluripotent stem cells from adult human fibroblasts by defined factors. *Cell*. 2007;131(5):861-872.
10. Takahashi K, Yamanaka S. Induction of pluripotent stem cells from mouse embryonic and adult fibroblast cultures by defined factors. *Cell*. 2006;126(4):663-676.
11. Cong L, Ran FA, Cox D, et al. Multiplex genome engineering using CRISPR/Cas systems. *Science*. 2013;339(6121):819-823.
12. Niwa-Kawakita M, Ferhi O, Soilihi H, Le Bras M, Lallemand-Breitenbach V, de The H. PML is a ROS sensor activating p53 upon oxidative stress. *J Exp Med*. 2017;214(11):3197-3206.
13. Chang HR, Munkhjargal A, Kim MJ, et al. The functional roles of PML nuclear bodies in genome maintenance. *Mutat Res*. 2018;809:99-107.

14. Niwa-Kawakita M, Wu HC, The H, Lallemand-Breitenbach V. PML nuclear bodies, membrane-less domains acting as ROS sensors? *Semin Cell Dev Biol*. 2018;80:29-34.
15. Bernardi R, Pandolfi PP. Structure, dynamics and functions of promyelocytic leukaemia nuclear bodies. *Nat Rev Mol Cell Biol*. 2007;8(12):1006-1016.
16. Maarifi G, Chelbi-Alix MK, Nisole S. PML control of cytokine signaling. *Cytokine Growth Factor Rev*. 2014;25(5):551-561.
17. Sahin U, de The H, Lallemand-Breitenbach V. PML nuclear bodies: assembly and oxidative stress-sensitive sumoylation. *Nucleus*. 2014;5(6):499-507.
18. Tessier S, Martin-Martin N, de The H, Carracedo A, Lallemand-Breitenbach V. Promyelocytic Leukemia Protein, a Protein at the Crossroad of Oxidative Stress and Metabolism. *Antioxid Redox Signal*. 2017;26(9):432-444.
19. Dong F, van Buitenen C, Pouwels K, Hoefsloot LH, Lowenberg B, Touw IP. Distinct cytoplasmic regions of the human granulocyte colony-stimulating factor receptor involved in induction of proliferation and maturation. *Mol Cell Biol*. 1993;13(12):7774-7781.
20. Ward AC, Smith L, de Koning JP, van Aesch Y, Touw IP. Multiple signals mediate proliferation, differentiation, and survival from the granulocyte colony-stimulating factor receptor in myeloid 32D cells. *J Biol Chem*. 1999;274(21):14956-14962.
21. Germeshausen M, Ballmaier M, Welte K. Incidence of CSF3R mutations in severe congenital neutropenia and relevance for leukemogenesis: Results of a long-term survey. *Blood*. 2007;109(1):93-99.
22. Tidow N, Pilz C, Teichmann B, et al. Clinical relevance of point mutations in the cytoplasmic domain of the granulocyte colony-stimulating factor receptor gene in patients with severe congenital neutropenia. *Blood*. 1997;89(7):2369-2375.
23. Bellissimo DC, Speck NA. RUNX1 Mutations in Inherited and Sporadic Leukemia. *Front Cell Dev Biol*. 2017;5:111.
24. Cai Z, Kotzin JJ, Ramdas B, et al. Inhibition of Inflammatory Signaling in Tet2 Mutant Preleukemic Cells Mitigates Stress-Induced Abnormalities and Clonal Hematopoiesis. *Cell Stem Cell*. 2018;23(6):833-849 e835.
25. Donadieu J, Beaupain B, Fenneteau O, Bellanne-Chantelot C. Congenital neutropenia in the era of genomics: classification, diagnosis, and natural history. *Br J Haematol*. 2017;179(4):557-574.
26. Veiga-da-Cunha M, Gerin I, Chen YT, et al. The putative glucose 6-phosphate translocase gene is mutated in essentially all cases of glycogen storage disease type I non-a. *Eur J Hum Genet*. 1999;7(6):717-723.
27. Boocock GR, Morrison JA, Popovic M, et al. Mutations in SBDS are associated with Shwachman-Diamond syndrome. *Nat Genet*. 2003;33(1):97-101.

28. Gorlin RJ, Gelb B, Diaz GA, Lofsness KG, Pittelkow MR, Fenyk JR, Jr. WHIM syndrome, an autosomal dominant disorder: clinical, hematological, and molecular studies. *Am J Med Genet*. 2000;91(5):368-376.
29. Collin M, Dickinson R, Bigley V. Haematopoietic and immune defects associated with GATA2 mutation. *Br J Haematol*. 2015;169(2):173-187.
30. Barth PG, Wanders RJ, Vreken P, Janssen EA, Lam J, Baas F. X-linked cardioskeletal myopathy and neutropenia (Barth syndrome) (MIM 302060). *J Inherit Metab Dis*. 1999;22(4):555-567.
31. Dale DC, Person RE, Bolyard AA, et al. Mutations in the gene encoding neutrophil elastase in congenital and cyclic neutropenia. *Blood*. 2000;96(7):2317-2322.
32. Horwitz M, Benson KF, Person RE, Aprikyan AG, Dale DC. Mutations in ELA2, encoding neutrophil elastase, define a 21-day biological clock in cyclic haematopoiesis. *Nat Genet*. 1999;23(4):433-436.
33. Klein C, Grudzien M, Appaswamy G, et al. HAX1 deficiency causes autosomal recessive severe congenital neutropenia (Kostmann disease). *Nat Genet*. 2007;39(1):86-92.
34. Devriendt K, Kim AS, Mathijs G, et al. Constitutively activating mutation in WASP causes X-linked severe congenital neutropenia. *Nat Genet*. 2001;27(3):313-317.
35. Boztug K, Appaswamy G, Ashikov A, et al. A syndrome with congenital neutropenia and mutations in G6PC3. *N Engl J Med*. 2009;360(1):32-43.
36. Vilboux T, Lev A, Malicdan MC, et al. A congenital neutrophil defect syndrome associated with mutations in VPS45. *N Engl J Med*. 2013;369(1):54-65.
37. Person RE, Li FQ, Duan Z, et al. Mutations in proto-oncogene GFI1 cause human neutropenia and target ELA2. *Nat Genet*. 2003;34(3):308-312.
38. Boztug K, Jarvinen PM, Salzer E, et al. JAGN1 deficiency causes aberrant myeloid cell homeostasis and congenital neutropenia. *Nat Genet*. 2014;46(9):1021-1027.
39. Triot A, Jarvinen PM, Arostegui JI, et al. Inherited biallelic CSF3R mutations in severe congenital neutropenia. *Blood*. 2014;123(24):3811-3817.
40. Manoharan S, Guillemin GJ, Abiramasundari RS, Essa MM, Akbar M, Akbar MD. The Role of Reactive Oxygen Species in the Pathogenesis of Alzheimer's Disease, Parkinson's Disease, and Huntington's Disease: A Mini Review. *Oxid Med Cell Longev*. 2016;2016:8590578.
41. Liou GY, Storz P. Reactive oxygen species in cancer. *Free Radic Res*. 2010;44(5):479-496.
42. Sies H, Berndt C, Jones DP. Oxidative Stress. *Annu Rev Biochem*. 2017;86:715-748.
43. Zambetti NA, Ping Z, Chen S, et al. Mesenchymal Inflammation Drives Genotoxic Stress in Hematopoietic Stem Cells and Predicts Disease Evolution in Human Pre-leukemia. *Cell Stem Cell*. 2016;19(5):613-627.

44. Grignani F, Testa U, Rogaia D, et al. Effects on differentiation by the promyelocytic leukemia PML/RARalpha protein depend on the fusion of the PML protein dimerization and RARalpha DNA binding domains. *EMBO J*. 1996;15(18):4949-4958.
45. de The H, Le Bras M, Lallemand-Breitenbach V. The cell biology of disease: Acute promyelocytic leukemia, arsenic, and PML bodies. *J Cell Biol*. 2012;198(1):11-21.
46. Kollner I, Sodeik B, Schreek S, et al. Mutations in neutrophil elastase causing congenital neutropenia lead to cytoplasmic protein accumulation and induction of the unfolded protein response. *Blood*. 2006;108(2):493-500.
47. Grenda DS, Murakami M, Ghatak J, et al. Mutations of the ELA2 gene found in patients with severe congenital neutropenia induce the unfolded protein response and cellular apoptosis. *Blood*. 2007;110(13):4179-4187.
48. Horwitz MS, Corey SJ, Grimes HL, Tidwell T. ELANE mutations in cyclic and severe congenital neutropenia: genetics and pathophysiology. *Hematol Oncol Clin North Am*. 2013;27(1):19-41, vii.
49. Horwitz MS, Duan Z, Korkmaz B, Lee HH, Mealiffe ME, Salipante SJ. Neutrophil elastase in cyclic and severe congenital neutropenia. *Blood*. 2007;109(5):1817-1824.
50. Makaryan V, Zeidler C, Bolyard AA, et al. The diversity of mutations and clinical outcomes for ELANE-associated neutropenia. *Curr Opin Hematol*. 2015;22(1):3-11.
51. Germeshausen M, Deerberg S, Peter Y, Reimer C, Kratz CP, Ballmaier M. The spectrum of ELANE mutations and their implications in severe congenital and cyclic neutropenia. *Hum Mutat*. 2013;34(6):905-914.
52. Skokowa J, Dale DC, Touw IP, Zeidler C, Welte K. Severe congenital neutropenias. *Nat Rev Dis Primers*. 2017;3:17032.
53. Venselaar H, Te Beek TA, Kuipers RK, Hekkelman ML, Vriend G. Protein structure analysis of mutations causing inheritable diseases. An e-Science approach with life scientist friendly interfaces. *BMC Bioinformatics*. 2010;11:548.
54. Dannenmann B, Zahabi A, Mir P, et al. Human iPSC-based model of severe congenital neutropenia reveals elevated UPR and DNA damage in CD34(+) cells preceding leukemic transformation. *Exp Hematol*. 2019;71:51-60.
55. Hiramoto T, Ebihara Y, Mizoguchi Y, et al. Wnt3a stimulates maturation of impaired neutrophils developed from severe congenital neutropenia patient-derived pluripotent stem cells. *Proc Natl Acad Sci U S A*. 2013;110(8):3023-3028.
56. Nayak RC, Trump LR, Aronow BJ, et al. Pathogenesis of ELANE-mutant severe neutropenia revealed by induced pluripotent stem cells. *J Clin Invest*. 2015;125(8):3103-3116.

57. Guo L, Giasson BI, Glavis-Bloom A, et al. A cellular system that degrades misfolded proteins and protects against neurodegeneration. *Mol Cell*. 2014;55(1):15-30.
58. Barreyro L, Chlon TM, Starczynowski DT. Chronic immune response dysregulation in MDS pathogenesis. *Blood*. 2018;132(15):1553-1560.
59. Essers MA, Offner S, Blanco-Bose WE, et al. IFNalpha activates dormant haematopoietic stem cells in vivo. *Nature*. 2009;458(7240):904-908.
60. Pietras EM. Inflammation: a key regulator of hematopoietic stem cell fate in health and disease. *Blood*. 2017;130(15):1693-1698.
61. Walter D, Lier A, Geiselhart A, et al. Exit from dormancy provokes DNA-damage-induced attrition in haematopoietic stem cells. *Nature*. 2015;520(7548):549-552.
62. Schneider RK, Schenone M, Ferreira MV, et al. Rps14 haploinsufficiency causes a block in erythroid differentiation mediated by S100A8 and S100A9. *Nat Med*. 2016;22(3):288-297.
63. Hanada T, Yoshimura A. Regulation of cytokine signaling and inflammation. *Cytokine Growth Factor Rev*. 2002;13(4-5):413-421.
64. Touw IP, Beekman R. Severe congenital neutropenia and chronic neutrophilic leukemia: an intriguing molecular connection unveiled by oncogenic mutations in CSF3R. *Haematologica*. 2013;98(10):1490-1492.
65. Rosenberg PS, Alter BP, Bolyard AA, et al. The incidence of leukemia and mortality from sepsis in patients with severe congenital neutropenia receiving long-term G-CSF therapy. *Blood*. 2006;107(12):4628-4635.
66. Touw IP, van de Geijn GJ. Granulocyte colony-stimulating factor and its receptor in normal myeloid cell development, leukemia and related blood cell disorders. *Front Biosci*. 2007;12:800-815.
67. Maxson JE, Gotlib J, Pollyea DA, et al. Oncogenic CSF3R mutations in chronic neutrophilic leukemia and atypical CML. *N Engl J Med*. 2013;368(19):1781-1790.
68. Hemmati S, Haque T, Gritsman K. Inflammatory Signaling Pathways in Preleukemic and Leukemic Stem Cells. *Front Oncol*. 2017;7:265.
69. Leimkuhler NB, Schneider RK. Inflammatory bone marrow microenvironment. *Hematology Am Soc Hematol Educ Program*. 2019;2019(1):294-302.
70. Mangan JK, Speck NA. RUNX1 mutations in clonal myeloid disorders: from conventional cytogenetics to next generation sequencing, a story 40 years in the making. *Crit Rev Oncog*. 2011;16(1-2):77-91.
71. Michaud J, Wu F, Osato M, et al. In vitro analyses of known and novel RUNX1/AML1 mutations in dominant familial platelet disorder with predisposition to acute myelogenous leukemia: implications for mechanisms of pathogenesis. *Blood*. 2002;99(4):1364-1372.

72. Matheny CJ, Speck ME, Cushing PR, et al. Disease mutations in RUNX1 and RUNX2 create nonfunctional, dominant-negative, or hypomorphic alleles. *EMBO J*. 2007;26(4):1163-1175.
73. Owen CJ, Toze CL, Koochin A, et al. Five new pedigrees with inherited RUNX1 mutations causing familial platelet disorder with propensity to myeloid malignancy. *Blood*. 2008;112(12):4639-4645.
74. Miyoshi H, Shimizu K, Kozu T, Maseki N, Kaneko Y, Ohki M. t(8;21) breakpoints on chromosome 21 in acute myeloid leukemia are clustered within a limited region of a single gene, AML1. *Proc Natl Acad Sci U S A*. 1991;88(23):10431-10434.
75. Miyoshi H, Kozu T, Shimizu K, et al. The t(8;21) translocation in acute myeloid leukemia results in production of an AML1-MTG8 fusion transcript. *EMBO J*. 1993;12(7):2715-2721.
76. Chang KS, Fan YH, Stass SA, et al. Expression of AML1-ETO fusion transcripts and detection of minimal residual disease in t(8;21)-positive acute myeloid leukemia. *Oncogene*. 1993;8(4):983-988.
77. Golub TR, Barker GF, Bohlander SK, et al. Fusion of the TEL gene on 12p13 to the AML1 gene on 21q22 in acute lymphoblastic leukemia. *Proc Natl Acad Sci U S A*. 1995;92(11):4917-4921.
78. Romana SP, Mauchauffe M, Le Coniat M, et al. The t(12;21) of acute lymphoblastic leukemia results in a tel-AML1 gene fusion. *Blood*. 1995;85(12):3662-3670.
79. Shurtleff SA, Buijs A, Behm FG, et al. TEL/AML1 fusion resulting from a cryptic t(12;21) is the most common genetic lesion in pediatric ALL and defines a subgroup of patients with an excellent prognosis. *Leukemia*. 1995;9(12):1985-1989.
80. Song WJ, Sullivan MG, Legare RD, et al. Haploinsufficiency of CBFA2 causes familial thrombocytopenia with propensity to develop acute myelogenous leukaemia. *Nat Genet*. 1999;23(2):166-175.
81. Satoh Y, Matsumura I, Tanaka H, et al. C-terminal mutation of RUNX1 attenuates the DNA-damage repair response in hematopoietic stem cells. *Leukemia*. 2012;26(2):303-311.
82. Wang CQ, Krishnan V, Tay LS, et al. Disruption of Runx1 and Runx3 leads to bone marrow failure and leukemia predisposition due to transcriptional and DNA repair defects. *Cell Rep*. 2014;8(3):767-782.
83. Alcalay M, Meani N, Gelmetti V, et al. Acute myeloid leukemia fusion proteins deregulate genes involved in stem cell maintenance and DNA repair. *J Clin Invest*. 2003;112(11):1751-1761.
84. Krejci O, Wunderlich M, Geiger H, et al. p53 signaling in response to increased DNA damage sensitizes AML1-ETO cells to stress-induced death. *Blood*. 2008;111(4):2190-2199.

85. Liddiard K, Hills R, Burnett AK, Darley RL, Tonks A. OGG1 is a novel prognostic indicator in acute myeloid leukaemia. *Oncogene*. 2010;29(13):2005-2012.
86. Forster VJ, Nahari MH, Martinez-Soria N, et al. The leukemia-associated RUNX1/ETO oncoprotein confers a mutator phenotype. *Leukemia*. 2016;30(1):250-253.
87. Cai X, Gaudet JJ, Mangan JK, et al. Runx1 loss minimally impacts long-term hematopoietic stem cells. *PLoS One*. 2011;6(12):e28430.
88. Cai X, Gao L, Teng L, et al. Runx1 Deficiency Decreases Ribosome Biogenesis and Confers Stress Resistance to Hematopoietic Stem and Progenitor Cells. *Cell Stem Cell*. 2015;17(2):165-177.
89. Motoda L, Osato M, Yamashita N, et al. Runx1 protects hematopoietic stem/progenitor cells from oncogenic insult. *Stem Cells*. 2007;25(12):2976-2986.
90. Bellissimo DC, Chen CH, Zhu Q, et al. Runx1 negatively regulates inflammatory cytokine production by neutrophils in response to Toll-like receptor signaling. *Blood Adv*. 2020;4(6):1145-1158.
91. Sun W, Downing JR. Haploinsufficiency of AML1 results in a decrease in the number of LTR-HSCs while simultaneously inducing an increase in more mature progenitors. *Blood*. 2004;104(12):3565-3572.
92. Jacob B, Osato M, Yamashita N, et al. Stem cell exhaustion due to Runx1 deficiency is prevented by Evi5 activation in leukemogenesis. *Blood*. 2010;115(8):1610-1620.
93. Speidel D, Wellbrock J, Abas M. RUNX1 Upregulation by Cytotoxic Drugs Promotes Apoptosis. *Cancer Res*. 2017;77(24):6818-6824.
94. Goyama S, Schibler J, Cunningham L, et al. Transcription factor RUNX1 promotes survival of acute myeloid leukemia cells. *J Clin Invest*. 2013;123(9):3876-3888.
95. Sakurai M, Kunimoto H, Watanabe N, et al. Impaired hematopoietic differentiation of RUNX1-mutated induced pluripotent stem cells derived from FPD/AML patients. *Leukemia*. 2014;28(12):2344-2354.
96. Lu H, Sun J, Wang F, et al. Enhancer of zeste homolog 2 activates wnt signaling through downregulating CXXC finger protein 4. *Cell Death Dis*. 2013;4:e776.

Addendum

List of abbreviations

2HG	octyl-(R)-2hydroxyglutarate
5hmC	5-hydroxymethylcytosine
5mC	5-methylcytosine
ALL	acute lymphoblastic leukemia
AML	acute myeloid leukemia
APL	acute promyelocytic leukemia
As_2O_3	arsenic trioxide
ATG	anti-thymocyte globulin
BM	bone marrow
CBF	core-binding factor
CFU	colony-forming unit
CNL	chronic neutrophilic leukemia
CsA	cyclosporine-A
CSF3	colony-stimulating factor 3 (a.k.a. G-CSF)
CSF3R	colony-stimulating factor 3 receptor
CSF3R-d715	mutated colony-stimulating factor 3 receptor at amino acid 715 (Q739*)
ER	endoplasmic reticulum
FAB	French-American-British
FACS	fluorescence-activated cell sorter
FDR	false discovery rate
FPD	familial platelet syndrome
G-CSF	granulocyte-colony-stimulating factor (a.k.a. CSF3)
gnomAD	genome aggregation database
GSEA	gene set enrichment analysis
GSR	gluthation reductase
GvHD	graft-versus-host disease
HDAC	histone deacetylase
HOVON	Dutch–Belgian cooperative trial group for hematology–oncology
HPC	hematopoietic progenitor cell
HSCT	hematopoietic stem cell transplantation
HSPC	hematopoietic stem and progenitor cell
iBMF	inherited bone marrow failure syndrome
IFN	interferon
iPSC	induced pluripotent stem cell
IPSS	international prognostic scoring system

IST	immunosuppressive therapy
ITD	internal tandem duplication
L	liter
LK	lineage negative, Sca-1 negative, c-Kit positive cell
LSK	lineage negative, Sca-1 positive, c-Kit positive cell
LT-HSC	long-term hemataopoietic stem cell
MDS	myelodysplastic syndrome
MPN	myeloproliferative neoplasms
MPP	multipotent progenitor
NAC	N-acetylcysteine
NE	neutrophil elastase
NES	normalized enrichment score
NGS	next generation sequencing
NMD	nonsense-mediated mRNA decay
PB	peripheral blood
PML	promyelocytic leukemic protein
PML-NBs	promyelocytic leukemic protein nuclear bodies
PRC2	polycomb repressor complex 2
RAEB	refractory anemia with excess of blasts
RAEB-t	refractory anemia with excess of blasts in transformation
RARA	retinoic acid receptor α
redox	reduction-oxidation
RHD	runt-homology domain
ROS	reactive oxygen species
SAA	severe aplastic anemia
SAKK	Swiss group for clinical cancer research
SCN	severe congenital neutropenia
sMDS	secondary myelodysplastic syndrome
SUMO	small ubiquitin-like modifier
TAD	transactivation domain
TPM	transcripts per million
UPR	unfolded protein response
VAF	variant allele frequency
WES	whole exome sequencing
WGS	whole genome sequencing
WT	wildtype

Nederlandse samenvatting

Ernstige aangeboren neutropenie (SCN) is een erfelijke beenmerg stoornis veroorzaakt door een uitrijpingsdefect van neutrofielen. Mutaties (genetische veranderingen) in verschillende genen kunnen SCN veroorzaken. De meeste Europese SCN-patiënten hebben een mutatie in de genen *ELANE* (~50%) of *HAX1* (~11%). SCN wordt gekarakteriseerd door een differentiatie blok ter hoogte van het promyelocyt stadium en een sterk tekort aan uitgerijpte neutrofielen in het bloed (<0.5x10^9/L). Uitgerijpte neutrofielen zijn een belangrijk onderdeel van het primaire afweermechanisme van het lichaam en zorgen ervoor dat bacteriën en schimmels worden opgeruimd. Patiënten met SCN vertonen veel, ernstige en vaak ook levens-bedreigende bacteriële infecties die onder andere tandvlees-, oor-, long- en huidontstekingen veroorzaken. Deze ontstekingen beginnen vaak al vier weken na de geboorte. Gelukkig is SCN een zeldzame aandoening (3-8,5 gevallen per miljoen individuen) en worden SCN-patiënten tegenwoordig effectief behandeld met de groeifactor CSF3 (ook bekend als G-CSF). CSF3-therapie resulteert in voldoende uitgerijpte neutrofielen in het bloed in meer dan 90% van de SCN-patiënten, waardoor hun kwaliteit van leven sterk verbeterd. Verontrustend is wel dat SCN-patiënten die behandeld worden met CSF3 een sterk verhoogd risico hebben op het ontwikkelen van myelodysplastisch syndroom (MDS) en acute myeloïde leukemie (AML). Tijdens de leukemische progressie van SCN worden vaak nieuw verkregen mutaties gevonden in de receptor voor CSF3 (*CSF3R*). Deze mutaties resulteren in een verkorte vorm van de receptor waardoor deze niet meer afgebroken kan worden en op een andere manier signaleert. Deze mutante CSF3R klonen zijn vaak al jaren voor de ontwikkeling van MDS/AML in het lichaam aanwezig en regelmatig worden er zelfs meerdere kleine CSF3R-mutant klonen gevonden. Op het moment dat SCN-patiënten gediagnosticeerd worden met MDS of AML hebben ze vaak, bovenop de *CSF3R*-mutatie, ook een mutatie verkregen in het gen *RUNX1*. RUNX1 is een transcriptiefactor welke erg belangrijk is voor de vorming van bloedcellen. Het werk beschreven in dit proefschrift focust zich op de mechanismen die betrokken zijn bij de leukemische progressie van SCN door deze verschillende stappen in geïnduceerde pluripotente stamcellen (iPSCs) en muizen na te bootsen.

Hoofdstuk 2 is een boekhoofdstuk gefocust op het gebruiken van iPSCs voor het bestuderen van SCN. iPSCs zijn cellen die geherprogrammeerd zijn tot een pluripotente stamcel vanuit uitgerijpte cellen. Deze cellen kunnen vervolgens onder de juiste condities uitgroeien tot alle type lichaamscellen. De ontwikkeling van deze technologie is een revolutie voor het bestuderen van zeldzame ziektes doordat nu patiënt-specifieke modellen kunnen worden gemaakt. Voor SCN in het bijzonder zijn iPSCs een bijzonder nuttig model, omdat muismodellen met SCN-patiënt-specifieke mutaties in *ELANE* of *HAX1* geen tekenen van

neutropenie vertonen. Voordat iPSC modellen beschikbaar waren werden humane cellijnen, gemaakt van niet SCN-gerelateerde leukemische cellen, gebruikt waar met een retrovirus het mutante *ELANE*-gen in werd ingebracht. De uitkomsten van deze experimenten zijn gemixt en cellijnen worden nu beschouwd als minder geschikt voor het bestuderen van de SCN-biologie. Sinds de introductie van de iPSC technologie zijn er verschillende lijnen beschreven die gemaakt zijn van materiaal van SCN-patiënten. Met de introductie van CRISPR-Cas9-gemedieerde genoommodificatie kwam de mogelijkheid om specifieke veranderingen aan te brengen in de iPSCs, waarbij bijvoorbeeld SCN-veroorzakende mutaties kunnen worden gecorrigeerd of extra mutaties kunnen worden aangebracht. Doordat deze cellen verder identiek zijn aan de niet-gemodificeerde cellen kan goed gekeken worden naar de effecten van deze specifieke veranderingen, zonder de aanwezigheid van verstorende factoren door bijvoorbeeld virale over-expressie of verschillen in iPSC lijnen of klonen.

In **Hoofdstuk 3** worden vier nieuwe iPSC-lijnen beschreven, gegenereerd van drie SCN-patiënten (met SCN-veroorzakende mutaties *ELANE*-I60F, *ELANE*-R103L en *HAX1*-W44X) en een gezonde controle. Deze iPSCs zijn gebruikt om onrijpe bloedcellen, de zogenaamde hematopoietische voorlopercellen (HPCs), van te maken waarin de effecten van de *ELANE/HAX1* mutaties zijn bestudeerd. De HPCs verkregen uit de SCN-patiënten iPSCs vertoonde tekenen van verhoogde oxidatieve stress, met als gevolg dat de NRF2-gemedieerde antioxidant respons werd geactiveerd. In *ELANE* SCN-patiënten waarin de mutatie resulteert in verkeerde vouwing van het NE-eiwit werden verhoogde aantallen van PML-lichaampjes (PML-NBs) in de kernen van de cellen gevonden. PML-NBs zijn een kenmerk van meer acute oxidatieve stress, maar zijn ook gelinkt aan verschillende andere processen zoals metabolisme, het herstellen van DNA-schade en apoptose. In het geval van *ELANE*-mutaties die resulteren in een verkeerd gevouwen NE-eiwit zorgde PML voor een verhoogde metabole staat van de HPCs, terwijl ook de expressie van mutant *ELANE* sterk werd verhoogd, suggestief voor een versterkende rol van PML in de ziekteontwikkeling. Daarnaast remde PML de CSF3-geinduceerde uitrijping van neutrofiel voorlopercellen van deze *ELANE*-mutant HPCs, duidend op een belangrijke rol van PML in CSF3-therapie respons en SCN-pathogenese.

In **Hoofdstuk 4** is CRISPR-Cas9-gemedieerde genoommodificatie gebruikt om de patiënt-specifieke CSF3R mutatie d715 (Q739X), resulterend in een verkorte (getrunceerde) vorm van de receptor, in te brengen in de hierboven beschreven iPSCs. RNA sequencing analyses lieten grote verschillen zien tussen controle- en SCN-HPCs wanneer de gemuteerde CSF3R werd geïntroduceerd. Waar CSF3R-d715 controle HPCs de bevindingen die eerder in cellijnen en muismodellen zijn gedaan bevestigde, resulteerde de CSF3R-d715 in SCN-HPCs niet in verhoogde proliferatie maar in activatie van inflammatoire signaleringsroutes, terwijl

neutrofiel uitrijping werd geïnduceerd in plaats van geremd. Deze data verklaren mogelijk waarom *CSF3R*-mutante klonen jaren in het lichaam aanwezig kunnen zijn als kleine kloon voordat leukemie klinisch detecteerbaar wordt. Verder verklaren deze data mogelijk ook de hoge frequentie van *CSF3R* mutaties in de leukemische kloon, aangezien de activering van inflammatoire signaleringsroutes mogelijk de selectie en uitgroei bevorderd van klonen met extra mutaties die ervoor zorgen dat de cellen hier beter tegen bestand zijn. Het is beschreven dat cellen met mutaties in bijvoorbeeld *RUNX1* en *TET2*, beiden vaak gemuteerd in AML, hogere resistentie hebben tegen een inflammatoire omgeving. Deze data geven hierdoor mogelijk een verklaring voor de vele *RUNX1* mutaties die gevonden worden in *CSF3R*-mutante klonen in SCN-patiënten.

Hoofdstuk 5 bevat een (p)review dat de rol van *RUNX1* mutaties in SCN bespreekt. De focus ligt voornamelijk op het *Csf3r*-d715/*RUNX1*-D171N muismodel dat beschreven wordt in **Hoofdstuk 6**. In dit muismodel lijdt de combinatie van deze twee mutaties, in combinatie met CSF3-behandeling, tot een selectieve expansie van onrijpe lineage- c-Kit+ (LK) myeloblasten. Aanvullende experimenten in iPSC laten ook een verminderde neutrofiel-uitrijping zien als de *RUNX1*-D171N mutatie wordt ingebracht in *CSF3R*-d715 cellen van een gezonde controle.

Hoofdstuk 6 beschrijft hoe de combinatie van CSF3-behandeling, *CSF3R* en *RUNX1* mutaties bijdraagt aan de ontwikkeling van AML. CSF3-behandelde, maar niet PBS-behandelde, *Csf3r*/*RUNX1* mutante muizen laten een selectieve expansie van onrijpe lineage negatieve, c-Kit positieve, Sca-1 negatieve (LK) myeloblasten zien, maar dit lijdt niet tot AML. Een van de *Csf3r*/*RUNX1* mutante muizen die behandeld werd met CSF3 (1/9) ontwikkelde AML nadat de beenmergcellen van deze muis opnieuw getransplanteerd werden. Deze muis had een extra mutatie verkregen in het gen *Cxxc4*, wat resulteerde in een insertie van 2 glycines in een glycine-repeat. Deze verandering zorgde voor een stabieler CXXC4 eiwit, resulterend in verhoogde CXXC4 levels en verlaagde TET2 eiwit levels. Verder vertoonde de muis AML-cellen verhoogde expressie van inflammatoire signaleringsroutes, welke ook hoger tot expressie kwamen in menselijke SCN-AML cellen. Deze verhoogde inflammatoire signaleringsroutes konden worden nagebootst in iPSC door (TET2's functie in) de rekrutering van HDACs te remmen, duidend op een mogelijke belangrijke rol voor verhoogde inflammatoire signaleringsroutes door verlaagde TET2-activiteit in de leukemische transformatie van SCN.

In **Hoofdstuk 7** worden 1706 MDS/AML patiënten beschreven die mee hebben gedaan aan verschillende HOVON klinische trials. Het DNA van deze patiënten werd gescreend op mutaties in de glycine-repeat regio van CXXC4, welke veranderd was in de leukemische muizen beschreven in **Hoofdstuk 6**. Inserties, deleties en missense mutaties in *CXXC4* werden gevonden in 46 MDS/AML patiënten. Speeksel materiaal was beschikbaar van 12

CXXC4-mutante patiënten, welke allemaal de aanwezigheid van de mutatie in het kiembaan-materiaal lieten zien wat betekent dat deze mutatie aangeboren/erfelijk is. Van vijf aanvullende patiënten was materiaal beschikbaar van remissiemateriaal, het stadium waarop de MDS/AML niet meer detecteerbaar is, en ook deze patiënten lieten de aanwezigheid van de mutatie in dit materiaal zien. Ook al werden *CXXC4* mutaties in het kiembaanmateriaal gevonden, meer *CXXC4*-mutante patiënten vertoonde een pre-leukemische ziekte waarvan beschreven is dat inflammatoire signaleringsroutes een belangrijke rol spelen, zoals hoog risico MDS en myeloproliferatieve neoplasmata (MPN) (p=0.008). Deze data suggereren dat *CXXC4*-mutaties mogelijk een rol spelen in, maar niet de enige veroorzakers zijn van, de leukemische transformatie door een inflammatoire omgeving te creëren die belangrijk is voor de klonale uitgroep van hematopoietische stamcellen. Leukemische transformatie is vervolgens afhankelijk van het verwerven van aanvullende mutaties die vaak voorafgegaan worden door een pre-leukemisch stadium zoals MDS.

In **Hoofdstuk 8** wordt een patiënt beschreven met ernstige aplastische anemie (SAA) die een chronische neutrofiele leukemie (CNL) heeft ontwikkeld. De verworven driver-mutaties in *CSF3R, RUNX1* en een van de polycomb onderdrukkende complex 2 (PRC2) genen (*EZH2*) in deze SAA-CNL patiënt overlappen met de mutaties in een eerder beschreven SCN-AML patiënt (mutatie in PRC2 gen *SUZ12*). Transcriptoom analyses gedaan op niet-leukemische $CD34^{++}$ HPCs van de SAA-CNL patiënt of de SCN-patiënt in vergelijking met 3 gezonde controles liet een sterk overlappend transcriptioneel profiel zien met verhoogde interferon (IFN)-gedreven inflammatoire responses. Deze bevindingen wijzen op de aanwezigheid van een pro-inflammatoir milieu in SAA en SCN, welke mogelijk bijdragen aan de pre-leukemische staat van deze cellen. Verder geven deze resultaten nieuwe inzichten in de mogelijke mechanismen die onderliggend zijn aan de leukemische transformatie van beenmerg stoornissen.

Concluderend, dit proefschrift onthult nieuwe mechanismen in hoe SCN-mutaties, en mogelijk andere beenmerg stoornissen zoals SAA, bijdragen aan de leukemische progressie. Een aparte groep SCN-patiënten met mutaties in *ELANE* die lijden tot een verkeerd gevouwen NE-eiwit zijn geïdentificeerd, waarin PML-NBs een belangrijke rol spelen in de ziekteontwikkeling en CSF3-therapie respons. Daarnaast laat dit proefschrift zien dat inflammatoire signalerings-routes een belangrijke rol spelen in de leukemische transformatie van SCN en wordt een *Cxxc4*-mutatie beschreven, welke ook in mensen voorkomt, als extra driver-mutatie in AML-cellen van een SCN-muismodel.

Curriculum Vitae

Personal information

- Name: Patricia Anita Olofsen-Dieleman
- Date of birth: 13-09-1990
- Place of birth: Amsterdam, the Netherlands
- Nationality: Dutch

Education

- **Master's in Biomedical Sciences (2011-2013)**
  Leiden University/Leiden University Medical Centre (LUMC) , Leiden, the Netherlands
- **Bachelor's in Biomedical Sciences (2008-2011)**
  Leiden University/LUMC, Leiden, the Netherlands
- **Pre-university education (VWO, 2002-2008)**
  Kaj Munk College, Hoofddorp, the Netherlands
  Profiles: Nature & Techniques (N&T), and Nature & Health (N&G), including Economy 1

Research experience

- **PhD student (January 2014 - January 2021)**
  Department of Hematology, Erasmus MC, Rotterdam, the Netherlands
  Laboratory of Professor Ivo P. Touw
  Title: Molecular and Cellular Defects Driving the Leukemic Progression of Severe Congenital Neutropenia
- **Master internship II (September 2012 - June 2013)**
  Department of Molecular Cell Biology, LUMC, Leiden, the Netherlands
  Laboratory of Professor Peter ten Dijke
  Title: The effect of over-expression of inhibitory SMADs on breast cancer cell invasion and metastasis.
- **Master internship I (Februari 2012 – August 2012)**
  Ludwig Institute for Cancer Research/Oxford University, Oxford, United Kingdom
  Laboratory of Professor Xin Lu
  Title: The Apoptosis Stimulating Protein of p53-2 inhibits Epithelial-to-Mesenchymal Transition by keeping β-catenin at the cell-cell junctions.
- **Bachelor internship (March 2011 - August 2011)**
  Department of Immunology, LUMC, Leiden, the Netherlands
  Laboratory of Professor Frank Staal
  Title: Transduction efficiency of various pseudotyped self-inactivating lentiviral vectors for RAG-SCID gene therapy.

List of publications

Olofsen PA, Bosch DA*, Roovers O*, van Strien PMH*, de Looper HWJ, Hoogenboezem RM, Barnhoorn S, Mastroberardino PG, Ghazvini M, van der Velden VHJ, Bindels EMJ, de Pater EM, Touw IP. “PML-controlled responses in severe congenital neutropenia with ELANE-misfolding mutations”. Blood Advances. 2021 Feb; 5(3):775-786.

Olofsen PA*, Schmied L*, Lundberg P, Tzankov A, Kleber M, Halter J, Uhr M, Valk PJM, Touw IP, Passweg J, Drexler B. “Secondary CNL after SAA reveals insights in leukemic transformation of bone marrow failure syndromes”. Blood Advances. 2020 Nov; 4(21):5540-5546.

Olofsen PA, Fatrai S, van Strien PMH, Obenauer JC, de Looper HWJ, Hoogenboezem RM, Erpelinck-Verschueren CAJ, Vermeulen PWM, Roovers O, Haferlach T, Jansen JH, Ghazvini M, Bindels EMJ, Schneider RK, de Pater EM, Touw IP. “Malignant Transformation Involving CXXC4 Mutations Identified in a Leukemic Progression Model of Severe Congenital Neutropenia”. Cell Reports Medicine. 2020 Aug; 1(5): 100074

Olofsen PA and Touw IP. “Recent Advances in iPSC Disease Modeling, Volume 1, Chapter 5 - Modeling severe congenital neutropenia in induced pluripotent stem cells”. Academic Press. 2020; 1 (1): 85-101.

Touw IP and **Olofsen PA**. “Educational Updates in Hematology Book, Severe Congenital Neutropenia-Biological Insights”. HemaSphere. 2020 Jun; 4(S2):44-46.

Olofsen PA and Touw IP. “RUNX1 Mutations in the Leukemic Progression of Severe Congenital Neutropenia”. Mol Cells. 2020 Feb; 43(2):139-144.

Ribezzo F, Snoeren IAM, Ziegler S, Stoelben J, **Olofsen PA**, Henic A, Ferreira MV, Chen S, Stalmann USA, Buesche G, Hoogenboezem RM, Kramann R, Platzbecker U, Raaijmakers MHGP, Ebert BL, Schneider RK. “Rps14, Csnk1a1 and miRNA145/miRNA146a deficiency cooperate in the clinical phenotype and activation of the innate immune system in the 5q-syndrome”. Leukemia. 2019 Jul; 33(7):1759-1772.

Wang Y, Bu F, Royer C, Serres S, Larkin JR, Soto MS, Sibson NR, Salter V, Fritzsche F, Turnquist C, Koch S, Zak J, Zhong S, Wu G, Liang A, **Olofsen PA**, Moch H, Hancock DC, Downward J, Goldin RD, Zhao J, Tong X, Guo Y, Lu X. “ASPP2 controls epithelial plasticity and inhibits metastasis through β-catenin-dependent regulation of ZEB1”. Nat Cell Biol. 2014 Nov; 16(11):1092-104.

PhD portfolio

Courses and workshops	ECTS	Year
Annual Course on Molecular Medicine	0.7	2014
MGC Technology Facilities	1.2	2014
Course and Master Classes on Molecular Aspects of Hematological Disorders	1	2014
Browsing Genes and Genomes with UCSC: Basic and Advanced Workshop	0.8	2015
Course on Molecular Aspects of Hematological Disorders	0.7	2015
Microscopic Image Analysis: From Theory to Practice	0.8	2016
Course on Molecular Aspects of Hematological Disorders	0.7	2016
Introduction in Graph Pad Prism 6	0.3	2016
Galaxy for NGS	1	2017
Course on Molecular Aspects of Hematological Disorders	0.7	2017
Workshop on Photoshop and Illustrator CS6	0.3	2017
Workshop Indesign	0.3	2017
Course on Molecular Aspects of Hematological Disorders	0.7	2018
Gene expression data analysis using R: How to make sense out of your RNA-Seq/microarray data	2	2019

Scientific meetings department of Hematology	ECTS	Year
Work discussions department (weekly)	14	2014-2020
Hematology seminar series (monthly)	3.5	2014-2020
PhD lunch with seminar speakers (monthly)	3.5	2014-2020
AIO/Postdoc presentations (monthly)	1	2014-2015
Journal club (bi-weekly)	10.5	2014-2020

Attendance national/international conferences	ECTS	Year
Molecular Medicine day, Rotterdam, NL	3	2014-2016
Daniel den Hoed day, Rotterdam, NL	3	2014-2016
Dutch Hematology congress, Arnhem, NL	1	2016
Dutch Society of Stem Cell Research meeting, Utrecht, NL	1	2015
Annual iPSC user meeting, NL	2	2016-2017
24th Congress of the European Hematology Association, Amsterdam, NL	1	2019

Poster presentations at national/international meetings	ECTS	Year
9th Annual meeting of the Dutch Society for Stem Cell Research, Utrecht, NL	1	2016
23th Congress of the European Hematology Association, Stockholm, Sweden	1	2018

Oral presentations at national/international meetings	**ECTS**	**Year**
Annual iPSC user meeting, Nijmegen, NL	2	2015
9th Dutch Hematology Congress, Arnhem, NL	2	2015
60th Annual meeting of the American Society of Hematology, San Diego, USA	2	2018
61st Annual meeting of the American Society of Hematology, Orlando, USA	2	2019

Invited presentations	**ECTS**	**Year**
Annual iPSC user meeting, Rotterdam, NL	2	2014
Molecular Aspects of Hematological Disorders, Rotterdam, NL	2	2018
12th Dutch Hematology Congress, Arnhem, NL	2	2018
Meeting of the Young European Hematology Association, Amsterdam, NL	2	2019
13th Dutch Hematology Congress, Arnhem, NL	2	2019
14th Dutch Hematology Congress, Arnhem, NL	2	2020
1st European Network for Innovative Diagnosis and Treatment of Chronic Neutropenias (EuNet-INNOCHRON) meeting, online	2	2020
2nd European Network for Innovative Diagnosis and Treatment of Chronic Neutropenias (EuNet-INNOCHRON) meeting, online, 2 presentations	3	2021
Total	**81.70**	

Awards	**Prize**	**Year**
European Hematology Association Travel Grant Award	€500	2018
American Society of Hematology Abstract Achievement Award	$500	2019

Committees and organization activities	**Year**
Lab day committee	2015-2016
Organization and supervision PhD lunch with seminar speakers	2015-2016
Young EuNet-INNOCHRON committee	2020

Dankwoord

Ja, het is zo ver, mijn proefschrift is af! Wie had gedacht dat deze dag toch nog zou komen?! Uiteraard had ik dit nooit alleen kunnen halen, dus via deze weg wil ik graag de mensen bedanken die direct of indirect een bijdrage hebben geleverd aan dit proefschrift.

Te beginnen met natuurlijk mijn promotor. Beste Professor Touw, beste **Ivo**, bedankt dat je mij de kans hebt gegeven om mijn promotieonderzoek in jouw groep te doen. Het zijn een aantal bewogen jaren geweest maar we hebben het tot een mooi einde weten te breien. Ik heb veel respect voor je kritische blik, je tomeloze inzet in het verbeteren van projecten en het proberen te behouden van wetenschappelijke kwaliteit. Bedankt voor je enthousiasme en de vele discussies die we de afgelopen jaren hebben mogen voeren. Veel succes in de toekomst. Ik hoop dat je nog een tijdje door mag/kan hobbyen!

Beste dr. de Pater, beste **Emma**, ik weet nog goed dat je op de afdeling kwam en begon aan de uitdaging om je eigen groep op te starten. Je kwam terecht op een afdeling met voornamelijk mannen, maar daar heb je je geen moment door uit het veld laten slaan. Bedankt voor de vele peptalks en adviezen door de jaren heen en dat je mijn copromotor hebt willen zijn. Ik wens je veel succes in je verdere carrière!

Beste Professor Raaijmakers, dr. von Lindern en dr. van der Reijden, beste **Marc**, **Marieke** en **Bert**, bedankt dat jullie in de beoordelingscommissie willen plaats nemen. Ik heb altijd genoten van onze discussies tijdens werkbesprekingen en/of congressen en kijk er dan ook naar uit om nogmaals met jullie van gedachten te wisselen over mijn proefschrift.

Dear dr. Drexler and dr. Schmied, dear **Beatrice** and **Laurent**, I remember our first meeting like yesterday, where you, Beatrice, approached me after my talk at the ASH meeting in San Diego to discuss a SAA-CNL patient with very similar mutations as our SCN-AML patient. I'm glad that conversation resulted in a fruitful collaboration and a nice publication. Dear Professor Vertegaal, Professor Shimamura, and Professor Newburger, dear **Alfred**, **Akiko**, and **Peter**, thank you for the nice collaborations. I hope everything will result in a nice publication, even though I'm not there to finish the projects anymore. Beste dr. Erkeland en Professor Delwel, beste **Stefan** en **Ruud**, bedankt voor de vele adviezen en gezellige gesprekken door de jaren heen. Ik kon altijd bij jullie terecht voor uitdagende discussies over mijn werk of wetenschap in het algemeen en ik ben dan ook erg blij dat jullie in de grote commissie willen plaatsnemen. Beste dr. Bartels, beste **Marije**, mensen die geïnteresseerd zijn in SCN zijn erg schaars in Nederland, maar ik ben blij dat jij altijd erg betrokken bent geweest bij het SCN-onderzoek. Bedankt voor de vele patiëntensamples die je hebt

opgestuurd door de jaren heen en ik hoop dat je je altijd blijft inzetten voor onderzoek naar dit soort zeldzame ziektes. Beste dr. van der Velden, beste **Vincent**, bedankt voor de vele flow cytometry analyses die je voor ons hebt gedaan met het EuroFlow panel. Ik ben blij dat dit mooie publicaties heeft opgeleverd en dat alle moeite en energie die jullie erin hebben gestoken niet voor niets is geweest.

Beste **Paulette** en **Onno**, bedankt voor alle hulp de afgelopen 7 jaar. Zonder jullie had ik nu nog steeds iPSCs zitten kweken of achter de confocal gezeten! Ik wens jullie veel succes in de toekomst en hoop dat jullie een leuke nieuwe groep vinden. Beste **Dennis**, wat had ik zonder jouw hulp in de laatste jaren van mijn PhD moeten beginnen?! Bedankt voor de vele uren iPSCs kweken, CRISPR lijnen maken en experimenten doen. Veel succes in de groep van Mathijs en ik hoop dat je je enthousiasme voor de wetenschap behoudt! Beste **Hans**, ook jouw hulp is van ontschatbare waarde geweest voor meerdere hoofdstukken van mijn proefschrift. Bedankt voor je hulp met het maken en screenen van de CRISPR lijnen en je doorzettingsvermogen om CXXC4 gesequenced en gekloneerd te krijgen! Succes met de brouwerij, ik kom snel weer biertjes halen!

In dit rijtje mag natuurlijk ook labpapa **Eric** niet ontbreken! Dr. Bindels, bedankt voor de vele keren dat je in het weekend voor onze celletjes wilden zorgen. Vooral Liesbeth is je hier heel dankbaar voor (en ik ook wel een beetje hoor :p). Ook wil ik je bedanken voor de vele adviezen en peptalks die je me door de jaren heen hebt gegeven. Je bent echt onmisbaar voor de afdeling en alle PhD studenten!

Dear Professor Schneider, dear **Rebekka**, you have been, and are, a huge example for many of us. Being a PI hasn't changed you and you still behave like one of the mere mortal lab people. Thanks for the many nice, motivating, and inspiring talks we had over the years. I wish you all the best for the rest of your career, and a lot of happy times with your beautiful family. I hope our paths cross again in the future!

Dear Dr. Gleitz-Brothers, dear **Hélène**, we've been hitting it of since you joined Rebekka's lab and I'm glad I get to call you my friend! Although you're way too young to be a postdoc, you are more talented and experienced than many others. Thanks for having my back during my defense by acting as my paranimf. Beste **Inge Snoeren**, ook jij mag natuurlijk niet in het rijtje ontbreken! Toen je als analist begon in Rebekka's groep was ik meteen onder de indruk van je skills om naast experimenten uit te voeren deze ook zelf te bedenken en te analyseren. Waarom je nooit een PhD bent gaan doen is me nog steeds een raadsel. Ook wij hadden meteen een klik en ik ben blij dat we in contact zijn gebleven! Hopelijk kunnen we snel weer barbecuen bij ons in de tuin :).

Dear office 1330b, what would I have done without you guys? All of you made this experience more fun and I miss all our work and non-work discussions every day. Dear **Julia**, dear Germy, thanks for being there for me when I started my PhD. We've had many nice moments together and I recall our sarcastic jokes fondly. I'm glad we stayed in touch and picked up our monthly Skype talks again! Beste **Davine**, succes met het afronden van je PhD en het oppakken van het werk in de kliniek. Hopelijk vind je snel een baan die bij je past! Dear dr. Avelino, dear **Roberto**, I admire your (scientific) knowledge and insights and I've always been impressed by the amount of papers you seem to know by heart! Thanks for all the peptalks and the faith you've always had in me. I wish you the best of luck in Israel. Beste dr. Smeenk, beste **Leonie**, you've had some big shoes to fill nadat je Julia's plek op kantoor had overgenomen, maar je hebt je er knap door heen weten te slaan. Ook al verpestte je het Hufflepuf karakter van 1330b, we hebben een hoop mooie en gezellige momenten gedeeld samen. Ik wens je veel succes met het uitvogelen van je vervolgstap maar heb er alle vertrouwen in dat het goed gaat komen! Beste **Maurice**, beste Swinki, je verhuizing naar de 13e was een schot in de roos. Niet alleen kwam je terecht in het leukste kantoor, het kwam ook je project en je liefdesleven ten goede. Ik wens je veel succes met het afronden van je PhD en het vinden van een passende nieuwe baan. Hopelijk is het niet al te ver van Rotterdam ;-). Beste **Dorien** en **Emma B**, de nieuwste aanwinsten van 1330b, bedankt voor alle gezellige momenten en succes met jullie PhD. Hopelijk kunnen we snel ons geplande spelletjes avond houden!

Waar zou de afdeling zijn zonder jullie? Gedurende de afgelopen 7 jaar heb ik heel veel gehad aan jullie lab expertises en ik ben erg dankbaar voor jullie hulp **Lianne**, **Eline**, **Pia**, **Anke**, de rest van de **BMT**, de dames van de **moleculaire diagnostiek**, **François**, **Michael**, **Elwin**, **Claudia**, **Marije** en **Claire**. Uiteraard was dit proefschrift er ook nooit gekomen zonder de hulp van de bioinformatici **Remco**, **Mathijs**, **Roger** en **Elodie**. Dankjulliewel voor de vele analyses die jullie voor mij hebben gedaan! Ook de secretaresses **Tessa**, **Leenke**, **Ans** en **Annelies** zijn onmisbaar. Bedankt voor het vele papierwerk wat jullie telkens in orde hebben gemaakt!

To all the current PhD students, **Cansu**, **Emanuele**, **Paola**, **Eline**, **Martijn**, **Jacqueline**, **Tim**, **Sophie**, **Madelon**, **Jess** and **Bella**, I wish you lots of luck finishing your PhDs, and during the rest of your careers. Furthermore, I would like to thank **Iris**, **Petra**, **Stanley**, **Stijn**, **Isabel**, **Andrea**, **Joyce** and the rest of the current and former Hematology department members for the fun times in- and outside of the lab. I also wish to thank the other PIs of the department including dr. **Ruben** Bierings, dr. **Tom** Cupedo, dr. **Peter** Valk, Prof. **Jan** Cornelissen, Dr. **Mojca** Jongen-Lavrencic, Prof. **Bob** Löwenberg, and Prof. **Frank** Leebeek for discussions and advice in the lab and during the floor meetings**.**

Niet alleen de mensen die direct hebben bijgedragen aan de verschillende hoofdstukken zijn belangrijk geweest voor de totstandkoming van dit proefschrift, de mensen die indirect een bijdrage hebben geleverd zijn minstens net zo belangrijk! Lieve **Martijn**, **Silke**, **Mariska**, **Inge Loonen** en **Jennifer**, bedankt dat jullie mij van tijd tot tijd uit het lab hebben getrokken. Ik kon altijd bij jullie terecht om mijn gedachten te verzetten en te ontspannen en ik ben blij dat ik jullie tot mijn beste vrienden mag rekenen! Lieve **familie**, lieve **Bob**, **Ad**, **Martha**, **Wouter**, **opa**, **oma**, **Ada**, **Richard**, **Steven**, **Marieke**, **Tineke**, **Peter**, **Bianca**, **Rob**, **Edwin** en **Claudia**, bedankt voor alle gezelligheid. Ook al begrijpen jullie niet veel van mijn onderzoek jullie hebben altijd interesse getoond en jullie best gedaan om er iets van te snappen. Ik kijk uit naar de nieuwe familiebijeenkomsten zodra deze weer plaats kunnen vinden!

Lieve **papa** en **mama**, bedankt voor jullie vertrouwen in mij. Zonder jullie had ik het nooit aangedurfd om naar de Universiteit te gaan, laat staan aan een promotieonderzoek te beginnen. Ook al zien we elkaar nu minder vaak, ik koester alle momenten dat we samen zijn en kijk er naar uit om dit succes met jullie te vieren. Lieve **Natascha**, mijn niet meer zo kleine zusje, bedankt dat je mijn paranimf wilt zijn! Ook jij bent essentieel geweest voor het succes van mijn PhD door altijd een luisterend oor te bieden en voor afleiding te zorgen. Bedankt dat ik altijd bij je terecht kan als er iets is!

Last but not least: mijn wifey. Lieve **Liesbeth**, toen jij in mijn leven kwam werd alles een stuk mooier. Bedankt dat je er altijd voor me bent, of ik nou een luisterend oor of een knuffel nodig heb. Thuiskomen bij jou is elke dag een feestje en ik kan niet wachten om met jou een gezinnetje te starten.